

**UNIVERSIDADE FEDERAL DO RIO GRANDE DO SUL
INSTITUTO DE GEOCIÊNCIAS
PROGRAMA DE PÓS-GRADUAÇÃO EM GEOCIÊNCIAS**

**MORFODINÂMICA E EVOLUÇÃO DE CAMPOS DE
DUNAS TRANSGRESSIVOS QUATERNÁRIOS DO
LITORAL DO RIO GRANDE DO SUL**

Caroline Thaís Martinho

ORIENTADOR: Prof. Dr. Sérgio Rebello Dillenburg

CO-ORIENTADORES: Prof. Dr. Patrick Hesp

Prof. Dr. Luiz José Tomazelli

BANCA EXAMINADORA: Prof. Dr. Paulo César Fonseca Giannini

Prof. Dr. Rodolfo J. Angulo

Pro. Dr. Eduardo Guimarães Barboza

Tese de Doutorado apresentada como
requisito parcial para a obtenção do Título
de Doutor em Geociências.

Porto Alegre – 2008

Livros Grátis

<http://www.livrosgratis.com.br>

Milhares de livros grátis para download.

*“Água parada apodrece,
tal qual aquele que estaciona no tempo.
Somos viajantes.”*

(Antonio Martinho)

Somos cientistas...

“The answer is blowing in the wind...”

(Bob Dylan)

AGRADECIMENTOS

Agradeço ao Conselho Nacional de Desenvolvimento Científico e Tecnológico (CNPq) pelo auxílio na forma de bolsa de estudos e projeto de pesquisa, sem os quais a realização dessa tese não seria possível.

À Comissão Permanente de Aperfeiçoamento de Pessoal de Nível Superior (CAPES) pela de doutorado sanduíche.

Ao Centro de Estudos de Geologia Costeira e Oceânica (CECO) pelos equipamentos de campo e laboratório.

Ao Departamento de Geografia e Antropologia da Louisiana State University (LSU) pela infra-estrutura oferecida para o desenvolvimento dos trabalhos no exterior.

Ao IBAMA pela concessão de licença para pesquisa no Parque Nacional da Lagoa do Peixe.

Ao meu orientador Prof. Dr. Sérgio R. Dillenburg e ao meu co-orientador Prof. Dr. Luis J. Tomazelli por toda ajuda e apoio ao longo desses anos e por me apresentarem a fascinante planície costeira do Rio Grande do Sul.

Ao meus amigos Prof. Dr. Patrick Hesp, também meu co-orientador, e Prof. Dra. Graziela Miot, pelo muito que aprendi com vocês, pela hospitalidade, pela hospedagem, por toda a ajuda pessoal e profissional, pelas correções no inglês, pelas discussões, pelas viagens, pelas festas. Os oito meses que passamos juntos foram maravilhosos!

À todo o pessoal do CECO pela companhia; aos meus bolsistas Daniel Bayer, Luciana Dornelles e José Becker pelas análises granulométricas e pela ajuda em campo; aos colegas Rodrigo (Alemão), Clerot, André, Felipe, Leonardo (Thunder), Rafael, Eduardo, Nelson, Tabajara pela ajuda voluntária nos trabalhos de campo; ao Eduardo e à Maria Luíza pela amizade e ajuda com as imagens de satélite e com o ArcGIS. Especialmente ao amigo Gilberto Santos e família que me mostraram a hospitalidade gaúcha, pelas conversas e churrascos, e por serem minha família em Porto Alegre.

Ao secretário do PPGGEO Roberto, pela atenção e ajuda desde minha chegada à Porto Alegre.

À todos os amigos queridos que fiz no Rio Grande do Sul, os quais me fizeram gostar ainda mais daqui. Especialmente Denise, Cristina, Paula, Melissa pelas

conversas, risadas momentos de descontração que me faziam esquecer os campos de dunas.

À minha família pelo apoio incondicional e por sempre acreditar em mim e no meu potencial.

E ao meu marido Ezequiel, pela ajuda em campo, por ter sempre me apoiado, incentivado, encorajado e estar sempre do meu lado; e por toda paciência, amor e carinho. Sem essa força não teria conseguido terminar. Obrigada por ter me encontrado!

Muito obrigada a todos!

RESUMO

O trecho do litoral do Rio Grande do Sul entre Torres e Mostardas apresenta três tipos diferentes de barreiras: progradantes, agradantes e retrogradantes, e campos de dunas transgressivos se desenvolvem sobre todas elas. Contudo, o tamanho e a morfologia desses campos variam ao longo da costa, e têm apresentado mudanças nas últimas décadas. O objetivo deste trabalho é analisar os fatores responsáveis pelas variações espaço-temporais na morfologia dos campos de dunas e compreender sua evolução ao longo do Holoceno médio e tardio (últimos 5000 anos A.P.).

De Mostardas a Jardim do Éden, as altas energia de ondas e taxas de transporte longitudinal de sedimentos (TLS) provocam a erosão da linha de costa e a consequente retrogradação da barreira. Essa erosão disponibiliza maior volume de areia para o transporte eólico. Desse modo, o alto aporte sedimentar juntamente com a baixa umidade e o alto potencial de deriva (PD) eólica, observados nessa região, são responsáveis pela formação de grandes campos de dunas.

De Atlântida Sul a Torres, trecho adjacente às escarpas da Serra Geral, a umidade é alta, devido à precipitação orográfica e o PD eólica é menor devido à barreira topográfica. A baixa energia de ondas e a desaceleração do TLS, observados nessa região, criam balanço positivo de sedimentos, promovendo a progradação da barreira. Contudo, a baixa energia de ondas não tem capacidade de transportar grandes volumes dessa areia para o estirâncio e pós-praia. Assim, apesar do balanço positivo e do caráter progradante da barreira, o volume de areia disponível para o transporte eólico é menor. Com o baixo aporte sedimentar, alta umidade e baixo PD eólica, os campos de dunas dessa região são mais estreitos e restritos.

Variações climáticas foram observadas ao longo das últimas décadas. De 1948 a 2003 a precipitação aumentou e o PD eólica diminuiu de 1964 a 1988. Os campos de dunas de Atlântida Sul a Torres, menores e com menor volume de areia, responderam rápido ao aumento da precipitação e decréscimo no PD eólica, e encontram-se em estágio avançado de estabilização. Os campos de dunas de Mostardas a Jardim do Éden, maiores e com maior volume de areia levaram maior tempo para iniciarem sua estabilização e crescimento da vegetação. Quanto maior o volume de areia e o tamanho do campo de dunas, maior será o intervalo de tempo para sua estabilização.

O estudo da evolução dos campos de dunas foi realizado a partir de análise estratigráfica. Analisando as idades ^{14}C de paleossolos e informações sobre paleoclima observou-se que os três períodos principais de formação de solo (de 4820 a 3970 anos cal A.P.; em 2760-2460 anos cal A.P.; e de 1570 a 710 anos cal A.P.) coincidem com períodos de clima mais úmido. Este fato indica que o clima pode estar controlando a evolução dos campos de dunas desde pelo menos 5000 anos A.P.. A partir de informações estratigráficas, idades de paleossolos e descrição de fácies, 10 fases de ativação e estabilização eólica foram reconhecidas no litoral médio do RS.

ABSTRACT

The Rio Grande do Sul coastal stretch between Torres and Mostardas present three different types of barriers: progradational, aggradational and retrogradational, and transgressive dunefields have developed over all of them. Nevertheless, the size and the morphology of these dunefields vary along the coast and have been changing over the last decades. The aim of this study is to analyze the factors responsible for the spatio-temporal variations in the dunefields morphology and to understand their evolution through mid and late Holocene (last 5000 yrs BP).

From Mostardas to Jardim do Éden, the wave energy and the longshore sediment transport (LST) promote the coastline erosion and, consequently, the barrier retrogradation. The erosion increases the volume of sand available to the aeolian transport. Thus, the large sand supply along with the observed low humidity and high wind drift potential (DP) are responsible for the formation of large transgressive dunefields.

From Atlântida Sul to Torres, coastal stretch adjacent to the Serra Geral scarps, the humidity is higher due to the orographic precipitation and the wind DP is lower due to the topographic obstruction. The low wave energy and the decrease of the LST, observed in this region, create a positive sediment imbalance, promoting barrier progradation. Nevertheless, the low wave energy is not capable to transport large volumes of sand to the foreshore and backshore. Thus, despite the positive imbalance and the progradational character of the barrier, the volume of sand available to aeolian transport is lower. With low sand supply, high humidity and low wind DP, the dunefields in this area are narrow and restrict.

Climatic changes were observed through the last decades. From 1948 to 2003 the precipitation has increased and the wind DP has decreased from 1964 to 1988. The dunefields from Atlântida Sul to Torres, smaller and with low sand volume, have responded faster to the increase in precipitation and the decrease in the wind DP, and nowadays are in an advanced stabilization stage. The dunefields from Mostardas to Jardim do Éden, larger and with high amount of sand, have taken longer to initiate the stabilization processes and vegetation growth. The larger the sand volume and the dunefields size, the longer it will be the time period to stabilize it.

The study of the dunefield evolution was realized by stratigraphic analysis. Analyzing the ^{14}C ages from paleosol layers and the paleoclimatic information, it was observed that the three main soil formation periods (from 4820 to 3970 cal yrs BP; in 2760-2460 cal yrs BP; and from 1570 to 710 cal yrs BP) coincide with periods of wetter climate. This fact indicates that the climate might be controlling the dunefield evolution since at least 5000 yrs BP. From stratigraphic information, paleosol ages and facies description, 10 phases of aeolian activation and stabilization were recognized in the RS mid littoral.

LISTA DE FIGURAS

CAPÍTULO 1

Figura 1: Principais vias de acesso à área de estudo. A linha preta delimita a área de estudos, dos municípios de Torres a Mostardas. Os pontos brancos representam municípios e os pontos pretos representam as localidades estudadas.	22
Figura 2: Método de testemunhagem a percussão manual, tendo como testemunhador um tubo de PVC de 6m de comprimento. A) Fase de penetração no solo através de um peso batente. B) Fase de retirada do testemunho utilizando-se tripé e talha.	26
Figura 3: Mesa de abertura de testemunhos, acoplada à serra elétrica circular.	27

CAPÍTULO 2

Figura 1: Diagrama esquemático de uma barreira, observar os depósitos da fase transgressiva, produzidos pela ascensão do NRM durante o início do Holoceno.	32
Figura 2: Série contínua de variações geomorfológicas de barreiras, proposta por Roy <i>et al.</i> (1994), apresentando a nomenclatura de barreiras proposta por Morton (1994).	34

CAPÍTULO 3

Figure 1: Location of Rio Grande do Sul coast and Pleistocene and Holocene Barrier-Lagoon systems.	45
Figure 2: Coastline of Rio Grande do Sul showing location of shelf profiles.	47
Figure 3: Georeferenced 1999 satellite image of the RS coast showing the location of the 24 beaches studied. The wave energy and longshore sediment transport calculated for those beaches is shown at the right, and classified as high, medium and low. On the left, the capital letters correspond to the Holocene barrier types shown in Fig. 4.	55
Figure 4: Schematic stratigraphical sections of barrier types found along the RS coast, based on geomorphology and drill-holes (Dillenburg <i>et al.</i> 2000; Dillenburg <i>et al.</i> 2004a; Travessas <i>et al.</i> 2005; Dillenburg <i>et al.</i> 2006).	57

CAPÍTULO 4

Figure 1: Rio Grande do Sul coast and location of meteorological stations.	68
Figure 2: (A) ITCZ position near the Equator during winter and beginning of spring. (B) During summer and beginning of fall ITCZ migrates southward induced by SASM. The arrows indicate prevailing wind direction.	70
Figure 3: Monthly average precipitation of Imbé and Porto Alegre stations.	78
Figure 4: Yearly average precipitation for Imbé station. The trend line shows an increase in the precipitation.	78
Figure 5: Yearly average precipitation for Imbé station. Light gray bars represent cold events (La Niña) and dark gray bars represent warm events (El Niño).	79
Figure 6: Wind roses showing the direction, frequency and velocity of winds at (A) Torres, (B) Imbé, (C) Tramandaí, (D) Mostardas, (E) Rio Grande, (F) Chuí.	81
Figure 7: Sand roses of the stations showing the drift potential (DP) for each direction. The arrow represents the resultant drift potential (RDP) and the resultant drift direction (RDD).	82
Figure 8: Wind roses showing the direction, frequency and velocity of winds at (A) Itapeva, (B) Imbé and (C) Mostardas, during the period of December 1998 to September 1999.	84
Figure 9: Sand roses of the Itapeva, Imbé and Mostardas stations for the period of	

December 1998 to September 1999, showing the DP for each direction. The arrow represents the RDP and the RDD.	84
Figure 10: Sand roses of the seasons at Imbé station. The lines represent the DP for each direction and the arrow represents the RDP and RDD.	86
Figure 11: Sand roses of the seasons at Mostardas station. The lines represent the DP for each direction and the arrow represents the RDP and RDD.	86
Figure 12: Yearly total DP for Imbé station. Light gray bars represent cold events (La Niña) and dark gray bars represent warm events (El Niño).	87
Figure 13: Yearly DP of NE winds for Imbé station. Light gray bars represent cold events (La Niña) and dark gray bars represent warm events (El Niño).	88
Figure 14: Annual total DP showing trends of interdecadal variations.	88

CAPÍTULO 5

Figure 1: The northern and mid littoral of Rio Grande do Sul coast. Black dots indicate the studied dunefields. White dots are the location of meteorological stations. The continuous lines represent the isobaths of 20m and 50m. Sand roses of three stations show the drift potential (DP) for each direction in vector units (v.u.). The arrow represents the resultant drift potential (RDP) and the resultant drift direction (RDD).	105
Figure 2: Annual total drift potential (DP) from 1948 to 2003 for Imbé station.	107
Figure 3: Rondinha dunefield. A) Aerial photo from 1974, black arrows represent the washouts. White arrows represent the main dune migration direction (a) and the main dunefield migration direction (b); B) Aerial photo from 1989 and C) Satellite image from 2000.	109
Figure 4: Capão Novo dunefield. A) Aerial photo from 1948, black arrows represent the washouts and the white arrow the main migration direction; B) Aerial photo from 1989 and C) Satellite image from 1999.	111
Figure 5: Atlântida Sul dunefield. A) Aerial photo from 1948, black arrows represent the washouts and the white line show the relict deflation plains, dunefields and precipitation ridges; B) Aerial photo from 1974 and C) Satellite image from 1999.	113
Figure 6: Jardim do Édem dunefield. A) Aerial photo from 1948, black arrows are some examples of washouts in the area; B) Aerial photo from 1974, black arrows point to examples of parabolic dunes that feed the dunefield (“corredores de alimentação” <i>sensu</i> Tomazelli 1994); C) Satellite image from 1999.	115
Figure 7: Magistério dunefield. A) Aerial photo from 1948; B) Aerial photo from 1974, white arrows point to some examples of gegenwalle ridges; C) Satellite image from 1999.	117
Figure 8: Dunas Altas dunefield. A) Aerial photo from 1974, white arrows point to examples of trailing ridges and the black arrow points to an example of parabolic sand sheet; B) Satellite image from 1987 and C) Satellite image from 1999.	120
Figure 9: Solidão dunefield. A) Satellite image from 1980, black line represents the dunefield inner margin, the white arrows point to places where the active dunefield reached in 1980 and the black arrows represent the washouts; B) Satellite image from 1987 and C) Satellite image from 1999.	122
Figure 10: São Simão dunefield. A) Satellite image from 1973, black arrows represent the large washouts; B) Satellite image from 1988, black arrows point to the wet bush pockets; and C) Satellite image from 1999.	124
Figure 11: Dendritic pattern of drainage on deflation plain at São Simão dunefield. Satellite image from 1999.	125
Figure 12: Mostardas dunefield. A) Satellite image from 1973; B) Satellite image from 1988, black arrows point to some examples of sand sheets that can evolve to parabolic dunes and the white arrows point to some examples of the regularly spaced small washouts; and C) Satellite image from 1999, black arrows display	

the difference of deflation plain width from the north and to the south of the dunefield.	126
Figure 13: Jardim do Éden dunefield. White arrows point to some examples of small deltas silting the lake, formed by washout at the landward margin of the dunefield. Black arrows represent washouts at the seaward margin of the dunefield.	130
Figure 14: Small deltas formed by sand transported by the washouts, silting the lakes.	130
Figure 15: Topographic section of the barrier at Magistério dunefield showing that the central portion is higher.	131
Figure 16: Progressive stages that RS dunes are experiencing for the last 58 years, driven by an increase in moisture, decrease in wind energy, and decrease in sediment supply. Transverse dune (a); Barchanoid chain (b); Isolated barchan dunes with some vegetation growth starting in the deflation areas (c); Barchan dunes leaving behind gegenwalle ridges and trailing ridges, trapped by vegetation (d); Low parabolic dunes (e); and flat sand sheets with parabolic shapes.	136

CAPÍTULO 6

Figure 1: Aerial photo of Curumim progradational barrier with the overlapping dunefields. The lines A and B represent the survey lines. (A) and (B) are the topographic section of those lines, illustrating the location and the TL/OSL age of the aeolian phase. Ages in bold represent ^{14}C dates (non calibrated) of shoreface (nearshore) sediments from subsurface drill holes. Each phase from P1 to P11 is represented in the horizontal bar.	150
Figure 2: Cross geological section of Curumim barrier with the average TL/OSL age and width of each aeolian phase. The subsurface information is based on drill holes data of Dillenburg <i>et al.</i> (2006). White dots represent the location of ^{14}C samples in the core. The ^{14}C dates were obtained from shells of shoreface deposits.	151
Figure 3: The study area located on the northern and mid-littoral of RS coast. Black dots indicate the location of the drill-holes in each of the nine profiles. White dots are the location of meteorological stations. The continuous lines represent the isobaths of 20m and 50m.	154
Figure 4: The barrier types present along the study area.	155
Figure 5: Dashed line represent the sea level envelope of Angulo <i>et al.</i> (2006) for the southern State of Santa Catarina. The solid line represent the paleosea-level behavior predicted by the geophysical simulations made by Milne <i>et al.</i> (2005) <i>apud</i> Angulo <i>et al.</i> (2006).	156
Figure 6: Capão Novo profile. Position and height of the cores in the topographic section. The diagram illustrates the cores, the observed sedimentary facies, the depositional environment in which these facies where deposited and, if discernible, the phases of aeolian activity.	162
Figure 7: Jardim do Éden profile. Position and height of the cores in the topographic section. The diagram illustrates the cores, the observed sedimentary facies, the depositional environment on which these facies where deposited, the position and age of the ^{14}C samples and, if discernible, the phases of aeolian activity.	165
Figure 8: Magistério profile. Position and height of the cores in the topographic section. The diagram illustrates the cores, the observed sedimentary facies, the depositional environment on which these facies where deposited, the position and age of the ^{14}C samples and, if discernible, the phases of aeolian activity.	166
Figure 9: Dunas Altas profile. Position and height of the cores in the topographic section. The diagram illustrates the cores, the observed sedimentary facies, the depositional environment on which these facies where deposited, the position and age of the ^{14}C samples and, if discernible, the phases of aeolian activity.	167
Figure 10: São Simão profile. Position and height of the cores in the topographic section. The diagram illustrates the cores, the observed sedimentary facies, the	

depositional environment on which these facies where deposited, the position and age of the ^{14}C samples and, if discernible, the phases of aeolian activity.

169

Figure 11: Radiocarbon dates of soil samples (palaeosols) plotted with paleoclimatic data (from Neves 1991; Behling 1997; Behling 1998; Ledru *et al.* 1998; Behling *et al.* 1999; Prieto *et al.* 1999; Ybert *et al.* 2001; Bauermann 2003). Gray bars represent a humid climate and white bars represent dry climates. The ellipses indicate major periods of soil formation. In the X axis are labeled the samples used to make this comparison.

173

Figure 12: Stratigraphic correlation of the cores DA-BD, MA-CD and SS-BD. Along each core, the observed sedimentary facies, the depositional environment, the position and age of the ^{14}C samples and the phases of aeolian activity. Dashed lines are inferred correlations; wavy lines represent erosion and unconformity. The numbers inside the circles are the recognized phases of aeolian activity from 1 the oldest to 10 the youngest.

175

LISTA DE TABELAS

CAPÍTULO 3

Table 1: Gradients of the shelf slopes. The profiles are 25 km distance apart.	47
Table 2. A- Data calculated from Calliari & Klein (1993) H_b measurements, for the RS Southern Littoral. B- Data calculated from Barletta (2000) H_b measurements, for the RS Middle Littoral. C- Data calculated from H_b measurements presented in this paper, for the Northern Littoral. N= number of observations; H_b = breaking waves height (m); T= wave period (s); Mz= mean sediment grain size (mm); w_f =sediment fall velocity (cm/s); K= dimensionless coefficient; θ = coastline orientation ($^{\circ}$); α_b = angle that the wave direction (S) makes with the shoreline ($^{\circ}$); E= wave energy $\times 10^3$ (Nm/m 2); P= wave power $\times 10^3$ (N/s); P ℓ = longshore energy flux $\times 10^3$ (N/s); I ℓ = immersed weight transport rate $\times 10^3$ (N/s); Q= volumetric sediment transport rate $\times 10^6$ (m 3 /year).	54

CAPÍTULO 4

Table 1: Chosen wind direction classes and their angles.	73
Table 2: Wind velocity classes utilized in this study.	74
Table 3: Grain size for each station	75
Table 4: Fryberger and Deans' (1979) wind energy classification converted from knots to m/s.	76
Table 5: Fryberger and Deans' Index of directional variability classification.	77

CAPÍTULO 5

Table 1: Satellite images and aerial photographs available for each dunefield and their acquisition year.	103
Table 2: Coastline orientation (A), dune movement direction (B), relationship of coastline orientation to dune movement (C), and dunefield width (D). In (A) two values for one place means that the coastline orientation changes along the dunefield from North to South.	110
Table 3: Mean migration and migration rate of three types of dunes, for the period of 1974 to 1987 in Magistério dunefield.	118
Table 4: Mean migration and migration rate of three types of dunes, for the period of 1974 to 1987 in Dunas Altas dunefield.	119
Table 5: Mean migration and migration rate of two types of dunes, for the period of 1987 to 1999 in Dunas Altas dunefield.	121

SUMÁRIO

AGRADECIMENTOS	iii
RESUMO	v
ABSTRACT	vi
ORGANIZAÇÃO E ESTRUTURA DA TESE	16
CAPÍTULO 1. INTRODUÇÃO	18
1.1. Apresentação e justificativas	19
1.2. Localização da área de estudo e vias de acesso	20
1.3. Objetivos	22
1.4. Métodos	23
1.4.1. Levantamento de dados regionais pré-existentes	23
1.4.2. Análise de fotografias aéreas e imagens de satélites	24
1.4.3. Trabalhos de campo	25
1.4.4. Atividades laboratoriais	27
1.4.5. Tratamento dos dados obtidos	29
CAPÍTULO 2. DEFINIÇÃO DE TERMOS E CLASSIFICAÇÃO DE BARREIRAS E DUNAS	30
2.1. Definição de termos	31
2.2. Classificação de barreiras	31
2.3. Classificação de depósitos eólicos	35
2.3.1. Depósitos eólicos com influência da vegetação	35
2.3.2. Depósitos eólicos sem influência da vegetação	37
2.4. Pulsos eólicos e superfícies de separação em campos de dunas	37
CAPÍTULO 3. WAVE ENERGY AND LONGSHORE SEDIMENT TRANSPORT GRADIENTS CONTROLLING BARRIER EVOLUTION IN RIO GRANDE DO SUL, BRAZIL	40
Abstract	43
3.1. Introduction	43
3.2. Study area	44
3.3. Factors that could influence the barrier type	45

3.4. Methods	48
3.4.1. Wave Energy	49
3.4.2. Longshore Sediment Transport	50
3.5. Results and discussion	52
3.5.1. Wave Energy Gradients	52
3.5.2. Longshore Sediment Transport	52
3.5.3. Barrier Types	56
3.6. Conclusions	57
Acknowledgements	59
References	59
 CAPÍTULO 4. CLIMATE PATTERNS AND VARIATIONS ON THE RIO GRANDE DO SUL COAST AND COASTAL DUNEFIELD DYNAMICS	 62
Abstract	65
4.1. Introduction	65
4.2. Regional settings	67
4.3. Climate of southern brazil	68
4.4. Anomalies in the climate	70
4.4.1. El Niño and La Niña events	71
4.5. Methods	72
4.5.1. Precipitation data	72
4.5.2. Wind data	72
4.5.3. Drift Potential and sand roses	73
4.5.4. Classification	76
4.6. Precipitation and ENSO events	77
4.7. Regional wind pattern and sand drift potentials	79
4.7.1. Effects of the scarp in the wind pattern	83
4.7.2. Seasonal changes in the wind pattern	84
4.7.3. Yearly changes in the wind drift potential	86
4.8. Discussion and conclusions	88
Acknowledgments	91
References	91

CAPÍTULO 5. MORPHOLOGICAL AND TEMPORAL VARIATIONS OF TRANSGRESSIVE DUNEFIELDS OF THE NORTHERN AND MID- LITTORAL RIO GRANDE DO SUL COAST	95
Abstract	98
5.1. Introduction	98
5.2. Methods	102
5.3. Regional settings	103
5.3.1. Coastline and inner shelf slope	104
5.3.2. Waves and longshore sediment transport (LST)	104
5.3.3. Barrier types	104
5.3.4. Precipitation	106
5.3.5. Winds	106
5.4. Dunefields description	107
5.4.1. Rondinha	107
5.4.2. Capão Novo	110
5.4.3. Atlântida Sul	112
5.4.4. Jardim do Éden	114
5.4.5. Magistério	116
5.4.6. Dunas Altas	118
5.4.7. Solidão	121
5.4.8. São Simão	123
5.4.9. Mostardas	125
5.5. Discussion	127
5.5.1. Dunefield Migration	127
5.5.2. Spatial Dunefields Changes	129
5.5.3. Temporal Dunefield Changes	132
5.5.4. Changes in dune morphology	135
5.6. Conclusions	137
Acknowledgments	138
References	138

CAPÍTULO 6. MID TO LATE HOLOCENE EVOLUTION OF TRANSGRESSIVE DUNEFIELDS FROM RIO GRANDE DO SUL COAST, SOUTHERN BRAZIL	145
Abstract	148
6.1. Introduction	148
6.2. Regional settings	151
6.2.1. Holocene relative sea level in southern Brazil	155
6.2.2. Climate changes during the mid to late Holocene in southern Brazil	156
6.3. Methods	157
6.3.1. Drilling	157
6.3.2. Dating	158
6.4. Results	158
6.4.1. Sedimentary Facies	158
6.4.2. Drill-hole profiles from Rondinha to Atlântida Sul	160
6.4.3. From Jardim do Éden to Dunas Altas	163
6.4.4. From Solidão to Mostardas	168
6.5. Discussion	170
6.5.1. Potential of aeolian deposits preservation	170
6.5.2. Soil formation periods	172
6.6. Conclusions	176
Acknowlegments	177
References	177
CAPÍTULO 7. CONCLUSÕES FINAIS	183
REFERÊNCIAS BIBLIOGRÁFICAS	189
ANEXO A - DESCRIÇÃO DAS FÁCIES SEDIMENTARES	196
ANEXO B - LOCALIZAÇÃO DOS PERFIS E TESTEMUNHOS	199
ANEXO C - TESTEMUNHOS DE SONDAGEM	205
ANEXO D - PERFIS COM OS TESTEMUNHOS DE SONDAGEM	232

ORGANIZAÇÃO E ESTRUTURA DA TESE

A presente tese é apresentada na forma de artigos submetidos a revistas indexadas e está organizada da seguinte maneira:

No **Capítulo 1**, são apresentadas a introdução, as justificativas, as características da área de estudos, os objetivos e os métodos empregados.

O **Capítulo 2** apresenta a definição de termos técnicos e as classificações de barreiras e de dunas que serão utilizadas ao longo da tese.

O primeiro passo para a compreensão do funcionamento e da evolução dos campos de dunas parece ser o entendimento do tipo de ambiente, ou no caso, o tipo de barreira sobre o qual eles se desenvolveram. No **Capítulo 3**, a partir de dados de altura de ondas na arrebentação, foram calculados valores de energia de ondas e transporte longitudinal de sedimentos (TLS) ao longo da costa do RS. Esse capítulo mostra como a energia de onda e o TLS variam ao longo da costa, e como essa variação influencia no tipo de barreira costeira. Esse capítulo é apresentado na forma do artigo intitulado: “*Wave Energy and Longshore Sediment Transport Gradients Controlling Barrier Evolution in Rio Grande do Sul, Brazil*”, aceito para publicação no periódico *Journal of Coastal Research*.

Identificados e descritos os fatores colaboradores para a variação do tipo de barreira ao longo da costa, é necessário identificar os fatores que podem influenciar no transporte eólico e na formação de campos de dunas. O **Capítulo 4** comprehende a análise de dados de ventos e precipitação para o litoral do RS. Esse capítulo descreve como a precipitação e o padrão de ventos variam ao longo da costa e ao longo das últimas décadas, e sugere como essas variações climáticas podem interferir na morfodinâmica dos campos de dunas. É apresentado na forma do artigo intitulado “*Climate patterns and variations on the Rio Grande do Sul Coast and coastal dunefield dynamics*” e submetido ao periódico *Earth Surface Processes and Landforms*.

Após descrever o comportamento do clima ao longo da costa e ao longo das últimas décadas, é importante observar como esse clima influenciou a morfologia dos campos de dunas. O **Capítulo 5** descreve como a morfologia dos campos de dunas varia ao longo do trecho costeiro entre Torres a Mostardas, e ao longo das últimas décadas. Os resultados encontram-se no artigo intitulado “*Morphological and Temporal Variations of Transgressive dunefields of the Northern and Mid-littoral of Rio Grande do Sul coast, Southern Brazil*”, submetido ao periódico *Geomorphology*.

O **Capítulo 6**, com a ajuda das informações da morfodinâmica atual, estuda a evolução dos campos de dunas ao longo do Holoceno médio e tardio (últimos 5000 anos antes do presente). Esse capítulo trata da estratigrafia dos campos de dunas presentes entre os municípios de Torres e Mostardas e, a partir de testemunhos de sondagem e datações ^{14}C , descreve como os campos de dunas se comportaram ao longo do Holoceno médio e tardio. Os resultados encontram-se sob forma de artigo submetido ao periódico *Marine Geology*, intitulado “*Mid to Late Holocene evolution of transgressive dunefields from Rio Grande do Sul coast, Southern Brazil*”.

O **Capítulo 7** apresenta a análise integradora de todos os capítulos anteriores, e as conclusões finais obtidas nesse estudo.

As **Referências** listam os trabalhos citados nos capítulo 1, 2 e 7. As referências utilizadas nos artigos (capítulos 3, 4, 5 e 6) estão localizadas no final dos respectivos capítulos.

No **Anexo 1** estão listadas todas as fácies sedimentares descritas nos testemunhos de sondagem e seus ambientes deposicionais. No **Anexo 2** estão a localização dos perfis e dos testemunhos de sondagem. O **Anexo 3** apresenta a descrição detalhada e fotografia de cada testemunho. O **Anexo 4** apresenta a posição e altitude dos testemunhos na seção topográfica de cada perfil.

Como a presente tese é apresentada sob forma de artigos, informações como área de estudo, métodos, resultados e referências bibliográficas podem aparecer repetidas.

A numeração das figuras e tabelas ao longo da tese é reiniciada a cada capítulo. Desse modo, cada capítulo possui sua própria numeração de figuras e tabelas.

CAPÍTULO 1

INTRODUÇÃO

1.1. APRESENTAÇÃO E JUSTIFICATIVAS

Há na literatura um consentimento de que costas progradantes formariam apenas cordões litorâneos (*beach-ridges* e *foredune ridges*), e que para haver campos de dunas seria necessária a erosão da linha de costa e da face litorânea (*shoreface*) (Pye & Bowman 1984). Short (1988), também mostra campos de dunas se desenvolvendo apenas quando há erosão (pg.123). Contudo, ao longo da costa do Rio Grande do Sul há a coexistência de barreiras progradantes, agradantes e retrogradantes e nota-se a presença de campos de dunas transgressivos sobre todas elas. Por esse motivo questiona-se, será mesmo preciso erosão da linha de costa pra a formação de campos de dunas? Não seria preciso apenas ter areia disponível suficiente para o transporte eólico?

Campos de dunas transgressivos holocênicos, no mundo todo, têm sido descritos e datados, e o que se observa é que eles têm se desenvolvido em episódios de sedimentação eólica, separados por períodos de estabilidade e formação de solos. As informações obtidas a partir do detalhamento da estratigrafia e do reconhecimento, e datação das superfícies formadas pela estabilização desses campos de dunas, podem ser correlacionados a variações climáticas e a mudanças do nível relativo do mar (NRM). Desse modo, podem contribuir para melhor compreensão da evolução de campos de dunas durante o Holoceno.

O estudo detalhado do conjunto de feições geomorfológicas existentes em campos de dunas costeiros ativos e de suas variáveis controladoras (como variação do NRM, clima, vegetação, aporte sedimentar etc) também é importante não só para caracterizar as fácies eólicas como para compreender a evolução de campos de dunas mais antigos. Diversos autores (Fisher 1983; Karpeta 1990; Soares 1992; Giannini 1993, 1998; Martinho *et al.* 2003) baseiam-se em tipos morfológicos de dunas e na morfologia e constituição das interdunas para reconhecer e delimitar fácies, uma vez que as texturas e estruturas eólicas são, aparentemente, bastante monótonas, em comparação com outros sistemas deposicionais. No Quaternário costeiro, faciologias fundadas em tipos morfológicos parecem adequadas, uma vez que estes tipos são quase sempre reconhecíveis em campo ou em aerofotografias, mantêm entre si relações dinâmicas discerníveis, e tendem a distribuir-se geograficamente segundo padrões determinados, que poderão deixar registros de sucessões verticais previsíveis (Giannini 1993).

Esse estudo da morfodinâmica de dunas costeiras depende da análise de distribuição espacial e temporal de fácies morfológicas em campos de dunas ativos e dos processos de destruição e reconstrução destas fácies. No Brasil, a investigação destes temas encontra-se em estágio inicial (Tomazelli 1990; Giannini 1993; Giannini & Santos 1994; Giannini 1998; Giannini 2002; Martinho 2004; Martinho *et al.* 2006). Martinho (2004) através de fotografias aéreas mapeou e descreveu mudanças na morfologia das dunas em um período de 40 anos, em campos de dunas de Santa Catarina. A autora notou que com o aumento da umidade e da vegetação, dunas sem influência da vegetação, como cadeias barcanóides e dunas transversais, acabam se transformando em dunas parabólicas. Com a evolução da estabilização das dunas parabólicas, notou-se que o que fica preservado morfologicamente são apenas os braços das parabólicas (*trailling ridges*), assim como os cordões de precipitação (*precipitation ridges*). Marcomini & Maidana (2006) também reconheceram mudanças na morfologia das dunas da província de Buenos Aires, Argentina, e associaram essa mudança ao aumento da precipitação na região, nos últimos 40 anos.

A compreensão da dinâmica e evolução de campos de dunas é um estudo de interesse aplicado, pois a previsão da direção, sentido, velocidade e modificação morfológica de dunas eólicas, a partir de suas variáveis controladoras, é necessária no planejamento da ocupação costeira e de obras de engenharia.

Neste contexto, a costa do Rio Grande do Sul aparece como laboratório natural para testar o controle do NRM e do clima na formação e evolução de campos de dunas durante o Holoceno. Ao longo de seus 625 km quase ininterruptos de extensão, a costa gaúcha alterna trechos de progradação e erosão costeira e possui um dos mais importantes campos de dunas transgressivos ativos da costa brasileira. Além disso, apresenta também campos de dunas holocênicos antigos, já totalmente vegetados.

1.2. LOCALIZAÇÃO DA ÁREA DE ESTUDO E VIAS DE ACESSO

A área de estudos a ser detalhada nos capítulos a seguir localiza-se na planície costeira do RS. Os capítulos 3 e 4, utilizando-se de dados regionais, analisam toda a costa, de Torres ao Chuí. Contudo, a área ao longo da costa compreendida entre os municípios de Torres e Mostardas, entre as latitudes 29° e 31° e longitudes 49° e 51°, foi tomada como alvo principal de estudo e onde foram realizados os trabalhos de campo. Segundo a FEPAM (Fundação Estadual de Proteção Ambiental -

www.fepam.rs.gov.br/programas/gerco.asp) o litoral do RS pode ser dividido em Litoral Norte (de Torres a Balneário Pinhal), Litoral Médio (de Quintão a São José do Norte) e Litoral Sul (de Rio Grande ao Chuí). Desse modo, a área estudada compreende todo o litoral norte e parte do litoral médio do RS. Com aproximadamente 250 km de linha de costa quasi-contínuos, interrompidos apenas pela desembocadura da laguna de Tramandaí, esse trecho costeiro apresenta alta variação topográfica, tendo a norte as escarpas da Serra Geral muito próximas à costa, e a sul extensa planície costeira apresentando terreno extremamente plano e aberto (Fig. 1).

As principais vias de acesso para o litoral norte, saindo de Porto Alegre, são a rodovia BR-290 até Osório, de onde se segue pela RS-389 (também conhecida como Estrada do Mar) até Torres. A saída de Porte Alegre para o litoral médio é feita por Viamão, pela RS-040. Para os balneários de Cidreira, Pinhal, Quintão e Dunas Altas, da RS-040 segue-se pela RS-789 ou RS-784. Para o balneário de Mostardas, extremo sul da área estudada, utiliza-se a RS-040 até o trevo de Capivari do Sul, pegando a seguir a rodovia RS-101 (BR-101) (Fig. 1). Como, especialmente no litoral médio, há escassez de vias de acesso secundário, muitas vezes o acesso aos pontos de testemunhagem, como Farol da Solidão e São Simão, foi feito pela praia ou através do leito de sangradouros.

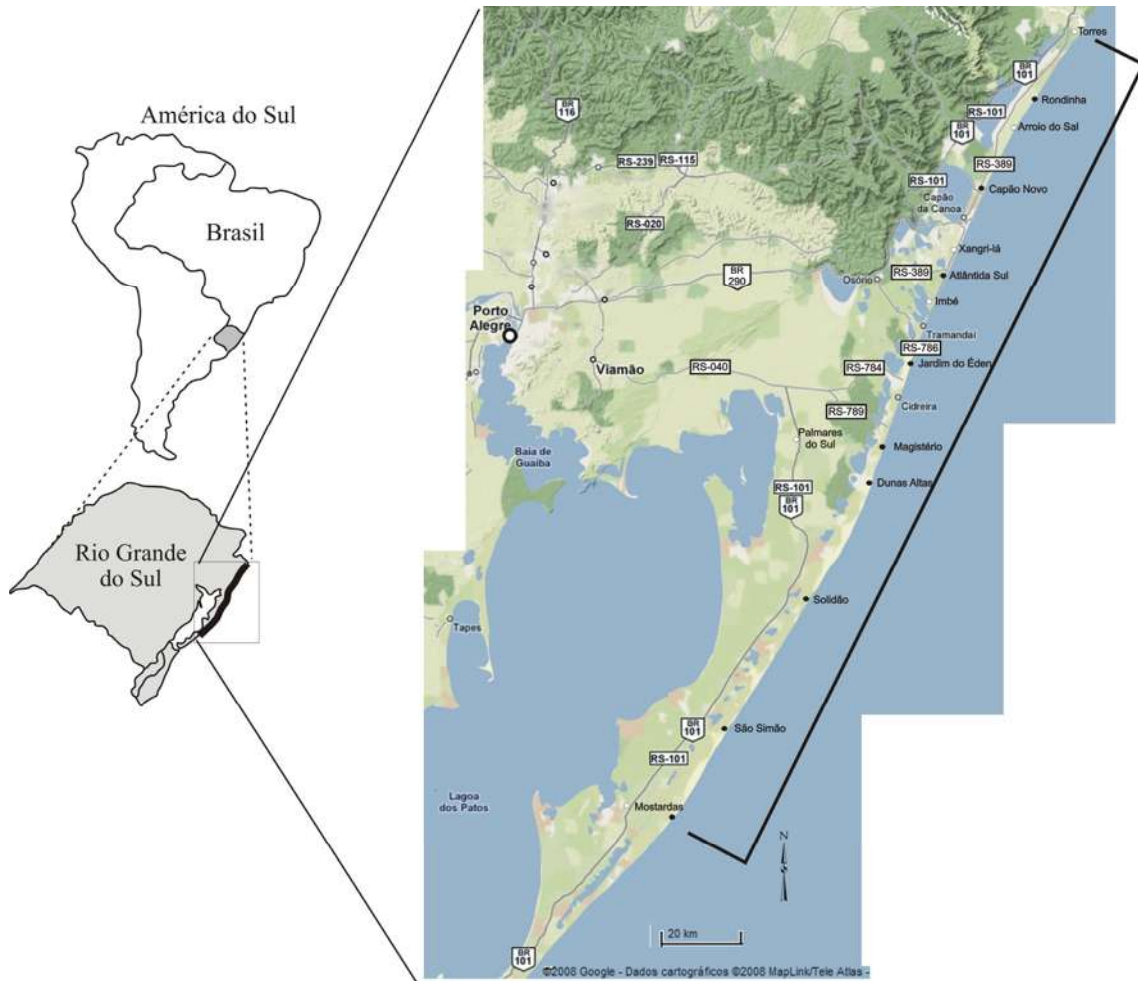


Figura 1: Principais vias de acesso à área de estudo. A linha preta delimita a área de estudos, dos municípios de Torres a Mostardas. Os pontos brancos representam municípios e os pontos pretos representam as localidades estudadas (Extraído de Google Maps).

1.3. OBJETIVOS

O objetivo mais geral desta tese foi contribuir para: o entendimento dos fatores e processos que controlam a morfodinâmica de sistemas deposicionais eólicos costeiros do Rio Grande do Sul; o aprimoramento dos critérios de reconhecimento dos ‘pulsos’ eólicos durante o Holoceno e sua relação com as flutuações climáticas e do NRM; e, a partir disso, compreender a evolução, não só dos campos de dunas como também da barreira holocênica do Rio Grande do Sul, no trecho compreendido entre os municípios de Torres e Mostardas. Por morfodinâmica, entende-se aqui como a distribuição tempo-espacial da morfologia das dunas. Espera-se que o conhecimento da dinâmica destes campos de dunas possa ser aplicado no planejamento da ocupação costeira.

Os objetivos mais específicos foram:

- Análise de fotos aéreas e imagens de satélite para avaliar e descrever a variação da morfologia, dimensão e distribuição dos campos de dunas ao longo da costa e ao longo do tempo.
- Análise de variações no aporte, velocidade, direção e freqüência dos ventos, energia de onda, largura da plataforma, transporte litorâneo longitudinal, orientação da linha de costa em relação ao vento efetivo, cobertura vegetal, atividade antrópica e clima ao longo da costa.
- Verificação de qual(is) fator(es) analisado(s) exerce(m) maior influência na presença e no tipo de campos de dunas, e na determinação das feições morfológicas a eles associadas.
- Identificação de diferentes fases de formação/ativação de campos de dunas através da:
 - Descrição de estruturas sedimentares, arquitetura de fácies e superfícies de separação;
 - Análise textural dos depósitos eólicos;
 - Datação da matéria orgânica presente nos solos desenvolvidos sobre depósitos eólicos que foram estabilizados.
- Correlação das fases de atividade/estabilidade eólica às variações de fatores como aporte sedimentar, NRM e clima.
- Elaboração de um modelo final dos mecanismos de ativação, deposição, preservação e estabilização de sistemas eólicos costeiros, contribuindo assim para entender a evolução dos campos de dunas holocênicos do Rio Grande do Sul.

1.4. MÉTODOS

1.4.1. Levantamento de dados regionais pré-existentes

Dados de precipitação pluviométrica para Porto Alegre no período de março de 1965 a julho de 1983 foram obtidos através do website <http://isohis.iaea.org>, do IAEA/WMO, Global Network for Isotopes in Precipitation (GNIP) Database (IGBP PAGES/World Data Center for Paleoclimatology Data Contribution Series 94–005 NOAA/NGDC Paleoclimatology Program, Boulder, Colorado, 1994).

Na Superintendência de Portos e Hidrovias (SPH) do Governo do Estado do Rio Grande do Sul foram obtidos dados de pluviosidade, direção e velocidade dos ventos para a estação meteorológica de Imbé, com três valores diários, para o período de 05/03/1948 a 31/12/2003.

Dados horários de direção e velocidade de ventos foram obtidos nas estações meteorológicas do Projeto RECOS, do Instituto do Milênio, nos períodos de 10/09/2003 a 14/10/2005 para a estação de Tramandaí; 2/10/2003 a 21/03/2006 para a estação de Chuí; e 12/01/1998 a 09/09/1999 para a estação de Itapeva.

Do banco nacional de dados oceanográficos da Diretoria de Hidrografia e Navegação da Marinha do Brasil foram obtidas informações, três vezes ao dia, de direção e velocidade de ventos na estação meteorológica de Mostardas, para o período de 22/03/1957 a 01/05/2000.

Os dados de vento, do período de janeiro de 1970 a dezembro de 1982, para as estações de Torres e Rio Grande foram compilados do artigo de Tomazelli (1993), e pertencem ao INEMET (Instituto Nacional de Meteorologia).

Dados adicionais como declividade da plataforma, variações granulométricas ao longo da costa, direção e altura de ondas e transporte litorâneo longitudinal foram compilados da bibliografia, com destaque para os trabalhos de Calliari & Klein (1993), Barletta (2000), Lima *et al.* (2001), Toldo Jr. *et al.* (2006), Dillenburg *et al.* (2000), Weschenfelder & Zouain (2002) e Dillenburg *et al.* (2003).

1.4.2. Análise de fotografias aéreas e imagens de satélites

As imagens de satélite e fotografias aéreas foram utilizadas para determinar, ao longo do litoral gaúcho e ao longo das últimas décadas, as variações morfológicas da linha de costa, variações da dimensão e geometria dos campos de dunas, a velocidade de migração das dunas, variação das áreas vegetadas e deflacionares e a interferência antrópica.

O registro de imagens de satélite e fotos aéreas não é uniforme para todo o trecho estudado. Os campos de dunas do litoral médio possuem o menor registro (Tabela 1, Capítulo 5). As imagens de satélite utilizadas foram: LANDSAT-7 ETM+ possuindo pixel com 15m de resolução, LANDSAT-5 TM com 30m de resolução, LANDSAT MSS com 60m de resolução e o modelo de elevação digital possuindo pixel com 90m de resolução. Tanto as imagens de satélite como o modelo de elevação digital

foram obtidos através do website do *Global Land Cover Facility* (<http://glcfapp.umiacs.umd.edu:8080/esdi/search>).

As coleções de fotografias aéreas disponíveis no Brasil foram obtidas pelo DAER, datam de 1974 e 1989, e possuem escala 1:20.000. Na *Louisiana State University* obteve-se uma coleção de fotografias aéreas, do litoral norte e médio do RS, que data de 1948, obtida pelo USGS, em escala 1:20.000. As fotos aéreas foram digitalizadas e os mosaicos de cada faixa foram georreferenciados a partir das imagens de satélite, utilizando o programa *ArcGIS 9.0*. A digitalização final dos mapas foi realizada através do mesmo programa. A partir da interpretação de fotos aéreas e imagens de satélites foram elaborados mapas geomorfológicos, procurando-se destacar as principais feições erosivas e deposicionais dos campos de dunas ativos.

Perfis altimétricos com a localização dos testemunhos (ilustrados no Capítulo 6 e Anexo 4) foram realizados a partir do modelo de elevação digital, a partir do programa *ArcGIS 9.0*.

1.4.3. Trabalhos de campo

Os trabalhos de campo dividiram-se em dois. O primeiro teve como objetivo a obtenção de medidas mensais de altura de onda na arrebentação (H_b), período de onda (T) e largura da praia, ao longo de um ano (Setembro 2004/2005). Para a obtenção de H_b foi utilizado o método visual nomeado por Patterson & Blair (1983) como “Linha da Visão” e descrito originalmente por Ingle (1966). Neste método, um observador posiciona-se na linha d’água média, na praia, e lê a altura da onda em uma régua topográfica, alinhando a altura dos seus olhos com a crista da primeira onda quebrando (mais externa) e a linha do horizonte. Esse levantamento da altura de ondas na arrebentação foi realizado nas seguintes praias do litoral norte e médio: Paraíso, Arroio do Sal, Arroio Teixeira, Xangri-lá, Mariluz, Jardim do Éden, Pinhal, Dunas Altas e Bacupari (Fig. 3, Capítulo 3). Em cada local de coleta de dados de H_b , dois observadores mediram a altura de dez ondas. A média desses valores foi o valor de H_b utilizado nos cálculos de energia de onda e transporte longitudinal de sedimentos (Capítulo 3).

O segundo tipo de trabalho de campo realizado consistiu na obtenção de testemunhos de sondagem ao longo de perfis orientados, sempre que possível, na direção do avanço dos campos de dunas. O método de testemunhagem utilizado foi o da

percussão manual, tendo como amostrador um tubo de PVC de 6m de comprimento (Fig. 2). Após o tubo ser cravado no terreno, antes de ser retirado, a compactação dos sedimentos dentro do tubo foi medida a partir das alturas internas e externas do tubo, para posterior correção das profundidades.



Figura 2: Método de testemunhagem a percussão manual, tendo como testemunhador um tubo de PVC de 6m de comprimento. A) Fase de penetração no solo através de um peso batente. B) Fase de retirada do testemunho utilizando-se tripé e talha.

Os primeiros furos foram realizados ainda com a intenção da amostragem de sedimentos para datação por Termo-Luminescência (TL) e/ou Luminescência Opticamente Estimulada (LOE), e por esse motivo, ainda no campo, logo após a retirada do testemunho do solo, eles eram imediatamente enrolados em lona preta a fim de evitar exposição dos sedimentos às radiações ultra-violetas.

Foram realizados perfis de testemunhagem nas localidades de Rondinha, Capão Novo, Atlântida Sul, Jardim do Éden, Magistério, Dunas Altas, Solidão, São Simão e Mostardas. A localização de todos os furos realizados em todos os perfis encontram-se no Anexo 2.

A altitude dos furos foi medida através de nivelamento topográfico, para os furos no litoral norte. No litoral médio, devido à grande largura dos campos de dunas e a dificuldade de acesso às áreas, a altitude dos furos foi medida por um equipamento

Trimble GPS 4600, de precisão submétrica. A medida foi feita com o aparelho estático, realizando uma medida a cada 2 segundos, por um período de 15 a 20 minutos. Essas medidas foram posteriormente corrigidas a partir das estações fixas de rádio-farol.

1.4.4. Atividades laboratoriais

- Abertura de testemunhos e amostragem: a abertura dos testemunhos foi realizada com serra elétrica circular acoplada à mesa de alumínio (Fig. 3). A abertura dos 18 primeiros testemunhos foi realizada em sala escura. Sendo que uma das seções do testemunho permaneceu na sala escura para posterior coleta de amostras para datação por TL/LOE. Na outra seção, os sedimentos do testemunho de sondagem foram fotografados, descritos e separados em fácies sedimentares de acordo com o tamanho dos grãos, estruturas sedimentares, grau de compactação, presença de matéria orgânica e vegetação em meio aos sedimentos. As duas últimas propriedades foram indicativas do grau de pedogênese. A lista das fácies sedimentares, a descrição e fotografia de todos testemunhos encontram-se nos Anexos 1 e 3.



Figura 3: Mesa de abertura de testemunhos, acoplada à serra elétrica circular.

A coloração das fácies foi descrita utilizando o manual *Rock Color Chart* (Goddard 1975). Uma amostra de cada fácie foi coletada para análises granulométricas. Amostras para datação por Termoluminescência (TL) foram coletadas na sala escura, sob luz vermelha. Níveis com matéria orgânica suficiente para datação por ^{14}C AMS foram amostrados e acondicionados em estufa, à temperatura de aproximadamente 30°C, para secagem.

- Análises Granulométricas: As amostras foram quarteadas, lavadas para eliminação de sais e finos pelíticos eventuais, seguida de peneiramento a seco, em intervalos de 0,5 Ø. Nas amostras com teor de finos maior que 5%, foram realizadas pipetagens. Os produtos de peneiramento foram pesados em balança analítica e embalados para arquivamento.
- Datações por TL e LOE: Dos 26 furos de sondagem realizados, os 18 primeiros foram realizados visando a coleta de sedimentos para datação por TL/LOE. Cerca de 41 amostras foram coletadas para datações. Contudo, o primeiro lote de 10 amostras enviado ao laboratório Labvidro (FATECSP) apresentou sérios problemas nos resultados. Os métodos utilizados foram os de análise da paleodose e da dose anual. Os resultados, mesmo após as análises terem sido refeitas, apresentaram diversos problemas: algumas amostras não apresentaram sinal de TL/LOE residual, algumas não apresentaram sinal (LOE) reproduutivo para a datação, houve problemas de inversões estratigráficas e todas as idades apresentaram-se superestimadas.

Os erros que implicaram nos problemas descritos acima podem ter origem variada, e decorrerem de métodos incorretos de: coleta, retirada e manuseio do testemunho no campo; manuseio do testemunho em laboratório; abertura e amostragem na sala escura; acondicionamento das amostras coletadas; e por fim, de erros analíticos do próprio laboratório de datação.

Após os primeiros resultados, as datações por TL/LOE de sedimentos dos testemunhos foram suspensas pela falta de confiança no método.

- Datações por ^{14}C : Após a falta de êxito dos resultados de datações por TL/LOE, como saída para tentar estimar a idade dos campos de dunas do RS e sua evolução, iniciaram-se amostragens de sedimentos ricos em matéria orgânica com o intuito de datá-las por radiocarbono. O número de amostras, evidentemente, foi bastante reduzido pela relativa escassez de sedimentos desse tipo em diversos testemunhos. Devido ao baixo teor de matéria orgânica nos sedimentos, todas as amostras foram datadas por AMS (*accelerator mass spectrometry*) no laboratório da Beta Analytic Inc. (Miami, Florida, EUA). O tipo de material coletado para datação foram: lamas orgânicas, de fundo lagunar, e areia ricas em matéria orgânica impregnada, bem como turfas.

1.4.5. Tratamento dos dados obtidos

- Ondas e transporte longitudinal: As fórmulas utilizadas para calcular energia de onda e transporte longitudinal de sedimentos foram obtidas no Manual de Engenharia Costeira (*Coastal Engineering Manual*, US Army 2003). A seqüência de cálculos, fórmulas e os valores nelas utilizados encontram-se detalhados no item *Methods* do Capítulo 3.
- Ventos: Os dados de vento foram analisados quanto à freqüência, velocidade e direção. Rosas de freqüência de ventos foram confeccionadas para cada estação meteorológica, utilizando o programa *WRPLOT*. O potencial de transporte eólico também foi calculado para cada estação meteorológica, assim como para cada estação do ano. O método utilizado para o cálculo do transporte eólico potencial foi o proposto por Fryberger & Dean (1979), tendo como resultado gráfico a construção de rosas de areia. A descrição completa deste método, bem como suas fórmulas, encontram-se no item *Methods* do Capítulo 4.
- Testemunhos: Os cálculos de descompactação dos sedimentos foram realizados seguindo os métodos utilizados por Dillenburg (1994) e as profundidades dos limites de fácies e das amostras foram corrigidas. O método de descompactação admite composição homogênea ao longo de todo testemunho. A base do testemunho representa compactação mínima (0% de compactação) e o topo do testemunho é considerado o local de máxima compactação (100% de compactação). A confecção dos perfis colunares dos testemunhos foi realizada utilizando o programa *CorelDraw 11*. A descrição detalhada de todos os testemunhos encontra-se no Anexo 3.
- Dados analíticos laboratoriais: Balanços de massa, em valores de distribuição percentual, foram executados, para cada amostra, ao término das análises granulométricas. Os resultados de distribuição granulométrica foram convertidos em valores de parâmetros estatísticos (diâmetro médio, desvio-padrão, assimetria e curtose) pelo método analítico dos momentos, através do programa *Momento4.123*, de Paulo C.F. Giannini.

CAPÍTULO 2

**DEFINIÇÃO DE TERMOS E CLASSIFICAÇÃO DE BARREIRAS E
DUNAS**

2.1. DEFINIÇÃO DE TERMOS

Ao revisar a literatura sobre barreiras e sistemas deposicionais costeiros percebe-se muitas vezes o mau uso de termos, causando certa confusão de conceitos. Por esse motivo, parece necessária, antes de tudo, a definição desses termos, seus significados e a nomenclatura adotada que será utilizada ao longo da presente tese.

Os termos transgressão e regressão, neste trabalho, serão utilizados *sensu* Curray (1964), ou seja, serão sinônimos de migração de linha de costa. **Transgressão** é o processo de migração da linha de costa em direção ao continente. **Regressão** é o processo de migração da linha de costa em direção ao mar.

Alguns autores utilizam os termos transgressão e regressão como sinônimos de variações do nível do mar (elevação e rebaixamento, respectivamente). Contudo, Curray (1964) em seu capítulo sobre transgressões e regressões já enfatizava que os termos referem-se exclusivamente à migração da linha de costa, não necessariamente ligados à variações de nível relativo do mar (NRM). Ele demonstra ainda que pode haver casos de regressão com nível do mar subindo, e de modo oposto, transgressão mesmo com nível do mar caindo.

Os termos Progradação, Agradação e Retrogradação referem-se ao preenchimento sedimentar da bacia e à arquitetura estratigráfica, e são o resultado das variações na criação de espaço de acomodação da bacia versus o suprimento sedimentar (Assine & Perinotto 2001). A **Progradação** acontece quando a taxa de aporte sedimentar supera a taxa de criação de espaço na bacia, o que faz com que os sistemas deposicionais migrem em direção ao centro da bacia. **Agradação** ocorre quando a geração de espaço na bacia e o suprimento sedimentar estão em equilíbrio. Nesse tipo de arquitetura as fácies se empilham verticalmente, não ocorrendo a migração dos sistemas deposicionais nem para o continente nem para o centro da bacia. A **Retrogradação** acontece quando a taxa de criação de espaço na bacia supera a taxa de suprimento sedimentar, provocando a migração dos ambientes deposicionais em direção à borda da bacia.

2.2. CLASSIFICAÇÃO DE BARREIRAS

Barreiras holocênicas são o resultado das mudanças do NRM ocorridas após o fim do último máximo glacial, em regiões de plataforma continental de baixo

gradiente e dominada por ondas. De 18000 anos até aproximadamente 6500 anos antes do presente (A.P.) o nível do mar subiu a taxas bastante elevadas, o que resultou na formação de depósitos de tratos de sistemas transgressivos. Tais depósitos podem ser reconhecidos em quase todas as barreiras holocénicas no mundo (Fig. 1) (Thom *et al.* 1981; Morton 1994; Roy *et al.* 1994). Assim, as barreiras no início do Holoceno apresentam comportamento semelhante, contudo, com o fim da Última Transgressão Marinha Pós-Glacial (TMP), variações locais de aporte sedimentar, e pequenas variações no NRM, fizeram com que diferentes tipos de barreiras fossem construídas durante o Holoceno médio e tardio. Duas renomadas escolas apresentam classificações de barreiras baseadas em parâmetros e exemplos diferentes, a “Escola Americana” (Fisher & McGowen 1969; Boyd *et al.* 1992; Morton 1994) e a “Escola Australiana” (Roy *et al.* 1994; Hesp & Short 1999).

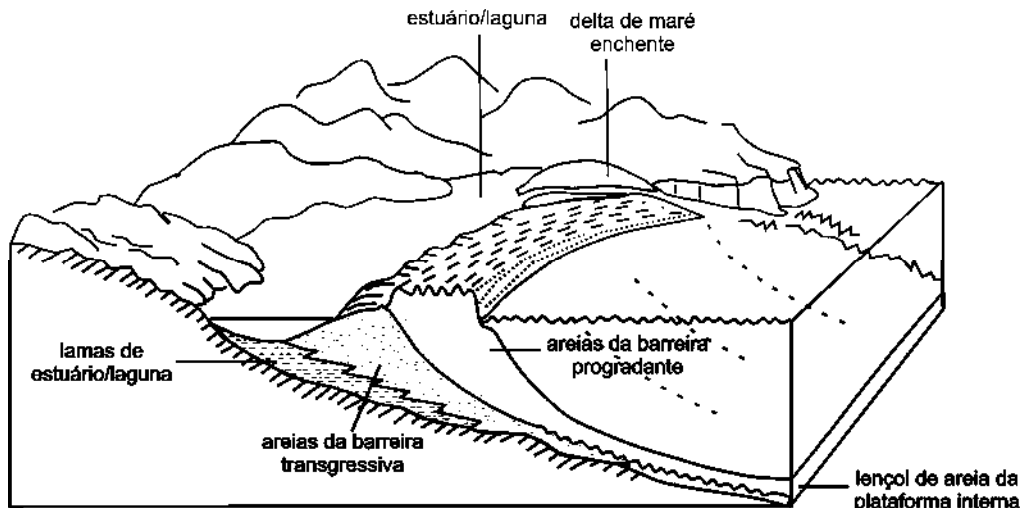


Figura 1: Diagrama esquemático de uma barreira, observar os depósitos da fase transgressiva, produzidos pela ascensão do NRM durante o início do Holoceno (modificado de Roy *et al.* 1994).

Analizando criticamente as classificações dessas escolas, percebe-se que ambas possuem problemas e qualidades (Martinho 2006). Por esse motivo, as classificações e definições de barreira nesta tese não seguirá uma única escola.

A definição do termo **Barreira** empregado na presente tese, será utilizada segundo a escola australiana. Eles propõem o termo “Barreira costeira arenosa” para ser usado como o elemento deposicional básico para todas as costas dominadas por ondas. Ou seja, o termo “barreira” na escola australiana significa acumulação detritica subaérea e subaquática de sedimentos (areia e cascalho), paralela à costa, formada por ondas, marés e processos eólicos, com ou sem um corpo aquoso na retaguarda (Hesp & Short 1999). Ela atua essencialmente como uma “barreira” entre o

mar e o continente. Os sedimentos que compõem a barreira podem ser depositados em diferentes ambientes como: duna, praia compreendendo o pós-praia e antepraia (*backshore* e *foreshore*), face litorânea (*shoreface*), canal de maré, delta de maré e leques de sobrelavagem (Roy *et al.* 1994).

A classificação de barreiras da escola australiana propõe uma série de estágios evolutivos pelos quais as barreiras podem passar. Essa série contínua de variações geomorfológicas de barreiras parte de uma costa aberta, com gradiente suave e depósitos de ilha barreira. Conforme o gradiente da plataforma interna aumenta, o corpo aquoso presente na retaguarda da barreira torna-se cada vez mais estreito, até desaparecer completamente formando as designadas “*mainland beaches*” ou praias anexas, o membro final da série (Fig. 2). No entanto, a nomenclatura dessa classificação não segue um critério definido, mas ao contrário, mistura critérios diferentes como preenchimento de bacia (ex. barreira progradante) com morfologia/elementos morfológicos da barreira (ex. esporões de promontório, barreira de dunas transgressivas). Por esse motivo, na classificação australiana os tipos de barreira podem se sobrepor, por exemplo, pode haver uma barreira progradante com esporões, ou barreira recessiva com campos de dunas. Adicionalmente, os termos regressivo e transgressivo são apresentados como sinônimos de variações do nível do mar, contudo, como visto anteriormente no item 2.1. eles não foram originalmente definidos como sinônimos.

As classificações de barreiras americanas foram feitas no âmbito da geologia do petróleo, de modo a compreender a organização e distribuição dos ambientes sedimentares na bacia e assim conseguir prever a localização de fácies de reservatório e fácies orgânicas (fonte do óleo). Por esse motivo seu enfoque é mais geológico. Desse modo, iremos adotar na presente tese a classificação de barreiras da escola americana, mais precisamente a terminologia adotada por Morton (1994) que enfatiza o aspecto deposicional e de preenchimento de bacia. Morton (1994) divide as barreiras em três tipos:

Barreiras Progradantes (*Progradational Barriers*) têm como principal característica o crescimento em direção ao oceano, devido a um abundante aporte sedimentar e/ou à decida do NRM. Morton (1994) relaciona esse tipo de barreira a lugares onde o NRM encontra-se relativamente estável (após a TMP) e onde a linha de costa é ligeiramente côncava. A feição geomorfológica característica desse tipo de barreira são os cordões litorâneos (*beach ridges* ou *foredune ridges*).

Barreiras Retrogradantes (*Retrogradational Barriers*) são aquelas que durante o Holoceno migraram em direção ao continente devido à pequenas elevações do NRM e/ou ao escasso aporte sedimentar. Situam-se geralmente em setores onde a linha de costa é ligeiramente convexa e há concentração da energia de ondas causando perda de sedimentos e erosão. A principal feição geomorfológica desse tipo de barreira são os canais e leques de sobrelavagem.

Barreiras Agradantes (*Aggradational Barriers*) são aquelas que durante o Holoceno se mantiveram relativamente estáveis, ou seja, que não migraram de forma expressiva em direção ao continente, nem em direção ao oceano. Esse tipo de barreira é caracterizada pelo equilíbrio entre processos de progradação e de retrogradação. Elas retratam um balanço entre aporte sedimentar e criação de espaço de acomodação.

Apesar de utilizar nesta tese a terminologia e classificação de Morton (1994), os estágios evolutivos propostos pela escola australiana serão considerados. A Figura 2 apresenta esses estágios evolutivos, entretanto, apresentando a nomenclatura de Morton (1994).

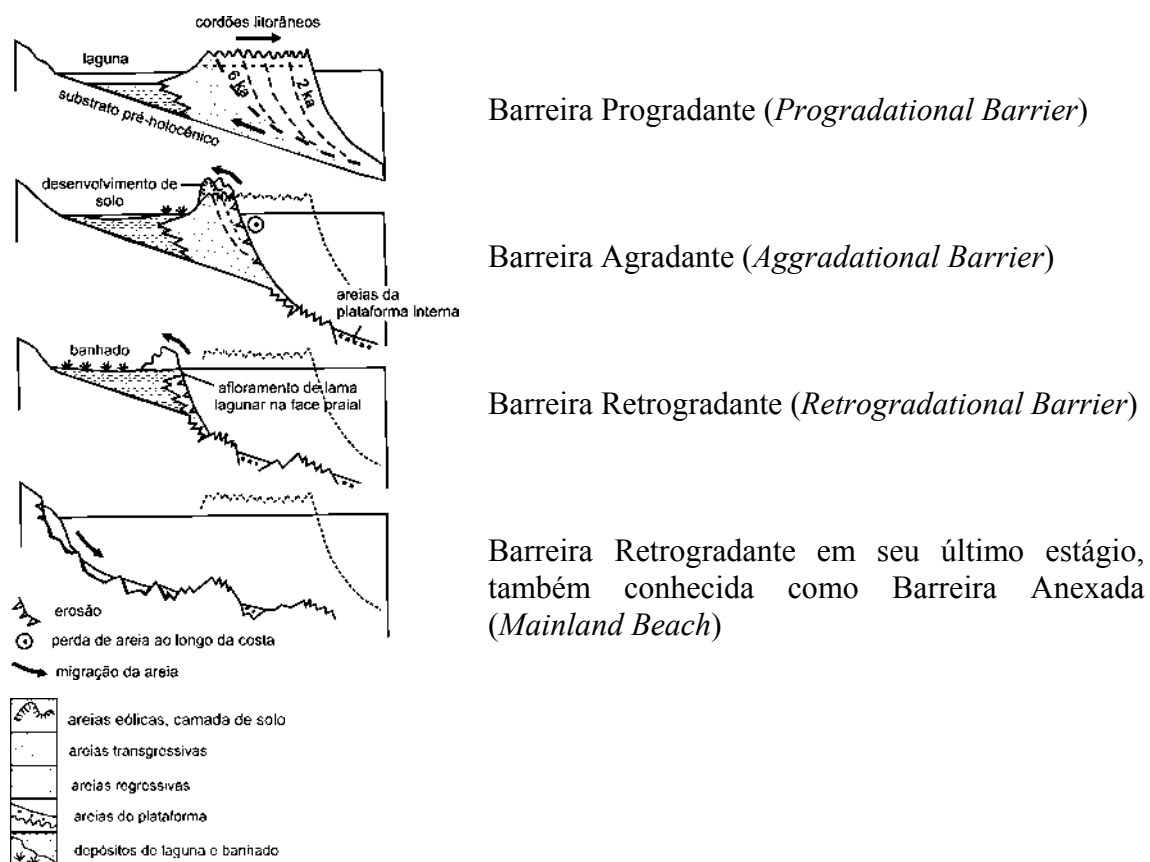


Figura 2: Série contínua de variações geomorfológicas de barreiras, proposta por Roy *et al.* (1994), apresentando a nomenclatura de barreiras proposta por Morton (1994). (Modificado de Roy *et al.* 1994).

2.3. CLASSIFICAÇÃO DE DEPÓSITOS EÓLICOS

Há numerosos tipos de classificação de dunas eólicas. Historicamente, nota-se que a maioria das abordagens, definições e tipos de classificação de dunas foram feitas a partir da observação de dunas e campos de dunas de grandes desertos interiores. Os autores dificilmente tentavam identificar as diferenças existentes entre dunas costeiras e dunas desérticas. Somente a partir da década de 80 (Short & Hesp 1982; Hesp 1983; Pye 1983; Goldsmith 1985; Carter 1988; Nordstrom *et al.* 1990), com o avanço do conhecimento sobre dunas costeiras começaram surgir trabalhos mais específicos sobre formação, classificação e influência da vegetação nas dunas costeiras. Alguns nomes típicos de dunas desérticas foram incorporados à nomenclatura costeira, porém eles geralmente referem-se a morfologias ligadas à ausência de vegetação.

A classificação adotada para este trabalho, é a proposta por Giannini *et al.* (2005) (também utilizada por Martinho 2004 e Martinho *et al.* 2006) baseada no critério da presença da vegetação para classificar os depósitos eólicos costeiros ativos em dois tipos: dunas com muita influência da vegetação e dunas com pouca ou nenhuma influência da vegetação. Estes dois tipos de depósitos eólicos não são completamente independentes, pois feições vegetadas, como dunas parabólicas e rastros lineares, associam-se, com freqüência, a zonas de deflação a barlavento de campos de dunas transgressivos. Além disso, é possível a passagem, no tempo e no espaço, de um tipo para outro, na dependência de variações no equilíbrio entre a taxa de aporte sedimentar e a taxa de crescimento de vegetação (Giannini & Santos 1994).

2.3.1. Depósitos eólicos com influência da vegetação

- Dunas frontais (*foredunes*): são acumulações de areia eólica em meio à vegetação pioneira acima da zona de pós-praia. Podem exibir geometria de cordão, rampa ou terraço (Hesp 2000) e podem ser divididas em dois tipos principais: incipientes e estabilizadas, dentro das quais pode haver grandes variações morfológicas e ecológicas (Hesp 1999). As dunas frontais incipientes são formadas por areia eólica recém depositada em meio à vegetação pioneira. As dunas frontais estabelecidas desenvolvem-se a partir de frontais incipientes e podem ser distintas pelo crescimento de vegetação secundária e pela maior complexidade de forma, altura e largura (Hesp 1988).

- Rupturas de deflação (blowouts): são feições mistas (erosivo-depositacionais), formada pela erosão eólica de depósitos arenosos pré-existentes seguida de redeposição local a sotavento. Sua morfologia consiste em uma bacia de deflação delimitada por paredes erosivas subparalelas que se fecham, rumo sotavento, em lobos deposicionais com formato em U (Hesp 2000).
- Dunas parabólicas (parabolic dunes): caracterizam-se por apresentar geometria plana em U, com convexidade voltada para sotavento. As dunas parabólicas possuem componentes similares às rupturas de deflação (*blowouts*), porém as dunas parabólicas diferem pelo maior alongamento das paredes, em forma de rastro linear residual (*trailing ridges*).
- Rastros lineares residuais (trailing ridges): podem ser apresentar-se em dois tipos: como braços alongados de dunas parabólicas (acima); e como cordões longos e estreitos formados pela colonização da vegetação nas margens externas de dunas transversais. Conforme a duna transversal avança, sua lateral externa, colonizada e estabilizada pela vegetação, é deixada para trás formando cordões retilíneos de areia. Os rastros lineares são paralelos ao vento efetivo e apresentam caráter deposicional em sua parte externa, vegetada e caráter erosivo em sua parte interna, desvegetada (Hesp 2004).
- Retrocordões (gegenwalle ridges): são cordões baixos e ondulados formados pela deposição de areia em meio à vegetação que cresce ao longo das margens do barlavento de dunas e campo de dunas. As plantas retêm a areia transportada pelo vento durante eventos de ventos reversos, num processo semelhante ao de formação de dunas frontais incipientes. Com a migração da duna ou campo de dunas, os retrocordões são deixados para trás, preservando a geometria em planta do lado barlavento da duna e/ou campo de dunas.
- Nebkhas: são montículos de areia formados pela deposição eólica em meio à vegetação. Os *nebkhas* são tipicamente circulares, sem faces de avalanche e com rampa a sotavento tênu e lisa. Podem possuir caudas alongadas no sentido do vento. Nesse caso, recebem a denominação dunas de sombra (*shadow dunes*).
- Cordões de precipitação (precipitation ridges): são longos cordões de areia formados pelo empilhamento de areia “precipita” sobre a vegetação presente ao longo da margem interna de campos de dunas. São vegetados, mais íngremes e possuem caráter deposicional em sua face externa, e desvegetados na face interna (Hesp & Thom 1990).

O grau de sinuosidade da crista depende da presença de frentes secundárias de avanço (Giannini 1993).

- Superfícies interdunares (interdunes): são áreas aproximadamente planas situadas entre dunas transversais/barcanóides, onde a deflação pode predominar sobre a deposição eólica. Caracterizam-se por apresentar-se constantemente úmidas, periodicamente alagadas e com vegetação pioneira esparsa.

2.3.2. Depósitos eólicos sem influência da vegetação

- Dunas transversais (transverse dunes): são formas de leito com orientação transversal ao vento efetivo, com crista linear retilínea.
- Dunas Barcanas (barchan dunes): são formas de leito em formato de meia-lua, com concavidade apontada para o rumo do vento efetivo.
- Cadeias barcanóides (barchanoid chains): são formadas por dunas barcanas lateralmente coalescidas, com crista sinuosa e orientação transversal ao vento efetivo.
- Lobos deposicionais (depositional lobes): referem-se às frentes de avanço principais dos campos de dunas. Possuem formato parabólico, com convexidade apontando para o mesmo rumo do vento efetivo.
- Lençóis de areia (sand sheets): são massas de areia eólica em movimento, com superfície de relevo negligenciável, sem superimposição de dunas.

2.4. PULSOS EÓLICOS E SUPERFÍCIES DE SEPARAÇÃO EM CAMPOS DE DUNAS

As primeiras tentativas de interpretação da evolução de sistemas eólicos iniciaram-se com o reconhecimento de importantes superfícies de separação entre séries e co-séries de estratificações cruzadas em afloramentos de arenitos eólicos e campos de dunas gigantes de desertos. A migração de dunas e campos de dunas, e/ou interrupções e mudanças bruscas na deposição eólica, podem resultar nessas superfícies de descontinuidade física (Brookfield 1977; Kocurek 1988). A análise destas superfícies eólicas possibilita caracterizar prováveis mudanças na dinâmica e morfologia dos sistemas deposicionais ao longo do seu período de existência.

Stokes (1968) sugeriu que estas superfícies seriam formadas por planos de deflação horizontais controlados pelo lençol freático. Talbot (1985) descreve as

chamadas super-superfícies que recobrem grandes áreas e estão associadas a períodos de não-acumulação ou de erosão. A gênese destas superfícies é controlada principalmente pelo comportamento do nível freático e do regime de fluxo eólico. Estas superfícies podem ser classificadas em instabilizadas e estabilizadas (Kocurek & Havholm 1993), conforme o seu substrato esteja disponível ou não, respectivamente, para o retrabalhamento eólico. Um problema prático é o reconhecimento de super-superfícies no registro geológico. A identificação é especialmente difícil em depósitos de sistemas eólicos úmidos, como o caso da maioria dos campos de dunas costeiros, pois muitas feições que se desenvolvem com a formação das super-superfícies são as mesmas que caracterizam superfícies interdunares.

Brookfield (1977) e Kocurek (1981, 1988) observaram que superfícies de truncamento formam-se com a migração das formas de leito eólicas. Seu desenvolvimento é determinado por variáveis como regime de fluxo eólico, suprimento de sedimentos a partir da área fonte, características granulométricas dos sedimentos, topografia e quantidade de água. Os mesmos autores hierarquizaram estas superfícies em três ordens, com base na sua extensão lateral e mútuas relações de truncamento.

Kocurek & Havholm (1993) tentaram relacionar as superfícies de descontinuidade física de depósitos eólicos aos fatores controladores de preenchimento de bacias previstos nos modelos de estratigrafia de seqüências (aporte e nível relativo do mar). Nesse contexto, estudos de caso de evolução de sistemas eólicos costeiros quaternários constituem um dos desafios mais importantes da estratigrafia moderna, pois é no quaternário costeiro que as oscilações de suprimento e nível do mar podem ser reconhecidas com maior detalhe (Giannini *et al.* 2001a, b).

Contudo, deve-se destacar que a relação entre a morfodinâmica de campos de dunas e a produção de superfícies de truncamento de diferentes hierarquias começou a ser compreendida através dos trabalhos de Brookfield (1977) e Kocurek (1988) em arenitos eólicos e campos de dunas gigantes (*ergs*) de desertos, mas não teve uma investigação detalhada em pequenos campos de dunas vegetados de regiões costeiras úmidas.

Estudos de morfoestratigrafia costeira mostram que a formação de dunas no Holoceno tem sido episódica, com períodos ou ‘pulsos’ de atividade eólica alternados com períodos de estabilização e intemperismo dos depósitos. Durante os períodos de estabilidade, há freqüentemente o desenvolvimento de solos e/ou depósitos de *lag* (Thom *et al.* 1981; Pye & Bowman 1984; Pye & Rhodes 1985; Illenberger 1988;

Short 1988a; Bressolier *et al.* 1990; Borówka 1990; Illenberger & Verhagen 1990; Shulmeister & Lees 1992; Tastet & Pontee 1998; Clarke *et al.* 1999; Loope & Alborgast 2000; Shepard 2000; Murray & Clemmensen 2001; Wilson *et al.* 2001; Orford 2005). O controle dos períodos de estabilização e ativação eólica se dá, principalmente, a partir de variações do lençol freático em resposta a variações climáticas e/ou variações do nível do mar.

CAPÍTULO 3

**WAVE ENERGY AND LONGSHORE SEDIMENT TRANSPORT
GRADIENTS CONTROLLING BARRIER EVOLUTION IN RIO
GRANDE DO SUL, BRAZIL**

Artigo aceito pelo *Journal of Coastal Research*

[Print - Close Window](#)

Date: Wed, 12 Dec 2007 14:19:18 UT
To: ctmartinho@yahoo.com
Subject: Manuscript 06-0645R Accepted after revision
CC: thals@lsu.edu
From: cfinkl@coastalplanning.net

Dear Ms. Martinho,

Revision of your manuscript was received in good condition. I have now completed my final adjudication of your contribution and am pleased to formally accept the paper for publication in the Journal of Coastal Research (JCR).

I hope that you will be pleased with the final production of your work. Thank you for thinking of the JCR as a source of publication for your research.

Sincerely,

Charles W. Finkl
Journal of Coastal Research
Editor
1656 Cypress Row Drive
West Palm Beach, FL 33411
United States of America
561.391.8102 (Work)
561.391.9116 (Fax)
cfinkl@coastalplanning.net

Wave Energy and Longshore Sediment Transport Gradients Controlling Barrier Evolution in Rio Grande do Sul, Brazil

Caroline Thaís Martinho[†]; Sérgio Rebello Dillenburg[‡]; Patrick Hesp[§]

† Universidade Federal do Rio Grande do Sul
Instituto de Geociências
Programa de Pós-Graduação em Geociências
Av. Bento Gonçalves 9500
91509-900, Porto Alegre, RS, Brasil
ctmartinho@yahoo.com

‡ Universidade Federal do Rio Grande do Sul
Instituto de Geociências
Centro de Estudos de Geologia Costeira e Oceânica
Av. Bento Gonçalves 9500
91509-900, Porto Alegre, RS, Brasil

§ Louisiana State University
Department of Geography and Anthropology
227 Howe/Russell Geosciences Complex
Baton Rouge, LA 70803-4105, USA

ABSTRACT

This paper aims to verify how wave energy and longshore sediment transport rates could have influenced the evolution of the RS Holocene barriers in the last 5000 years, assuming that wave climate conditions did not change much during the Middle and Late Holocene.

Calculations of wave energy based on visual observations and longshore sediment transport show that both wave energy and sediment transport decrease as the coastline becomes concave (embayed) and increase as the coastline becomes convex (projected). These variations alongshore created a positive and negative imbalance respectively in the sediment budget. The long-term operation of these processes has produced progradational barriers in embayments and retrogradational barriers along projections. In the transition zones between embayed to convex coastlines, neither depositional nor erosional processes predominate, creating a sediment balance and producing aggradational barriers.

3.1. INTRODUCTION

Recent studies have noted that along the Rio Grande do Sul (RS) coastal plain (29° to 34° south latitude), at least during the Holocene, the barriers have behaved in different ways along the coast. Progradational, aggradational and retrogradational barriers co-exist in this area.

Dillenburg *et al.* (2003) have stated an hypothesis that wave energy gradients along the coast would be an important factor in the Holocene barrier evolution, especially when the relative sea level (RSL) is roughly stable for the last 5000 years (5 ky). But until now no one has combined real wave energy data along the entire RS coastline in order to verify if there really is a variation.

Toldo Jr. *et al.* (2006) believe that the behavior of the RS shoreline, in the short-term (last three decades) is controlled by wave energy flux variations along the coast, i.e. variations in the longshore sediment transport rate. However, they did not apply their study for a long-term period, nor for the Holocene barrier evolution.

The aim of this paper is to test the assumptions of Dillenburg *et al.* (2003) and Toldo Jr. *et al.* (2006), to confirm if there really is a wave energy gradient along the coast, and what role it has on the barrier evolution. In addition, we aim to

verify how the longshore sediment transport can vary along the coast as the coastline orientation changes, and if this variation could influence long term Holocene barrier evolution, assuming that the actual conditions were similar in the past.

3.2. STUDY AREA

The Rio Grande do Sul (RS) littoral is characterized by a barrier-lagoon depositional system, dominated by waves. With 625 km length, it has a quasi-continuous, gently undulating coastline, orientated NE-SW (Fig. 1). According to Lima *et al.* (2001), waves from the N-NE represent the most frequent waves, occurring approximating 13% of the time. However, these waves are generated by local winds near the coast, so their longshore transport capacity is less than 2%. Although less frequent (9%), waves from S are the most important for longshore sediment transport. They are responsible for more than 30% of the sediment transported alongshore, producing a drift to the NE. Mean tide range is 0.5m (microtidal) with semidiurnal tides (Tomazelli & Villwock 1992). The adjacent inner shelf is wide (100 to 200 km), shallow (100 to 140 m) and has gentle slopes (0.03 to 0.08). At present the RS beaches receive very little sediment supply from the continent. All sediments, transported by rivers that drain the coastal plain, are deposited into lagoons and lakes located behind the barrier, or in other coastal plain environments (Tomazelli *et al.* 1998). Thus, the barrier only receives sediments from the adjacent shelf and from the longshore drift currents.

According to the Holocene sea level curve proposed by Angulo *et al.* (1999) and Angulo *et al.* (2006) for the southern littoral of Santa Catarina, an adjacent area, it is estimated that the RSL had been approximately 2 m above the actual position, during the maximum of the Post-Glacial Marine Transgression (PMT) at 5ky before present. This RSL behavior can be considered stable or quasi-stable for the last 5ky, because the rate of sea level fall is relatively low (0.4 mm/year), principally when it is compared to rates of 1.2 cm/year rise observed between 17.5 to 6.5 ky, after the Last Glacial Period in the Pleistocene (Corrêa 1995).

The accepted evolution model for the RS coastal plain is the one proposed by Villwock *et al.* (1986), on which the authors identify four Barrier-Lagoon depositional systems formed by successive RSL rise and drop during the Quaternary. From the latest to the earliest, they are designated as Barrier-Lagoon I, II, III, and IV

(Fig. 1). These four systems were formed during the last four Interglacials, the first three during the Pleistocene and the last during the Holocene.

The IV Barrier-Lagoon system is the main object of this study, the Holocene barrier. This barrier was formed around 7-8 *ky* ago, as a result of the migration of a transgressive barrier, during the final stages of the PMT (Hesp *et al.* 2005; Dillenburg *et al.* 2006). The barrier IV formation had isolated large lagoons, which were segmented during the RSL lowering after the transgressive maximum at 5 *ky*. Besides the modern beach, the barrier consists of large dunefields, from 2 to 8 km in width (Tomazelli 1990; Hesp *et al.* 2005). These predominantly transgressive dunefields are some of the most important in Brazil, in amount of sand and size.

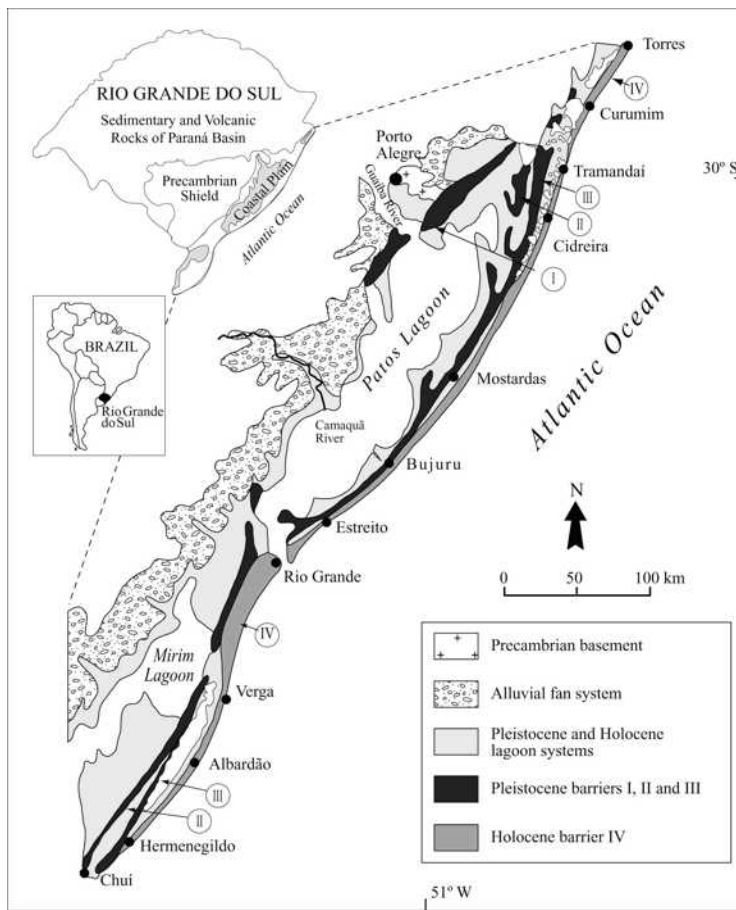


Figure 1: Location of Rio Grande do Sul coast and Pleistocene and Holocene Barrier-Lagoon systems (after Villwock *et al.* 1986).

3.3. FACTORS THAT COULD INFLUENCE THE BARRIER TYPE

According to Roy *et al.* (1994), on a wave dominated coast, the barrier type is determined by four main factors: 1) inner shelf slope; 2) wave energy versus tide range; 3) sediment supply versus accommodation space and 4) rates of sea level change.

Short & Hesp (1982) argue that barrier types develop as a function of surfzone-beach types (related to wave energy and sediment size and supply). Thus, if on the RS coast the regime is microtidal, there is not a significant neotectonic setting creating accommodation space, the RSL has been quasi-stable (gently falling) for the last 5 ky, and the surfzones-beaches are predominantly dissipative, the main factors that control the different types of barriers along the coast have to be the inner shelf slope, the wave energy and the sediment supply.

As stated above, the coast receives almost no sediment supply from the continent. So, the sediment budget of RS barriers depends on the sediment transference across the shoreface and between the shoreface and inner shelf, as well as on the longshore sediment transport.

Dillenburg *et al.* (2000) have calculated the slope of the RS inner shelf, from 25 profiles, perpendicular to the coast. From +2 to 70 m isobaths the slope varies from 0.027° to 0.125° (Table 1 and Fig. 2). The inner shelf slopes vary with the coastline orientation. When the coastline changes from concave to convex, the inner shelf slope tends to become steeper (see profiles 1 to 10 and 17 to 21), and when the coastline changes from convex to concave, the inner shelf changes to gentler slopes (see profiles 10 to 17 and 21 to 25).

Using the graphic model of May & Tanner (1973) for littoral sediment transport, Dillenburg *et al.* (2003) related the RS barrier types formed over the Holocene to the wave energy, which is controlled by processes of wave energy refraction and dissipation, over the inner shelf and nearshore. Thus, a coastal projection (convex coastline) concentrates wave energy, resulting in coastal erosion and formation of retrogradational barriers, while the coastal embayments (concave coastline), with gentle slopes on the inner shelf, dissipate wave energy and consequently induce sediment deposition, producing progradational barriers. The sediments eroded from the projections would be transported and deposited into the adjacent embayment.

Toldo Jr. *et al.* (2006) indicated that for the RS middle littoral (from Estreito to Pinhal), short-term coastal erosion and accretion are likely controlled by a relationship between longshore sediment transport and changes in the coastline orientation. According to these authors, in the last three decades, almost the entire middle littoral has experienced shore erosion. They found that the coastal projections are, in general eroding, except in the locations of Mostardas and Dunas Altas (local projections or convex shoreline segments) where the shoreline has accreted for the last

30 years. Lima *et al.* (2001) observed that the longshore sediment transport is highest along this coastal sector, which is probably the reason for the erosion. However, there is a decrease in the transport rates around Mostardas and Dunas Altas. From Figure 4 it can be seen that these two sites are inflection points, where the shoreline orientation changes, and to these authors, this is the reason for the decrease in the sediment transport. Toldo Jr. *et al.* (2006) noticed that the shoreface width increases at these points too, and concluded that the reduction of the transport rate due to change in shoreline orientation would produce a “jam” in the longshore transport, and because of that, the sediments would be deposited in the shoreface or deviated to offshore. With this positive sediment imbalance, produced by the jam, the shoreline at these locations has not eroded like the other areas, but accreted.

Profiles	Longshore distance (Km)	Overall slope m - 70 to + 2
01	0	0.064
02	25	0.057
03	50	0.058
04	75	0.067
05	100	0.075
06	125	0.084
07	150	0.104
08	175	0.113
09	200	0.120
10	225	0.125
11	250	0.104
12	275	0.086
13	300	0.070
14	325	0.057
15	350	0.045
16	375	0.031
17	400	0.027
18	425	0.029
19	450	0.032
20	475	0.034
21	500	0.034
22	525	0.031
23	550	0.033
24	575	0.035
25	600	0.033

Table 1: Gradients of the shelf slopes. The profiles are 25 km distance apart.

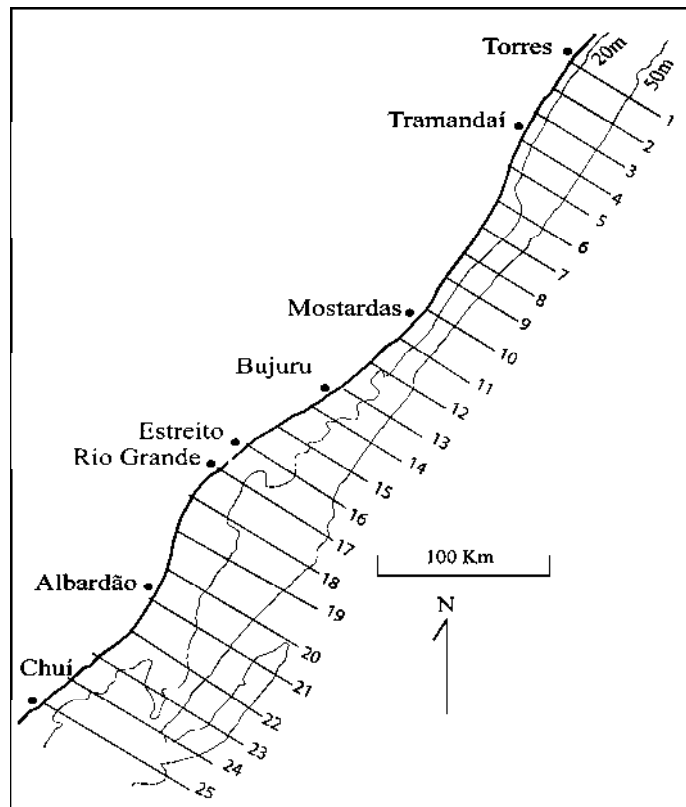


Figure 2: Coastline of Rio Grande do Sul showing location of shelf profiles (Modified from Dillenburg *et al.* 2000).

3.4. METHODS

To test Dillenburg and Toldo Jr. models, it is necessary to have wave height data along the entire RS shoreline. However there is a lack of deep water data for the whole coast, and there is no detailed bathymetric data for the area. The only data available is breaking wave height (H_b), measured visually at the beach. Munk (1944) stated that the average height of the waves estimated by an experienced observer is about equal to the significant wave height (H_s) defined as the average of the one-third highest waves.

Many authors divide the RS littoral into three regions, northern, middle and southern littoral. Data from the middle and southern littoral were obtained from pre-existing data; however there was a lack of data for the northern littoral, so, field observations over one year were initiated to cover this gap.

Calliari & Klein (1993), during one year (March 1991/1992), visually obtained the breaking wave height (H_b) and the wave period (T) at beaches of the southern littoral: Chuí, Hermenegildo, Concheiros, Albardão, Verga, Taim, Sarita, Querência, and Terminal (Fig. 3). The data were collected by measuring the difference between wave crest height and the trough, at a determined point inside the breaking zone.

Barletta (2000), from 1996 to 1999, collected H_b and T, for the Estreito, Conceição, Lagamarzinho, Mostardas, São Simão, and Solidão beaches, along the middle littoral (Fig. 3), by the qualitative visual method proposed by Melo (1991), used in the “Sea’s Sentinels” project.

To cover the entire RS coast, H_b and T data were collected from the northern littoral for a period of one year (September 2004/2005). The visual measurement method utilized was the “Line of Sight (LOS)” method, named by Patterson & Blair (1983) and originally described by Ingle (1966). In this method an observer stands at the mean water line on the beach, and reads wave height from a graduated staff by aligning the height of their eyes with the outermost breaker wave crest and the horizon line. The beaches surveyed were: Bacupari, Dunas Altas, Pinhal, Jardim do Éden, Mariluz, Xangri-lá, Arroio Teixeira, Arroio do Sal, and Paraíso (Fig. 3).

Since Lima *et al.* (2001) found that waves from the south (azimuth 180°) are responsible for most of the sediment transport alongshore, in this paper, this wave

direction was applied in the formulas for calculating the longshore energy flux as an exercise to observe how the longshore sediment transport can vary along the coast. It is important to state here that the numbers calculated do not represent the total amount of sand transported at the coast, since we are examining only one direction. But these numbers are valid for a qualitative evaluation, to see in general how they can vary, where the highest variations at the coast are, and why those variations take place.

The coastline orientation was measured from a geo-referenced satellite image, by subdividing the entire RS shoreline into ten straight lines, with different azimuths (θ in Table 2).

Most of the formulas used to calculate wave energy and longshore transport, described next, were taken from the *Coastal Engineering Manual* (U.S. Army 2003).

The parameter H_b was measured by slightly different methods, and because of that it cannot be compared quantitatively among the sectors. Thus, wave energy and longshore sediment transport (LST) parameters that are directly related to H_b , were classified qualitatively as high, medium and low (Fig. 3).

3.4.1. Wave Energy

From Airy wave theory the wave energy per unit surface area, also known as “specific energy” (U.S. Army 2003), can be directly related to the breaking wave height (H_b) by the formula

$$E_b = \frac{\rho g H_b^2}{8} \quad (1)$$

where E_b is the wave energy at the breaking line, given by Nm/m²;

ρ is the mass density of salt water = 1027 kg/m³; and

g is the gravity acceleration = 9.81 m/s²

With the wave energy calculated by equation (1), the energy flux, also called “wave power” (U.S. Army 2003), can be calculated by

$$P = E_b C_{gb} \quad (2)$$

where P is the energy flux, or wave power (N/s); and

C_{gb} is the breaking wave group celerity (m/s), given by the equation:

$$C_{gb} = \sqrt{g \frac{H_b}{\kappa}} \quad (3)$$

where κ is the breaker index (H_b/d_b) and is =0.78 for flat beaches (U.S. Army 2003).

3.4.2. Longshore Sediment Transport

Alongshore sediment transport occurs when waves approach the coast at an angle. According to the *Shore Protection Manual* (U.S. Army 1984), this transport can be calculated using the longshore energy flux, which is given by:

$$P_\ell = (EC_g)_b \sin \alpha_b \cos \alpha_b \quad (4)$$

where α_b is the angle that the wave breaking makes with the shoreline, and it depends on the coastline orientation and the wave direction.

When calculating longshore transport, a convention coordinate system has to be used, in which positive values of the angles, in degrees, mean that the waves are approaching the coast from the left (which means NE in the case of the RS coast) and negative angles mean that the waves are approaching the coast from the right (SW in this case). So, the transport rates with positive values will indicate that the transport is to the right as well as negative values will indicate that the transport is to the left. Consequently, for the calculations of the transport, the angle that the deep-water waves direction makes with the shoreline has to be converted to this system, by:

$$\alpha = \theta_n - \text{deep-water angle} \quad (5)$$

where θ_n is the azimuth angle of the outward normal to the shoreline (U.S. Army 2003).

However, to calculate longshore energy flux, α_b is needed (eq. 4), and it can be deduced by:

$$\sin \alpha_b = \sqrt{g \frac{H_b}{\kappa}} \frac{\sin \alpha}{C} \quad (6)$$

$$\text{where } C = \frac{gT}{2\pi} \quad (7)$$

The energy flux method for calculating longshore sediment transport, known as the “CERC formula” (U.S. Army 2003) is:

$$I_\ell = KP_\ell \quad (8)$$

where I_ℓ is the immersed weight transport rate (N/s) and K is a dimensionless coefficient.

The *Shore Protection Manual* (U.S. Army 1984), has proposed that K should be 0.39. However, the simple appliance of this value on the formula ignores the local sediment and hydrodynamic properties. Due to this, many authors (e.g. Lima *et al.* 2001, Williams *et al.* in press) have been using the Bailard (1981) formula to calculate different values of K , which depends on the beach characteristics of sediment size, sediment fall velocity and wave breaker height and angle.

$$K = 0.05 + 2.6 \sin^2(2\alpha_b) + 0.007 \frac{u_{mb}}{w_f} \quad (9)$$

where u_{mb} is the maximum oscillatory velocity magnitude at the breaking point, (U.S. Army 2003) given by:

$$u_{mb} = \frac{\kappa}{2} \sqrt{g \kappa H_b} \quad (10)$$

and w_f is the sediment fall velocity (cm/s) given by the Baba & Komar (1981) formula:

$$w_f = \frac{-3\mu + \sqrt{9\mu^2 + gr^2\rho(\rho_s - \rho)(0.015476 + 0.19841r)}}{\rho(0.011607 + 0.14881r)} \quad (11)$$

where μ is the water viscosity, at 20°C, known as 0.011 poise;

r is the grain size radius (cm);

ρ is the mass density of salt water = 1.027 g/cm³; and

ρ_s is the mass density of quartz = 2.65 g/cm³.

In order to express sediment transport rates in volumetric units (m³/s), the *Coastal Engineering Manual* (U.S. Army 2003) suggests the formula:

$$Q_\ell = \frac{I_\ell}{(\rho_s - \rho)g(1-n)} \quad (12)$$

where n is the sediment porosity, assumed as 0.4.

3.5. RESULTS AND DISCUSSION

3.5.1. Wave Energy Gradients

Table 2 presents the previously collected data of H_b , T and Mz from Calliari & Klein (1993) and Barletta (2000) as well as the results of this work, and the calculations of the wave energy (E) and the wave power (P) for the three coastal sectors, for a total of 24 beaches. As stated earlier it can be noted that there is a discrepancy of the H_b values in the three separate sectors (A, B and C Table 2) because of the different methods utilized to collect the data. Due to this fact, and since the focus of this paper is the wave energy gradient, not the numbers themselves, wave energy values were normalized and classified qualitatively as high, medium and low (Fig. 3).

The data show a clear pattern in the variation of wave height, energy and power along the coast (Table 2 and Fig. 3). The wave energy increases as the coastline becomes convex and decreases as the coastline becomes concave (see the changes from Paraíso to Solidão and from Terminal to Albardão), confirming Dillenburg *et al.* (2003) model. The cause of these wave energy and power gradients is likely the refraction and dissipation processes which the deep water waves encounter as they approach the coast. Inside the gentle embayments of the RS, the inner shelf is always wider and gentler, so these processes act for a longer period, and by the time the wave arrives at the coast and break, a large amount of energy is already lost having been dissipated by bottom friction. In contrast, when the coastline is convex, the inner shelf is narrower and steeper, so the refraction and dissipation processes are less, and the waves do not lose as much energy before they break. According to Dillenburg *et al.* (2000), if this pattern remained constant for a long period, at least the last 5ky, a positive imbalance would take place at the coastal sectors that have lower wave energy, and consequently, these sectors would prograde. In contrast, along the coastal sectors where the wave energy is higher, the sediment imbalance would be negative, leading to retreat of the coastline.

3.5.2. Longshore Sediment Transport

The results of the calculations of w_f , K , α_b and $P\ell$ for each location, as well as the results of longshore sediment transport ($I\ell$ and Q) are shown in Table 2. Similarly to wave energy, longshore sediment transport rates are different between the

sectors A, B and C (Table 2) due to the different methods of acquiring data. However, again, the aim of this study is not modeling LST at the RS coast, but rather to take the most import direction of transport and verify how it varies along the coast. So, the values of LST rates were also normalized and classified as high, medium and low (Fig. 3).

The volume of sediment transported alongshore tends to increase as the coastline becomes convex and decrease as the coastline becomes concave (Fig. 3). From Chuí, going northward, the rates increase, reaching highest values at Albardão, probably due its location at the outer most place in the southern littoral coastal projection. From Albardão to Terminal the values decrease, being the lowest at Querência, located approximate at the central part of the embayment.

The sector between Terminal and Solidão is characterized by the coastline becoming more and more convex, and so the rates of transport become higher too, however the increasing rates are not as continuous as in the southern littoral.

From Solidão to Paraíso the transport rates decrease, from high to low, as the coastline changes from convex to concave. The transport rates varies from medium to high between Bacupari and Jardim do Éden probably due to local characteristics, and then drop towards the embayment, showing the lowest rate at Arroio Teixeira, coincidently in the central part of the northern embayment.

Toldo Jr. *et al.* (2006) stated that a decrease in the longshore sediment transport rates, due to the changes in the shoreline, would produce a jam and, because of that, sediments would be deposited on the shoreface. The data presented in the Fig. 3 shows that the decreases in the transport rates are related to the coastline changing from convex to concave. Considering this, the sediment jam would be at the embayment's shoreface, what would produce a positive imbalance there, and consequently, the progradation of the coast. The sectors where the longshore transport rates are high coincide with the places where the coastline has been historically and geologically retrogradating.

A	Chuí	Hermenegild	Concheiros	Albardão	Verga	Taim	Sarita	Querência	Terminal
	O								
N	5	7	10	7	7	8	9	15	14
H_b	0.90	0.86	0.99	1.02	0.77	0.80	0.74	0.64	0.70
T	7.5	7.5	10.5	9.9	9.0	8.4	8.5	8.7	8.2
Mz	0.177	0.177	0.210	0.192	0.177	0.192	0.177	0.177	0.136
w_f	1.84	1.84	2.39	2.09	1.84	2.09	1.84	1.84	1.20
K	0.85	0.83	0.60	0.87	0.83	0.93	0.91	0.62	0.87
θ	45	45	45	22	22	10	10	43	43
α_b	-11.72	-11.45	-8.75	-12.40	-11.84	-13.77	-13.08	-8.78	-9.75
E	1.02	0.93	1.23	1.31	0.75	0.81	0.69	0.52	0.62
P	3.43	3.06	4.36	4.69	2.32	2.56	2.10	1.46	1.83
$P\ell$	-0.68	-0.60	-0.65	-0.98	-0.47	-0.59	-0.46	-0.22	-0.31
$I\ell$	-0.58	-0.49	-0.39	-0.86	-0.39	-0.55	-0.42	-0.14	-0.26
Q	-1.92	-1.62	-1.30	-2.84	-1.28	-1.81	-1.39	-0.45	-0.87
B	Estreito	Conceição	Lagamarzinho		Mostardas	São Simão	Solidão		
N	12	35	10		9	10	10		
H_b	0.8	1.00	1.30		1.10	1.00	1.30		
T	10	11	11		10	11	12		
Mz	0.225	0.203	0.203		0.215	0.225	0.210		
w_f	2.64	2.27	2.27		2.46	2.64	2.39		
K	0.42	0.51	0.73		0.68	0.64	0.75		
θ	58	58	43		43	32	32		
α_b	-32	-32	-47		-47	-58	-58		
E	0.81	1.26	2.13		1.52	1.26	2.13		
P	2.56	4.47	8.61		5.67	4.47	8.61		
$P\ell$	-0.27	-0.49	-1.46		-0.97	-0.77	-1.55		
$I\ell$	-0.12	-0.25	-1.06		-0.66	-0.50	-1.16		
Q	-0.38	-0.81	-3.51		-2.17	-1.64	-3.82		
C	Bacupari	Dunas Altas	Pinhal	Jardim do Éden	Mariluz	Xangri-lá	Arroio Teixeira	Arroio do Sal	Paraíso
N	8	10	10	10	10	10	10	10	10
H_b	1.45	1.60	1.48	1.53	1.39	1.21	1.21	1.26	1.25
T	9.5	10.2	10.4	9.8	9.6	9.6	10.3	9.7	9.8
Mz	0.184	0.186	0.183	0.183	0.196	0.193	0.196	0.196	0.187
w_f	1.96	1.98	1.94	1.94	2.15	2.11	2.15	2.15	2.00
K	1.10	1.22	1.14	1.19	1.09	0.99	0.85	0.93	0.95
θ	32	19	19	25	25	25	32	32	32
α_b	-58	-71	-71	-65	-65	-65	-58	-58	-58
E	2.66	3.23	2.77	2.95	2.45	1.86	1.84	1.99	1.97
P	11.38	14.49	11.95	12.93	10.26	7.26	7.20	7.93	7.79
$P\ell$	-2.70	-3.73	-2.90	-3.25	-2.52	-1.66	-1.44	-1.72	-1.68
$I\ell$	-2.97	-4.56	-3.30	-3.88	-2.74	-1.64	-1.23	-1.60	-1.60
Q	-9.82	-15.07	-10.91	-12.80	-9.05	-5.42	-4.07	-5.27	-5.27

Table 2. A- Data calculated from Calliari & Klein (1993) H_b measurements, for the RS Southern Littoral. B- Data calculated from Barletta (2000) H_b measurements, for the RS Middle Littoral. C- Data calculated from H_b measurements presented in this paper, for the Northern Littoral. N= number of observations; H_b = breaking waves height (m); T= wave period (s); Mz= mean sediment grain size (mm); w_f =sediment fall velocity (cm/s); K= dimensionless coefficient; θ = coastline orientation ($^{\circ}$); α_b = angle that the wave direction (S) makes with the shoreline ($^{\circ}$); E= wave energy x $10^3(\text{Nm/m}^2)$; P= wave power x $10^3(\text{N/s})$; $P\ell$ = longshore energy flux x $10^3(\text{N/s})$; $I\ell$ = immersed weight transport rate x $10^3(\text{N/s})$; Q= volumetric sediment transport rate x $10^6(\text{m}^3/\text{year})$

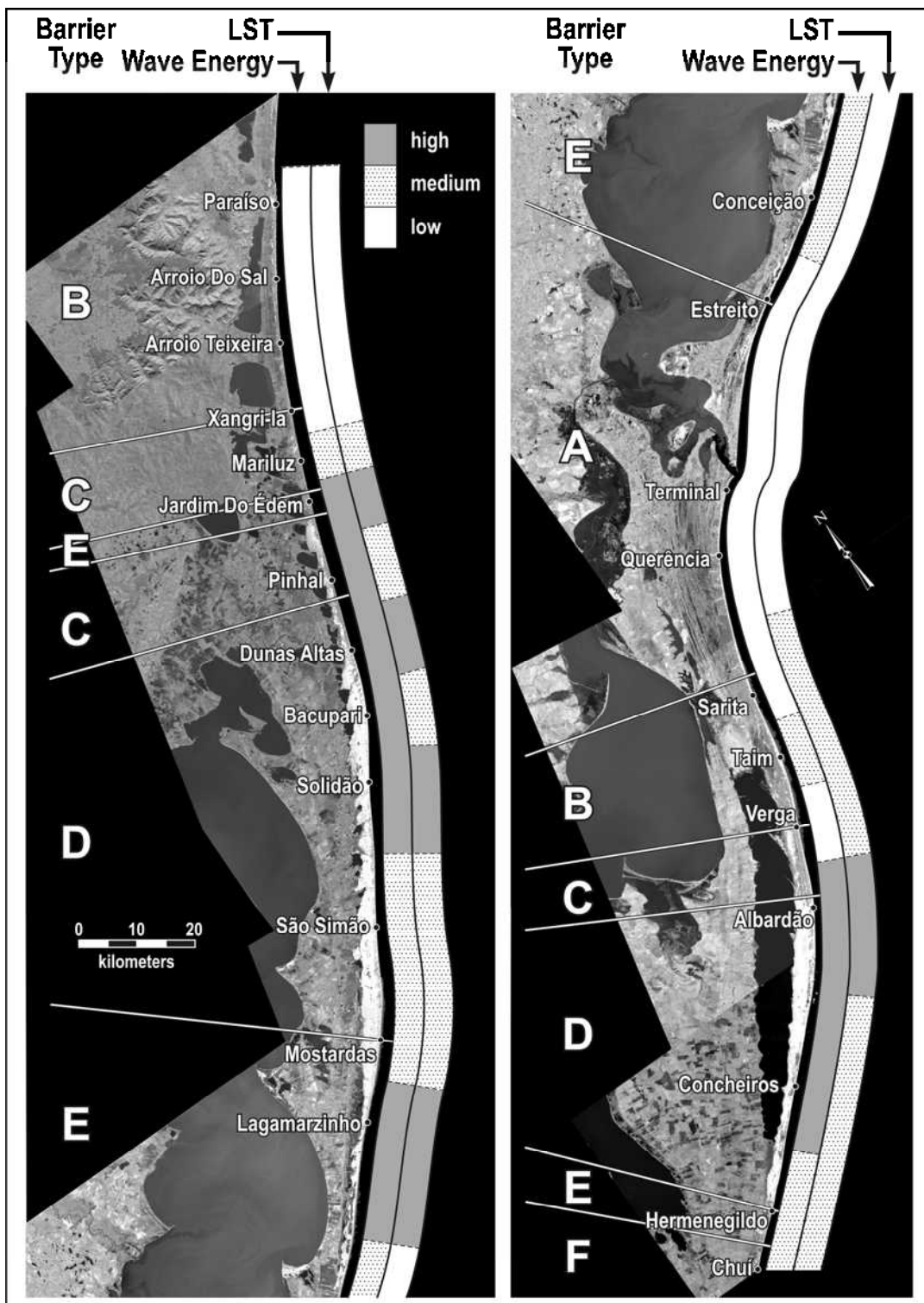


Figure 3: Georeferenced 1999 satellite image of the RS coast showing the location of the 24 beaches studied. The wave energy and longshore sediment transport calculated for those beaches is shown at the right, and classified as high, medium and low. On the left, the capital letters correspond to the Holocene barrier types shown in Fig. 4.

3.5.3. Barrier Types

Reviewing the literature of the RS coastal barriers (Dillenburg *et al.* 2000; Dillenburg *et al.* 2003; Dillenburg *et al.* 2004a, b; Hesp *et al.* 2005; Travessas *et al.* 2005; Dillenburg *et al.* 2006), the barrier types for the entire coast were plotted over a satellite image (Fig. 3), and they can be classified as progradational, aggradational and retrogradational following the terminology of Morton (1994).

The progradational barriers are characterized by migration of the coastline seawards, during the last 5 *ky* at least, and they are present on this coast in two different morphologies. The first progradational barrier (A) comprises suites of relict foredunes interspersed with transgressive dunefields, and no Holocene lagoonal system behind (Fig. 4A). It occurs in the southern littoral, from Estreito to Sarita, where the coastline is concave (Fig. 3). The second progradational type (B) occurs in the northern littoral, also on a concave coastline (between Paraíso and Xangri-lá, Fig. 3), but it differs from the first by presenting a lagoon system at the back and a succession of overlapping transgressive dunefields, which according to Hesp *et al.* (2005) are each separated by precipitation ridges (the downwind edge of transgressive dunefields) (Fig. 4B).

The retrogradational barriers are those barriers which, for the last 5*ky*, had their coastline migrating landwards, and they occur in three different evolutionary stages on this coast. The first (D), present from Dunas Altas to Mostardas and from Albardão to Hermenegildo, is characterized by eroding beaches and transgressive dunefields partially covering the lagoonal deposits behind the barrier (Fig. 4D). The progression of this stage (E) leads to the outcrop of lagoonal deposits at the beach face and backshore, with the transgressive dunefields on top of the lagoon deposits (Fig. 4E). This retrogradational barrier type can be found from Mostardas to Estreito, around Hermenegildo and Jardim do Éden area (Fig. 3). The last retrogradational type (F), found around the Chuí area (Fig. 3) (also known as “mainland beach”; Roy *et al.* 1994), is a barrier that has endured the entire erosion of the transgressive sediments and the lagoonal deposits and has reached the mainland. Here the transgressive dunefields partially overlie the Pleistocene barrier (the mainland) (Fig. 4F). From Fig. 3 it can be seen that all the retrogradational barrier types (D, E and F), excepting Jardim do Éden, occur from the middle to the south of the coastal projections.

Between the two end members, progradational and retrogradational barriers, are the aggradational barriers. This barrier type is characterized by the alternation of prograding and retrograding processes during the last 5 *ky*, which ends up with a quasi-stationary coastline (Fig. 4C). The places where this type of barrier is found are located in inflection points, where the coastline is changing from concave to convex (From Xangri-lá to Jardim do Éden, from Jardim do Éden to Dunas Altas and from Verga to Albardão) (Fig. 3).

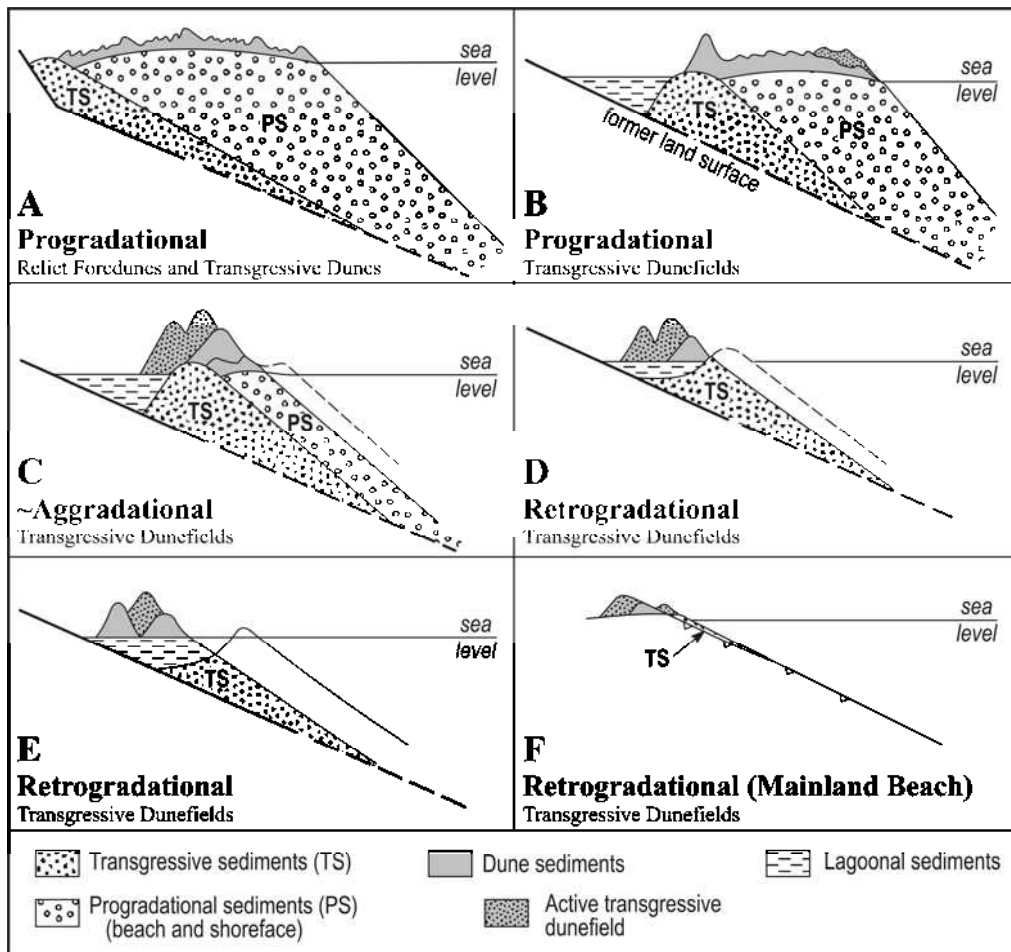


Figure 4: Schematic stratigraphical sections of barrier types found along the RS coast, based on geomorphology and drill-holes (Dillenburg *et al.* 2000; Dillenburg *et al.* 2004a; Travessas *et al.* 2005; Dillenburg *et al.* 2006).

3.6. CONCLUSIONS

Along the RS coastal plain there is a coexistence of progradational, aggradational and retrogradational barriers. Dillenburg *et al.* (2000), using simulations from the Shoreface Translation-Barrier Model (STM), predicted that at 5 *ky* the RS coastline configuration displayed better developed projections and embayments. Since

then, the projections have been eroding and the embayments prograding, smoothing the coastal profile somewhat, and creating the different types of barriers. According to the parameters of Roy *et al.* (1994), for the RS coast the main factors that control the different types of barriers have to be the inner shelf slope, the wave energy and the sediment supply.

The inner shelf slope is the gentlest inside the embayments and the steepest at coastal projections.

The data presented above shows that as the coastline orientation changes from convex to embayed (concave) and the inner shelf becomes wider and gentler alongshore, the wave energy as well as the longshore sediment transport rates decrease, creating a local positive imbalance in sediment supply. Assuming that the general wave behavior along the RS coast has not changed substantially during the Middle and Late Holocene, the long-term operation of this positive imbalance would produce progradation and, consequently, progradational barriers inside the embayments.

Alongshore, as the coastline orientation changes to convex, with a steeper and narrower inner shelf, the results point to an increase in wave energy and longshore sediment transport rates, which together can produce a local negative sediment imbalance. Again, considering that wave conditions were almost similar in the past, in the long-term this negative imbalance would cause erosion and, consequently, retrogradational barriers at coastal projections.

At the transition zones, between an embayment and a projection, neither depositional nor erosional processes would predominate, creating a sediment balance and producing aggradational barriers.

We conclude that differences in the local sediment budget along the RS coast are determined by components of the alongshore and cross-shore transport, driven by littoral drift and by sand transference inside the shoreface and between the inner shelf and shoreface respectively. Therefore, wave energy and the longshore transport have played an important role in the Holocene evolution of the RS barrier systems.

Finally, the Dillenburg *et al.* (2003) and Toldo Jr. *et al.* (2006) models were tested with real data and confirmed the wave energy gradient along the coast, hypothesized by Dillenburg *et al.* (2000). The analyses show that for the entire RS coast, changes in the orientation of the shoreline strongly affect the direction and magnitude of the LST causing either erosion or deposition. This means that Toldo Jr. *et*

al. model works not only for the rest of the coast, but it is important in the entire coastal barrier evolution.

ACKNOWLEDGEMENTS

This research was partly supported by grants of RECOS-Institutos do Milênio and Conselho Nacional de Desenvolvimento Científico e Tecnológico (CNPq). We thanks CNPq for the PhD. Scholarship and Comissão Permanente de Aperfeiçoamento de Pessoal de Nível Superior (CAPES) for the doctorate *sandwich* scholarship, to the first author. Thanks also to Luciana Dornelles and Daniel Bayer for their assistance in the field, and to Mary Lee Eggart (LSU) for cartographic assistance. Sérgio Dillenburg thanks CNPq for his scholarship, and Patrick Hesp LSU for support.

REFERENCES

- ANGULO, R.J.; GIANNINI, P.C.F; SUGUIO, K.; PESSENCIA, L.C.R. 1999. Relative sea-level changes in the last 5500 years in the southern Brazil (Laguna-Imbituba region, Santa Catarina State) based on vermetid ^{14}C ages. *Marine Geology*, **159**: 323-339.
- ANGULO, R.J.; LESSA, G.C. AND SOUZA, M.C. 2006. A critical review of the mid-to late Holocene sea-level fluctuations on the eastern brazilian coastline. *Quat Sci Reviews*, **25**: 486-506.
- BABA, J & KOMAR, P.D. 1981. Measurements and analysis of settling velocities of natural quartz sand grains. *Journal of Sedimentary Petrology*, **51** (2): 631-640.
- BAILARD, J. A., 1981. An energetics total load sediment transport model for a plane sloping beach. *Journal of Geophysical Research*, **86 C**(11): 10938–10954.
- BARLETTA, R.C. 2000. *Efeito da interação oceano-atmosfera sobre a morfodinâmica das praias do litoral central do Rio Grande do Sul, Brasil*. Rio Grande, Fundação Universidade Federal de Rio Grande, Dissertação de mestrado. 134p.
- CALLIARI, L.J. & KLEIN, A.H.F. 1993. Características morfodinâmicas e sedimentológicas das praias oceânicas entre Rio Grande e Chuí, RS. *Pesquisas*, **20** (1): 48-56.
- CORRÊA, I. C. S., 1995. Les variations du niveau de la mer durant les derniers 17.500 ans BP: l'exemple de la plate-forme continentale du Rio Grande do Sul-Brésil. *Marine Geology*, **130**: 163-178.

- DILLENBURG, S.R.; ROY, P.S.; COWELL, P.J.; TOMAZELLI, L.J. 2000. Influence of antecedent topography on coastal evolution as tested by shoreface translation-barrier model (STM). *Journal of coastal research*, **16** (1): 71-81.
- DILLENBURG, S.R., TOMAZELLI, L.J., CLEROT, L.C.P. 2003. Gradients of wave energy as the main factor controlling the evolution of the coast of Rio Grande do Sul in southern Brazil during the Late Holocene. *Proceedings of the 5th International Symposium on Coastal Engineering and Science of Coastal Sediment Process*. New York, NY: American Society of Civil Engineers, v.1, CD, 2003.
- DILLENBURG, S.R.; TOMAZELLI, L.J.; BARBOZA, E.G. 2004a. Barrier evolution and placer formation at Bujuru southern Brazil. *Marine Geology*, **203**: 43-56.
- DILLENBURG, S.R.; ESTEVES, L.S.; TOMAZELLI, L.J. 2004b. A critical evaluation of coastal erosion in Rio Grande do Sul, Southern Brazil. *Anais da academia brasileira de ciências*, **76**(3): 611-623.
- DILLENBURG, S.R.; TOMAZELLI, L.J.; HESP, P.A.; BARBOZA, E.G.; CLEROT, L.C.P.; SILVA, D.B. 2006. Stratigraphy and evolution of a prograded, transgressive dunefield barrier in southern Brazil. *Journal of Coastal research*, **SI 39** :132-135.
- HESP, P.A.; DILLENBURG, S.R.; BARBOZA, E.G.; TOMAZELLI, L.J.; AYUP-ZOUAIN, R.N.; ESTEVES, L.S.; GRUBER, N.L.S.; TOLDO JR., E.E.; TABAJARA, L.L.C.A.; CLEROT, L.C.P. 2005. Beach ridges, foredunes or transgressive dunefields? Definitions and an examination of the Torres to Tramandaí barrier system, Southern Brazil. *Anais da Academia Brasileira de Ciências*, **77** (3): 493-508.
- INGLE, J.C. 1966. *The movement of beach sand: an analysis using florescent grains*. Devel. in Sedimentology v. 5. Amsterdam, Elsevier.
- KOMAR, P. D. & INMAN, D. L., 1970. Longshore sand transport on beaches, *Journal of Geophysical Research*, **75** (30), 5514-5527.
- LIMA, S.F.; ALMEIDA, L.E.S.B.; TOLDO JR., E.E. 2001. Estimate of longshore sediments transport from waves data to the Rio Grande do Sul coast. *Pesquisas* **48** (2): 99-107
- MAY, J. P. AND TANNER, W. F. 1973. The littoral power gradient and shoreline changes. In: COATES, D.R. (Ed.), *Publications in Geomorphology*. Binghamton: State University of New York, 43-60.
- MELO, F.E. 1991. Projeto sentinelas do mar: Instruções para efetuar as observações. Comissão de Pós-graduação e Pesquisa em engenharia, COPPE/UFRJ, 12 p.
- MORTON, R. A. 1994. Texas Barriers, In: DAVIS, R.A. (Ed.) *Geology of Holocene Barrier Island Systems*, Springer-Verlag, Berlin: 75-114.

- PATTERSON, D.C. & BLAIR, R.J. 1983. Visually determined wave parameters. In: Sixth Australian Conference on Coastal & Ocean Engineering, 1983, Gold Coast. pp. 151-155.
- ROY, P.S.; COWELL, P.J.; FERLAND, M.A.; THOM, B.G. 1994. Wave-Dominated Coasts. IN: CARTER, R.W.G. & WOODROFFE, C.D. (Eds.), *Coastal evolution, Late Quaternary Shoreline Morphodynamics*. Cambridge, Cambridge University Press, p.121-186.
- SHORT, A.D. & HESP, P.A. 1982. Wave, beach and dune interactions on the SE Australian coast. *Marine Geology* 48: 259-284
- TOLDO JR. E.E.; NICOLODI, J.L.; ALMEIDA, L.E.S.B.; CORRÊA, I.C.S.; ESTEVES, L.S. 2006. Coastal dunes and shoreface width as a function of longshore transport. *Journal of Coastal research* SI 39 .
- TOMAZELLI, L.J., 1990. *Contribuição ao estudo dos sistemas deposicionais holocénicos do nordeste da província costeira do Rio Grande do Sul, com ênfase no sistema eólico*. PhD Thesis (unpublished). Porto Alegre, Universidade Federal do Rio Grande do Sul, 270 p.
- TOMAZELLI, L.J. & VILLWOCK, J.A. 1992. Considerações sobre o ambiente praial e deriva litorânea de sedimentos ao longo do Litoral norte do Rio Grande do Sul, Brasil. *Pesquisas*, 19 (1): 3-12.
- TOMAZELLI, L. J., VILLWOCK, J. A., DILLENBURG, S. R., BACHI, F. A., DEHNHARDT, B. A., 1998. Significance of present-day coastal erosion and marine transgression, Rio Grande do Sul, Southern Brazil. *Anais da Academia Brasileira de Ciências*, 70(2): 221-229.
- TRAVESSAS, F. A.; DILLENBURG, S.R.; CLEROT, L.C.P. 2005. Stratigraphy and evolution of the Holocene barrier of Rio Grande do Sul between Tramandaí and Cidreira. Estratigrafia e evolução da barreira holocênica do Rio Grande do Sul no trecho Tramandaí - Cidreira (RS). *Boletim Paranaense de Geociências*, 57: 57-73.
- U.S. ARMY, CECW-EW, 2003. *Coastal engineering manual*. Corps of Engineers Internet Publishing Group, Washington, DC, USA. EM 1110-2-1100.
- U.S. ARMY, COASTAL ENGINEERING RESEARCH CENTER/CERC, 1984. *Shore protection manual*. 4ed., vol. (1). Waterways Experiment Station, Corps of Engineers. Washington, DC, USA. 608p.
- VILLWOCK, J.A., TOMAZELLI, L.J., LOSS, E.L., DEHNHARDT, E.A., HORN FILHO, N.O., BACHI, F.A., DEHNHARDT, B.A., 1986. Geology of the Rio Grande do Sul Coastal Province. *Quaternary of South America and Antarctic Peninsula*, 4: 79-97.
- WILLIAMS, J.J.; TOLDO JR., E.E.; ESTEVES, L.S.; CALLIARI, L.J.; DILLENBURG, S.R. (in press). Predicting longshore sediment transport and morphological response of the coastline of Rio Grande do Sul, Brazil.

CAPÍTULO 4

CLIMATE PATTERNS AND VARIATIONS ON THE RIO GRANDE DO SUL COAST AND COASTAL DUNEFIELD DYNAMICS

Artigo submetido à *Earth Surface Processes and Landforms*

[Print - Close Window](#)

Date: Mon, 1 Oct 2007 16:50:31 -0400 (EDT)

From: f.kirkby@leeds.ac.uk

To: ctmartinho@yahoo.com

Subject: ESP-07-0198 successfully submitted

01-Oct-2007

Dear Ms Martinho,

Your manuscript entitled "Climate patterns and variations on the Rio Grande do Sul Coast and coastal dunefield dynamics" has been successfully submitted online and is presently being given full consideration for publication in Earth Surface Processes and Landforms.

Your manuscript number is ESP-07-0198. Please mention this number in all future correspondence regarding this submission.

You can view the status of your manuscript at any time by checking your Author Center after logging into <http://mc.manuscriptcentral.com/esp>. If you have difficulty using this site, please click the 'Get Help Now' link at the top right corner of the site.

Thank you for submitting your manuscript to Earth Surface Processes and Landforms.

Yours sincerely,
Earth Surface Processes and Landforms Editorial Office

Climate patterns and variations on the Rio Grande do Sul Coast and coastal dunefield dynamics

Caroline Thaís Martinho^{†‡}; Patrick Hesp[§]; Sérgio R. Dillenburg[‡]; Luiz J. Tomazelli[‡]

† Universidade Federal do Rio Grande do Sul
Instituto de Geociências
Programa de Pós-Graduação em Geociências
Av. Bento Gonçalves 9500
91509-900, Porto Alegre, RS, Brasil
ctmartinho@yahoo.com

‡ Universidade Federal do Rio Grande do Sul
Instituto de Geociências
Centro de Estudos de Geologia Costeira e Oceânica
Av. Bento Gonçalves 9500
91509-900, Porto Alegre, RS, Brasil

§ Louisiana State University
Department of Geography and Anthropology
227 Howe/Russell Geosciences Complex
Baton Rouge, LA 70803-4105, USA

ABSTRACT

Transgressive dunefields are present along the entire Rio Grande do Sul (RS) coast. This paper analyses the rainfall and wind patterns of the area, and their interdecadal and interannual variations driven by the North Atlantic Oscillations (NAO) or the Southern Oscillations (SO), and how they modify the dunefields.

The RS coast is dominated by the South America Summer Monsoon (SASM) on the northern littoral and by the mid-latitude climate on the mid and southern littoral. These two climate regimes, in addition with great topographic variation along the coast, create differences in wind patterns and precipitation. The mid and southern littoral with less rainfall and more strong winds is more susceptible to the formation of large dunefields. Spring is the season with the highest potential for dune migration.

During El Niño (EN) events and/or in the year after it, the precipitation increases. The year before EN tends to be drier. So, during EN it is likely that dunefields have their migration rate lowered, while the opposite tendency is expected in the year before the event. During La Niña (LN) events the precipitation decreases while the drift potential (DP) of NE winds increases. The low moisture and highest DP makes LN the event of expected high dune migration, death of foredune vegetation, and creation of new blowouts and even the initiation of new dunefields.

For a 55 years period there is a tendency of increasing precipitation. From 1964 to 1988 the DP decreased, associated with the interdecadal variation driven by the NAO. This decrease in DP associated with the increase in precipitation acting in concert will reduce significantly the dune movement rates and induce vegetation growth which is the key to dunefield stabilization. Thus, during this period it is highly likely that a large portion of the dunefields have been stabilized.

4.1. INTRODUCTION

To initiate a transgressive dunefield it is necessary to have a sand supply in an adequate grain size to be transported by winds with appropriate velocity and direction (Wilson 1972; Fryberg & Dean 1979; Lancaster 1988; Hesp & Thom 1990; Treinhaile 1997; Bauer & Sherman 1999). The formation and full activation, or complete stabilization of a dunefield can be produced by variations in sand supply, velocity, direction and frequency of wind, wave energy, shoreline orientation relative to

the wind direction, vegetation cover etc (Hesp & Thom 1990; Treinhaile 1997). Thus, climate plays an important rule in dunefield evolution. Large scale climate changes (millennial or centennial) like the Little Ice Age, or short scale climate variations like the southern oscillation (El Niño and La Niña), can have great importance in dunefield formation and development.

In Europe, especially in the high latitude countries, climatic events such as the Little Ice Age (LIA) have drastically altered the local climate. Denmark, British Islands and France relate dunefield formation produced by climatic changes in the LIA. These changes produce colder temperatures, death of vegetation cover, and increase the storminess and changes in the atmospheric circulation pattern, which produce an increase in the wind velocity and frequency as well as changes in the wind direction, from offshore to onshore (Clarke *et al.* 1999; Clemmensen *et al.* 2001; Murray & Clemmensen 2001; Wilson *et al.* 2001; Orford 2005). Murray & Clemmensen (2001) and Clemmensen *et al.* (2001) recognized in Denmark, during the Holocene, four episodes of colder climate similar to the LIA and they associate these events to millennial cycles recognized in the North Atlantic Ocean.

Periods of increased dryness can also influence dunefield formation by increasing fires, death of vegetation and lowering the water table producing an increase in the available sediments to be transported by winds (Filion 1984; Shulmeister & Lees 1992; Formann *et al.* 2005; Hugenholtz & Wolfe 2005). Formann *et al.* (2005) and Hugenholtz & Wolfe (2005) have describe the formation of recent interior dunefields, in USA and Canada, generated by the intense dryness period that predominated in these countries during the 40's (known as the 'dust bowl').

Maia *et al.* (2005) in northeastern Brazil have correlated El Niño events with dune migration, due to the local decrease of moisture produced by this phenomenon. In contrast, an increase in precipitation can increase the fluvial sand supply and, consequently increase the coastal supply, generating eolian pulses of sedimentation in these periods (Illenberger & Verhagen 1990).

Hesp (2003) observed the highest dune migration rates during an El Niño event, associated with an increase in the wind drift potential.

Marcomini & Maidana (2006) studied how the increase in rainfall in the last 60 years has modified the transgressive dunefields in Argentina by increasing vegetation cover and deflation processes and decreasing dune migration rates.

Climatic changes can not only initiate a dunefield but also stabilize them by increasing moisture and/or slowing the wind velocity, favoring vegetation growth (Hugenholtz & Wolfe 2005; Marcomini & Maidana 2006).

Transgressive dunefields are present along the entire Rio Grande do Sul (RS) coast, comprising both urban and natural areas. The aim of this paper is to examine how the actual climate works and how variations in climate possibly modify dunefield behavior by analyzing wind and precipitation records. This has an applied interest since understanding dunefield behavior could assist coastal management.

4.2. REGIONAL SETTINGS

The Rio Grande do Sul coast is located between 29° to 34° south latitude, is 625km long with a gentle undulating coastline orientated NE-SW (Fig. 1). It is a lagoon-barrier depositional system dominated by waves with a semidiurnal microtidal regime (Tomazelli & Villwock 1992; Hesp *et al.* 2005; Dillenburg *et al.* 2006). Waves from the N-NE are the most frequent but they have low energy and short periods, while waves from the S are less frequent but because of their high energy and long period they are responsible for the main littoral drift current northeastwards (Lima *et al.* 2001).

This coast receives a small sedimentary supply from the continent, so the main source of sediments is the inner shelf and the longshore littoral drift currents that transport sediments from SW to NE (Tomazelli *et al.* 1998).

This coast can be divided into three sectors: the Northern littoral from Torres to Pinhal, Mid-littoral from Pinhal to Estreito, and Southern littoral from Estreito to Chuí (Fig. 1).

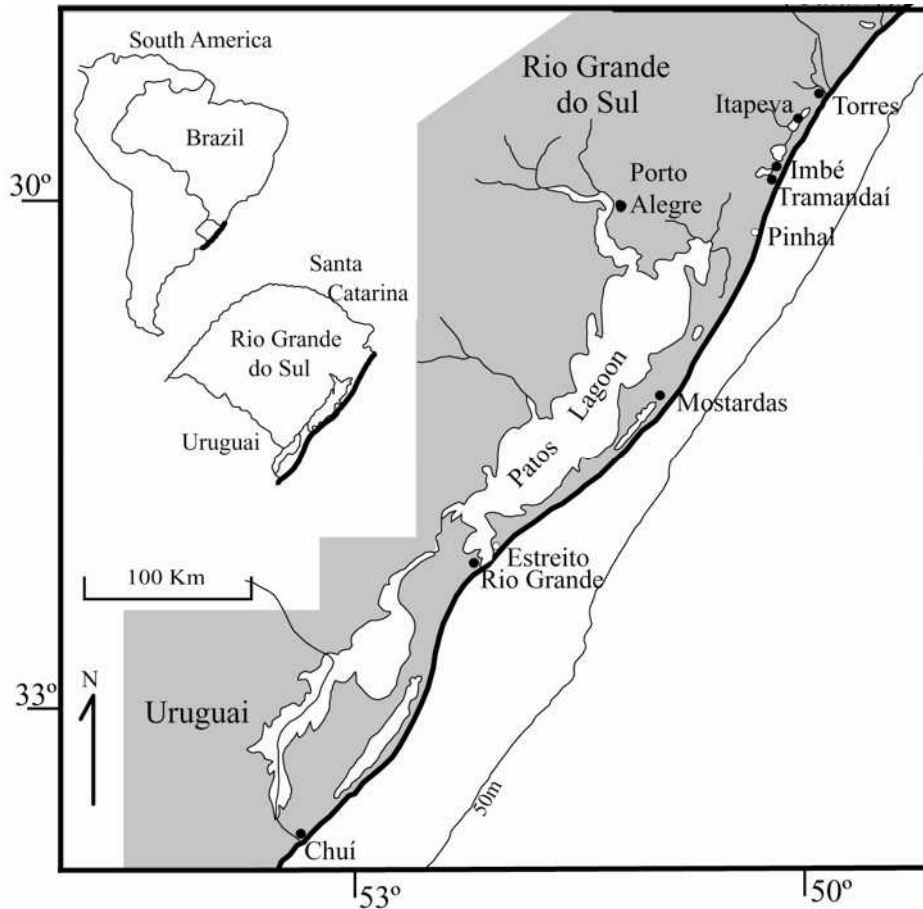


Figure 1: Rio Grande do Sul coast and location of meteorological stations.

4.3. CLIMATE OF SOUTHERN BRAZIL

Southern Brazil is affected by the South Atlantic Tropical Anticyclone, Polar Migratory Anticyclone and the West Low. The South Atlantic Tropical Anticyclone (SATA) is a high-pressure center composed of a warm and wet air mass, located between 18° and 35° S (Tomazelli 1990; Giannini 1993). The Polar Migratory Anticyclone (PMA) is a high pressure center, fed by cold air masses from Antarctica and it has a migratory character towards the NE (Tomazelli 1990; Giannini 1993). The displacement of the PMA induces the formation of two high pressure centers, which produces a low pressure center between them. This low pressure center, also known as a “cold front”, is always accompanied by cyclonic winds, weather instabilities and precipitation.

The West Low (WL), also known as the ‘Chaco Low’, is a quasi-stationary low-pressure center located around central-western Argentina and southern Bolivia (eastern border of the Andes) (Grimm *et al.* 2000, Barros *et al.* 2002). This

barometric depression is caused by the blockade that the Andes produces on the westerly flows associated with the intense heating of the low altitude plains in this area (Grimm *et al.* 2000; Barros *et al.* 2002). The WL is weaker during winter and it becomes deeper before the passage of cold fronts (Grimm *et al.* 2000; Barros *et al.* 2002).

The two anticyclones alternate seasonally. The SATA predominates during warmer months, spring-summer. Pressure gradients between the SATA and the WL generate winds from the E-NE along the entire RS coast (Zhou & Lau 1998; SEMC 2002). During colder seasons, fall-winter, the PMA is more active and consequently the S and SW cyclonic winds, produced by the cold fronts, predominate in this period (Tomazelli 1990).

The climate in Rio Grande do Sul State is subtropical temperate (SEMC 2002). The thermal amplitude of the region is high, varying from $< 0^{\circ}\text{C}$ during winter to $> 30^{\circ}\text{C}$ during summer (SEMC 2002). Although in a general view the rainfall is well distributed along the year, there are differences in precipitation along RS coast. The northern littoral is warmer and wetter than the mid and southern littoral (SEMC 2002). On the northern coast of RS, large gradients in the relief are responsible for the rainy season which has its peak during summer. The Serra Geral scarp enhances the land-sea temperature contrast and in association with the sea-land breeze that generates warm and wet air masses, produces orographic precipitation in this area (Grimm *et al.* 1998). At the mid and southern littoral of RS, the peak of the rainy season is during winter, which characterizes this area as a typical mid-latitude climate regime where precipitation comes from the frontal systems very active this time of the year (Grimm *et al.* 1998).

Thus, the RS coast is a region of transition between two adjacent regimes: mid-latitude winter conditions and the South American Summer Monsoon (SASM). These two regimes produce a seasonal variation in the origin of the precipitation by seasonal variations of the Intertropical Convergence Zone (ITCZ) through the year (Grim *et al.* 2000; Cruz Jr. *et al.* 2005).

During winter and the beginning of spring, the ITCZ stays near the Equator due to the migration of the cold air from mid-latitudes towards the Equator. The migration of the cold air produces cyclonic storms in the southern region which move moisture inland from the Atlantic Ocean (Fig. 2A). So, during winter, the main source of precipitation is the Atlantic Ocean (Cruz Jr. *et al.* 2005).

During late spring the SASM starts its development by creating an intense convection over the Amazon basin, by enhancing the NE trade winds which reach the Andes forming a strong NW low-level flow along the southwestern boundary of the Amazon basin, known as the Andean low-level jet (ALLJ), and finally by activating the South Atlantic Convergence Zone (SACZ) (Zhou & Lau 1998) (Fig. 2B). Thus, during summer and the beginning of fall, the convection over the Amazon basin induces an inland southward migration of the ITCZ, to the interior of the Amazon basin (Maslin & Burns 2000; Cruz Jr. *et al.* 2005). During this period, the continental moist air from the Amazon basin is transported by the ALLJ which blows it to the SACZ, producing high amounts of rainfall in southeastern and southern Brazil (Cruz Jr. *et al.* 2005).

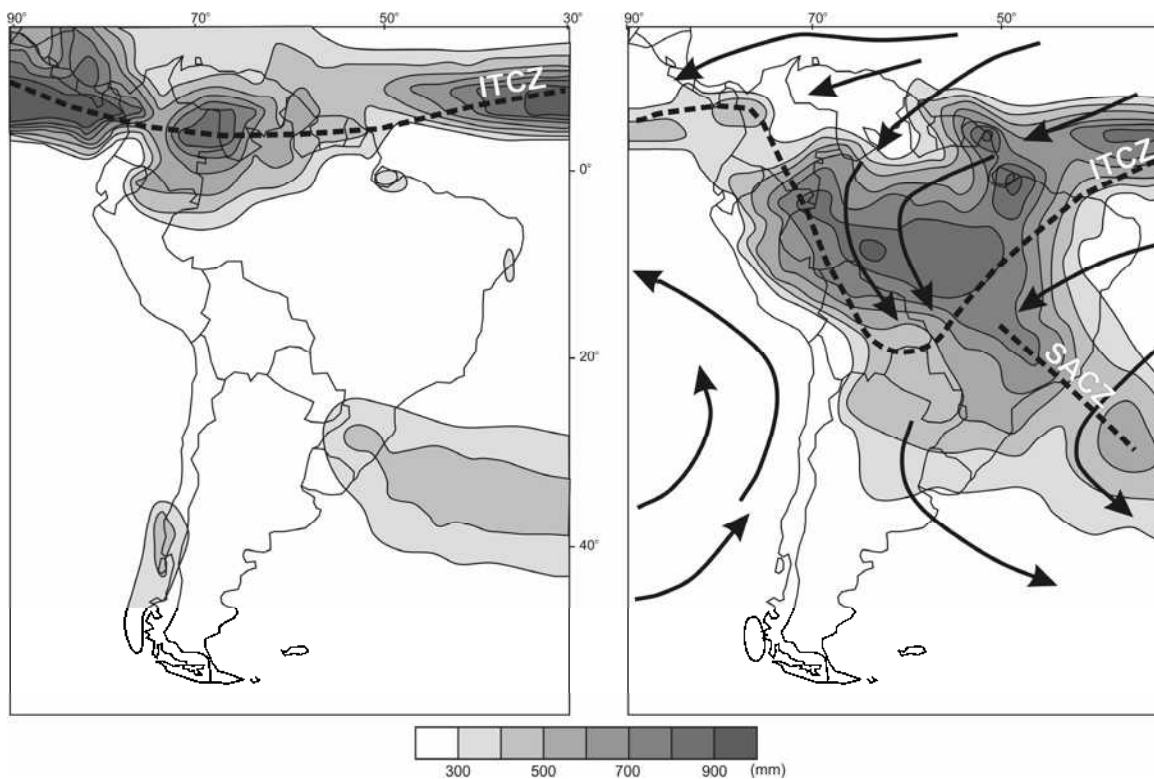


Figure 2: (A) ITCZ position near the Equator during winter and beginning of spring. (B) During summer and beginning of fall ITCZ migrates southward induced by SASM. The arrows indicate prevailing wind direction. Modified from Maslin & Burns (2000) and Cruz Jr. *et al.* (2005).

4.4. ANOMALIES IN THE CLIMATE

As stated above, the presence or absence of dunefields at the coast depends on the climate of the region as well as other factors such as sediment supply. Thus, any large or short scale climate variation may produce changes in the dunefields.

Induced by the Earth's precessional cycles, millennial scale changes in the oceanic and atmospheric circulation patterns driven by insolation variations have been described (Wang *et al.* 2001; Cruz Jr. *et al.* 2005). For Southern Brazil, Cruz Jr. *et al.* (2005) using isotopic climatology ($\delta^{18}\text{O}$) observed that when there is a minimum in the solar radiation during the summer of the tropical and subtropical southern hemisphere, the location of the SASM and ITCZ move northward and so, less moisture from the Amazon basin will be captured and transported to the south, decreasing the contribution of SASM rainfall. The opposite is true when the summer insolation is at a maximum (Cruz Jr. *et al.* 2005).

Robertson & Mechoso (1998) have observed an approximate 9 years cycle of variations in the Paraguai-Paraná rivers flux, which is associated with anomalies in the sea surface temperature in the tropical region of North Atlantic Ocean. Sea surface negative anomalies are associated with the increase in the flux of these rivers. Possibly the tropical North Atlantic Ocean influences the southeast of South America by a decadal variation of the SASM and the flux of moisture toward the south, associated with the ALLJ (Robertson & Mechoso 1998; Wanner *et al.* 2001). Negative anomalies in the sea surface in the North Atlantic during summer intensify the trade winds from the NE, what produces the displacement southward of the ITCZ (Robertson & Mechoso 1998; Wanner *et al.* 2001).

4.4.1. El Niño and La Niña events

Anomalies in the interannual sea surface temperature (SST) and atmospheric circulation over the Pacific Ocean directly influence the climate in the southern South America by the development of the Southern Oscillation (SO). Positive anomalies in the SST (warm phases) are known as El Niño events. During cold phases the La Niña events take place.

Grimm *et al.* (1998) described precipitation anomalies in southern Brazil associated with El Niño and La Niña events. They found very large positive precipitation anomalies during warm phases (El Niño), which occur mostly during spring of the event year. They also found for the RS coastal area that there is a consistent dry period in the year before the El Niño event and positive anomalies during autumn-winter of the following year. During cold phases (La Niña) there are strong

negative anomalies in precipitation during the spring of the event year (Grimm *et al.* 1998).

During El Niño events the subtropical westerly winds tend to be stronger than normal, weakening the SASM circulation (Grimm *et al.* 1998). La Niña events show opposite tendencies (Grimm *et al.* 1998).

Robertson & Mechoso (1998) and Krepper *et al.* (2003) described variations in the Negro-Uruguay river flux associated with El Niño and La Niña events, in cycles of 3 to 5 years. There is a clear tendency of a decrease in the river flux during La Niña from June to December, and an increase of the river flux during El Niño events, from November to February. The increase in flux during El Niño coincides with the warm phase in the sea surface temperature of the east equatorial portion of the Pacific Ocean, as well as with positive anomalies over the Atlantic, especially on the South American coast around 30° latitude (Robertson & Mechoso 1998; Krepper *et al.* 2003).

The study of El Niño/La Niña events in southern Brazil has a direct interest for this work once these events are associated to changes in rainfall and wind velocity, and may influence directly the formation, migration and/or stabilization of dunefields (Maia *et al.* 2005; Marcomini & Maidana 2006).

4.5. METHODS

4.5.1. Precipitation data

Precipitation data were obtained from two locations - Imbé and Porto Alegre (Fig. 1). The Imbé station belongs to Superintendência de Portos e Hidrovias (SPH) of Rio Grande do Sul State Government and the data extends from March 1948 to December 2003, with daily measurements in millimeters (mm). Precipitation data for Porto Alegre station were taken from the IAEA/GNIP database (<http://isohis.iaea.org>). The database extends from 1965 to 1982, with the 1970 and 1972 years missing, with mean monthly precipitation in mm (IAEA/WMO 1994).

4.5.2. Wind data

The wind data were obtained from five meteorological stations located along the Rio Grande do Sul coast. From north to south these are Itapeva, Imbé,

Tramandaí, Mostardas and Chuí (Fig. 1). In all the stations the wind speed is expressed in m/s.

The data from Itapeva station range from December 1998 to September 1999, with two readings per hour of mean wind velocity and 16 directions of provenance. The data from Imbé station range from April 1948 to December 2003 with three readings per day in 8 directions of provenance. At Tramandaí lighthouse station, hourly wind data were registered from September 2003 to October 2005. At the Mostardas station, wind data range from March 1957 to May 2000, with three readings per day. The Chuí lighthouse station recorded hourly wind data in the period of October 2003 to March 2006.

Wind data (direction and velocity) from Torres and Rio Grande were collected from the percentage wind frequency table of Tomazelli (1993), and they represent the period of January 1970 to December 1982.

The wind data were analyzed by mean velocity and direction. Wind roses were plotted for each station using *WRPLOT* software (www.lakes-environmental.com). Wind drift potentials and sand roses were calculated for each station and for each season of the year by the method described below.

4.5.3. Drift Potential and sand roses

Pearce & Walker (2005) observed that the Fryberger and Deans' model broadly used in the literature (Fryberger & Dean 1979) to calculate sand drift potential has systematic frequency and magnitude biases. So, to avoid and/or minimize these biases these authors describe methods which were used in this paper.

The first step to calculate sand drift potential is to build a wind frequency table (Fryberger & Dean 1979). As proposed by Pearce & Walker (2005), to minimize systematic frequency bias the wind direction classes chosen were 16 with equal interval ranges between them (22.5°) (Table 1).

Table 1: Chosen wind direction classes and their angles

Dir.	N	NNE	NE	ENE	E	ESE	SE	SSE	S	SSW	SW	WSW	W	WNW	NW	NNW
Angle	0	22.5	45	67.5	90	112.5	135	157.5	180	202.5	225	247.5	270	292.5	315	337.5

As stated by Pearce & Walker (2005), the aggregation of wind velocities into classes produces a bias, yet the more the wind speed classes chosen, the smaller the bias will be. So, the wind speed classes used were the ones chosen by Pearce & Walker (2005), transformed to m/s, and in addition five more complementary classes were utilized, totaling ten classes (Table 2). These complementary classes were added due to the specific characteristics of these wind data.

Table 2: Wind velocity classes utilized in this study.

Wind velocity classes (m/s)

0 - 3	3.01- 5.6	5.61 - 7	7.01 - 8.7	8.71-11.3	11.31-14.3	14.31-17.4	17.41-20.6	20.61-25	>25
-------	-----------	----------	------------	-----------	------------	------------	------------	----------	-----

With the wind direction and velocity classes chosen, a wind frequency table for each location was calculated, using the software *MATLAB Student 7.0.1*.

As stated above, Fryberger and Dean developed a method to analyze wind data and to calculate sand drift potentials (DP) represented as vector units (v.u.). Considering a flat, dry and unvegetated surface, composed of medium grain size (0.25-0.3mm) quartz sand with, they attempted to quantify the amount of aeolian sand (sand drift) that could be transported at a station during a determined period of time. However, different wind velocities can transport different amounts of sand. The higher the wind velocity, the greater the sand transport will be. So, modifying the Lettau and Lettau (1978) equation they created *weighting factors* to each velocity class:

$$Q \propto (\text{weighting factor}) * t$$

where

Q is the rate of sand drift in vector units (v.u.)

t is the amount of time that the wind blew, expressed as a percentage in the frequency tables

and the *weighting factor* is represented by :

$$\frac{V^2(V - Vt)}{100}$$

Fryberger and Dean use V as the midpoint of a velocity wind class; however, considering Pearce & Walker (2005) and trying to reduce biases in the DP

calculation, in this work V is the statistical mean of the velocity wind class (in m/s). V_t is the impact threshold wind velocity at 10m (in m/s).

To calculate the V_t , Fryberger and Dean use the Bagnold (1941) equation and assume a fixed grain size of 0.3mm. Nevertheless, in this work we assume the real and measured grain size (see Table 3), and because of that the impact threshold velocity is not necessarily the same for all locations.

$$V_t = 5.75 V_t^* \log \frac{Z'}{Z} + V_t'$$

Z is the pattern height = 10m

Z' is the surface roughness factor = $10*d_{(mm)}$, being $d_{(mm)}$ = grain diameter in millimeters, given by Belly (1964)

V_t' is the threshold wind velocity at height Z' , given by Zingg (1953)

as $20*d$ (in miles per hour), or $8.94*d$ (in m/s)

V_t^* is the threshold wind velocity at bed (in m/s) given by Belly (1964):

$$V_t^* = A \sqrt{\frac{\rho_s - \rho_a}{\rho_a} gd}$$

A is according to Bagnold (1941) ≈ 0.1

ρ_s is the sand grain density = 2650 Kg/m^3 for quartz

ρ_a is the air density = 1.22 Kg/m^3

g is the acceleration of gravity = 9.81 m/s^2

Table 3: Grain size for each station

Stations	Torres	Itapeva	Imbé	Tramandaí	Mostardas	Rio Grande	Chuí
Grain Size (mm)	0.177	0.177	0.177	0.177	0.210	0.105	0.177

The DP for each velocity class, then, is the product of the weighting factor and wind frequency. The total DP of a station is the sum of DPs from all directions. DPs of velocity classes lower than V_t are negative and because of that they are discarded and do not count in the total sum.

The drift potentials of all directions produce a resultant drift potential (RDP) and a resultant drift direction (RDD), which are calculated by:

$$RDP = \sqrt{x^2 + y^2}$$

$$RDD = \tan^{-1}(y/x)$$

where

$$x = \cos \alpha * DP$$

$$y = \sin \alpha * DP$$

being

α the angle of the class direction (in degrees)

DP the drift potential for the class direction (in v.u.)

All these DPs calculations are expressed in a sand rose diagram. In the sand rose each wind direction is represented as an arm and its length corresponds to its DP expressed in vector units (v.u.). The resultant drift direction (RDD) is represented as an arrow that points to the sand movement direction and its length is the value of RDP in v.u..

4.5.4. Classification

Fryberger and Dean studied wind patterns in many sand seas and created a wind-energy classification based on the DP values. However, Bullard (1997) observed that the magnitude of DP values depends on the wind velocity units and the results are not the same value using different units such as knots versus m/s. Fryberger and Dean used knots in their calculations but when using m/s the values are not the same magnitude. Because of that Bullard converted the Fryberger and Dean classification from knots to m/s (Table 4). In this paper m/s will be used as is Bullard's recalibration of the Fryberger and Deans' classification.

Table 4: Fryberger and Deans' (1979) wind energy classification converted from knots to m/s (after Bullard 1997).

DP values calculated in

knots	m/s	Wind energy classification
< 200	< 27	Low energy
200-400	27-54	Intermediate energy
>400	>54	High energy

To measure the directional wind variability Fryberger and Dean (1979) proposed an index RDP/DP. The greater the directional variability of the winds at the station, the lower the RDP/DP will be. Fryberger and Deans' classification of RDP/DP values are indicated in Table 5.

Table 5: Fryberger and Deans' Index of directional variability classification.

Index of directional variability (RDP/DP)	
0 to <0.3	low
0.3 to < 0.8	intemediate
≥0.8	high

4.6. PRECIPITATION AND ENSO EVENTS

Monthly precipitation data from Imbé and Porto Alegre station were analyzed. Both stations follow approximately the same trend with the peak of rain during the period of August/September while the driest periods are in April/May and November (Fig. 3).

Due to the longer period of observations (55 years), only Imbé station was analyzed by yearly average precipitation. From 1948 to 2003 yearly precipitation was very variable with values ranging from 57.6 mm in 1962 to 170 mm in 1972. Despite the high variability, when a trend line is calculated, the data show a tendency of increasing rainfall. In fifty five years of data, the average precipitation has increased around 20 mm (Fig. 4).

Historical records of El Niño and La Niña events were taken from Grimm *et al.* (1998), from the Climate Prediction Center of National Weather Service in NOAA's website (http://www.cpc.ncep.noaa.gov/products/analysis_monitoring/ensostuff/ensoyears.shtml) and from the Centro de Previsão do Tempo e Estudos Climático - CPTEC in INPE's website (<http://www.cptec.inpe.br/enos/>). The Climate Prediction Center of National Weather Service (NOAA) considers a threshold anomaly in the sea surface temperature of +/- 0.5°C to define the El Niño/La Niña events. Nevertheless, Hesp (2003) observed that only during strong El Niño events the dunefield migration rates were high. In order to avoid weak or non continuous events, in this paper it was considered only the sea surface temperature anomalies $\geq +0.8^{\circ}\text{C}$ in case of warm events (El Niño) and $\leq -0.8^{\circ}\text{C}$ in case of cold events (La Niña). Those

events were plotted with the annual precipitation of Imb   Station. There were a few strong events which reached or exceeded +/- 2.0  C. The strongest El Ni  os were in 1972, 1982 and 1997, while the strongest La Ni  as in 1955, 1973 and 1988.

Annual precipitation and the SO events were plotted together and they show a very consistent trend although there are some negative or positive precipitation anomalies that did not occur during SO events (Fig. 5). In similarity to Grimm *et al.* (1998) observations, in the year before an El Ni  o there is a tendency for dryness. During El Ni  o events the precipitation tends to increase. There is a lag in time between the start of the El Ni  o event in the tropical Pacific Ocean and its response in southern Brazil (Grimm *et al.* 1998) as seen elsewhere (for example, New Zealand; Hesp 2003). Sometimes the precipitation shows its response only in the average of the year after the start of the event, as in the case of the strongest El Ni  os' in 1982 and 1997. During La Ni  a events there is a decrease in the precipitation. Due to the precipitation behavior in the year before and after El Ni  o, and due to the short period between some El Ni  o and La Ni  a events, the anomalies can sometimes overlap each other, changing the magnitude or even the expected trend.

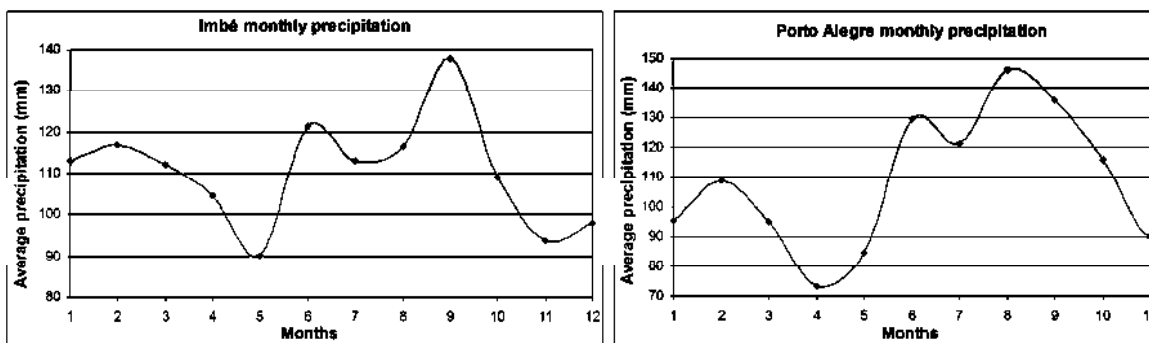


Figure 3: Monthly average precipitation of Imb   and Porto Alegre stations.

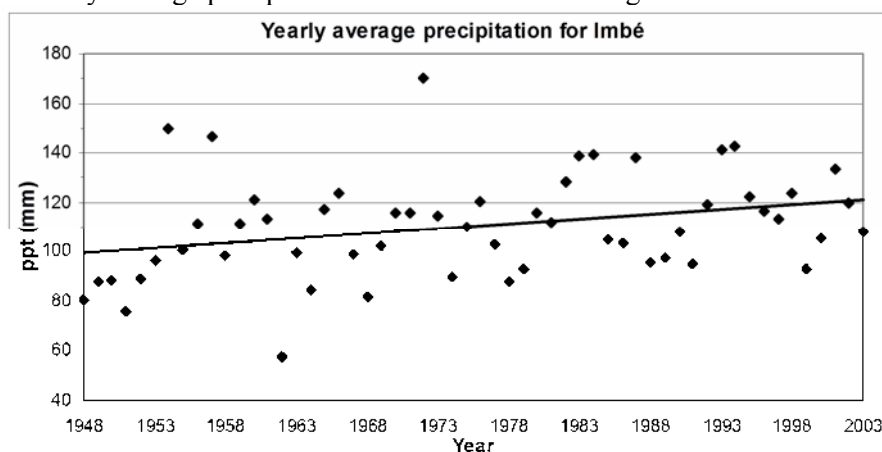


Figure 4: Yearly average precipitation for Imb   station. The trend line shows an increase in the precipitation.

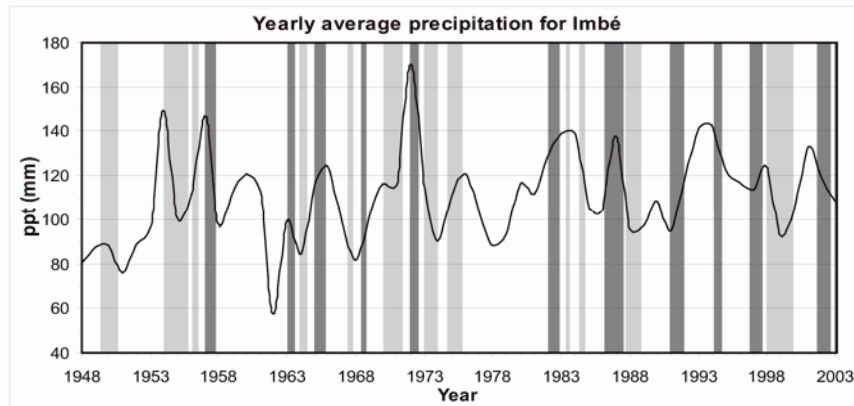


Figure 5: Yearly average precipitation for Imbé station. Light gray bars represent cold events (La Niña) and dark gray bars represent warm events (El Niño).

4.7. REGIONAL WIND PATTERN AND SAND DRIFT POTENTIALS

Analyzing the DP and sand roses along the RS coast, some differences in the wind patterns can be observed. From north to south the direction of the prevailing wind as well as their velocity changes significantly, as well as their DPs and RDPs.

The wind patterns in Torres show that the directions from E-NE and S-SW are very important in the area. Winds from NE display a frequency of 24.1%, followed by 12.2% (S) (Fig. 6A). Both have high speed and together they produce a sand drift to the NW. Winds from the N are very low (5%). Winds from the W are not important in this region of the coast due to the topography of the landward scarp (4.3%). The Torres RDP is onshore (Fig. 7).

At Imbé and Tramandaí, stations very close to each other, winds from the NE are by far more frequent and have the highest velocities. For Imbé, winds from the NE are 40.4% frequent and reach velocity classes of 17.4-20.6 m/s (Fig. 6B). For Tramandaí winds from the NE and NNE are 24.7% and 13.7% respectively (Fig. 6C). So, these winds produce a sand drift potential in this region predominantly to the SW (Fig. 7).

At Mostardas the range of wind directions is broader. Winds blow from every direction although from the NE-E and S-SW are the most important ones. Winds from the NE are the most frequent (17.3%) followed by winds from the S (10.7%) and the E (10.4%) (Fig. 6D). Together these directions produce a drift resultant to the W, onshore, making a 45° angle with the shoreline (Fig. 7). Winds from the NE, S and W are the strongest, with velocities higher than 17m/s. In comparison, with all the other

stations, Mostardas is the windiest station, with high frequencies for wind velocities higher than 14m/s, and with the smallest number of calms.

In Rio Grande NE and SW are the most frequent directions (22.3% ad 13.5%) and the winds are weaker when compared with other stations (Fig. 6E). To Rio Grande the most important DP directions are exactly opposite to each other, with the same wind velocity annulling each other, because of that the sand drift is very small to onshore (NW) (Fig. 7).

At Chuí, for the period of three years (2003-2006) winds blow from all directions, the most frequent is ENE at 10.5% (Fig. 6F). However, for sand transport, wind speed is more important than frequency, and 8% of winds from the south have higher velocities, changing the shape of the sand rose and producing a very high value for sand DP, towards the NNW (Fig. 7).

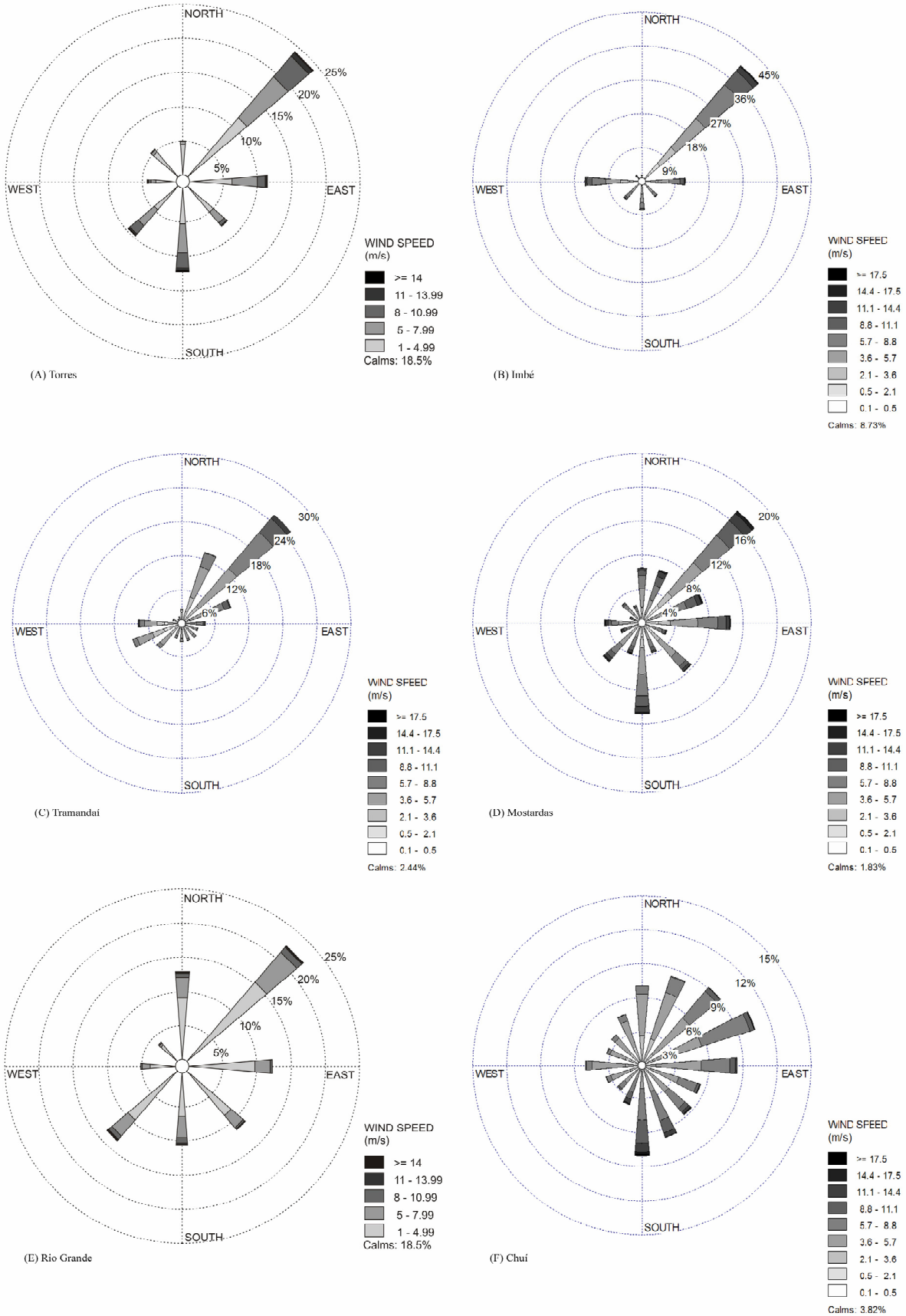


Figure 6: Wind roses showing the direction, frequency and velocity of winds at (A) Torres, (B) Imbé, (C) Tramandaí, (D) Mostardas, (E) Rio Grande, (F) Chuí.

The results show that winds from the S have more influence in the middle and southern littoral of RS. This probably occurs due to topographic effects. In the north, the scarps of the Serra Geral are a barrier for wind flow and definitely change the wind patterns in this area. On the other hand, the middle and southern littoral are flat and open regions, without significant topographic gradients, what make these places more susceptible to wind blowing from every direction (e.g. Mostardas sand rose).

Although the stations at Chuí and Tramandaí have a small period of observation and for that their data are not very representative of the wind pattern, they are important because they show how different the wind can blow over the northern littoral versus the southern littoral, at the same time, since they have the same period of data observations (daily and hourly).

According to Fryberger and Deans' classification, all station data shows that the winds are high energy, obtuse bimodal with low directional variability, shown by the low RDP/DP values.

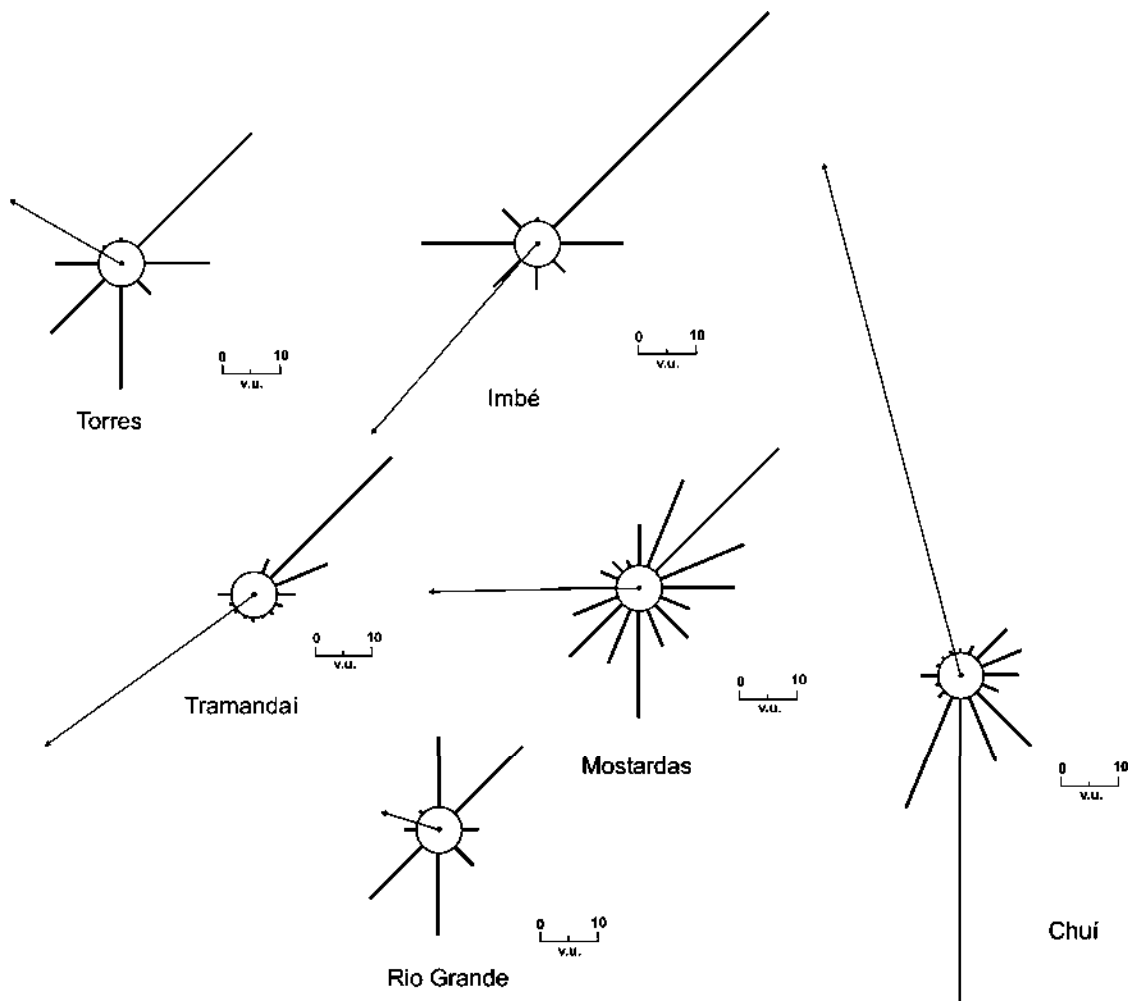


Figure 7: Sand roses of the stations showing the drift potential (DP) for each direction. The arrow represents the resultant drift potential (RDP) and the resultant drift direction (RDD).

4.7.1. Effects of the scarp in the wind pattern

The Itapeva station is very important because it is located on Itapeva lake (Fig. 1), near the base of the Serra Geral scarp, thus this station can show how the wind behaves as it approaches the scarps. Unfortunately, data from this station are very scarce with less than one year of measurements. So, data from Imbé and Mostardas for the same period of the Itapeva measurements were taken with an intention to compare the wind behavior along different stretches of the coast. The results show that wind blowing along the coast at the same time behaves very differently.

At Itapeva the most frequent winds are NNE and NE (16% and 13.8% respectively), but these winds do not reach high velocities, so winds from the SW (13.1%) and reaching velocity classes of 17.4 to 20.6 m/s (Fig. 8A), are dominant in the sand drift, producing a resultant to the NE (Fig. 9). What is clear here is that there are almost no winds from the SE and NW quadrants. For the same period at Imbé, winds blow from the NE 34% of the time (Fig. 8B), very similar to Itapeva. Considering that at Imbé the data have only 8 directions, so NE represents Itapeva's NNE and NE directions together. Nevertheless, the greatest difference between these places is that at Imbé the SE and NW directions are also important (19% and 14.4% respectively), and NW winds are very strong with velocities higher than 17m/s producing a very strong resultant to the SE (Fig. 9). The strong winds from the NW are not present at Itapeva due to the fact that the scarp acts like a barrier to the winds that come from this direction. At Mostardas, the wind during this period is completely different. The most frequent directions were ENE and E (12.8% and 13.5% respectively) (Fig. 8C). The highest speed winds blow from the W and SE, reaching velocity classes of 20.6-25 m/s and >25 m/s, creating a sand drift resultant to the NNE (Fig. 9).

As stated in the section above, the most important wind direction is NE and it does not appear here because the Itapeva data are from December 1998 to September 1999, consequently the data did not cover spring which is the most windy season and is responsible for the great importance of the NE drift.

Thus, the data show that at the scarp the wind blows predominantly parallel to it, orientated NE-SW, and with lower velocities. This wind behavior can influence the dunefields adjacent to the shoreline on this stretch of coast.

Comparing Itapeva with the data of other stations, Itapeva has intermediate wind energy while Imbé and Mostardas have high wind energy.

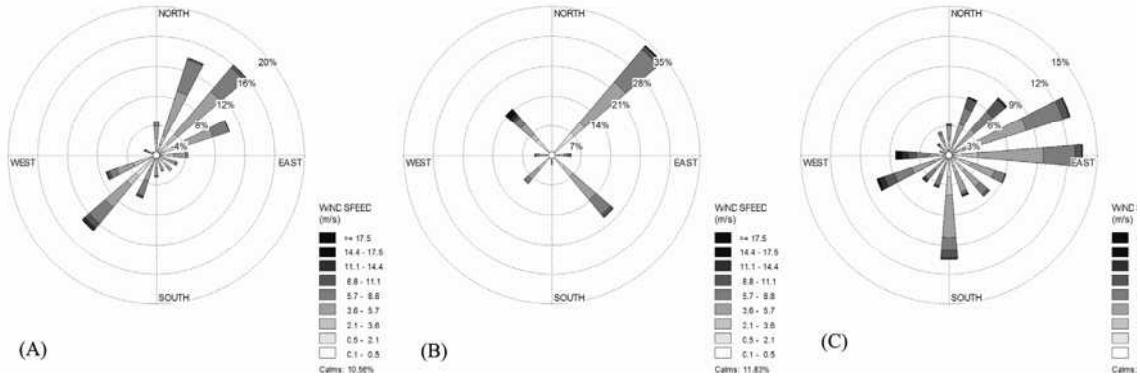


Figure 8: Wind roses showing the direction, frequency and velocity of winds at (A) Itapeva, (B) Imbé and (C) Mostardas, during the period of December 1998 to September 1999.

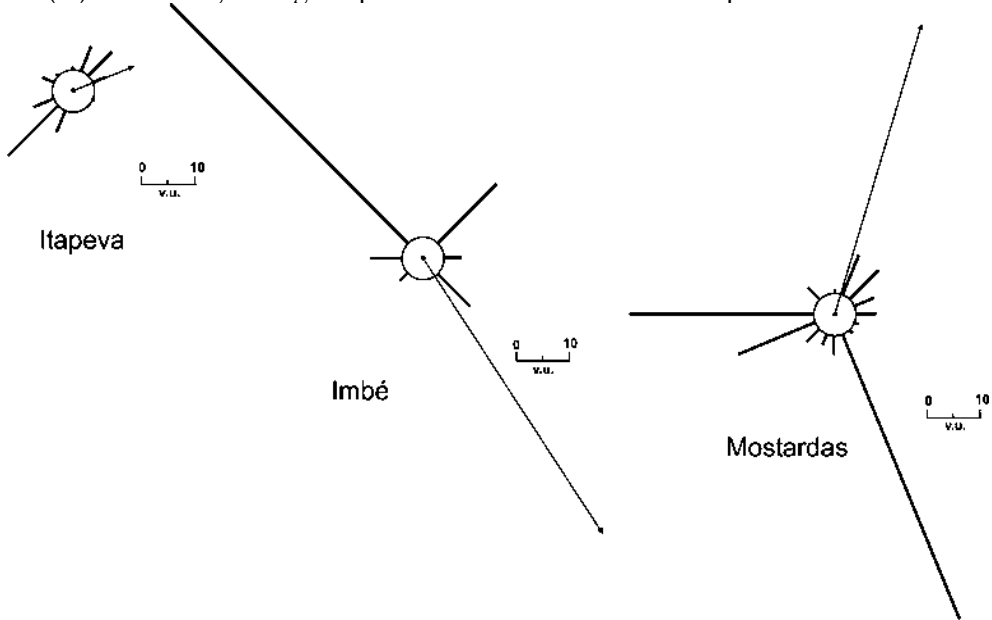


Figure 9: Sand roses of the Itapeva, Imbé and Mostardas stations for the period of December 1998 to September 1999, showing the DP for each direction. The arrow represents the RDP and the RDD.

4.7.2. Seasonal changes in the wind pattern

Due to the fact that only Mostardas and Imbé stations have longer period observations, and therefore they are more representative, these stations were chosen to verify seasonal changes in the wind. Despite the wind pattern at Imbé being well defined and predominantly from the NE, there are very important and clear seasonal variations in it. During summer NE and E winds predominate overall, and the predicted sand drift vector is very strong to the SW with 56 v.u. (Fig. 10). During fall the W winds are as strong as NE winds, creating an offshore sand drift to the SSE (Fig. 10). All through winter these characteristics remain the same, with NE winds a little more frequent and strong, producing a RDP still offshore to the S (Fig. 10). During spring,

despite the high frequency of W and S winds (10% each), winds from the NE predominates with the highest DP (93 v.u.) and the highest RDP to the SW (84 v.u.) (Fig. 10).

At Mostardas, winds blow from many directions but the ones from the NE quadrant are more important resulting in a RDP to the SW. During summer those characteristics remain, but in fall the wind regime changes, NE winds decrease their frequency (from 21.7% during summer to 12.2% during fall) and get weaker (Fig. 11). S and SW winds get stronger and more frequent producing a RDP to the N. Winds from the W and E also increase their potential, but they cancel each other in the RDP. During winter the scene remains almost the same, but with a gentle increase in the NE winds what causes a slight change in the RDP, which changes its direction to the NNW and get weaker 16.6 v.u. (Fig. 11). From winter to spring there are great differences in the wind pattern. During spring, despite the high velocity and frequency of the S wind, the NE wind is the most frequent (20.5%) and the strongest (61v.u.), accompanied by the NNE and ENE winds which increase their values too (Fig. 11). So, together they create a high potential sand drift (87v.u.) to the WSW along the coast.

A common situation for both stations is that in the passage from summer to fall winds the NE decreases in speed and frequency and there is an increase in the W winds. Spring is the windiest season and the NE wind has the highest frequencies and velocities. Because of that the potential sand drift is the highest and to the SW for both stations. Winds from the E are very frequent during spring and summer, but they are also very low velocities and not important for sand transport.

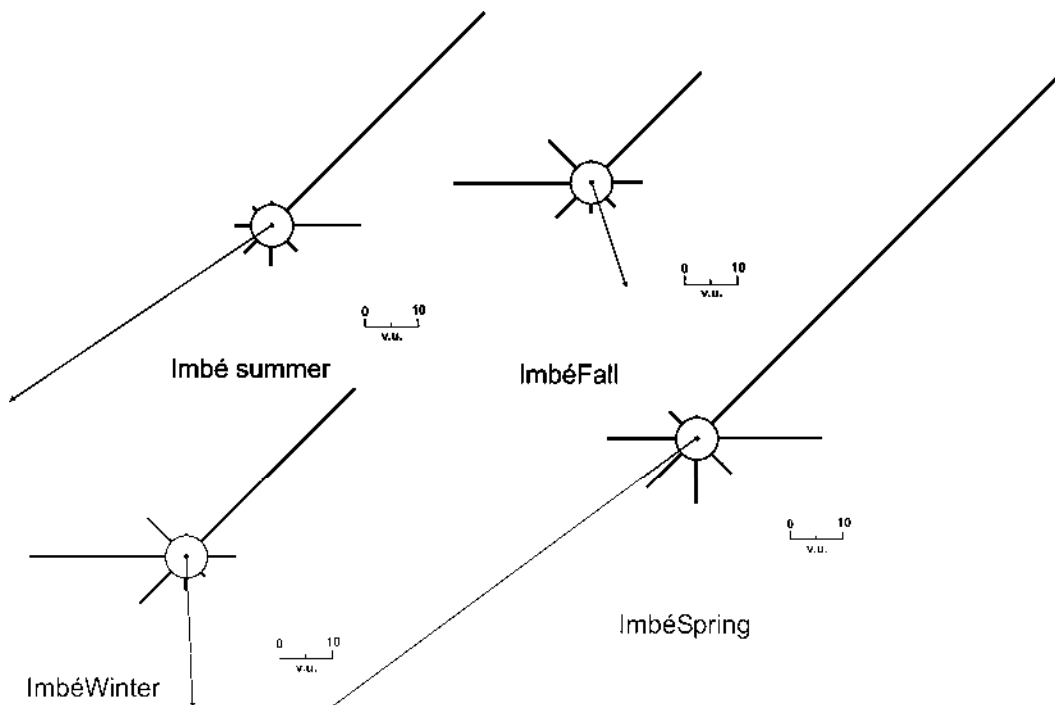


Figure 10: Sand roses of the seasons at Imbé station. The lines represent the DP for each direction and the arrow represents the RDP and RDD.

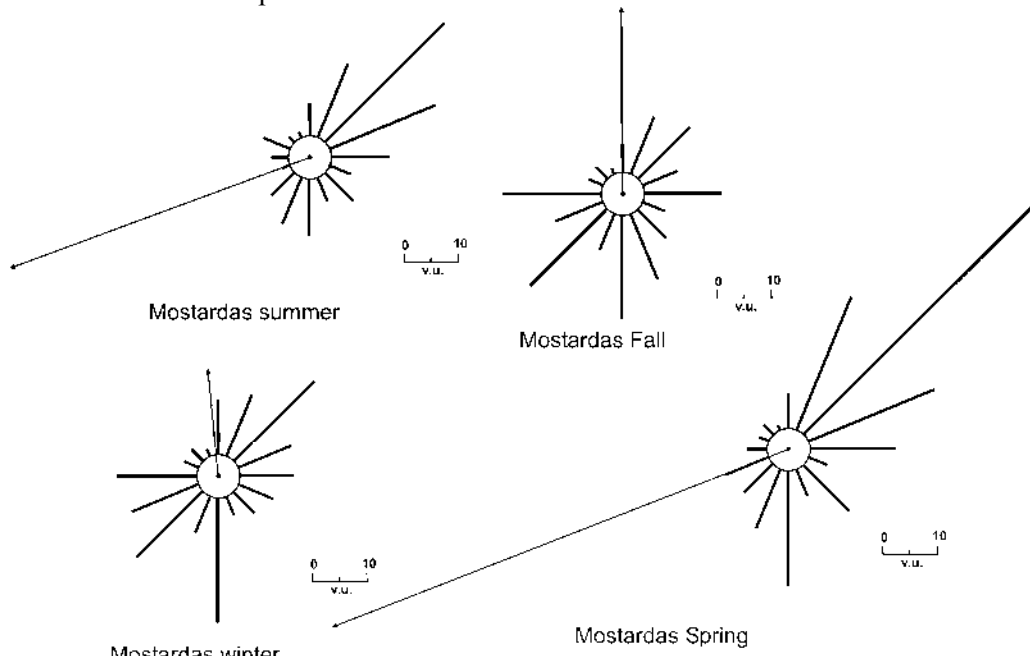


Figure 11: Sand roses of the seasons at Mostardas station. The lines represent the DP for each direction and the arrow represents the RDP and RDD.

4.7.3. Yearly changes in the wind drift potential

The Imbé data was analyzed by its yearly drift potential and these data were plotted with the records of SO events (in section - *Precipitation and ENSO events*) above. The total DP of winds and the DP of NE winds, the most important winds for sand transport, showed some trends. More clearly in the total DP than in the NE DP,

there is a tendency of increasing DP's during La Niña events (Fig. 12 and 13). These results combined with the observed decrease in precipitation during La Niña makes this event the perfect period for dune initiation and/or high dune migration rates.

Another tendency is the interdecadal DP variations. From 1948 to 1955 there was a decrease in the total DP's, from 1955 to 1965 a strong increase and from 1964 to 1988 a continuous decrease and then again from 1988 to 2003 a gentle increase (Fig. 14). Eden & Jung (2001) describe from 1960 to 1984 a negative anomaly in the North Atlantic sea surface temperature associated to the North Atlantic Oscillation (NAO). According to these authors this negative anomaly is a lagged response for the persistent low phase in the NAO which started in the 1950's. Perhaps with a lag around 4 years this negative anomaly in the North Atlantic sea surface temperature has been influencing the winds at southern Brazil.

This great decrease in the drift potential combined with an observed increase in precipitation (section above) could be responsible for the stabilization and vegetation of large dunefield areas.

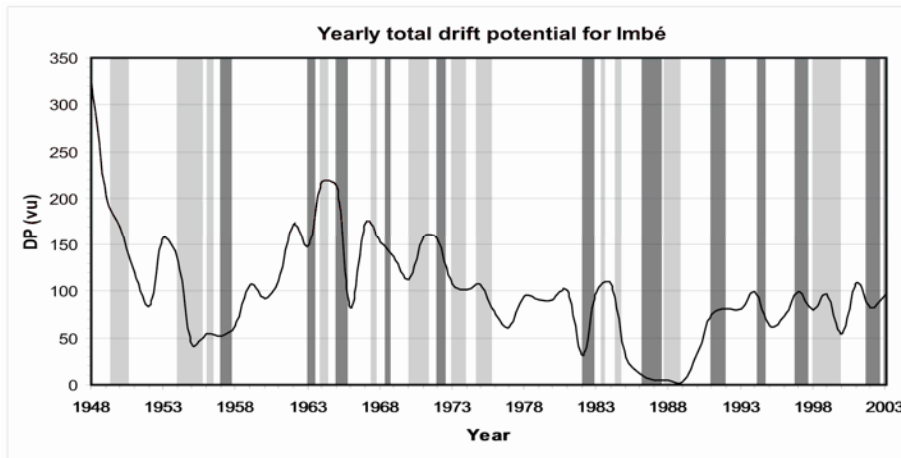


Figure 12: Yearly total DP for Imbé station. Light gray bars represent cold events (La Niña) and dark gray bars represent warm events (El Niño).

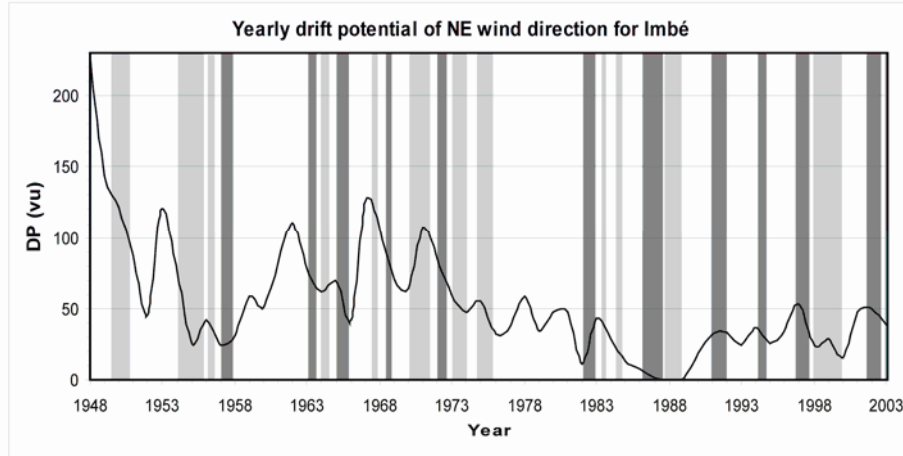


Figure 13: Yearly DP of NE winds for Imbé station. Light gray bars represent cold events (La Niña) and dark gray bars represent warm events (El Niño).

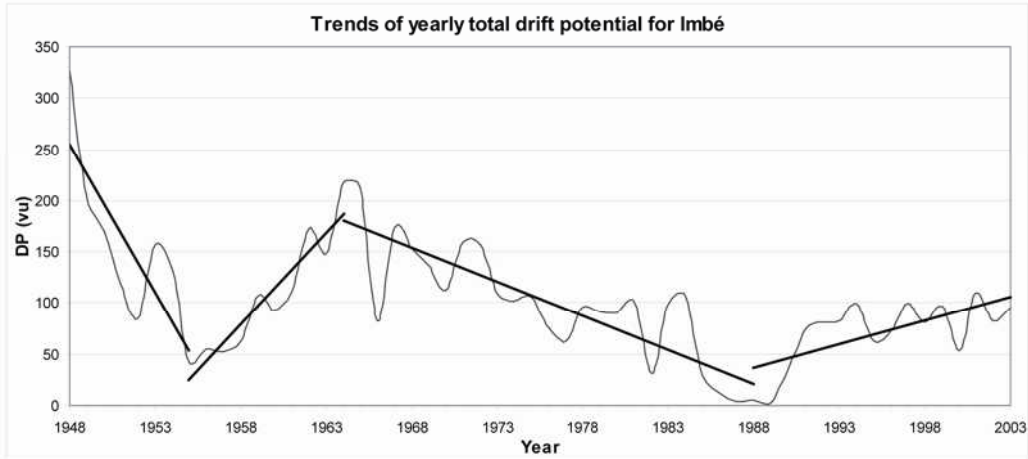


Figure 14: Annual total DP showing trends of interdecadal variations.

4.8. DISCUSSION AND CONCLUSIONS

Climate variations in Southern Brazil can have a strong influence on dunefields changes in this region. Interdecadal and interannual cycles produced by NAO or SO create variations in rainfall and winds. Understanding the actual climate patterns and the temporal variations could help in understanding dunefield behavior in the past and predict its future paths.

The RS coast is dominated by two climate patterns, the SASM and the mid-latitude climate. These two climate regimes, in addition with great topographic variation along the coast, create differences in wind patterns and precipitation between coastal sectors. At the northern littoral there are high gradients of the Serra Geral scarps near the coast and the SASM dominates. The rainfall in this area is higher due to

orographic precipitation, and NE-SW winds blow predominantly parallel to the scarps with lower velocities.

Mid-latitude climate predominates on the mid and southern littoral which are flat and open regions more susceptible to winds blowing stronger and from every direction.

The wind patterns and sand drift potential vary along the coast. At Torres the E-NE and S-SW winds are very important due to the topography of the landward scarp. Winds from NE and S are responsible for the sand drift potential to the NW in the area. At Imbé winds from the NE are the most frequent and the strongest, producing a sand drift potential predominantly to the SW. Mostardas has a broader range of wind directions, but the NE-E and S-SW are the most important. Together these directions produce a resultant drift potential to the W, making a 45° angle with the shoreline. Mostardas is the windiest station, with high frequencies of strong winds and with the smallest number of calms. At Rio Grande the winds velocity is low and the NE and SW are the most frequent directions, but they annul each other creating a very small sand drift potential to NW.

Chuí and Tramandaí, with not long but with the same period of observations showed how different the winds blow over the northern littoral versus the southern littoral. At Tramandaí the wind pattern was very similar to Imbé, the NE winds predominate and produce RDP to the SW. At Chuí the most frequent wind was ENE, but the S winds had higher velocities what produced a RDP to the NNW.

In general, winds from the S have more influence in the middle and southern littoral of RS. This probably occurs due to topographic effects. In the north, as showed the Itapeva data, the scarps of the Serra Geral are a barrier for wind flow and definitely change the wind patterns in this area. Along the scarp the wind blows predominantly parallel to it, orientated NE-SW, and with low velocities. At northern littoral, the large amount of rainfall (SEMC 2002) and the low wind velocities produce a small potential to develop large dunefields (Wilson 1972; Fryberg & Dean 1979; Lancaster 1988; Hesp & Thom 1990; Treinhaile 1997; Bauer & Sherman 1999). The middle and southern littoral are flat and open regions, without significant topographic gradients, making them more susceptible to wind blowing stronger and from many directions. This fact associated with less rainfall in this area (SEMC 2002) makes the middle and southern littoral more propitious areas for the formation of large dunefields

(Wilson 1972; Fryberg & Dean 1979; Lancaster 1988; Hesp & Thom 1990; Treinhaile 1997; Bauer & Sherman 1999).

The climate and wind patterns change not only along RS coast but also seasonally. In the passage from summer to fall the NE winds decrease in speed and frequency and the W winds increase. Months with the highest DP's are September, October and November, and the association with low values of precipitation in October and November, makes spring the season with the highest dune migration rates with the RDD to the SW. The end of winter (August/September) is the period of the year with highest rainfall and low DP's during August making this season the lowest potential dune migration period.

During SO events some consistent trends were observed, despite a few anomalies that did not occur during these events. During El Niño events and/or in the year after the event, there is an increase in precipitation. The year before El Niño tends to be drier. The increase in moisture disfavors the sand transport by increasing the threshold velocity (Bagnold 1941; Belly 1964), and facilitate the vegetation growth that also increase the threshold wind velocity by increasing the surface roughness (Bagnold 1941; Belly 1964; Hesp 1989). Taking these premises, due to high moisture, during El Niño events it is likely that dunefields would have their rate of migration lowered and even some of their area stabilized by vegetation (Marcomini & Maidana 2006), while the opposite tendency is expected in the year before the event.

During La Niña events the precipitation tends to decrease while the DP of NE winds increases. The low moisture associated with highest wind drift potentials makes La Niña the event of expected high dune migration (Bagnold 1941; Belly 1964). The decrease in moisture can also produces the decline or death of foredune vegetation and creates new blowouts and even the initiation of new dunefields (Davies 1980; Hesp 1988; Hesp & Thom 1990; Bauer & Sherman 1999; Hesp 2000).

For the 55 years period (1948 to 2003) there is a gentle tendency of increasing precipitation by about 20 mm. From 1964 to 1988 the total DP and the DP of NE winds have a trend of continuously decreasing, possibly associated with the interdecadal variation in the North Atlantic sea surface temperature driven by the NAO. The gentle increase in precipitation increase the threshold wind velocity and the decrease in DP means that less winds will have the capacity of transport, so both acting in concert will reduce significantly the dune movement rates (Bagnold 1941; Belly 1964). Furthermore, all these factors induce vegetation growth which, taking the

example of Marcomini & Maidana (2006), can be the key to dunefield stabilization. Thus, during this period it is highly likely that a large portion of the dunefields have been stabilized, as observed at Argentina coast for the same period (Marcomini & Maidana 2006).

ACKNOWLEDGMENTS

This research was partly supported by grants of RECOOS-Institutos do Milênio and Conselho Nacional de Desenvolvimento Científico e Tecnológico (CNPq). We thanks CNPq for the PhD. scholarship and Comissão Permanente de Aperfeiçoamento de Pessoal de Nível Superior (CAPES) for the doctorate *sandwich* scholarship, to the first author. Thanks also Marinha do Brasil, Superintendência de Portos e Hidrovias and RECOOS for provide the wind and precipitation data, to Graziela Miot da Silva for her assistance with the DP calculations and Patrick Hesp LSU for support. Sérgio Dillenburg thanks CNPq for his scholarship.

REFERENCES

- BAGNOLD, R.A. 1941. *The physics of blown sand and desert dunes*. London, Chapman & Hall, 265p.
- BARROS, V.R.; GRIMM, A.M.; DOYLE, M.E. 2002. Relationship between temperature and circulation in southeastern South America and its influence from El Niño and La Niña events. *J. Meteorological Society of Japan*, **80** (1): 21-32.
- BAUER, B.O.; SHERMAN, D.J. 1999. Coastal dune dynamics: Problems and prospects. In: GOUDIE, A.S.; LIVINGSTONE, I.; STOKES, S. (Eds.) *Aeolian environments, sediments and landforms*. John Wiley & Sons, Ltd. 71-104.
- BELLY, P.Y. 1964. *Sand Movement by Wind*. US Army Corps of Engineers Technical Memo No. 1.
- BULLARD, J.E. 1997. A note on the use of the Fryberger method for evaluating potential sand transport by wind. *J. Sediment. Res.*, **67** (3A): 499-501.
- CLARKE, M.L.; RENDELL, H.M.; PYE, K.; TASTET, J.P.; PONTEE, N.I.; MASSÉ, L. 1999. Evidence for the timing of dune development on the Aquitaine coast, southwest France. *Z. Geomorph. N.F. Suppl.Bd*, **116**: 147-163.
- CLEMMENSEN, L.B.; ANDREASEN, F.; HEINEMEIER, J.; MURRAY, A.S. 2001. A Holocene coastal aeolian system, Vejers, Denmark: landscape evolution and sequence stratigraphy. *Terra Nova*, **13**: 129-134.
- CRUZ JR, F.W.; BURNS, S. J.; KARMANN,I.; SHARP, W.D.; VUILLE, M.; CARDOSO, A.O.; FERRARI, J.A.; DIAS, P.L.S.; VIANA JR, O. 2005.

- Insolation-driven changes in atmospheric circulation over the past 116,000 years in subtropical Brazil. *Nature*, **434**: 63-66.
- DAVIES, J.L. 1980. *Geographical variation in coastal development*. Longman. London. 212 pp.
- DILLENBURG, S.R.; TOMAZELLI, L.J.; HESP, P.A.; BARBOZA, E.G.; CLEROT, L.C.P.; SILVA, D.B. (2006). Stratigraphy and evolution of a prograded, transgressive dunefield barrier in southern Brazil. *Journal of Coastal research SI* **39**: 132-135.
- EDEN, C.; JUNG, T. 2001. North Atlantic interdecadal variability: oceanic response to the North Atlantic Oscillation (1865-1997). *Journal of Climate*, **14**: 676-691.
- FILION, L. 1984. A relationship between dunes, fire and climate recorded in the Holocene deposits of Quebec. *Nature*, **309**: 543-546.
- FORMANN, S.L.; MARÍN, L.; PIERSON, J.; GÓMEZ, J.; MILLER, G.H.; WEBB, R.S. 2005. Aeolian sand depositional records from western Nebraska: landscape response to droughts in the past 1500 years. *The Holocene*, **15** (7): 973-981.
- FRYBERGER, S.G.; DEAN, G. 1979. Dune forms and wind regime. In: MCKEE, E.D. (Ed.) *A study of global sand seas*. USGS, Professional paper **1052**:137-169.
- GIANNINI, P.C.F. 1993. *Sistemas Deposicionais no Quaternário Costeiro entre Jaguaruna e Imbituba, SC*. São Paulo, Inst. Geoc. Univ. S. Paulo. Tese de Doutoramento (inéd.) 2v, 2 mapas, 439p..
- GRIMM, A.M.; FERRAZ, S.E.T.; GOMES, J. 1998. Precipitation anomalies in Southern Brazil associated with El Niño and La Niña events. *J. Climate*, **11**: 2863-2880.
- GRIMM, A.M.; BARROS, V.R.; DOYLE, M.E. 2000. Climate variability in Southern South America associated with El Niño and La Niña events. *J. Climate*, **13**: 35-58.
- HESP, P.A. 1988. Morphology, dynamics and internal stratification of some established foredunes in Southeast Australia. *Sediment. Geol.*, **55** (1/2): 17-41.
- HESP, P.A. 2000. *Coastal sand dunes. Form and Function*. CDNV Technical Bulletin No. 4. Massey University, 28 pp.
- HESP, P.A. 2003. El Niño winds and dune dynamics, west coast, North Island, New Zealand. *Canadian Coastal Conference Index*, 1-6.
- HESP, P.A. & THOM, B.G., 1990. Geomophology and evolution of active transgressive dunefields. In: NORDSTROM, K.F.; PSUTY, N.P.; CARTER, R.W.G. (Eds.) *Coastal Dunes: Form and Process*. Chichester, John Wiley & Sons Ltd. 253-288.
- HESP, P.A.; DILLENBURG, S.R.; BARBOZA, E.G.; TOMAZELLI, L.J.; AYUP-ZOUAIN, R.N.; ESTEVES, L.S.; GRUBER, N.L.S.; TOLDO JR., E.E.; TABAJARA, L.L.C.A.; CLEROT, L.C.P. 2005. Beach ridges, foredunes or

- transgressive dunefields? Definitions and an examination of the Torres to Tramandaí barrier system, Southern Brazil. *Anais da Academia Brasileira de Ciências* 77 (3): 493-508.
- HUGENHOLTZ, C.H.; WOLFE, S.A. 2005. Recent stabilization of active sand dunes on the Canadian prairies and relation to recent climate variations. *Geomorphology*, **68**: 131-147.
- IAEA/WMO. 1994. Global Network for Isotopes in Precipitation (GNIP) Database. IGBP PAGES/World Data Center-A for Paleoclimatology Data Contribution Series # 94-005. NOAA/NGDC Paleoclimatology Program, Boulder, Colorado, USA. <http://isohis.iaea.org>
- ILLENBERGER, W.K.; VERHAGEN, B.T. 1990. Environmental history and dating of coastal dunefields. *Suid-Afrikaanse Tydskrif vir Wetenskap*, **86**: 311-314.
- KREPPER, C.M.; GARCÍA, N.O.; JONES, P.D. 2003. Interannual variability in the Uruguay river basin. *International journal of climatology* **23**: 103-115.
- LANCASTER, N. 1988. The development of large aeolian bedforms. *Sedimentary geology*, **55**: 69-89.
- LETTAU, K.; LETTAU, H.H. 1978. Experimental and micrometeorological fields studies on dune migration. In: LETTAU, K.; LETTAU, H.H. (Eds.), *Exploring the world's driest climate*: Wisconsin. Univ. Wisconsin-Madison, Institute of Environmental Sciences, 110-147.
- LIMA, S.F.; ALMEIDA, L.E.S.B.; TOLDO JR., E.E. 2001. Estimate of longshore sediments transport from waves data to the Rio Grande do Sul coast. *Pesquisas*, **48** (2): 99-107.
- MAIA, L.P.; FREIRE, G.S.S.; LACERDA, L.D. 2005. Accelerated dune migration and aeolian transport during El Niño events along the NE Brasilian coast. *Journal of coastal research*, **21** (6): 1121-1126.
- MASLIN, M. A.; BURNS, S.J. 2000. Reconstruction of the Amazon basin effective moisture availability over the past 14,000 yrs. *Science* **290** (5500): 2285-2287.
- MARCOMINI, S.C.; MAIDANA N. 2006. Response of eolian ecosystems to minor climatic changes. *Journal of Coastal research* **SI 39**: 204-208.
- MURRAY, A.S.; CLEMENSEN, L.B. 2001. Luminescence dating of Holocene aeolian sand movement, Thy, Denmark. *Quaternary Sciences Reviews*, **20**: 751-754.
- ORFORD, J.D. 2005. The controls on Late-Holocene coastal dune formation on leeside coasts of the British Isles. *Z. Geomorph. N. F.*, **141**: 135-152.
- PEARCE, K.I.; WALKER, I.J. 2005. Frequency and magnitude biases in the 'Fryberger' model, with implications for characterizing geomorphically effective winds. *Geomorphology* **68**: 39-55.

- ROBERTSON, A.W.; MECHOSO, C.R. 1998. Interannual and decadal Cycles in River flows of Southeastern South America. *Journal of climate* **11**: 2570-2581.
- SEMC – SECRETARIA de ENERGIA, MINAS e COMUNICAÇÕES. 2002. *Atlas Eólico: Rio Grande do Sul*. Porto Alegre: SEMC, 70p.
- SHULMEISTER, J.; LEES, B. 1992. Morphology and chronostratigraphy of coastal dunefield: Groote Eylandt, northern Australia. *Geomorphology*, **5**: 521-534.
- TOMAZELLI, L.J. 1990. *Contribuição ao Estudo dos Sistemas Depositionais Holocénicos do Nordeste da Província Costeira do Rio Grande do Sul, com Ênfase no Sistema Eólico*. Porto Alegre, Univ. Federal Rio Grande do Sul. Tese de Doutoramento (inéd). 270p.
- TOMAZELLI, L.J. 1993. Regime de ventos e taxa de migração de dunas eólicas costeiras do Rio Grande do Sul, Brasil. *Pesquisas*, **21**(1): 64-71.
- TOMAZELLI, L.J.; VILLWOCK, J.A. 1992. Considerações sobre o ambiente praial e deriva litorânea de sedimentos ao longo do Litoral norte do Rio Grande do Sul, Brasil. *Pesquisas*, **19** (1): 3-12.
- TOMAZELLI, L. J., VILLWOCK, J. A., DILLENBURG, S. R., BACHI, F. A., DEHNHARDT, B. A., 1998. Significance of present-day coastal erosion and marine transgression, Rio Grande do Sul, Southern Brazil. *Anais da Academia Brasileira de Ciências*, **70**(2): 221-229.
- TRENHAILE, A.S., 1997. Sand Dunes. In: TRENHAILE, A.S. (Ed.) *Coastal Dynamics and Landforms*. Oxford, Clarendon Press, p.144-169.
- WANG, Y.J.; CHENG, H.; EDWARDS, R.L.; AN, Z.S.; WU, J.Y.; SHEN, C.C.; DORALE, J.A. 2001. A high-resolution absolute-dated Late Pleistocene monsoon record from Hulu Cave, China. *Science* **294**: 2345-2348.
- WANNER, H.; BRÖNNIMANN, S.; CASTY, C.; GYALISTRAS, D.; LUTERBACHER, J.; SCHMUTZ, C.; STEPHENSON, D.B.; XOPLAKI, E. 2001. North Atlantic Oscillation – Concepts and Studies. *Surveys in Geophysics*, **22**: 321-382.
- WILSON, I.G., 1972. Aeolian bedforms – Their development and origins. *Sedimentology* **19**: 173-210.
- WILSON, P.; ORFORD, J.D.; KNIGHT, J.; BRALEY, S.M.; WINTLE, A.G. 2001. Late-Holocene (post-4000 years BP) coastal dune development in Northumberland, northeast England. *The Holocene*, **11** (2): 215-229.
- ZINGG, A.W., 1953. Wind tunnel studies of the movement of sedimentary material. *Proc. 5th Hydraulics Conf. Bull.* **34**, Inst. of Hydraulics, Iowa City, pp. 111-135.
- ZHOU, J.; LAU, K.M. 1998. Does a monsoon climate exist over South America? *J. Climate*, **11**: 1020-1040.

CAPÍTULO 5

MORPHOLOGICAL AND TEMPORAL VARIATIONS OF TRANSGRESSIVE DUNEFIELDS OF THE NORTHERN AND MID- LITTORAL RIO GRANDE DO SUL COAST

Artigo submetido à *Geomorphology*



[Print](#) - [Close Window](#)

From: "Geomorphology" <submissionsupport@elsevier.com>

To: ctmartinho@yahoo.com

Date: 20 Feb 2008 22:27:53 +0000

Subject: Submission Confirmation

Dear Thais,

Your submission entitled "Morphological and Temporal Variations of Transgressive dunefields of the Northern and Mid-littoral of Rio Grande do Sul coast, Southern Brazil" has been received by Geomorphology

You may check on the progress of your paper by logging on to the Elsevier Editorial System as an author. The URL is
<http://ees.elsevier.com/qgeomor/>.

Your username is: Thais

Password: [if you have forgotten your password, please click the "Forgot your password?" link located on the login screen.]

Your manuscript will be given a reference number once an Editor has been assigned.

Thank you for submitting your work to this journal.

Kind regards,

Elsevier Editorial System
Geomorphology

Morphological and Temporal Variations of Transgressive dunefields of the Northern and Mid-littoral Rio Grande do Sul coast, Southern Brazil

Caroline T. Martinho^a, Patrick A. Hesp^b, Sergio R. Dillenburg^c

^a Universidade Federal do Rio Grande do Sul
Instituto de Geociências
Programa de Pós-Graduação em Geociências
Av. Bento Gonçalves 9500
91509-900, Porto Alegre, RS, Brasil
Tel: + 55 51 30295689 Fax: + 55 51 33086332
ctmartinho@yahoo.com

^b Louisiana State University
Department of Geography and Anthropology
227 Howe/Russell Geosciences Complex
Baton Rouge, LA 70803-4105, USA
pahesp@lsu.edu

^c Universidade Federal do Rio Grande do Sul
Instituto de Geociências
Centro de Estudos de Geologia Costeira e Oceânica
Av. Bento Gonçalves 9500
91509-900, Porto Alegre, RS, Brasil
sergio.dillenburg@ufrgs.br

ABSTRACT

Transgressive dunefields are present along the entire stretch of the Rio Grande do Sul (RS) coast from Rondinha to Mostardas, although the dunefields change their morphology and size along the coast and through time. The aim of this paper is describe these changes and understand the factors responsible for them. At the northern littoral, the dunefields are narrow (1300 to 1400m wide) due to the local higher precipitation, lower wind drift potential (DP) and smaller sand supply. Southwards the dunefields increase in size, reaching 6900m in width due to the decrease in precipitation, increase in wind Drift Potential (DP) and possibly a larger volume of sand supply.

For the last 58 years, all the studied dunefield have experienced an enlargement in the extent of deflation zone, vegetation cover, and humid/moist areas promoted by an historical increase in precipitation and a decrease in wind DP. The northern dunefields have less sand, and are more susceptible to stabilization, whereas in the mid-littoral dunefields, the stabilization processes take longer due to the larger amount of sand, and ongoing coastline erosion.

5.1. INTRODUCTION

Transgressive dunefields are relatively large-scale coastal sand bodies with little vegetation when active that migrate perpendicular, obliquely landwards or alongshore (Hesp & Thom 1990; Trenhaile 1997; Hesp 1999). Within the dunefields may be found a large variety of dune types such as dome dunes, barchans, barchanoid chains, transverse dunes, aklé or network dunes, and depositional lobes (Hesp & Thom 1990; Hesp 1999; Martinho *et al.* 2006). The margins are often formed by precipitation ridges (Hesp & Thom 1990). The development of a dunefield can create sub-environments dominated by erosional landforms, particularly deflation plains or basins (or slacks) (Ranwell 1972; Hesp & Thom 1990; Trenhaile 1997; Hesp 1999). The deflation plains are relatively flat, humid and frequently vegetated areas separating the barchanoid and transverse dune area from the beach. Although they display a predominantly erosive character, within the deflation plain there is a range of depositional morphologies which usually are dune types dominated by vegetation and typical from humid areas like parabolic dunes, trailing ridges, gegenwalle ridges and

nebkhas (Paul 1944; Hesp & Thom 1990; Piotrowska & Gos 1993; Martinho *et al.* 2006). The seaward margin of many transgressive dunefields may be composed of foredunes, whether incipient or established ridges. Locally these foredunes rupture forming blowouts that can migrate over the deflation plain, evolving into parabolic dunes and eventually feed the mobile sand dune area (Hesp 1999). Some dunefields do not have foredunes at all, especially where the dunefield is migrating alongshore, sand supply is high, or the coast is moderately to highly erosional (Hesp 2004; Hesp & Martinez 2007).

One rule for the initiation and maintenance of a dunefield is sand availability in adequate grain size and winds with velocity and direction appropriate to transport the sand (Bagnold 1941; Belly 1964). The main control agents that can initiate the formation or complete stabilization of a dunefield are variations in the relative sea level (RSL), climatic changes, antecedent topography, surfzone-beach morphodynamic type, and human activities. All those agents can influence the dunefield behavior by changing the sand supply, wind velocity, direction and frequency, wave energy, coastline orientation in relation of effective winds, vegetation cover etc.

In the literature there is a general consensus that only beach ridges or foredune ridges form on prograding coasts and that it is necessary for the coastline and shoreface to be erosional in order to build coastal dunefields (Pye & Bowman 1984; Short 1988a; Roy *et al.* 1994). Nevertheless, along the RS coast, as elsewhere (e.g. NZ coast; Shepherd & Hesp, 2003) there is a co-existence of progradational, aggradational and retrogradational barriers and transgressive dunefields form the predominant terrestrial landform on all of them (Dillenburg *et al.* 2000; Hesp *et al.* 2005, 2007; Martinho *et al.* accepted). Thus, is it really necessary to have coastline erosion in order to have transgressive dunefield formation? Would it only be necessary to have enough available sand supply and wind with potential to transport the sand?

Dunefield development related to RSL rise is broadly accepted in the literature and is described for coasts all over the world including Australia (Pye 1983; Pye & Bowman 1984; Pye & Rhodes 1985; Carter 1988; Short 1988b; Roy *et al.* 1994; Carter & Chance 1997; Hesp & Short 1999); New Zealand (Shepherd & Hesp 2003), British Islands (Wilson *et al.* 2001; Orford 2005); Brazil (Tomazelli 1990, 1994; Dillenburg *et al.* 2000; Giannini *et al.* 2001a, b; Hesp *et al.* 2007); France (Bressolier *et al.* 1990; Tastet & Pontee 1998, Clarke *et al.* 1999); Lake Michigan (Loope & Arbogast

2000); South Africa (Illenberger 1988; Illenberger & Verhagen 1990); USA (Cooper 1958, 1967) etc.

These authors associate the formation of transgressive dunefields with the eustatic sea level rise during the early Holocene, related to the last post-glacial period. The sea level rise induces the coastline erosion, and as a result, a large volume of sand may be emplaced on the shoreface (Roy *et al.* 1994). With an adequate wave regime and inner shelf slope, it is possible to transfer this sand from the shoreface to the backshore. Subsequently, the sediments became available to be transported by wind feeding a new transgressive dunefield (also known as primary dunes *sensu* Davies 1980, Short 1988b). If foredunes are present, the foredune erosion also induces blowout formation (Hesp 1999). So, the sand that previously was protected by the vegetation becomes available to be transported landwards and to initiate a new transgressive dunefield (also known as secondary dunes *sensu* Davies 1980, Short 1988b).

Nevertheless, in many places, including the Rio Grande do Sul (RS) coast, the RSL has remained stable or with very small variations (~2m) after it reached its actual position at ~ 7000 - 6500 years before present (yr BP) (Dillenburg *et al.* 2006; Hesp *et al.* 2007). If the RSL has been approximately stable for the last 7000-6500 yr in these places, how can one explain the dunefield formation in this period? Many authors attribute the dunefield formation during the early Holocene to the marine transgression, while those portions of the dunefields formed during the mid and late Holocene would be produced by changes in climate. These climate changes would include changes in temperature, moisture, wind and wave regimes (Thom 1978; Davies 1980; Filion 1984; Short 1988b; Shulmeister & Lees 1992; Young *et al.* 1993; Clarke *et al.* 1999; Clemmensen *et al.* 2001; Murray & Clemmensen 2001; Wilson *et al.* 2001; Formann *et al.* 2005; Hugenholtz & Wolfe 2005; Orford 2005).

Climatic changes may produce a variety of changes including:

- (1) Events of colder temperatures can induce the death of vegetation cover, reducing the dune stability and consequently creating the possibility for dunefield formation (Wilson *et al.* 2001).
- (2) An increase in the storminess or in the breaker wave energy is also described in the literature as responsible for dune formation as the increase in wave energy or storminess allows for an increase in sediment supply particularly in shelf supplied beach systems (Thom 1978; Short 1988b; Clarke *et al.* 1999; Orford 2005). In

addition, an increase in storminess could reduce the foredune stability (Short 1988b; Clarke *et al.* 1999; Wilson *et al.* 2001; Orford 2005).

- (3) An increase in the wind velocity is also considered to be potentially responsible for dunefield formation and high rates of migration (Hesp 2003; Chase & Thomas 2006, 2007) as well as changes in the wind direction, from offshore to onshore (Clemmensen *et al.* 2001; Murray & Clemmensen 2001; Wilson *et al.* 2001; Orford 2005).
- (4) Periods of increased dryness or drought can also be responsible for dunefield formation by increasing fires, death of vegetation and lowering the water table producing an increase in the available sediments to be transported by winds (Filion 1984; Shulmeister & Lees 1992; Formann *et al.* 2005; Hugenholtz & Wolfe 2005). In contrast, an increase in precipitation can increase grain cohesion and threshold velocity, reducing the wind transport and favoring vegetation growth (Hesp 1999; Clemmensen *et al.* 2001; Hugenholtz & Wolfe 2005; Marcomini & Maidana 2006; Martinho *et al.* submitted).

The antecedent topography of the coast can also influence the dynamics of aeolian processes. Regions where the coastline is convex and the inner shelf is steep and narrow tend to concentrate the wave energy, and as stated above, an increase in wave energy can be responsible for the formation of dunefields (May & Tanner 1973; Pye & Rhodes 1985; Short 1988b; Dillenburg *et al.* 2000, 2003, 2004 a,b; Martinho *et al.* accepted). Abrupt changes in coastline orientation can also locally decrease the longshore sediment transport rates and provoke a local positive sand budget on the shoreface, and with an adequate wave regime this sand can be transported to the backshore and become available for wind transport (Lees 2006; Toldo Jr. *et al.* 2006).

Short & Hesp (1982) and Hesp (1988) relate the presence or absence of particular dunefield and barrier types with surfzone-beach morphodynamic type. In this model, subsequently tested and validated by Sherman & Lyons (1994), dissipative beaches, being flatter and wider than reflective beaches have a longer wind fetch, and consequently their aeolian transport would be higher. Thus, the probability of large scale and often transgressive dunefield formation adjacent to dissipative beaches is much higher than on reflective beaches.

On the Rio Grande do Sul coast, in the stretch from Torres to Mostardas, all beaches are dissipative and the barrier types change from progradational to retrogradational (Dillenburg *et al.* 2000; Hesp *et al.* 2005; Martinho *et al.* accepted).

Nevertheless, principally transgressive dunefields are present along the entire coast, although their shape, sediment volume and size change along the coast and through time. The aim of this paper is to describe their spatio-temporal changes and to attempt to provide an understanding of the factors which are responsible for them.

5.2. METHODS

Along the study area from Torres to Mostardas, nine dunefields were analyzed and described, from north to south: Rondinha, Capão Novo, Atlântida Sul, Jardim do Éden, Magistério, Dunas Altas, Solidão, São Simão and Mostardas (Fig. 1). The coastal stretch from Rondinha to Magistério is considered the Northern littoral of RS, while from Magistério to Mostardas is Mid- littoral (according to FEPAM – www.fepam.rs.gov.br/programas/gerco.asp).

Satellite images and aerial photographs were used to map the dunefield morphologies over time. The record of those images and photos is not uniform for the entire area and the southern profiles have less data (Table 1). Satellite images from LANDSAT-7 ETM+ with 15m of resolution, LANDSAT-5 TM with 30m of resolution, LANDSAT MSS with 60m of resolution and digital elevation data with 90m of resolution were taken from the Global Land Cover Facility website (<http://glcfapp.umiacs.umd.edu:8080/esdi/search>).

The aerial photographs from 1974 and 1989 were obtained by DAER and those from 1948 were obtained from the USGS, all with a scale of 1:20,000. From the image and photo interpretation, geomorphological maps of the main features in the dunefield were created and then digitized with *ArcGIS 9.0* software.

All the dunefields studies had, or presently have mobile, active transverse dunes, barchanoidal chains, and barchan dunes as well as other dune types (e.g. blowouts, parabolic dunes etc). In order to distinguish the various types, and particularly distinguish the partially vegetated but still active types (e.g. parabolic dunes) from the unvegetated types, we refer to all active barchanoidal, barchan and transverse dunes as b/t dunes in this paper.

Table 1: Satellite images and aerial photographs available for each dunefield and their acquisition year.

Resolution/ Scale	LANDSAT- 7 ETM+	LANDSAT- 5 TM	LANDSAT MSS	Photos from 1989	Photos from 1974	Photos from 1948
	15m	30m	60m	1:20,000	1:20,000	1:20,000
Rondinha	2000	1986	1980	X	X	
Capão Novo	1999	1987	1980	X	X	X
Atlântida Sul	1999	1987	1980		X	X
Jardim do Éden	1999	1987	1980		X	X
Magistério	1999	1987	1980		X	X
Dunas Altas	1999	1987	1980		X	
F. Solidão	1999	1987	1980			
São Simão	1999	1988	1973			
Mostardas	1999	1988	1973			

5.3. REGIONAL SETTINGS

The study area is located in the RS coastal plain, in the stretch from Torres to Mostardas, with approximated 250 km in length and a quasi-continuous coastline, interrupted only by the Tramandaí Lagoon inlet. This coastal stretch present high topographic gradients, having in the northern littoral the scarps from Serra Geral very close to the coast, and southwards a wide coastal plain with extremely flat and open surface.

The RS coast is characterized by a barrier-lagoon depositional system, dominated by waves. The accepted evolution model for the RS coastal plain is the one proposed by Villwock *et al.* (1986), on which the authors identify four Barrier-Lagoon depositional systems formed by successive RSL rise and drop during the Quaternary. The latest one, built during Holocene, is designated IV Barrier-Lagoon (Villwock *et al.* 1986). This barrier was formed around 7-8 ka BP, as a result of the migration of a transgressive barrier, during the final stages of the post-glacial marine transgression (PMT) (Hesp *et al.* 2005; Dillenburg *et al.* 2006). The IV Barrier-Lagoon formation had isolated large lagoons, which were segmented during the relative sea-level (RSL) lowering after the transgressive maximum. Besides the modern beach, the barrier consists of large dunefields, from 2 to 8 km in width (Tomazelli 1990; Hesp *et al.* 2005; Martinho *et al.* submitted b).

5.3.1. Coastline and inner shelf slope

The coastline from Torres to Mostardas is undulatory: from Torres to Imbé the coastline forms a gentle embayment, while from Imbé to Mostardas the coastline is projected. This change in the coastline orientation is paralleled by the inner shelf which is wider and gentler inside the embayment and narrower and steeper adjacent to the coastal projection (Dillenburg *et al.* 2000) (Fig. 1).

5.3.2. Waves and longshore sediment transport (LST)

Wave energy and LST vary along the coast (Dillenburg *et al.* 2003; Martinho *et al.* accepted). From Torres to Imbé, due to the fact that the coastline orientation is embayed (concave) and the inner shelf is wider and gentler (Fig. 1), the processes of refraction and dissipation by bottom friction act for a long period until the waves reach the coast, causing the waves to lose their energy (Dillenburg *et al.* 2003; Martinho *et al.* accepted). Thus, inside the coastal embayment, the wave energy and the LST rates decrease. In contrast, from Imbé to Mostardas, as the coastline orientation changes to convex, with a steeper and narrower inner shelf (Fig. 1), the refraction and dissipation processes do not act for so long and waves do not lose as much energy, resulting in an increase in wave energy and longshore sediment transport rates (Dillenburg *et al.* 2003; Martinho *et al.* accepted).

5.3.3. Barrier types

Dillenburg *et al.* (2000) states that the antecedent topography and the slope variation in the RS inner shelf, cited above, were responsible for the Holocene barrier evolution in the area and for the barrier types present along the coast. There is a coexistence of progradational, aggradational and retrogradational barriers along the RS coast. At least since 5000 yr BP, the RS coastline projections have been eroding and the coastline embayments have been prograding, smoothing the coastal profile and creating different types of barriers (Dillenburg *et al.* 2000). The change in coastline orientation from convex to embayed (concave) and the inner shelf becoming wider and gentler alongshore produce a decrease in wave energy and LST rates. This decrease creates a local positive imbalance in sediment supply (Martinho *et al.* accepted). Assuming that

this general wave and LST behavior along the RS coast has not changed substantially during the Mid and Late Holocene, the long-term operation of this positive imbalance would produce progradational barriers inside the coastal embayments.

Alongshore, as the coastline orientation changes to convex, with a steeper and narrower inner shelf, the wave energy and LST rates increase, producing a local negative sediment imbalance (Martinho *et al.* accepted). Again, considering that these conditions were roughly similar in the past, the long-term negative imbalance would cause erosion, creating retrogradational barriers along the coastal projections.

At the transition zones, between an embayment and a projection, neither depositional nor erosional processes would predominate, creating a sediment balance and producing aggradational barriers.

Thus, in the northern littoral progradational barriers predominate and retrogradational barriers are present in mid-littoral.

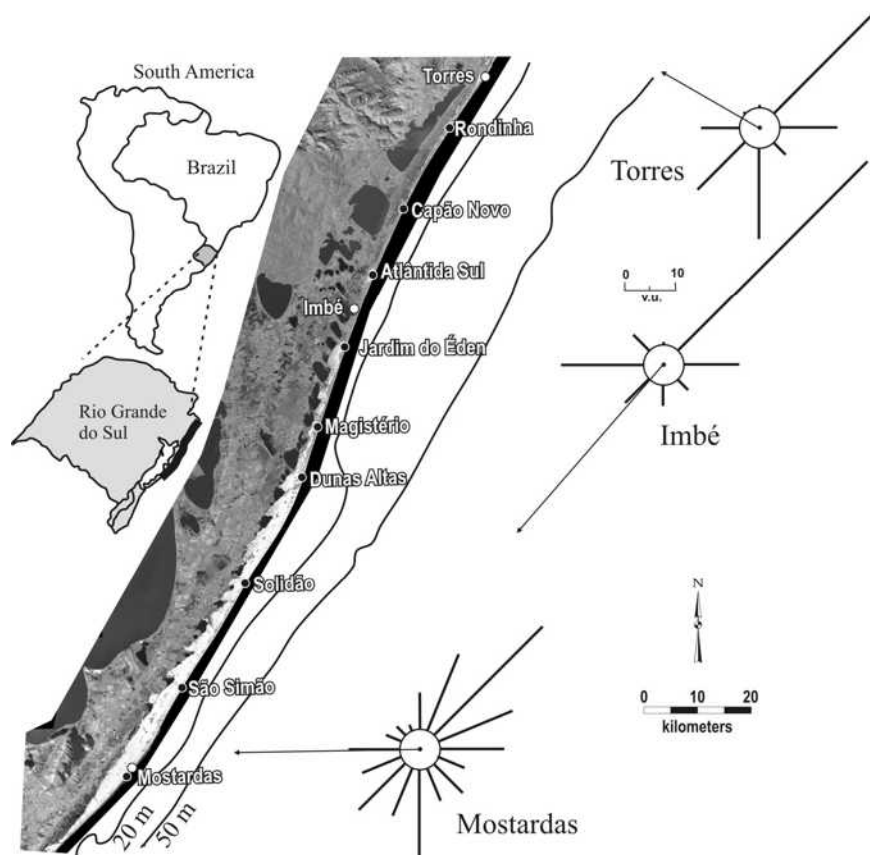


Figure 1- The northern and mid littoral of Rio Grande do Sul coast. Black dots indicate the studied dunefields. White dots are the location of meteorological stations. The continuous lines represent the isobaths of 20m and 50m. Sand roses of three stations show the drift potential (DP) for each direction in vector units (v.u.). The arrow represents the resultant drift potential (RDP) and the resultant drift direction (RDD).

5.3.4. Precipitation

The northern littoral is warmer and wetter than the rest of the coast due to the influence of the large gradients of the Serra Geral scarps. These gradients enhance the land-sea temperatures contrast and in association with the sea-land breeze that blows warm and wet air masses, produce orographic precipitation in this area (Grimm *et al.* 1998; SEMC 2002). Martinho *et al.* (submitted) analyzed the mean precipitation data of Imbé from 1948 to 2003 and observed that despite the high dispersion, the data show a tendency of increasing rainfall. In fifty five years of data, the average precipitation has increased around 20 mm. Marcomini & Maidana (2006) also observed an increase in precipitation in northern Buenos Aires province, Argentina, for the last 60 years. They describe how the transgressive dunefields have been modified by an increase in vegetation cover and a decrease in dune migration rates.

5.3.5. Winds

Martinho *et al.* (submitted) described how the winds vary along the coast using the Fryberger and Dean (1979) method calculating sand drift potentials and constructing sand roses for meteorological stations at Torres, Imbé and Mostardas (Fig. 1). In Torres the most frequent wind direction is from the E-NE. The topographic gradients of the scarp adjacent to the coast narrow the wind directions in the area, which blows predominantly parallel to the scarp, orientated NE-SW and with reduced velocity. This wind behavior can influence the dunefields in this stretch of coast. With a high frequency of the NE winds and strong S winds the resultant drift direction (RDD) results in an onshore transport to WNW, perpendicular to the coastline (Fig. 1).

In Imbé, without the presence of the scarp, winds from the NE are by far more frequent and have the highest velocities, producing a sand drift potential predominantly to the SW in this area (Fig. 1).

Due to the fact that Mostardas is a flat and open region, the area is much more susceptible to the wind blowing stronger and from every direction. So at Mostardas the range of wind directions is broader, although winds from the NE-E and the S are the most important. Together those directions produce a RDD to the W, onshore, making a 45° angle with the shoreline (Fig. 1). Winds from the NE, S and W are the strongest, with velocities higher than 17m/s. In comparison with all the other

stations, Mostardas is the windiest station, with high frequencies for wind velocities higher than 14m/s, and with the smallest number of calms.

Interdecadal variations in drift potential (DP), in Imbé, show that from 1948 to 1955 the total DP decreased and from 1955 to 1964 it increased strongly. But from 1964 to 1988 the total DP decreased continuously with a gentle increase from 1988 to 2003 (Fig. 2) (Martinho *et al.* submitted). This strong and continuous decrease in the wind from 1964 to 1988 may be crucial to dunefield behavior (Martinho *et al.* submitted).

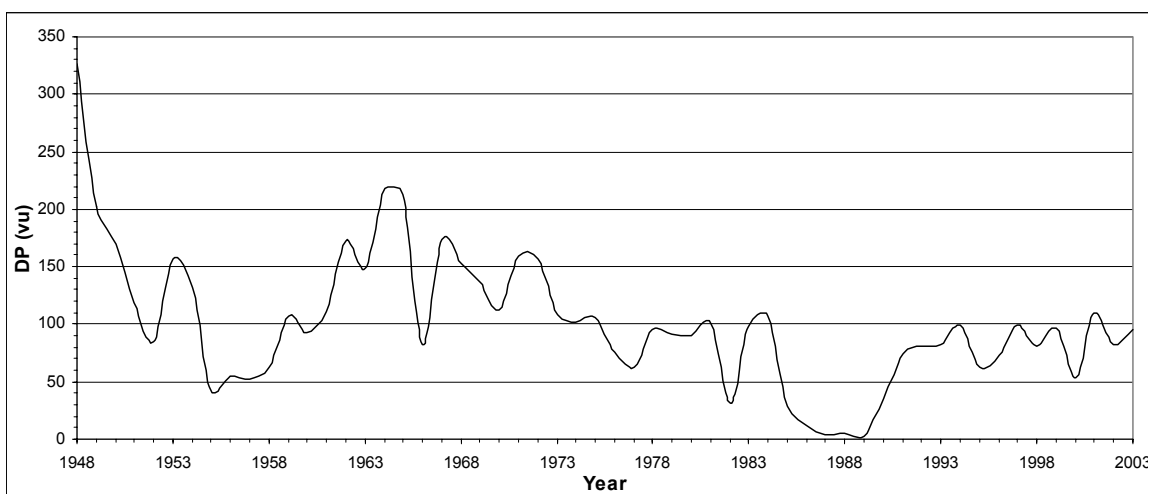


Figure 2. Annual total drift potential (DP) from 1948 to 2003 for Imbé station (Martinho *et al.* submitted).

5.4. DUNEFIELDS DESCRIPTION

5.4.1. Rondinha

Rondinha is the northernmost studied dunefield and is under the influence of the Torres sand rose (Fig. 1). At Rondinha there are two directions of sand movement, one at the dunefield scale and the other at dune scale. The dunefield migrates landwards mostly normal to the shore, blowing away from the beach, to the WNW in accord with the Torres RDD (Martinho *et al.* submitted). Its continuous migration has lead to a detachment of the main sand body from the beach, allowing the formation of a seaward deflation plain. The repetition of this process creates a new dunefield that migrates inland over the deflation plain of the previous dunefield. The overlapping dunefield phases create a morphology of successive ridges, each ridge

corresponding to the landward margin of the dunefield in the form of low precipitation ridges (Hesp 1999; Hesp *et al.* 2005, 2007) (Fig. 3).

The other important direction of migration at Rondinha is the dune migration. The transverse dunes present on the b/t dunes area, instead of migrating landwards like the dunefield, migrate roughly parallel to the coast towards the SW (Table 2). This occurs because the NE wind predominates during the dry periods while SW and S winds usually come with precipitation from the frontal systems (Tomazelli 1990; Giannini 1993; Martinho *et al.* submitted).

Hesp *et al.* 2007 described the dunefield morphology as lobate and discontinuous with its b/t dune area restricted by the presence of regularly spaced washouts that come from the center of the barrier, through stabilized dunefields and finally cut the active dunefield area (Fig. 3; Hesp *et al.* 2007).

Comparing aerial photos from 1974 with satellite images from 2000, many changes can be observed in the dunefield. In 1974 a section from the beach to the inner margin of the dunefield was composed by: beach, small sand sheet behind the backshore (~ 120m wide), very wet deflation plain with nebka fields and many creeks and washouts, and finally a b/t dune area 500m in width, with transverse and barchanoid dunes that moved parallel to the coast (Fig. 3A). In places there are several discrete b/t dune phases separated by narrow deflation plains (e.g. near-center portion of Fig. 3A). Fifteen years later, in the 1989 photos, the b/t dune area had decreased in size and height with no dune crests discernible (Fig. 3B). In 2000, a large area which was formerly b/t dunes had become either vegetated or converted to an undulating sand sheet. In addition, the deflation plain was divided into lots and urbanized, the washouts were canalized, with very little of the active dunefield remained (Fig. 3C).

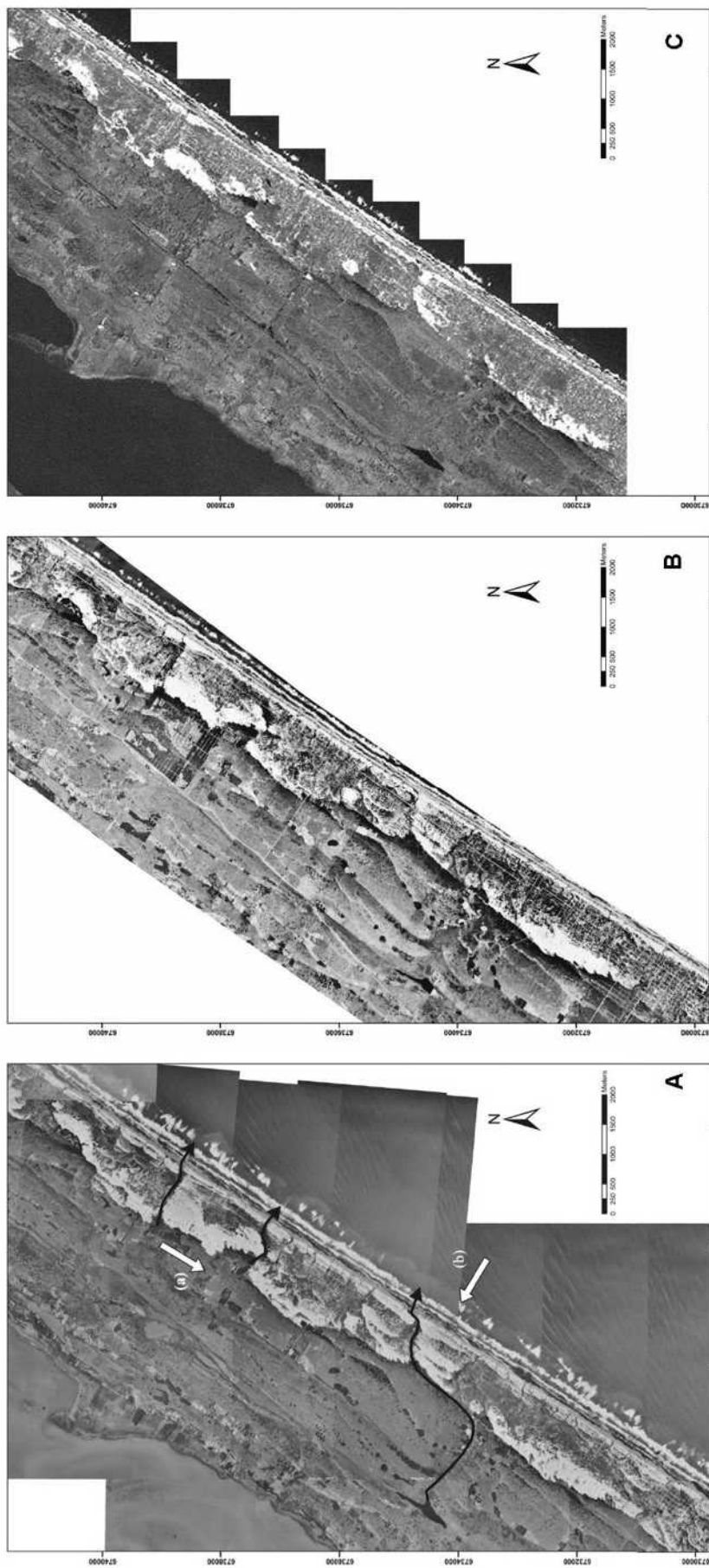


Figure 3: Rondinha dunefield. A) Aerial photo from 1974, black arrows represent the washouts. White arrows represent the main dune migration direction (a) and the main dunefield migration direction (b); B) Aerial photo from 1989 and C) Satellite image from 2000.

Table 2: Coastline orientation (A), dune movement direction (B), relationship of coastline orientation to dune movement (C), and dunefield width (D). In (A) two values for one place means that the coastline orientation changes along the dunefield from North to South.

Dunefield	A) Coast line orientation	B) Dune movement direction	(C) Angle A with B	(D) Max active dunefield width (m)
Rondinha	32°	214°	2°	1300
Capão Novo	27°	218°	11°	1400
Atlântida Sul	24°	216°	12°	2500
Jardim do Éden	21°	224°	23°	3700
Magistério	21°	234°	33°	4000
Dunas Altas	18°/24°	227°	29°/23°	5500
Solidão	35° / 30°	233°	18° / 23°	6500
São Simão	34° / 31°	230°	16° / 19°	6900
Mostardas	32° / 40°	232°	20° / 12°	6000

5.4.2. Capão Novo

Capão Novo is located adjacent to the scarps of Serra do Mar and is still under the Torres sand rose wind pattern although perhaps there is the beginning of the Imbé sand rose influence (Fig. 1). Rondinha and Capão Novo dunefields are similar in their discontinuous and lobate shape limited in alongshore movement by washouts that cut the dunefield (Hesp *et al.* 2007). Nevertheless, in Capão Novo, the dunefield migrates obliquely landward due to the angle that the coastline makes with the NE wind (Table 2). There is no deflation plain parallel to the shore between the beach and the b/t dune area. Dunes start to develop adjacent to the beach, where they are smaller with their crests tending to be parallel to the coast. Landwards, the dunes increase their size migrating to the SW, 11° oblique to the coast showing that NE winds are important in this dunefield. The main deflation areas are located around washouts. By the shape of the old dunefield the RDD from Torres, almost normal to shoreline, is a secondary movement direction and it spreads the edge of the dunefields into a quasi-parallel to shore precipitation ridge overlapping stabilized dunefields similar to Rondinha (Fig. 4).

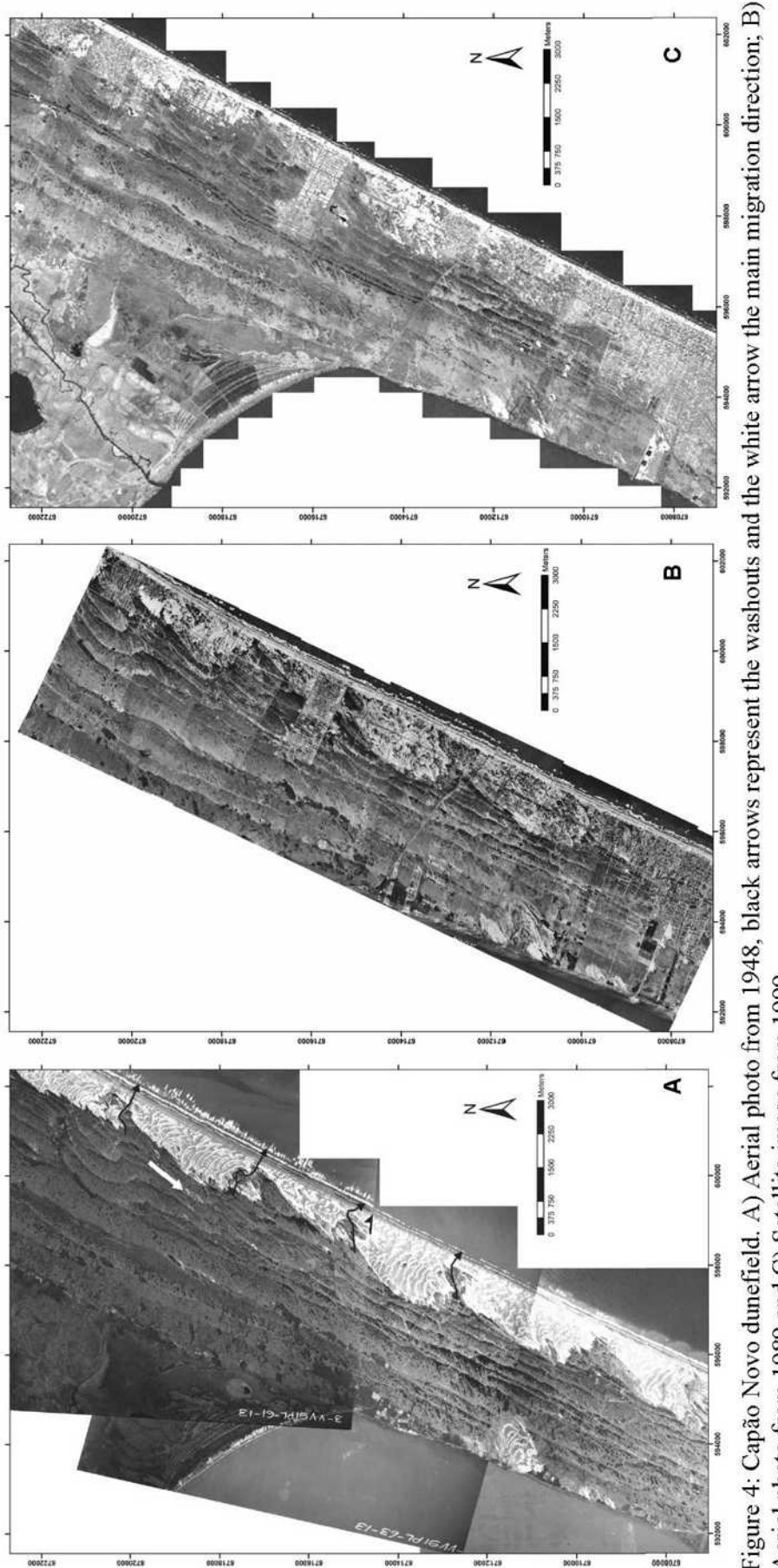


Figure 4: Capão Novo dunefield. A) Aerial photo from 1948, black arrows represent the washouts and the white arrow the main migration direction; B) Aerial photo from 1989 and C) Satellite image from 1999.

In 1948 Capão Novo was an area with 1300 m width of completely active dunefields with barchanoidal and transverse dunes from beach to the landward margin. There was no deflation plain in the area. The dunefield was segmented by strong washouts that flowed to the sea (Fig. 4A). In 1974 the dunefield had developed some deflation areas, especially around washouts where there was more moisture. Interdune areas also became wetter and more vegetated which induced a change in the dunes shape from barchanoid to parabolic. In 1989 the dunefield was much more vegetated and deflated with dunes flattened. A town started to develop over portions of the deflation area, mainly near the beach. In the remaining landward b/t dune area, the moisture transformed barchanoid dunes into parabolic sand sheets or into solitary flat barchans which left behind gegenwalle ridges as they moved (Fig. 4B). In 1999 the town had been built over the entire dunefield area, leaving locally small flat sand sheets (Fig. 4C).

5.4.3. Atlântida Sul

There is a considerable increase in dunefield width at Atlântida Sul. In the north, along its first 6 km, the active dunefield width varies from 700 m to 2500 m. In the northernmost portion relict deflation plains, dunefields and precipitation ridges are present (Fig. 5, upper portion) but in the central to southern portions the active dunefield covers the entire Holocene barrier (Fig. 5). The reason for this is likely the lack of the Serra do Mar scarp adjacent to the shore. Without the influence of the scarp, rainfall decreases, the coastal plain enlarges and the wind velocity increases building a wide dunefield (Martinho *et al.* submitted). The Imbé sand rose prevails in the Atlântida Sul dunefield with the RDD to the SW and a strong DP of the NE winds. With this wind regime, the dunes move oblique to the coastline (12° , see Table 2), facilitating the increase in dunefield width.

The larger width and amount of sand reduce the impact of the washouts and they do not appear to influence the dunefield shape, so the Atlântida Sul dunefield is continuous along the coast. Washouts primarily flow along the interdunes, from the middle of the dunefield to the lakes behind the barrier at the landward margin and to the beach at the seaward margin (Fig. 5).

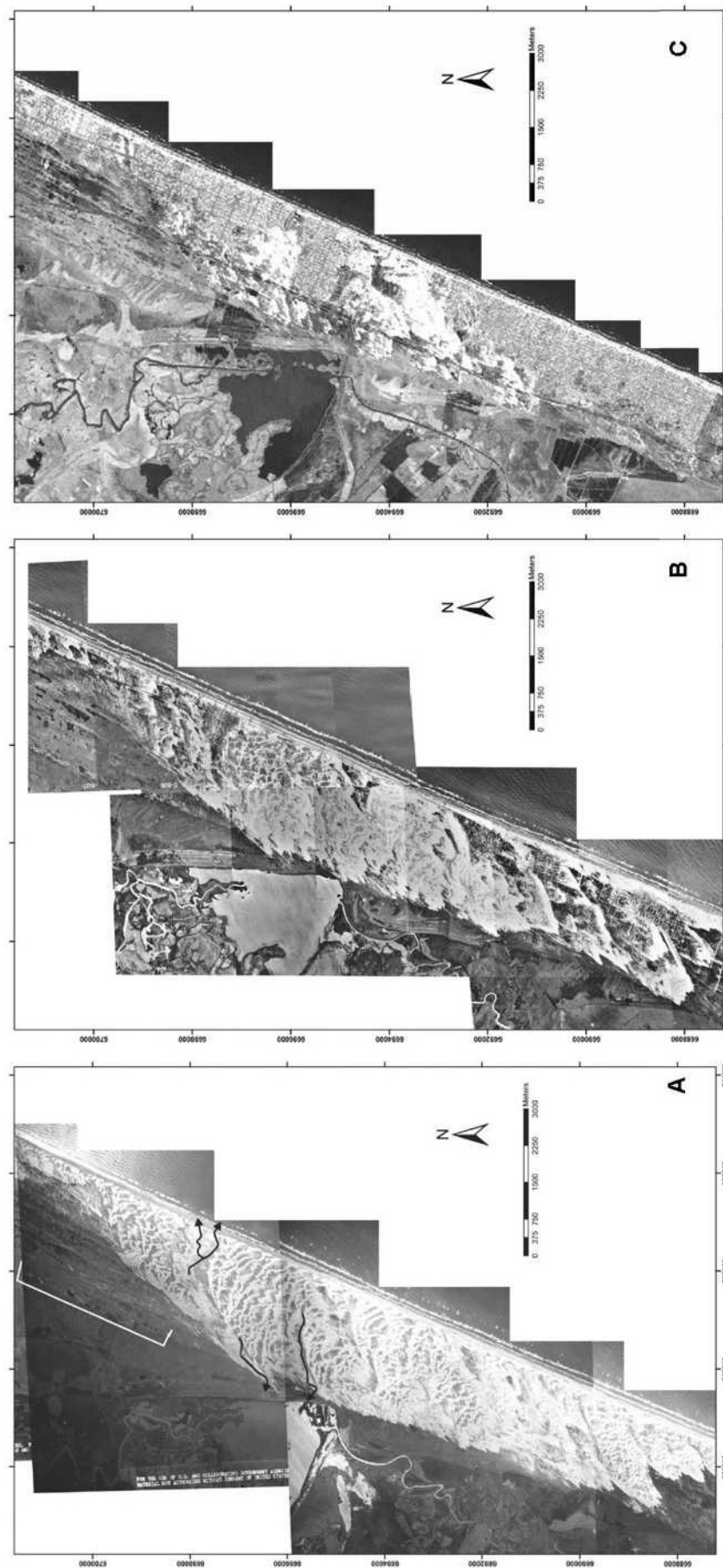


Figure 5: Atlântida Sul dunefield. A) Aerial photo from 1948, black arrows represent the washouts and the white line show the relict deflation plains, dunefields and precipitation ridges; B) Aerial photo from 1974 and C) Satellite image from 1999.

In 1948 the dunefield seemed to have a larger amount of sand than Rondinha and Capão Novo, and from the beach to the inland edge there were only b/t dunes with no deflation nor vegetated areas. The areas with more humid sand were restricted around the washouts and on these areas dunes were small and more parabolic in shape. Downwind, the dunefield finished as large lobate forms migrating over wet or vegetated areas (Fig. 5A). In 1974 the upwind area was reduced and was deflated, wetter and vegetated, the barchanoid dunes changed to parabolic dunes and developed gegenwalle ridges at their upwind margin. The humid areas were enlarged and vegetated, and due to this, the dunes and the dunefield became more parabolic, with trailing ridges on the margin of these vegetated areas. Downwind the landward most marginal lobes became parabolic dunes. An incipient urbanization started over part of the deflation areas (Fig. 5B). In 1999, almost the entire downwind area was destroyed with the development of the town. Upwind most of the dunefield area was urbanized also, especially the deflated areas, and only small areas with sand sheets and flat parabolic dunes remained in the landward portion (Fig.5C).

5.4.4. Jardim do Éden

At Jardim do Éden the dunefield width is large, and the entire Holocene barrier is covered with aeolian sand (Table 2). The Imbé sand rose prevails here too, with NE being the effective wind direction moving the sand to the SW. At the landward margin of the dunefield, the sand is very humid because dunes migrate into the lakes, silting them. Landwards washouts flow from the interdunes to the lakes while at the dunefield seaward margin, washouts flow to the sea. The large-scale dunefield shape is influenced by the lakes; it is continuous along the barrier and when the dunefield reaches a lake the migration rate is locally lowered, while the dry part continues to migrate. This process produces a lobate shape in the dunefield (Fig. 6).

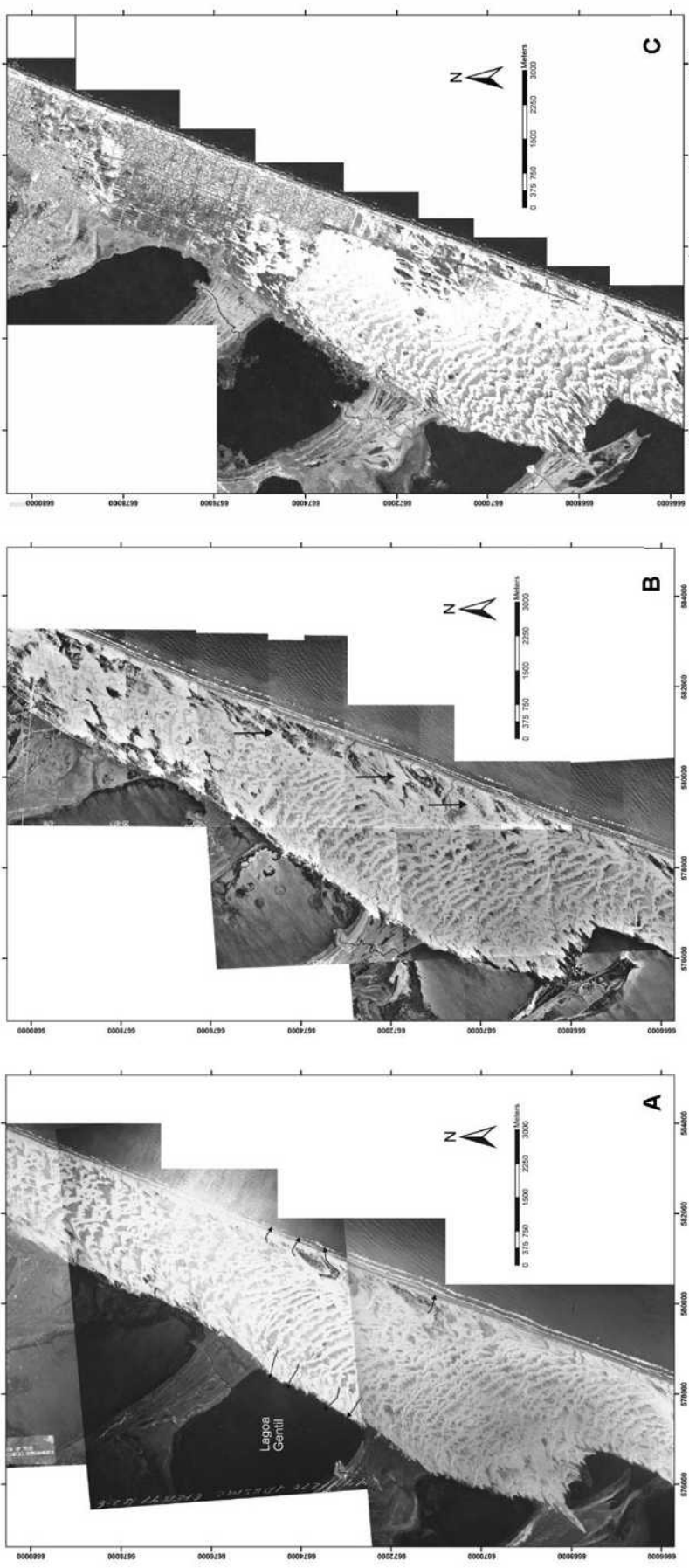


Figure 6: Jardim do Édem dunefield. A) Aerial photo from 1948, black arrows are some examples of washouts in the area; B) Aerial photo from 1974, black arrows point to examples of parabolic dunes that feed the dunefield (“corredores de alimentação” *sensu Tomazelli 1994); C) Satellite image from 1999.*

In 1948 the dunefield was a massive sand body, with very incipient deflation areas. Upwind, with less sand, barchan dunes and small barchanoid chains predominated and the interdune was more humid, but without vegetation. Downwind, the dune crests were straightened forming long (~2000m) barchanoid and transverse dunes. The interdune area was narrow and dry. In front of Lagoa Gentil, an incipient deflation plain had started to develop as a very flat and wet sandy area dominated by washouts, separating the b/t dunes area from the beach (Fig. 6A). By 1974, the upwind area was reduced by urbanization, the humid area was transformed into a large deflated and vegetated area and barchan dunes changed to low parabolic dunes and sand sheets. Along the entire dunefield, a vegetated deflation plain was developed separating the beach from the b/t dune area. With the dunefield detachment from the beach, the only sand supply for the dunefield came from the parabolic dunes, evolved from blowouts in the incipient foredunes or from the sand sheets adjacent to the backshore. These dunes transport sand from the beach across the deflation plain to the dunefield (“corredores de alimentação” *sensu* Tomazelli 1994). The long barchanoid chains and transverse dunes have migrated around 150m from 1948 to 1974 (Fig. 6B). By 1999, the upward side of the dunefield had been reduced by around 7500 m, due to the urbanization of the area. The deflation plain was also urbanized in many places. Downwind, the area with more sand still had b/t dunes but they were smaller and single barchans started to appear. At the front, where the dunefield was silting the lake, parabolic dunes dominated (Fig. 6C).

5.4.5. Magistério

Also under the influence of the Imbé sand rose, Magistério dunefield migrates to the SW. The angle that the direction of dune migration makes with the coastline is the highest (Table 2). Due to this, the dunefield detachment of the beach is favored and it can reach further inland, silting the lake behind the barrier (Fig. 7).

In 1948 the entire dunefield was active. Adjacent to the backshore, there were a few parabolic dunes and parabolic shaped sand sheets migrating over a humid area, with no vegetation and dominated by washouts. Landwards, barchanoid and transverse dunes predominated, with long crests. In places where the humid area was absent, transverse dunes started at the beach. The interdunes were dry and had small size dunes over them. The large-scale U-shaped lobe (center of photo) moving into the lake had dry sand and small barchanoid chains (Fig. 7 A).

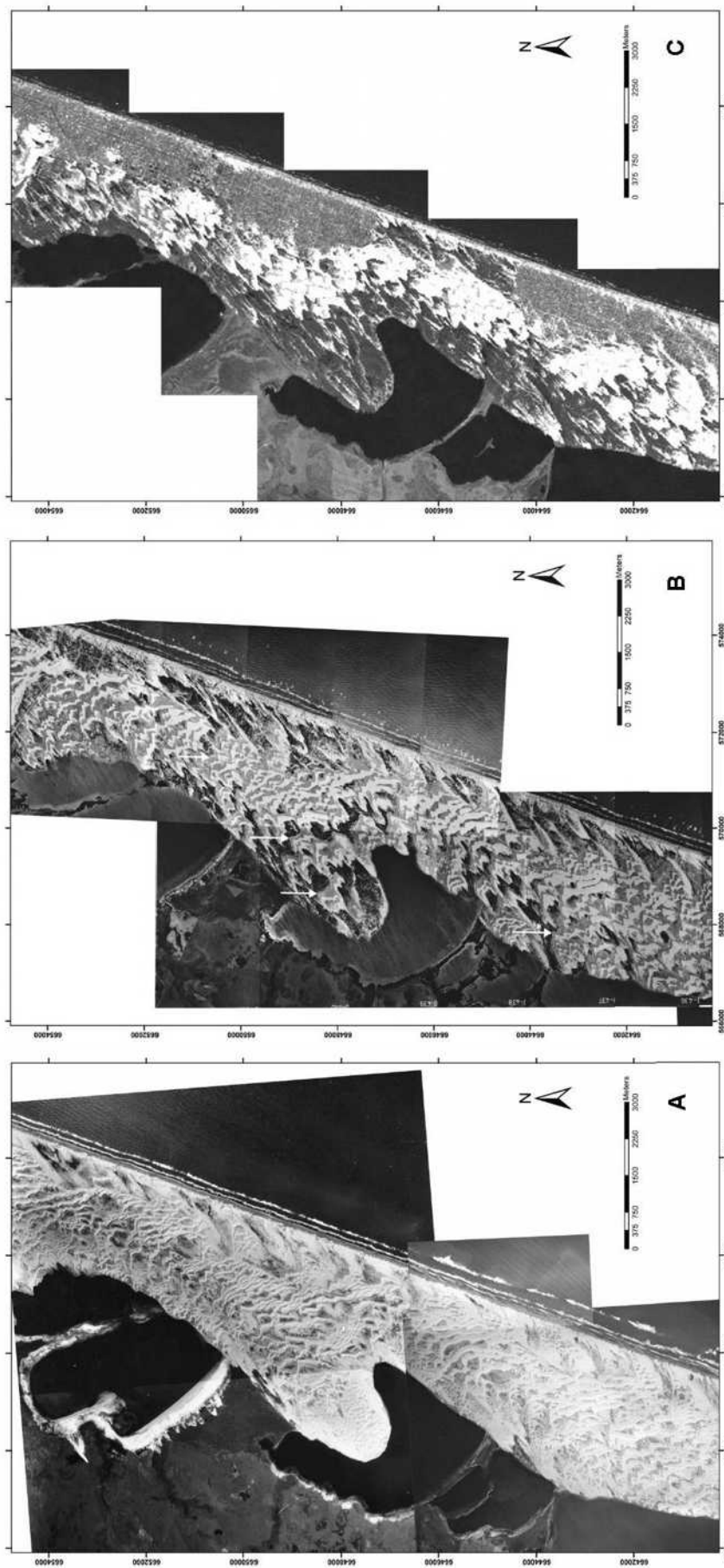


Figure 7: Magistério dunefield. A) Aerial photo from 1999. B) Aerial photo from 1948; C) Satellite image from 1974, white arrows point to some examples of gegenwalle ridges; C)

In 1974 the dunefield had changed significantly, becoming more humid and with more deflation areas. Some low, segmented and highly erosional foredunes developed and had small sand sheets behind them. Washouts flowed through the vegetated deflation plain, and parabolic dunes migrated over the deflation plain connecting the foredunes to the b/t dunes area. On the b/t dunes area, small barchanoid dunes or barchans alone predominated, and the moisture and vegetation increased on interdunes allowing the development of gegenwalle ridges at the upwind edge of barchan dunes. The landward margin of the dunefield continued to silt the lakes, and due to that a large amount of washouts ran from the wet interdunes lakewards. The dunefield U-shaped lobe became wet, vegetated and dominated by parabolic dunes (Fig. 7B). Migration rates of some dune types, from 1974 to 1987 were measured (Table 3).

Table 3: Mean migration and migration rate of three types of dunes, for the period of 1974 to 1987 in Magistério dunefield.

	Mean migration (m)	Migration rate (m/year)
Parabolic dunes on the frontal lobe	316	24.3
Parabolic dunes on the deflation plain	346	26.6
Barchan	191	14.7

The moisture and the deflation areas continue increasing and in 1999 both landward and seaward margins of the dunefield were dominated by deflation and parabolic dunes. Only a narrow area remained without vegetation, where barchans and barchanoid dunes have changed to predominantly parabolic dunes. The deflation plain next to the beach was almost entirely urbanized (Fig. 7C).

5.4.6. Dunas Altas

Dunas Altas dunefield can be considered to be under the influence of the Imbé sand rose and despite the high proximity to Magistério, it has some important differences. The angle of the coastline changes along the dunefield (Table 2) and according to Toldo Jr. *et al.* (2006) this change provokes deceleration of the littoral sand transport drift. This deceleration causes a sediment “jam”, an increase in sediments on the shoreface which are transported by waves to the foreshore and become available for wind transport landwards to feed the dunefield. Due to this, Dunas Altas dunefield seems to have more sand than Magistério, confirmed by larger b/t dune areas and lower moisture.

As dunes evolve from foredune blowouts and sand sheets and migrate obliquely over the deflation plain, a seaward arm (trailing ridge) develops within the vegetation present along that margin due to the high water table and washout channels. As the dunefield migrates, the seaward trailing ridge is left behind creating a series of relatively straight ridges crossing the deflation plain and reaching the b/t dune area (Fig. 8).

In similarity to Magistério, Dunas Altas had the same beach-lake profile in 1974, but apparently there was more sand in the b/t dune area. Erosional foredunes, blowouts and sand sheets provided sand to feed the sand sheets behind them. The sand sheets were lobate and U-shaped and eventually several evolved into parabolic dunes that migrated over the deflation plain. Near the deflation plain, a more humid area, the barchanoid chains and barchans dunes had small sizes and the interdune was large and wet. Landwards, the long barchanoid chains were better developed. Large washouts are present in both landward and seaward margins of the dunefield draining water to the lakes and to the beach respectively. Like Magisterio, the central part of the dunefield was the driest (Fig. 8A).

In 1988 the deflation plain had expanded and the seawards humid area with small size barchans became more vegetated and dominated by parabolic dunes. Washout areas became vegetated too. The sand sheet behind the foredunes migrated landward over the deflation plain, evolving into parabolic dunes (Fig. 8B). Some dune migration rates were measured for the period of 1974 to 1987 (Table 4)

Table 4: Mean migration and migration rate of three types of dunes, for the period of 1974 to 1987 in Dunas Altas dunefield.

	Mean migration (m)	Migration rate (m/year)
Large-scale U-shaped lobe	442	34
Parabolic dunes on the deflation plain	570	43.8
Barchanoids	274	21

In 1999 the deflation plain with low parabolic dunes was larger and the b/t dune area decreased. Migration rates for the period of 1987 to 1999 were measured (Table 5). Parabolic dunes migrate faster than barchanoid chains because they are lower and have less sand; as barchanoid chains are higher and have more sand, they take longer to migrate (Fig. 8C).

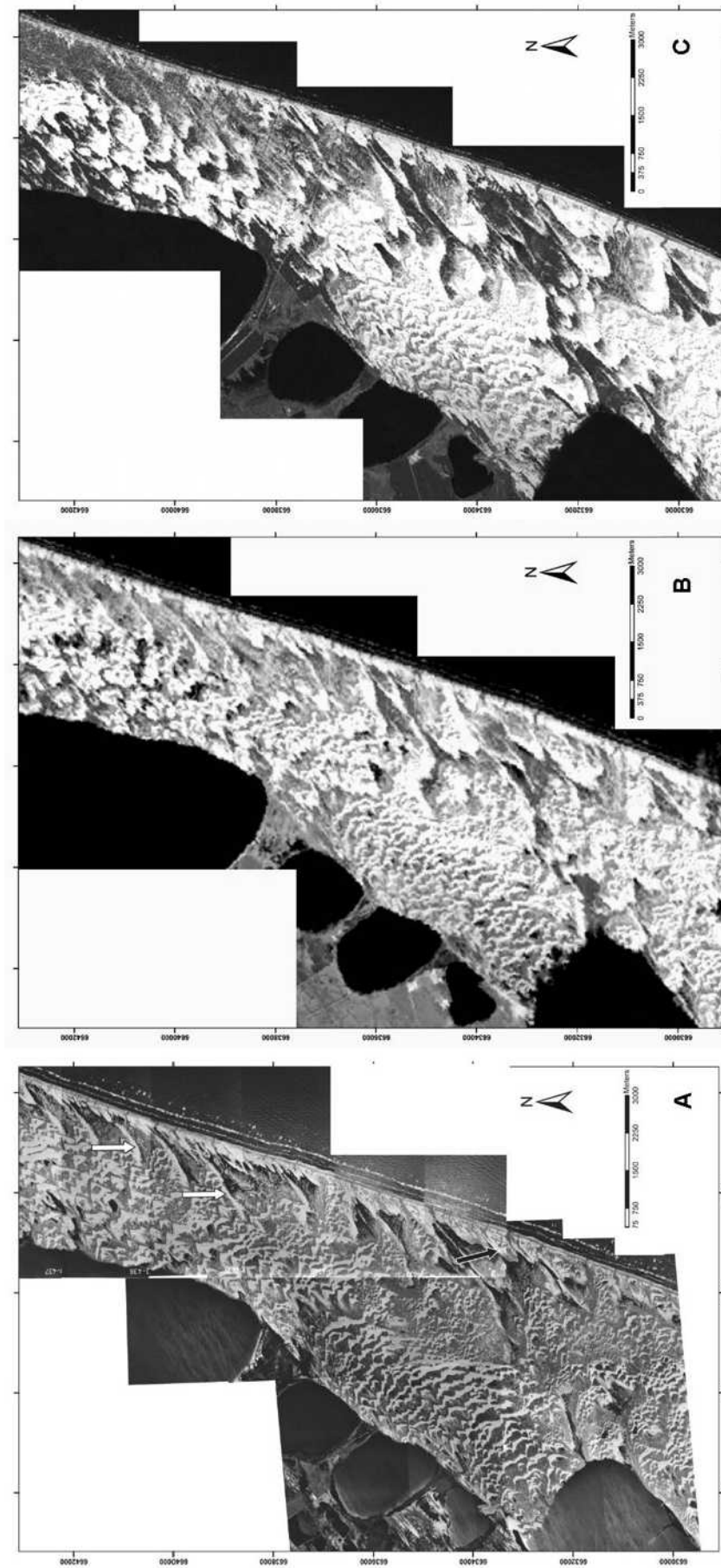


Figure 8: Dunas Altas dunefield. A) Aerial photo from 1974, white arrows point to examples of trailing ridges and the black arrow points to an example of parabolic sand sheet; B) Satellite image from 1987 and C) Satellite image from 1999.

Table 5: Mean migration and migration rate of two types of dunes, for the period of 1987 to 1999 in Dunas Altas dunefield.

	Mean migration (m)	Migration rate (m/year)
Parabolic dunes on the deflation plain	335	28
Barchanoids	270	22.5

5.4.7. Solidão

The coastline orientation along Solidão dunefield changes five degrees (Table 2) and this change seems to be important enough to change the dunefield morphology. In the north the dunefield has no deflation plain, but small dunes and sand sheets moving along the back of the backshore. Southwards, as the coastline orientation changes, the dunefield is detached from the beach with the development of a deflation plain (Fig. 9). In addition, Solidão is under the influence of the Mostardas sand rose that is characterized by having stronger winds and an onshore RDD which can contribute to this dunefield detachment.

Despite the very low resolution of the 1980 satellite image, in this period the dunefield had a large amount of sand, with very long barchanoid chains and transverse dunes that varied from 1000m to more than 2000m in extension and showed no deflation area. By this time the dunefield was wide (5800m) and its large-scale lobes surrounded the inner and outer margins of the lakes, migrating into them. This means that aeolian sand covered not only the entire Holocene barrier but also part of the Pleistocene barrier (Barrier III *sensu* Villwock *et al.* 1986). The silting of the lakes by aeolian sand created swamp areas on the interdunes. These areas were dominated by washouts that streamed from the lakes towards the beach (Fig. 9A). In 1987, the U-shaped lobes of the dunefield along the inner margin of the lakes were completely stabilized by vegetation, grazing and farming. The sand around the lake as well as the swamp areas became vegetated deflation areas, and long barchanoid chains changed to barchan dunes. Separating the dunefield from the beach, there was a deflation plain, vegetated and with trailing ridges, the register of parabolic dunes that had migrated over the area. Adjacent to the backshore there was a sand sheet, sometimes evolving to parabolic dunes (Fig. 9B). In 1999 large areas were stabilized. As the dunefield migrated landwards the deflation plain enlarged, and with less sand supply, the long barchanoid and transverse dunes changed to small barchanoid chains or to barchans alone, leaving behind gegenwalle ridges. The U-lobes were also deflated and dominated by parabolic dunes (Fig. 9C).

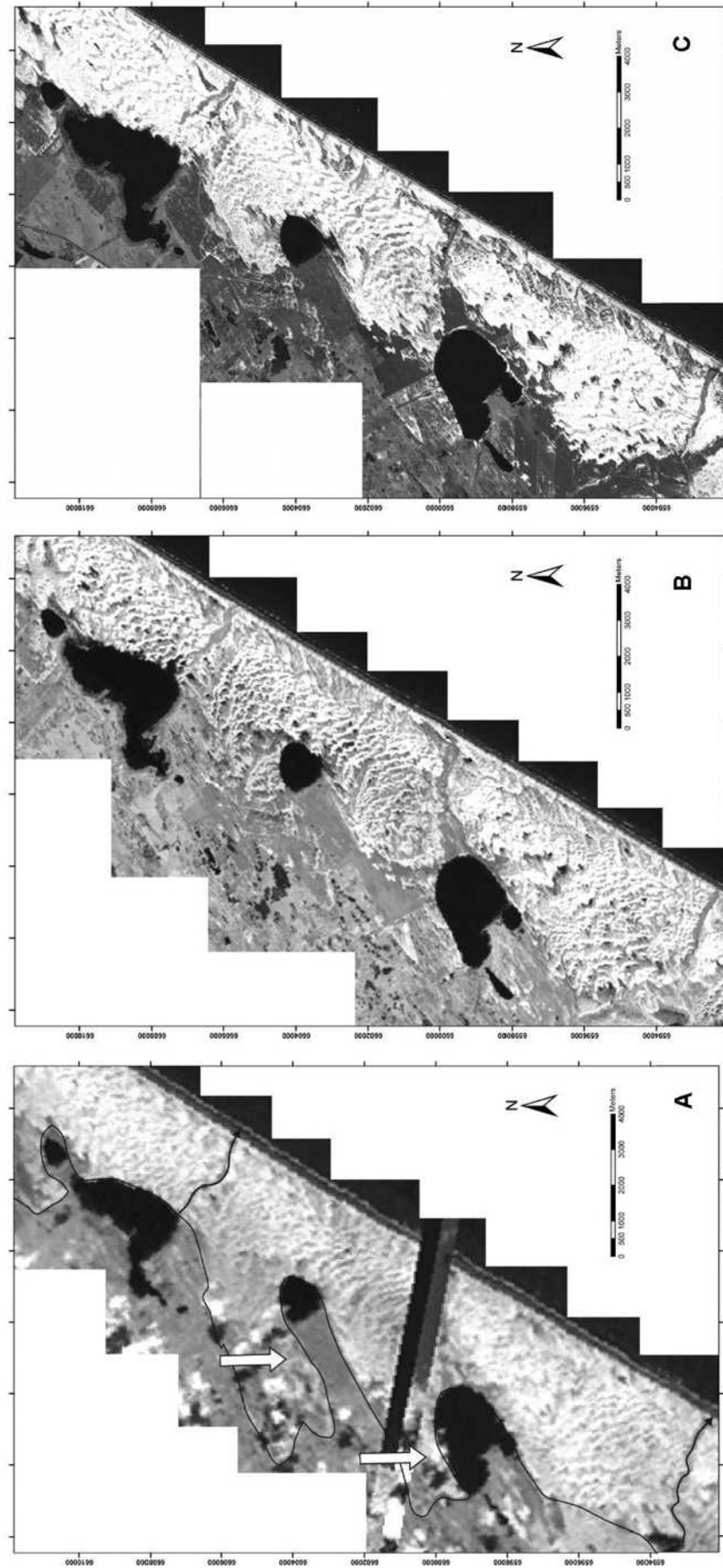


Figure 9: Solidão dunefield. A) Satellite image from 1980, black line represents the dunefield inner margin, the white arrows point to places where the active dunefield reached in 1980 and the black arrows represent the washouts; B) Satellite image from 1987 and C) Satellite image from 1999.

5.4.8. São Simão

São Simão dunefield is very similar to Solidão, and is also dominated by the Mostardas sand rose and is the largest dunefield with 6900 m width. Large-scale U-shaped lobes are also present at the inner and outer margin of the lakes, covering part of the Pleistocene barrier. Large washouts and drainage areas flow from the lakes to the sea, crossing the b/t dune area and the deflation plain to reach the beach. In the north, the dunefield migrates more parallel to the coast while southwards the coastline orientation changes three degrees (Table 2), and the deflation plain width increases slightly (Fig. 10).

In 1973, in the north, a sandy humid area separated the sand sheets adjacent to the backshore from the b/t dune area. In the south, this area was smaller and locally the b/t dunes migrated along the beach. The central area of the dunefield seemed to be drier and with the highest dunes (Fig. 10A). In 1988, the deflation areas enlarged especially in the south where wet bush pockets appear in the middle of the b/t dune area (Fig. 10B). In 1999, the deflation and the increase in moisture continued, starting at the seaward margin of the b/t dune area and spreading over the entire deflation plain (Fig. 10C). A large drainage area has developed showing a dendritic pattern of small creeks and streams that converged into many washouts or small ponds that break through the foredunes and sand sheets and reach the beach (Fig. 11).

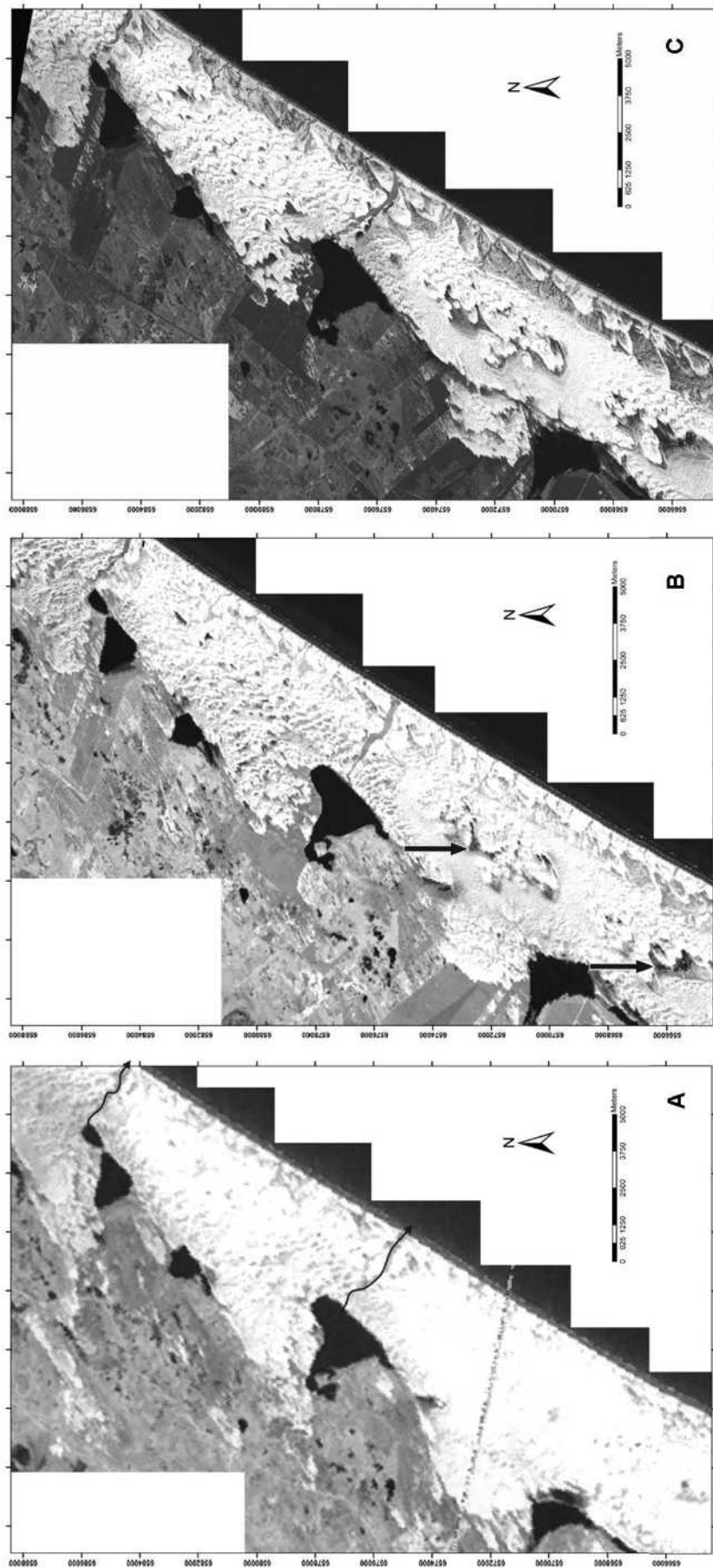


Figure 10: São Simão dunefield. A) Satellite image from 1973, black arrows represent the large washouts; B) Satellite image from 1988, black arrows point to the wet bush pockets; and C) Satellite image from 1999.



Figure 11: Dendritic pattern of drainage on deflation plain at São Simão dunefield. Satellite image from 1999.

5.4.9. Mostardas

A major difference between Mostardas dunefield and the others is the absence of large scale U-shaped lobes, and, while multiple washouts are present along the coastal fringe they do not exert a control on large-scale dunefield shape. The Mostardas dunefield is parallel to the coast and continuous alongshore (Fig. 12).

Mostardas dunefield is under the influence of the Mostardas sand rose. The coastline also changes orientation alongshore such that, in 20 km the coastline varies eight degrees (Table 2) producing a modification in the size of the deflation plain from 1500m wide in the north to 600m wide in the south (half the size) (Fig. 12C).

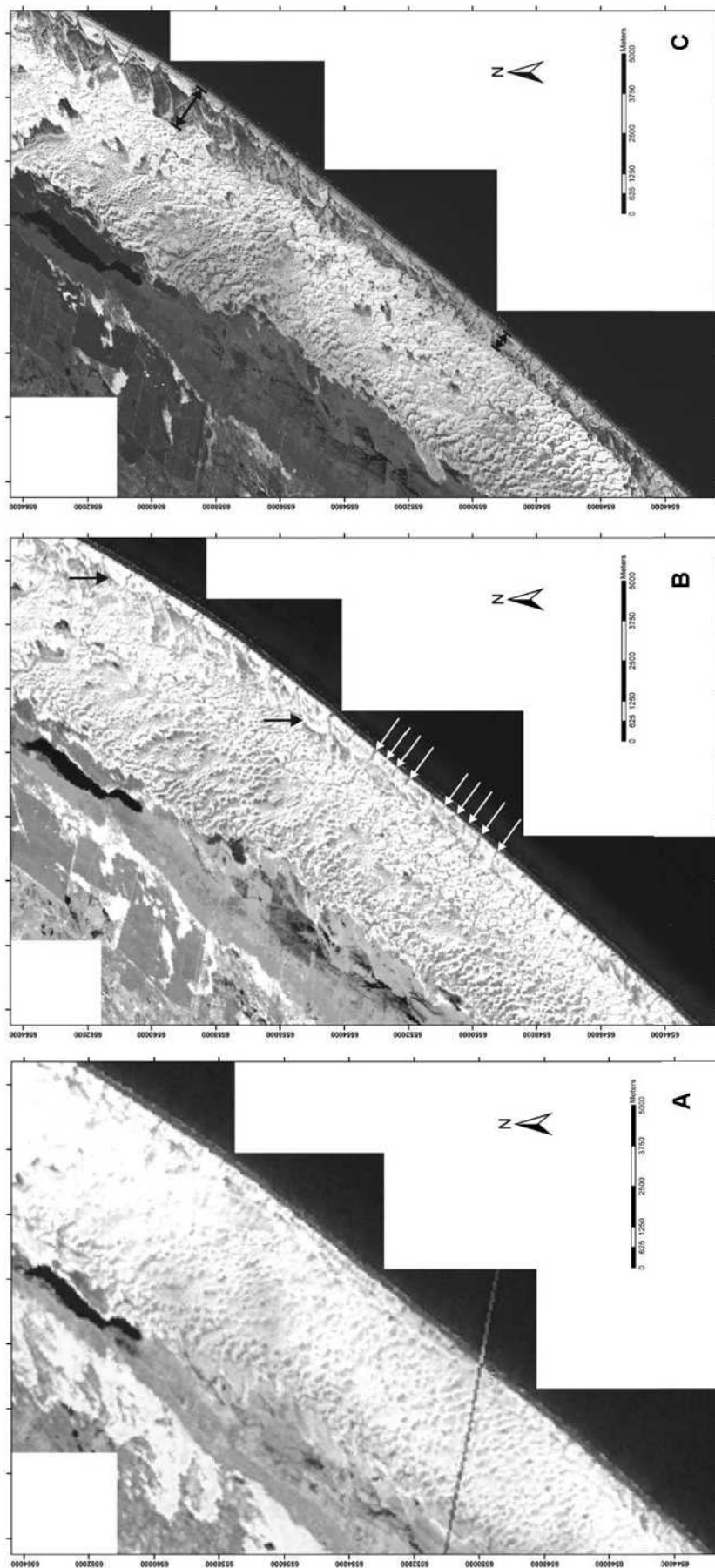


Figure 12: Mostardas dunefield. A) Satellite image from 1973; B) Satellite image from 1988, black arrows point to some examples of sand sheets that can evolve to parabolic dunes and the white arrows point to some examples of the regularly spaced small washouts; and C) Satellite image from 1999, black arrows display the difference of deflation plain width from the north and to the south of the dunefield.

In 1973 the dunefield was massive, over 6100 m wide with no deflation plain from the beach to the lake. Barchanoid chains reached 3km in length. In the north, behind the beach there was a flat sand sheet bordering the b/t dune zone, crossed by a few washouts (Fig. 12A). In 1988 a deflation plain had developed alongshore, being wider in the north and narrower in the south. Small sand sheets adjacent to the backshore were interrupted by regularly spaced small washouts that, in similarly to São Simão, start at the seaward border of the b/t dune area, forming a complex drainage system flowing to the sea. These washout creeks are spaced at a very regular spacing alongshore. (Figueiredo & Calliari 2005) Parabolic dunes formed from the evolution of the sand sheets migrated over the deflation plain and as described above, left their seaward trailing ridges (Fig. 12B). In 1999 the deflation plain was larger, more vegetated and with more trailing ridges present. There was a change in the dunes morphology on the b/t dune area; large barchanoid chains changed to flat barchans with gegenwalle ridges at their upwind border and in some wetter areas they became flat parabolics (Fig. 12C).

5.5. DISCUSSION

5.5.1. Dunefield Migration

Rondinha and Capão Novo are under the influence of the Torres wind pattern and Serra Geral scarp, so their direction of dune migration is very similar as the wind blows parallel to the scarp (Table 2). These dunefields are the narrowest probably due to the adjacent scarp that acts as a barrier obstructing the winds and decreasing their velocity, reducing landwards migration. The rainfall on the coastal plain adjacent to the scarp is also the highest, and this increases the threshold velocity for wind transport and contributes to the small size of the dunefields (Martinho *et al.* submitted). In addition, the dune migration at Rondinha is parallel to the coast (Table 2), consequently the flux of sand landwards is reduced and the dunefield width is restricted.

At Atlântida Sul, without the influence of the scarp, the wind velocity increases significantly and the rainfall decreases. In addition, the coast line orientation changes so the dunes migrate landward, oblique to the coast. All these facts together contribute to the increase in the dunefield width which is almost doubled in this area (Table 2).

Jardim do Éden dunefield is clearly dominated by the Imbé sand rose. The strong and persistent winds and the higher angle of dune movement with the coastline favor the landward dunefield migration, increasing its width (Table 2).

A similar situation occurs for Magistério and Dunas Altas, which also are under the Imbé sand rose wind pattern. Magistério has the highest angle of the dune migration with the coastline (Table 2). This landward migration produces a large loss of sand, since the sand leaves the beach system and can be trapped by the inland vegetation (Martinho 2004). It may be observed that the higher the angle, the higher the probability of deflation plain formation. This is clear in the Magistério dunefield which has the highest angle and the largest deflation area. This shows how important coastline orientation can be in relation to the main dune movement direction and dunefield development. Despite being next to Magistério, Dunas Altas dunefield does not have as large a deflation area due to its change in coastline orientation.

In Solidão, São Simão and Mostardas the dune migration direction is always over 230°, probably due to the influence of the Mostardas sand rose that has a strong inland component (Table 2, Fig. 1). These dunefields cover the entire Holocene barrier and part of the Pleistocene barrier. Nevertheless, the dunes in these dunefields do not migrate to the W as expected (calculated RDD). This occurs because the RDD and RDP are the calculated wind potential of transport; however, the calculated transport direction does not correspond to the effective transport direction. The EDD (effective drift direction) depends on the availability of noncohesive sand with grain sizes compatible to wind competence (Giannini *et al.* 2005). So, the EDD for these locations is to the WSW, the measured direction of dune migration (Table 2). The RDD is to the W due to the strong winds that blow from the S in this area, nevertheless those winds usually come with precipitation from the cold fronts, what increases their shear velocity and reducing significant sand transport (Bagnold 1941; Belly 1964; Tomazelli 1990; Giannini 1993; Martinho *et al.* submitted).

As described above, in Solidão, São Simão and Mostardas the coastline orientation changes along the dunefield, while the dune migration direction remains the same (Table 2). This difference in coastline orientation is important since it changes the width of the deflation plain in the dunefield.

Analyzing all the studied dunefields and their changes through time, it may be observed that when the sand supply is abundant, the coastline orientation is largely irrelevant and deflation is always inhibited (see dunefields in 1948, for

example). But, when there is less sand supply available for wind transport and the deflation processes start to develop, or are already present, small variations in the system like the change in coastline orientation is sufficient to control the deflation plain width.

5.5.2. Spatial Dunefields Changes

Analyzing the transgressive dunefields present along the coastal stretch from Torres to Mostardas some important differences was observed.

The narrowest dunefields are located on the northern littoral, adjacent to the Serra Geral scarps (Rondinha and Capão Novo). These dunefields have apparently less sand and they are more deflated. There are some b/t dunes but the main duneforms are typical from deflation plain (nebkas, shadow dunes etc). They develop in phases that overlap each other. These dunefields have their shape controlled by the regularly spaced washouts that cross them. The washouts start to flow from the middle of the barrier toward the sea, crossing paleodunefields and the active dunefield, and thus controlling their alongshore shape (Hesp *et al.* 2007). Southwards, as the dunefield width and amount of sand increases, the washouts lose their influence in the dunefield shape, and the lakes start to influence large-scale dunefield behavior and form.

Medium size dunefields are located on the northern littoral area where the scarps influence is finished (Atlântida Sul, Jardim do Éden and Magistério). In these dunefields b/t dunes predominate, but there are some duneforms from deflation areas such as sand sheets and parabolic dunes which help to feed the b/t dunes area. They cover the Holocene barrier and silt the lakes behind it. Atlântida Sul and Jardim do Éden have washouts on the seaward and the landward margins of the dunefield (Fig. 13). When the washouts that flow to the lakes reach the stagnate body of water they decelerate, building small deltas at the margin of the lakes (Fig. 13 and 14). So, the lakes were not only silted by aeolian sand but also by the development of small deltas. They also show the center of the barrier as the driest. All this might occur due to the barrier topography which is higher in the center (Fig. 15), so it would act as a drainage separator and thus, the driest part.

The largest dunefields are located in the mid-littoral (Dunas Altas, Solidão, São Simão and Mostardas), reaching more than 6 km in width. These dunefields have apparently more sand and in some places they cover the entire

Holocene barrier/lagoon system, reaching the Pleistocene barrier. B/t dunes are by far the most predominant duneforms in these dunefields.

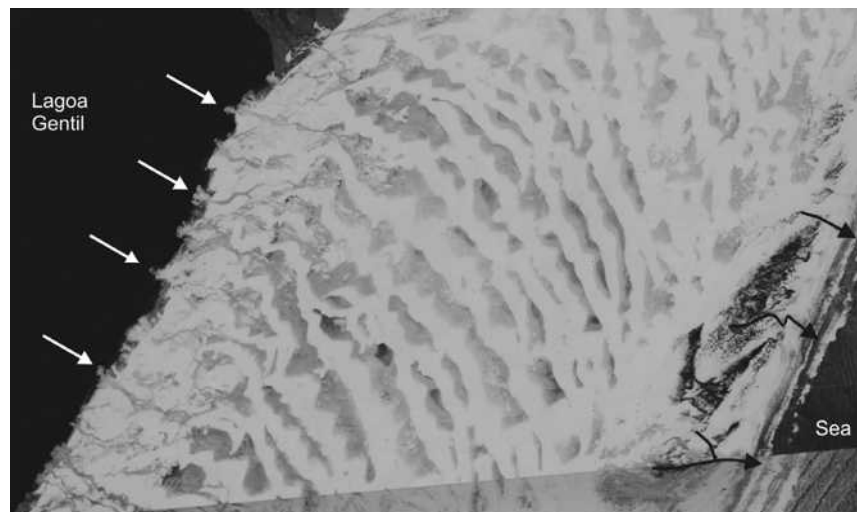


Figure 13: Jardim do Éden dunefield. White arrows point to some examples of small deltas silting the lake, formed by washout at the landward margin of the dunefield. Black arrows represent washouts at the seaward margin of the dunefield.

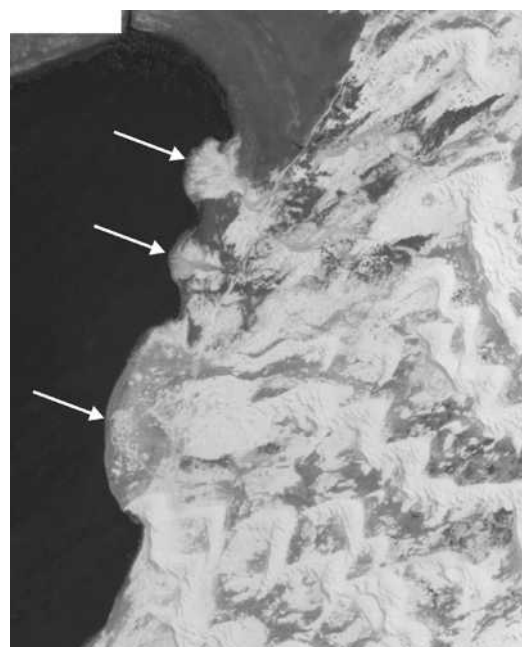


Figure 14: Small deltas formed by sand transported by the washouts, silting the lakes.

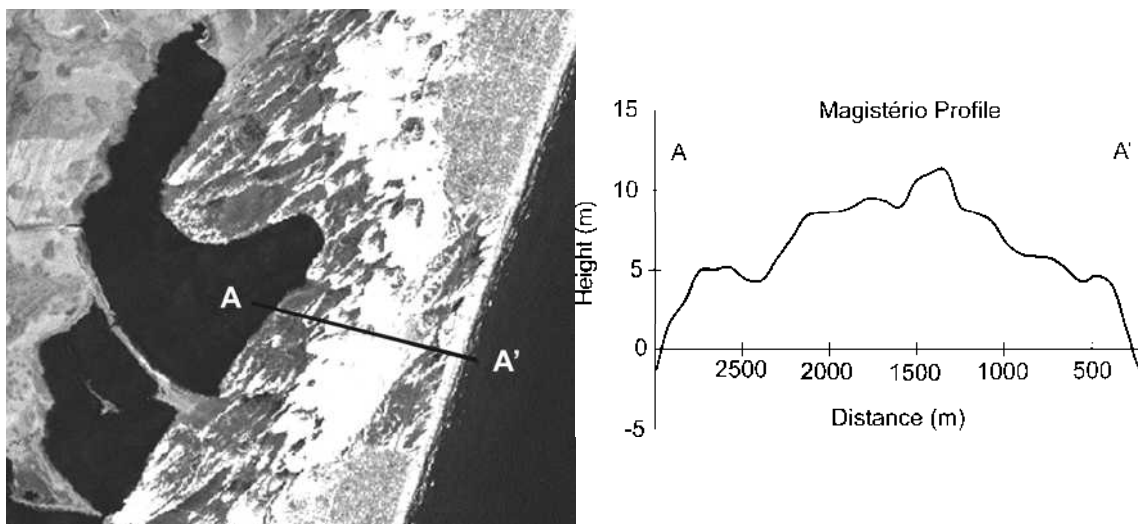


Figure 15: Topographic section of the barrier at Magistério dunefield showing that the central portion is higher.

These differences in the dunefields from the northern littoral to the mid-littoral could be explained by the variation along the coast of: rainfall, wind velocity and direction, sediment supply, wave energy, longshore sediment transport (LST) and antecedent topography which produces different types of barriers.

The precipitation can control dunefield size since an increase in humidity increases the grain cohesion and threshold velocity, reducing the wind transport and favoring vegetation growth (Hesp 1999; Clemmensen *et al.* 2001; Hugenholtz & Wolfe 2005; Marcomini & Maidana 2006; Martinho *et al.* submitted). In the studied area, the precipitation in the northern littoral is higher, influenced by the Serra Geral scarps (SEMC 2002). Southwards, precipitation decreases with the distance from the scarps (SEMC 2002; Martinho *et al.* submitted). With more rainfall in the north, the threshold velocity is higher, so less sand will be transported in the area, creating narrower dunefields. Less humidity in the south allows more sand to be transported, increasing dunefield size.

Wind velocity and direction can also directly influence the sand transport. The higher the wind velocity, the higher is the potential for sand transport (Fryberger & Dean 1979). A decrease in wind velocity would cause sand deposition (Fryberger & Dean 1979; Chase & Thomas 2006, 2007). The wind direction would also influence the dunefields as offshore and alongshore winds inhibit the sand migration landwards, influencing the dunefield width (Martinho 2004). In the studied area, the wind in the northern littoral is weaker and has lower drift potential. The strongest wind direction (to the NE) blows parallel to the coast due to the scarps (Martinho *et al.*

submitted). For all these reasons, the wind could be the main factor influencing the narrow dunefields in this area. In the mid-littoral, the winds are stronger, their DP are high, the main directions are obliquely onshore and the wind velocity is much higher due to the gentle topography of the coastal plain in this area (Martinho *et al.* submitted). Thus, in the mid-littoral, the wind could be responsible for the large dunefields.

The sand supply can be another factor responsible for the dunefield differences along the coast. The mid-littoral dunefields might have more sand supply than the northern dunefields. Sand supply along the RS coast depends on the wave energy and the longshore sediment transport (LST). Wave energy and LST vary along the coast due to the coastline and slope variations (Dillenburg *et al.* 2000, 2003; Martinho *et al.* accepted). These wave energy and LST variations along the coast can cause variations in sediment budget cross-shore and alongshore. Wave energy and LST are higher in the convex areas, from Mostardas to Atlântida Sul, and lower in the concave, from Atlântida Sul to Rondinha (Martinho *et al.* accepted). The high wave energy and LST rates in the mid-littoral would promote coastal erosion, form retrogradational barriers and would create more sand available on the foreshore and backshore to be transported by wind, thus forming large dunefields. Northwards, the decrease in wave energy and LST rates would create a local positive imbalance in sediment supply, forming progradational barriers, although this positive imbalance would stock sand on the shoreface not on the foreshore or backshore where the wind could transport it. So in these areas, despite the progradational character of the barrier, there is less sand available for wind transport, and consequently the dunefield size would be restricted.

Each of these factors could alone promote variations in dunefield size and morphology along the coast. Nevertheless, it is likely that all the factors cited above have been acting together and contributing to enhance the dunefield differences alongshore.

5.5.3. Temporal Dunefield Changes

Since 1948, the dunefields from Torres to Mostardas have experienced important changes. In 1948 the dunefields were completely active with no vegetation and no deflation areas even with the existing variations in coastline direction. Large b/t

dunes, with long and continuous crests migrated from the backshore landwards (Figs. 4A, 5A, 6A).

Since then, the dunefields have been experiencing a widespread stabilization. In the last 50 years, the b/t dune area has moved downwind away from the coast, creating a deflation plain between the b/t dunes and the beach. Foredunes have been developed and have increased their heights. Typical deflation plain dune forms, developed in vegetation, started to appear, such as nebkas, parabolic dunes, blowouts and sand sheets. The dune forms inside the dunefield have progressively changed from high barchanoid chains to single barchans with gegenwalle ridges at the upwind margin and finally to parabolic dunes or flat sand sheets with parabolic shapes (Fig. 16).

Due to the difference in the dunefields size along the coast, cited above, the stabilization has not been homogeneous for the northern and mid-littoral dunefields. In 1974 the northern littoral dunefields were starting to develop a deflation plain and deflation areas, with barchanoid dunes being converted to parabolics (Figs. 4B, 5B, 6B). Nowadays the northern dunefields have only very restricted areas of activity which resumes in foredune growth and a nebka field behind it.

In the mid-littoral dunefields, the development of deflation areas experienced by the northern littoral in 1974 is occurring now (Figs. 9C, 10C, 12C). This deflation phase includes foredune growth, development of parabolic dunes, blowouts and sandsheets, and the b/t dunes moving landwards, enlarging the deflation area.

So, there is a lag of ~25 years approximately between dunefield evolution in the northern littoral and the mid-littoral. This lag may occur because the northern dunefields are smaller and have less sand, so they might respond faster to small changes in climate, for example. In the RS mid-littoral, the dunefields are very large and the amount of sand is much higher. Due to this, it would likely that it will take longer to start the dunefield stabilization and vegetation growth; i.e. the larger the amount of sand and size of the dunefield, the longer it will take to stabilize it.

Dunefield stabilization can be a response to environmental changes, and they include changes in moisture, wind and wave regimes, sand supply (Thom 1978; Davies 1980; Filion 1984; Short 1988b; Shulmeister & Lees 1992; Young *et al.* 1993; Clarke *et al.* 1999; Clemmensen *et al.* 2001; Murray & Clemmensen 2001; Wilson *et al.* 2001; Formann *et al.* 2005; Hugenholtz & Wolfe 2005; Orford 2005). Thus, the hypotheses for the observed changes in RS dunefields in the last 50 years can be:

1. An increase in precipitation increases the threshold velocity, reducing significantly the dune movement rates and induces vegetation growth which is the key to dunefield stabilization (Hesp 1999; Clemmensen *et al.* 2001; Hugenholtz & Wolfe 2005; Marcomini & Maidana 2006; Martinho *et al.* submitted). The precipitation on the RS coast has increased since 1948 (Martinho *et al.* submitted), and this observed increased moisture levels might be responsible for the changes observed in the RS dunefields.

2. The wind velocity is also considered to be potentially responsible for dunefield formation and high rates of migration (Hesp 2003; Chase & Thomas 2006, 2007). A decrease in wind velocity and direction can cause dunefield stabilization (Chase & Thomas 2006, 2007), since a low volume of sand will be transported favoring vegetation growth (Hesp 1989). Martinho *et al.* (submitted) describes that, on the RS coast, the wind drift potential has a trend of continuously decreasing from 1964 to 1988. This 24 years period of weak winds could be responsible for the start of the stabilization process that has been continuing until today.

3. Change in sand supply can facilitate dunefield stabilization. The landward migration of a dunefield produces a large loss of sand, since the sand leaves the beach system and can be trapped by the inland vegetation (Tomazelli 1994; Martinho 2004). A decrease in sand supply along the years, together with the natural loss of sand can start a process of stabilization in the dunefields. In addition, the decrease in sand supply can also favor vegetation growth and the establishment of new vegetation species (Seelinger 1998; Hesp 2002, 2004).

No sand supply data are available for the RS coast. Nevertheless the sand supply may have been severely reduced with the construction of the 4km long jetties at the Patos Lagoon inlet, in 1919. These jetties retain the sediments transported alongshore northwards by the littoral drift currents (Esteves *et al.* 2003), reducing the alongshore supply.

4. Other factors like the frequency of storms, or periods with high wave energy can be responsible for dune formation since these events increase sediment supply in shelf supplied beach systems and reduce foredune stability (Thom 1978; Short 1988b; Clarke *et al.* 1999; Wilson *et al.* 2001; Orford 2005). There are no historical records of storm frequency or increasing breaker wave energy in the studied area, but the decrease of these types of events could be responsible for the dunefield stabilization by reducing sand supply, or reducing shoreline and dune erosional events.

5. Human activities can rapidly modify a dunefield's behavior. Seeliger *et al.* (2000) describes for the southern littoral of RS a 50 year change in foredunes caused by an increase in moisture. The moisture increased due to the construction of a highway near the coast which changed regional water table behavior obstructing the water flow and raising the water table. In the studied area, the mid-littoral has no expressive human activities, so this case would not apply for this area. Nevertheless, in the northern littoral the human occupation has increased drastically and this human impact may have aided the dunefield stabilization. Alternatively, dunefield stabilization may have occurred despite human habitation expansion. The water tables in the areas of urbanization have probably fallen due to high levels of extraction, so this may indicate that climatic or other factors are definitely playing a role rather than human factors.

As indicated above, there may have many factors that alone or together could induce the dunefield stabilization and changes observed in RS dunefields. Nevertheless, the lack of historical data of some factors makes it difficult to prove how, or if they have been acting to produce change. Even so, the available data on precipitation and wind can explain very well the dunefield changes with time. The observed increase in precipitation and decrease in windiness, both acting in concert will reduce significantly the dune movement rates (Bagnold 1941; Belly 1964). Furthermore, they will induce vegetation growth, and will contribute even more to dunefield stabilization (Marcomini & Maidana 2006).

5.5.4. Changes in dune morphology

Tomazelli (1994) observed that the dune types change along the RS dunefields produced by a decrease in sand supply as the distance from the beach (source of sand) increases. He describes along a dunefield, transverse dunes changing to barchanoid chains and finally to isolated barchans. We have observed a very similar dune progression through time.

An increase in moisture and a decrease in wind velocity reduces the sand availability to build large b/t dunes. The high and large barchanoid/transverse dune chains have been either trapped by vegetation or deposited on the wet interdunes. As the dune migrates, with a wet interdune, an amount of sand will stay behind forming gegenwalle ridges and trailing ridges. In all the studied dunefields it was observed that the increase in deflation area and the loss of sand promotes a decrease in the dune

height, and a change of dune shape (McKee 1979; Tomazzelli 1994). The progression of the dune morphology change temporally is from high barchanoid chains to single barchans with gegenwalle ridges at the upwind margin and finally to parabolic dunes or flat sand sheets with parabolic shapes (Fig. 16). In the northern dunefields this evolutionary development of the b/t active dunefields allowed or encouraged the growth of urbanization.

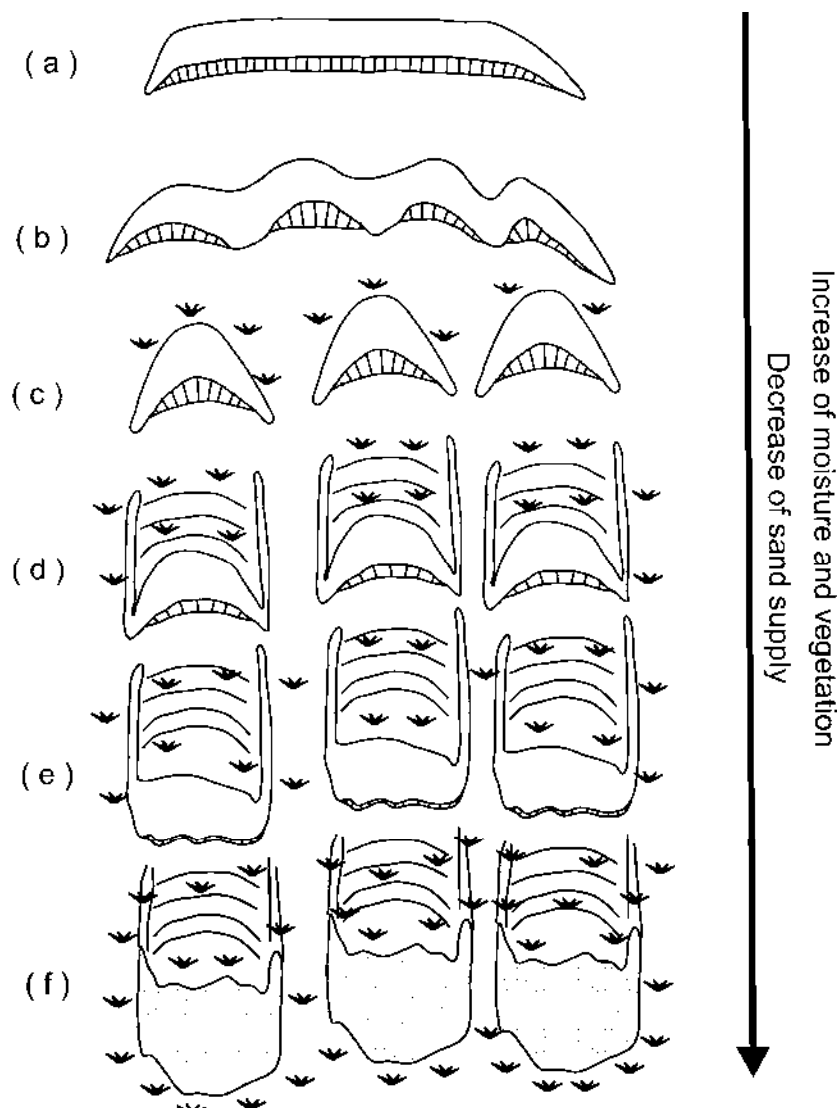


Figure 16: Progressive stages that RS dunes are experiencing for the last 58 years, driven by an increase in moisture, decrease in wind energy, and decrease in sediment supply. Transverse dune (a); Barchanoid chain (b); Isolated barchan dunes with some vegetation growth starting in the deflation areas (c); Barchan dunes leaving behind gegenwalle ridges and trailing ridges, trapped by vegetation (d); Low parabolic dunes (e); and flat sand sheets with parabolic shapes.

5.6. CONCLUSIONS

- The RS dunefields vary along the coast from Rondinha to Mostardas. They are narrow and restricted in the north and increase in size southwards. The factors responsible for this variation in dunefield morphology could be many, including variations in precipitation, wind velocity and direction, sediment supply, wave energy, LST and antecedent topography which produces different types of barriers. Nevertheless, the available data of rainfall, wind and wave energy together can explain those differences along the coast. In the south the dunefields are larger because there is higher wind energy capable to transport sand, less humidity and more sand supply, represented by the larger, wider dunefields and the high wave energy. While in the north the dunefields are smaller due to the weaker winds, higher rainfall and less sand supply.
- The RS dunefields have also changed through time. Wet, vegetated deflation areas have enlarged since 1948 in all studied dunefields. This process of dunefield stabilization could be a result of a number of factors including changes in moisture, wind, waves, frequency of storms, sand supply and human impacts. Nevertheless, the only historical data available are precipitation and wind. An observed increase in precipitation over 55 years and a decrease, for 25 years, in wind DP (*Martinho et al. submitted*) might have been responsible for this stabilization. In addition, in order for the expansion of deflation plains landwards, and the development of foredunes along the coast to take place, it is likely that there has been a decrease in either (i) sand supply, or (ii) storms. Both would allow the formation of foredunes, and the development and expansion of deflation plains.
- After these years of change in precipitation and wind, the less active, smaller and lower volume northern dunefields responded faster to changes in climate and they are in an advanced degree of stabilization. On the RS mid-littoral, the dunefields are large, the width of active dunefield is significant, and the sand volume is higher, so they take longer time to start the stabilization processes and vegetation growth. The larger the amount of sand and size of the active dunefield, the longer is the period required to stabilize it.

- Not only did dunefield morphologies change since 1948, but also the dune forms comprising the dunefields have changed significantly. As the increase in moisture and decrease in wind DP reduced the sand availability, the dune forms inside the dunefield have progressively changed from high barchanoid chains to single barchans with gegenwalle ridges at the upwind margin and finally to parabolic dunes or flat sand sheets with parabolic shapes.

ACKNOWLEDGMENTS

This research was partly supported by grants of RECOIS-Institutos do Milênio and Conselho Nacional de Desenvolvimento Científico e Tecnológico (CNPq). We thank CNPq for the PhD Scholarship and Comissão Permanente de Aperfeiçoamento de Pessoal de Nível Superior (CAPES) for the doctorate *sandwich* scholarship to Caroline Martinho, the Dept of Geography and Anthropology at LSU and CECO at UFRGS for provision of research facilities, and LSU for providing the USGS 1948 aerial photographic collection. Sérgio Dillenburg thanks CNPq for his scholarship, and Patrick Hesp thanks LSU and UFRGS for support. We also thank Graziela Miot da Silva for her assistance with the wind analyses.

REFERENCES

- BAGNOLD, R.A. 1941. *The Physics of Blown Sand and Desert Dunes*. London, Chapman & Hall, 265p.
- BELLY, P.Y. 1964. *Sand Movement by Wind*. US Army Corps of Engineers Technical Memo No. 1.
- BRESSOLIER, C.; FROIDEFOUND, J.M.; THOMAS, Y.F. 1990. Chronology of coastal dunes in the South-West of France. *Catena Supplement* **18**: 101-107.
- CARTER, R.W.G. 1988. *Coastal Environments*. Academic Press, London, 617 pp.
- CARTER, R.W.G. & CHANCE, S., 1997. Integrated management of coastal dunes in Ireland: Assessment and example. In: NOVO, F.G.; CRAWFORD, R.M.M.; BARRADAS, M.C.D. eds. *The Ecology and Conservation of European Dunes*. Universidad de Sevilla, Secretariado de Publicaciones, p.301-314.
- CHASE, B.M. & THOMAS, D.S.G. 2006. Late Quaternary dune accumulation along the western margin of South Africa: distinguishing forcing mechanisms through the analysis of migratory dune forms. *Earth Planet. Scien. Letters* **251**: 318-

- 333.CHASE, B.M. & THOMAS, D.S.G. 2007. Multiphase late Quaternary aeolian sediment accumulation in western South Africa: Timing and relationship to palaeoclimatic changes inferred from the marine record. *Quaternary International* **166**: 29-41.
- CLARKE, M.L.; RENDELL, H.M.; PYE, K.; TASTET, J.P.; PONTEE, N.I.; MASSÉ, L. 1999. Evidence for the timing of dune development on the Aquitaine coast, southwest France. *Z. Geomorph. N.F. Suppl.Bd* **116**: 147-163.
- CLEMMENSEN, L.B.; ANDREASEN, F.; HEINEMEIER, J.; MURRAY, A.S. 2001. A Holocene coastal aeolian system, Vejers, Denmark: landscape evolution and sequence stratigraphy. *Terra Nova*, **13**: 129-134.
- COOPER, W.S. 1958. *Coastal Sand Dunes of Oregon and Washington*. Geol. Soc. Am. Mem. **72**, 169 pp.
- COOPER, W.S. 1967. *Coastal Dunes of California*. Geol. Soc. Am. Mem. **104**, 131 pp.
- DAVIES, J.L. 1980. *Geographical Variation in Coastal Development*. Longman, London, 2nd ed. 212pp.
- DILLENBURG, S.R.; ROY, P.S.; COWELL, P.J.; TOMAZELLI, L.J. 2000. Influence of antecedent topography on coastal evolution as tested by shoreface translation-barrier model (STM). *Journal of coastal research*, **16**(1): 71-81.
- DILLENBURG, S.R., TOMAZELLI, L.J., CLEROT, L.C.P. 2003. Gradients of wave energy as the main factor controlling the evolution of the coast of Rio Grande do Sul in southern Brazil during the Late Holocene. *Proceedings of the 5th International Symposium on Coastal Engineering and Science of Coastal Sediment Process*. New York, NY: American Society of Civil Engineers, v.1, CD, 2003.
- DILLENBURG, S.R.; TOMAZELLI, L.J.; BARBOZA, E.G. 2004a. Barrier evolution and placer formation at Bujuru southern Brazil. *Marine Geology*, **203**: 43-56.
- DILLENBURG, S.R.; ESTEVES, L.S.; TOMAZELLI, L.J. 2004b. A critical evaluation of coastal erosion in Rio Grande do Sul, Southern Brazil. *Anais da academia brasileira de ciências*, **76**(3): 611-623.
- DILLENBURG, S.R.; TOMAZELLI, L.J.; HESP, P.A.; BARBOZA, E.G.; CLEROT, L.C.P.; SILVA, D.B. 2006. Stratigraphy and evolution of a prograded, transgressive dunefield barrier in southern Brazil. *Journal of Coastal research* SI **39**: 132-135.
- ESTEVES, L.S.; SILVA, A.R.P.; AREJANO, T.B.; PIVEL, M.A.G. VRANJAC, M.P. 2003. Coastal development and human impacts along the Rio Grande do Sul beaches, Brazil. *Journal of Coastal Research*, **SI 35**: 548-556.
- FIGUEIREDO, S.A. & CALLIARI, L.J. 2005. Sangradouro: Distribuição especial, variação sazonal, padrões morfológicos e implicação no gerenciamento costeiro. *Gravel* **3**: 47-57.

- FILION, L. 1984. A relationship between dunes, fire and climate recorded in the Holocene deposits of Quebec. *Nature*, **309**: 543-546.
- FORMANN, S.L.; MARÍN, L.; PIERSON, J.; GÓMEZ,J.; MILLER, G.H.; WEBB, R.S. 2005. Aeolian sand depositional records from western Nebraska: landscape response to droughts in the past 1500 years. *The Holocene* **15** (7): 973-981.
- FRYBERGER, S.G.; DEAN, G. 1979. Dune forms and wind regime. In: MCKEE, E.D. (Ed.) *A Study of Global Sand Seas*. USGS, Professional paper **1052**:137-169.
- GIANNINI, P.C.F.; SAWAKUCHI, A.O.; MARTINHO, C.T. 2001a. A estratigrafia de seqüências na evolução das dunas costeiras de Santa Catarina, Sul do Brasil. In: I CONGRESSO DO QUATERNÁRIO DOS PAÍSES DE LÍNGUA IBÉRICA, Lisboa. *Actas*, GTPEQ., AEQUA, SGP. p. 117-120.
- GIANNINI, P.C.F.; SAWAKUCHI, A.O.; MARTINHO, C.T. 2001b. O nível do mar e as dunas eólicas no litoral centro-sul catarinense: um modelo de estratigrafia de seqüências no Quaternário. In: VIII CONGRESSO ABEQUA, Imbé, RS. *Boletim de resumos*, ABEQUA. p. 45-46.
- GIANNINI, P.C.F.; ASSINE, M.L.; BARBOSA, L.M.; BARRETO, A.M.F.; CARVALHO, A.M.; CLAUDINO-SALES, V.; MAIA, L.P.; MARTINHO, C.T.; PEULVAST, J.P.; SAWAKUCHI, A.O. & TOMAZELLI, L.J. 2005. Dunas Eólicas Costeiras e Interiores. In: SOUZA, C.R.G.; SUGUIO, K.; DE OLIVEIRA, P.E. & OLIVEIRA, A.M.S. (Eds.). *Quaternário do Brasil*. Holos Editora, São Paulo. 235-257.
- GRIMM, A.M.; FERRAZ, S.E.T.; GOMES, J. 1998. Precipitation anomalies in Southern Brazil associated with El Niño and La Niña events. *J. Climate*, **11**: 2863-2880.
- HESP, P.A. 1989. A review of biological and geomorphological processes involved in the initiation and development of incipient foredunes. *Procc. Royal Soc. Edinburg*, **96B**: 181-201.
- HESP, P.A., 1999. The beach backshore and beyond. In: SHORT, A.D. (Ed.) *Handbook of Beach and Shoreface Morphodynamics*. Chichester, John Wiley & Sons Ltd, p. 145-270.
- HESP, P.A., 2002. Foredunes and blowouts: initiation, geomorphology and dynamics. *Geomorphology* **48**: 245-268.
- HESP, P.A. 2003. El Niño winds and dune dynamics, west coast, North Island, New Zealand. *Proceedings Canadian Coastal Conference*, 1-6.
- HESP, P.A. 2004. Coastal dunes in the Tropics and Temperate Regions: Location, formation, morphology and vegetation processes. In: MARTINEZ, M. & PSUTY, N. (Eds.) *Coastal Dunes, Ecology and Conservation. Ecological Studies* v. 171. Springer-Verlag, Berlin: 29-49.

- HESP, P.A. & THOM, B.G. 1990. Geomorphology and evolution of active transgressive dunefields. In: NORDSTROM, K.F.; PSUTY, N.P.; CARTER, R.W.G. (Eds.) *Coastal Dunes: Form and Process*. Chichester, John Wiley & Sons Ltd, 253-287.
- HESP, P.A. & SHORT, A.D., 1999. Barrier Morphodynamics. In: SHORT, A.D. (Ed.) *Handbook of Beach and Shoreface Morphodynamics*. Chichester, John Wiley & Sons Ltd, p. 307-333.
- HESP, P.A. & MARTINEZ, M. 2007. Disturbance in coastal dune ecosystems. In: E.A. Johnson and K. Miyaniishi (Eds.), *Plant Disturbance Ecology: The Process and Response*. Academic Press: 215-247.
- HESP, P.A.; DILLENBURG, S.R.; BARBOZA, E.G.; TOMAZELLI, L.J.; AYUP-ZOUAIN, R.N.; ESTEVES, L.S.; GRUBER, N.L.S.; TOLDO JR., E.E.; TABAJARA, L.L.C.A.; CLEROT, L.C.P. 2005. Beach ridges, foredunes or transgressive dunefields? Definitions and an examination of the Torres to Tramandaí barrier system, Southern Brazil. *Anais da Academia Brasileira de Ciências* **77** (3): 493-508.
- HESP, P.A.; DILLENBURG, S.R.; BARBOZA, E.G.; CLEROT, L.C.P.; TOMAZELLI, L.J.; AYUP-ZOUAIN, R.N. 2007. Morphology of the Itapeva to Tramandaí transgressive dunefield barrier system and mid- to late Holocene sea level change. *Earth Surf. Process. Landforms* **32**: 407-414.
- HUGENHOLTZ, C.H.; WOLFE, S.A. 2005. Recent stabilization of active sand dunes on the Canadian prairies and relation to recent climate variations. *Geomorphology* **68**: 131-147.
- ILLEMBERGER, W.K. 1988. The Holocene evolution of the Sundays estuary and adjacent coastal dunefields, Algoa Bay, South Africa. In: DARDIS, G.F. & MOON, B.P. (Eds.) *Geomorphological Studies in Southern Africa*. Balkema, Rotterdam, 389-405.
- ILLEMBERGER, W.K. & VERHAGEN, B.T. 1990. Environmental history and dating of coastal dunefields. *Suid-Afrikaanse Tydskrif vir Wetenskap* **86**: 311-314.
- LEES, B. 2006. Timing and formation of coastal dunes in Northern and Eastern Australia. *Journal of Coastal Research*, **22**(1): 78-89.
- LIMA, S.F.; ALMEIDA, L.E.S.B.; TOLDO JR., E.E. 2001. Estimate of longshore sediments transport from waves data to the Rio Grande do Sul coast. *Pesquisas*, **48** (2): 99-107.
- LOOPE, W.L.; ARBOGAST, A.F. 2000. Dominance of an ~150-year cycle of sand-supply change in the Late Holocene dune-building along the Eastern Shore of Lake Michigan. *Quaternary Research*, **54**: 414-422.
- MARCOMINI, S.C.; MAIDANA N. 2006. Response of eolian ecosystems to minor climatic changes. *Journal of Coastal Research SI* **39**: 204-208.

- MARTINHO, C.T. 2004. *Morfodinâmica e sedimentologia de campos de dunas transgressivos da região de Jaguaruna-Imbituba, Santa Catarina*. São Paulo, Inst. Geoc. Univ. S. Paulo. Dissertação de Mestrado, (ined.) 108p.
- MARTINHO, C.T.; GIANNINI, P.C.F.; SAWAKUCHI, A.O. 2006. Morphological and depositional facies of transgressive dunefields in the Imbituba-Jaguaruna region, Santa Catarina State, Southern Brazil. *Journal of Coastal Research*, SI 39: 673-677.
- MARTINHO, C.T.; DILLENBURG, S.R.; HESP, P.A. (Accepted). Wave energy and longshore sediment transport gradients controlling barrier evolution in Rio Grande do Sul, Brazil. *Journal of Coastal Research*.
- MARTINHO, C.T.; HESP, P.A.; DILLENBURG, S.R.; TOMAZELLI, L.J. (Submitted). Climate patterns and variations on the Rio Grande do Sul Coast and coastal dunefield dynamics. *Earth Surf. Process. Landforms*.
- MAY, J. P. & TANNER, W. F. 1973. The littoral power gradient and shoreline changes. In: COATES, D.R. (Ed.), *Publications in Geomorphology*. Binghamton: State University of New York, 43-60.
- McKEE, E.D. 1979. Introduction to a study of global sand seas. In: McKEE, E.D. (Ed.). *A Study of Global Sand Seas*. USGS, Professional paper **1052**:1-19.
- MURRAY, A.S. & CLEMMENSEN, L.B. 2001. Luminescence dating of Holocene aeolian sand movement, Thy, Denmark. *Quaternary Sciences Reviews*, **20**: 751-754.
- ORFORD, J.D. 2005. The controls on Late-Holocene coastal dune formation on leeside coasts of the British Isles. *Z. Geomorph. N. F.*, **141**: 135-152.
- PAUL, K. 1944. Morphologie und vegetation der Kurische Nehrung. *Acta Nova Leopoldina Carol.*, NF **13**: 217-378.
- PIOTROWSKA, H & GOS, K. 1993. Coastal dune vegetation in Poland; diversity and development. In: VAN DIJK, H.W.J. (Ed.) *Management and Preservation of Coastal habitats*. Euro. Union for Coastal Conservation: 71-83.
- PYE, K. 1983. Formation and history of Queensland coastal dunes. *Z. Geomorph. N.F.* Suppl.-Bd **45**: 175-204.
- PYE, K. & BOWMAN, G.M. 1984. The Holocene marine transgression as a forcing function in episodic dune activity on the Eastern Australian Coast. In: THOM, B.G. (Ed.) *Coastal Geomorphology in Australia*. Academic Press Australia, 179-196.
- PYE, K. & RHODES, E.G. 1985. Holocene development of an episodic transgressive dune barrier, Ramsay Bay, North Queensland, Australia. *Marine Geology*, **64**: 189-202.
- RANWELL, D.S. 1972. *Ecology of Salt Marshes and Sand Dunes*. Chapman & Hall, London, 258 pp.

- ROY, P.S.; COWELL, P.J.; FERLAND, M.A.; THOM, B.G. 1994. Wave-dominated coasts. In: CARTER, R.W.G. & WOODROFFE, C.D. (Eds.) *Coastal evolution, Late Quaternary Shoreline Morphodynamics*. Cambridge, Cambridge University Press, p.121-186.
- SEELIGER, U. 1998. O sistema de dunas frontais. In: SEELIGER, U.; ODEBRECHT, C.; CASTELLO, J.P. (Eds.) *Os Ecossistemas Costeiro e Marinho do Extremo Sul do Brasil*. Rio Grande. Editora Ecoscientia, p. 179-184.
- SEMC – SECRETARIA de ENERGIA, MINAS e COMUNICAÇÕES. 2002. *Atlas Eólico: Rio Grande do Sul*. Porto Alegre: SEMC, 70p.
- SHEPHERD, M.J. & HESP, P.A. 2003. New Zealand coastal barriers and dunes. In: ROUSE, H.; GOFF, J.; NICHOL, S. (Eds.) *The New Zealand Coast: Te Tai O Aotearoa*. Dunmore Press in assoc. with Whitireia Publishing and Daphne Brasell Associates Ltd., Palmerston North, NZ: 163-190.
- SHERMAN, D.J. & LYONS, W. 1994. Beach-state controls on aeolian sand delivery to coastal dunes. *Physical Geography* **15** (4): 381-395.
- SHORT, A.D. 1988a. The south Australia coast and Holocene sea-level transgression. *The Geographical Review*, **78**(2): 119-136.
- SHORT, A.D. 1988b. Holocene coastal dune formation in Southern Austrália: a case study. *Sed. Geol.*, **55** (1/2): 121 - 142.
- SHORT, A.D. & HESP, P.A. 1982. Wave, beach and dune interactions in South-eastern Austrália. *Marine Geol.*, **48**(4): 259-284.
- SHULMEISTER, J. & LEES, B. 1992. Morphology and chronostratigraphy of coastal dunefield: Groote Eylandt, northern Australia. *Geomorphology* **5**: 521-534.
- TASTET, J.P.; PONTEE, N.I. 1998. Morpho-chronology of coastal dunes in Médoc. A new interpretation of Holocene dunes in Southwestern France. *Geomorphology* **25**: 93-109.
- THOM, B.G. 1978. Coastal sand deposition in southeast Australia during the Holocene. In: DAVIS, J.L. & WILLIAMS, M.A.J. (Eds), *Landform Evolution in Australasia*. ANU Press, pp. 197-214.
- TOLDO JR, E.E. ; ALMEIDA, L.E.S.B.; NICOLODI, J.L.; ABSALONSEN, L.; GRUBER, N.L.S. 2006. O controle da deriva litorânea no desenvolvimento do campo de dunas e da antepraia no litoral médio do Rio Grande do Sul. *Pesquisas* **33** (2): 35-42.
- TOMAZELLI, L.J. 1990. *Contribuição ao Estudo dos Sistemas Depositionais Holocénicos do Nordeste da Província Costeira do Rio Grande do Sul, com Ênfase no Sistema Eólico*. Porto Alegre, Univ. Federal Rio Grande do Sul. Tese de Doutoramento (inéd). 270p.
- TOMAZELLI, L.J. 1994. Morfologia, organização e evolução do campo eólico costeiro do litoral norte do Rio Grande do Sul, Brasil. *Pesquisas*, **21** (1): 64-71.

- TRENHAILE, A.S., 1997. Sand Dunes. In: TRENHAILE, A.S. (Ed.), *Coastal Dynamics and Landforms*. Oxford, Clarendon Press, p.144-169.
- VILLWOCK, J.A., TOMAZELLI, L.J., LOSS, E.L., DEHNHARDT, E.A., HORN FILHO, N.O., BACHI, F.A., DEHNHARDT, B.A., 1986. Geology of the Rio Grande do Sul Coastal Province. *Quaternary of South America and Antarctic Peninsula*, **4**: 79-97.
- WILSON, P.; ORFORD, J.D.; KNIGHT, J.; BRALEY, S.M.; WINTLE, A.G. 2001. Late-Holocene (post-4000 years BP) coastal dune development in Northumberland, northeast England. *The Holocene*, **11** (2): 215-229.
- YOUNG, R.W.; BRYANT, E.A.; PRICE, D.M.; WIRTH, L.M.; PEASE, M. 1993. Theoretical constraints and chronological evidence of Holocene coastal development in central and southern New South Wales, Australia. *Geomorphology* **7**: 317-329.

CAPÍTULO 6

**MID TO LATE HOLOCENE EVOLUTION OF TRANSGRESSIVE
DUNEFIELDS FROM RIO GRANDE DO SUL COAST, SOUTHERN
BRAZIL**

Artigo submetido à *Marine Geology*

[Print - Close Window](#)

From: "Marine Geology" <margo-eo@elsevier.com>
To: ctmartinho@yahoo.com
Date: 28 Feb 2008 01:19:12 +0000
Subject: Acknowledgement of receipt of your submitted article

Dear Ms Martinho,

Your submission entitled "Mid to Late Holocene evolution of transgressive dunefields from Rio Grande do Sul coast, Southern Brazil" has been received by Marine Geology

Please note that submission of an article is understood to imply that the article is original and is not being considered for publication elsewhere. Submission also implies that all authors have approved the paper for release and are in agreement with its content.

You will be able to check on the progress of your paper by logging on to <http://ees.elsevier.com/margo/> as Author.

Your manuscript will be given a reference number in due course.

Thank you for submitting your work to this journal.

Kind regards,

Marine Geology

Mid to Late Holocene evolution of transgressive dunefields from Rio Grande do Sul coast, Southern Brazil

Caroline T. Martinho^a, Sérgio R. Dillenburg^b, Patrick A. Hesp^c

^a Universidade Federal do Rio Grande do Sul
Instituto de Geociências
Programa de Pós-Graduação em Geociências
Av. Bento Gonçalves 9500
91509-900, Porto Alegre, RS, Brasil
Tel: + 55 51 30295689 Fax: + 55 51 33086332
ctmartinho@yahoo.com

^b Universidade Federal do Rio Grande do Sul
Instituto de Geociências
Centro de Estudos de Geologia Costeira e Oceânica
Av. Bento Gonçalves 9500
91509-900, Porto Alegre, RS, Brasil
sergio.dillenburg@ufrgs.br

^c Louisiana State University
Department of Geography and Anthropology
227 Howe/Russell Geosciences Complex
Baton Rouge, LA 70803-4105, USA
pahesp@lsu.edu

ABSTRACT

The aim of this paper is to examine the dunefield evolution of the Rio Grande do Sul (RS) coastal stretch from Torres to Mostardas, which presents progradational, aggradational and retrogradational barriers. The stratigraphy and sedimentary facies of 26 cores along 9 profiles were analyzed. The stratigraphy of the cores along the profiles agreed with the suggested barrier types. The northern area comprises prograded barriers; in Jardim do Éden and Magistério, retrograded barriers; in Dunas Altas an aggradational barrier; and the southernmost profiles, Solidão, São Simão and Mostardas retrograded barriers.

Three major periods of soil formation and dunefield stabilization were found: from 4820 to 3970 yr BP, in 2760-2460 cal yr BP and from 1570 to 710 yr BP. These periods coincide with periods where the literature cites an increase in moisture during the mid to late Holocene. This coincidence of soil formation and wet climate indicates that the climate might be controlling dunefield evolution on the RS coast since 5000 yr BP. The stratigraphic data of the three most representative cores were correlated, and along with the available ages from palaeosols and the facies descriptions 10 phases of aeolian activity and stabilization were recognized for the mid-littoral of RS.

6.1. INTRODUCTION

Transgressive dunefields are sand deposits, formed by winds, which develop adjacent to the beach, by the onshore or alongshore sand migration (Hesp & Thom 1990; Hesp 1999). The term “transgressive” dunes was firstly adopted by Gardner (1955) to describe aeolian sand deposits that migrated landwards, from the beach, “transgressing” over the continent (Hesp & Thom 1990; Hesp 1999). These dunefields may occur in a variety of climate regimes, but they are more common in coasts with temperate humid climate, abundant sand supply, and especially in high wave energy beaches, exposed to strong onshore winds (Short 1988a, b; Hesp 1989; Hesp *et al.* 1989; Hesp & Thom 1990; Trenhaile 1997). They may have varied sizes, from hundreds of meters to many kilometers long, and present a complex suite of dunes and geomorphological features including deflation plains, blowouts, transverse dunes, barchanoid chains, sand sheets, parabolic dunes, precipitation ridges and others.

Transgressive dunefields are present along the entire Rio Grande do Sul (RS) coast, but studies on their evolution are still scarce. One of the first and more detailed studies on these dunefields was carried out by Tomazelli (1990, 1993 and 1994) where he described the dunefield morphology, dune migration rates and calculated a maximum age for the northern littoral dunefields. Taking the migration rates in m/year, the migration direction and the maximum dunefield width he estimated that the dunefields in the area would be younger than 1000-1500 years before present (yr BP), a very recent aeolian activity.

Dillenburg *et al.* (2004a) studied a highly erosive barrier at Bujuru, RS mid-littoral, and also found for the active dunefields the maximum age of 1060 ± 70 yr BP by dating a layer of peat under the aeolian deposits.

Hesp *et al.* (2005) observed that the Holocene progradational barrier at the RS northern littoral was not formed by beach ridges or foredune ridges as stated previously (Delaney 1963; Villwock 1984; Villwock and Tomazelli 1995; Dillenburg *et al.* 2000), but was formed by successive overlapping of low and vegetated transgressive dunefields, which were formed by phases of dune transgression. The last phase is the active dunefield. This means that dunefields were present throughout the entire Holocene, evolving in phases of activity and phases of stability. Hesp *et al.* (2007) analyzing aerial photos from Curumim, northern littoral, found 12 phases of dunefield transgression and dated some of them by TL and OSL. Later, Dillenburg *et al.* (in review) using 13 TL and OSL dates along the barrier and four ^{14}C dates from drill holes drafted a scheme with the ages of each phase (Figs. 1 and 2). The oldest phase dates around 7000 yr BP, the 11th phase dates around 3000 yr BP, so the modern and active phase would be younger than 3000 years.

In recent times the transgressive dunefields of the RS northern littoral progradational barrier are well studied; nevertheless, the dunefield evolution of the RS mid-littoral is still very poorly understood. The barriers in this area are aggradational to retrogradational (Dillenburg *et al.* 2000; Martinho *et al.* accepted) and the active dunefield sometimes covers the entire Holocene barrier, thereby making it impossible to recognize older aeolian phases from aerial photos. Would the aeolian phases described by Hesp *et al.* (2007) be vertically preserved, under the modern phase, in the mid-littoral?

This paper describes the stratigraphy of RS dunefields by analyzing data from 26 cores made in transgressive dunefields distributed from the northern to mid-

littoral of Rio Grande do Sul, and attempts to understand the dunefield evolution during the mid to late Holocene, over a stretch of the RS coast that comprises three different types of barriers. Within the cores, the aeolian phases are only recognizable when there is a paleosol layer separating them, showing a stabilization phase between the aeolian activity phases.

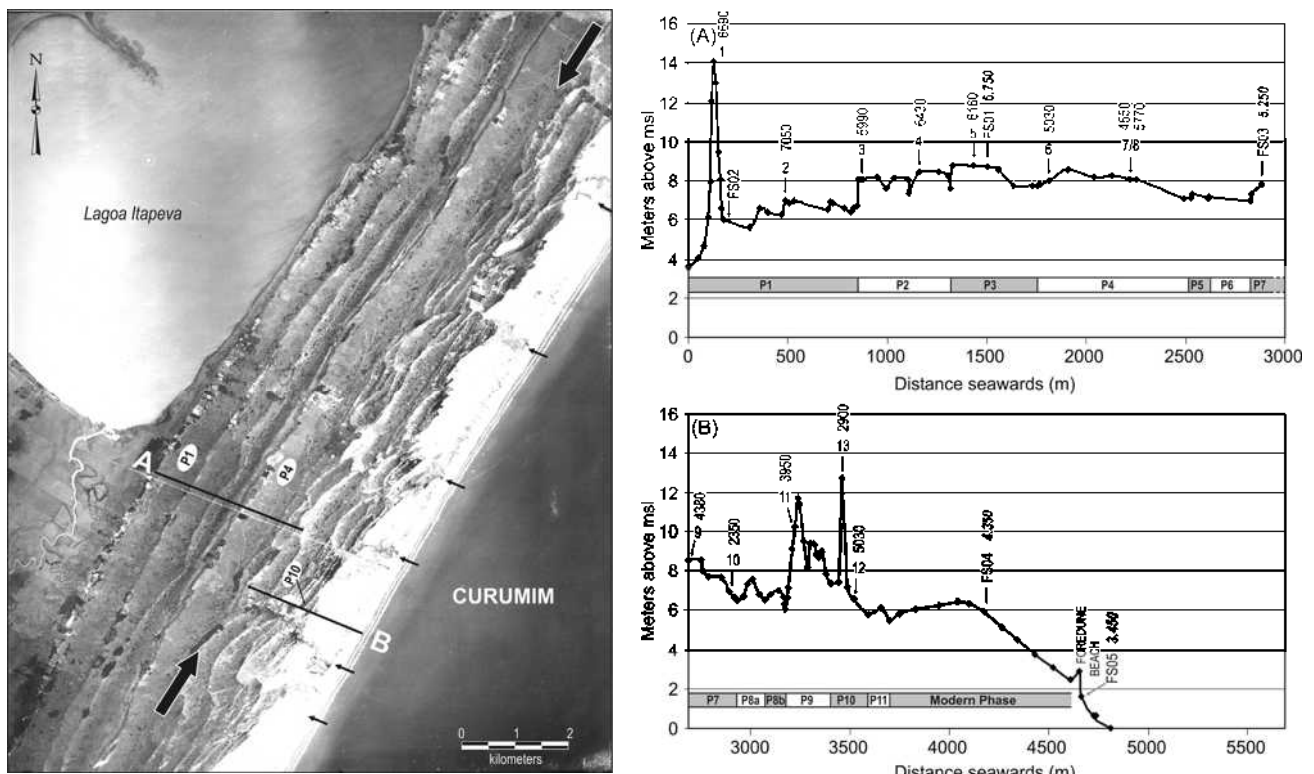


Figure 1: Aerial photo of Curumim progradational barrier with the overlapping dunefields. The lines A and B represent the survey lines. (A) and (B) are the topographic section of those lines, illustrating the location and the TL/OSL age of the aeolian phase. Ages in bold represent ^{14}C dates (non calibrated) of shoreface (nearshore) sediments from subsurface drill holes. Each phase from P1 to P11 is represented in the horizontal bar (data from Hesp *et al.* 2007 and Dillenburg *et al.* in review).

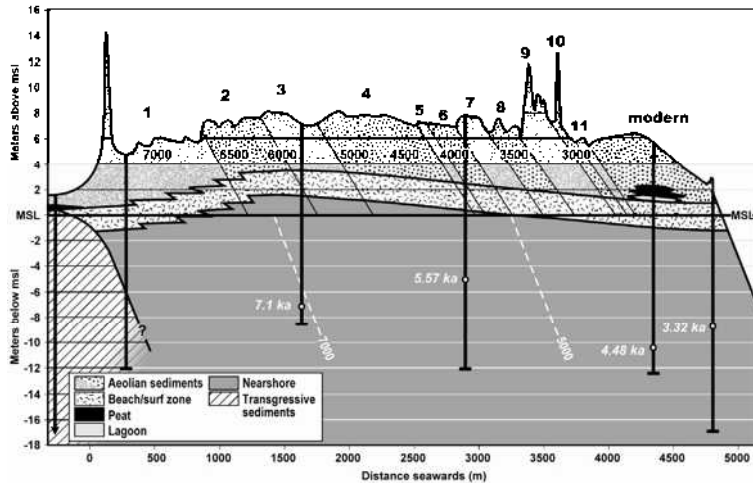


Figure 2: Cross geological section of Curumim barrier with the average TL/OSL age and width of each aeolian phase. The subsurface information is based on drill holes data of Dillenburg *et al.* (2006). White dots represent the location of ^{14}C samples in the core. The ^{14}C dates were obtained from shells of shoreface deposits (data from Hesp *et al.* 2007 and Dillenburg *et al.* in review).

6.2. REGIONAL SETTINGS

The RS coast is characterized by a barrier-lagoon depositional system, dominated by waves. Four barrier-lagoon systems have been formed during the Quaternary. The latest one, built during the Holocene, is designated Barrier-Lagoon IV (Villwock *et al.* 1986). The barrier started to form around 7-8 ka BP, as a result of the migration of a transgressive barrier, during the final stages of the post-glacial marine transgression (PMT) (Dillenburg *et al.* 2006; Hesp *et al.* 2005). Initially this barrier had isolated large lagoons, which were segmented during the relative sea-level (RSL) lowering after the transgressive maximum. Besides the modern beach, the barrier consists of large dunefields, from 2 to 8 km in width (Tomazelli 1990; Hesp *et al.* 2005; Martinho *et al.* submitted b).

The study area is the RS costal stretch from Torres to Mostardas (Fig. 3). The coastal stretch from Torres to Magistério is considered the Northern littoral of RS, while from Magistério to Mostardas is the Mid- littoral (according to FEPAM – www.fepam.rs.gov.br/programas/gerco.asp). The coastline is undulating, orientated to the NE-SW, with approximately 250 km in length. The tidal range is 0.5 m (microtidal) with semi-diurnal tides (Tomazelli & Villwock 1992). According to Lima *et al.* (2001), waves from the N-NE represent the most frequent direction, but their capacity for longshore transport is limited by their short period and low energy. Waves from the S

are less frequent but along with their high energy and long period, and are responsible for the main longshore transport direction, towards the NE.

The coast receives almost no sediment supply from the continent as the sediments transported by rivers are deposited in the lake/lagoon systems, behind the barrier (Tomazelli *et al.* 1998). So, the sediment budget of the RS barriers depends on the sediment transference across the shoreface and between the shoreface and inner shelf, as well as on the longshore sediment transport.

Dillenburg *et al.* (2000), using the Shoreface Translation-Barrier Model (STM), stated that the barriers present today along the RS coast are a response to the antecedent topography. During the Holocene, the antecedent topography represented by the substrate slope has defined the shape of the RS coast and, as a consequence, the type of barriers, since small differences in the slope produce important differences in barrier translation (Dillenburg *et al.* 2000; Travessas *et al.* 2005). Between the altitude of +2m and the isobath of -70m, the inner shelf slope varies from 0.027° to 0.125° along the RS coast (Dillenburg *et al.* 2000). This slope variation is accompanied by variations in coastline orientation. Where the inner shelf slope is steep, the coastline is convex and where the inner shelf slope is gentle, the coastline is concave (Dillenburg *et al.* 2000).

The STM predicted a more accentuated undulation of the RS coast at 5000 yr BP, and since then, Dillenburg *et al.* (2000, 2003) states that coastal processes would have been acting to attenuate the undulation and straighten the coastline. Thus, where the coastline is concave, progradational barriers would predominate and in the convex coastal stretches retrograding barriers would occur. Martinho *et al.* (accepted), in an attempt to test the Dillenburg *et al.* assumption, calculated wave energy and longshore sediment transport (LST) rates, using wave heights measured in the field. They observed that wave energy and LST vary along the coast, what can cause variations in sediment budgets cross-shore and alongshore. Wave energy and LST are higher in the convex areas, from Mostardas to Atlântida Sul, and lower in the concave area, from Atlântida Sul to Rondinha. Lima *et al.* (2001) calculated the resultant direction and the volume of sediment transported alongshore per year and also found that the transport rates decrease northwards. The high wave energy and LST rates in the south would promote coastal erosion and form retrogradational barriers. Northwards, the decrease in wave energy and LST rates would create a local positive imbalance in sediment supply, forming progradational barriers.

Martinho *et al.* (submitted a) observed that in Mostardas, south of the study area, wind drift potentials (DP) are stronger, decreasing northwards. Precipitation is lower in the south and higher in the north, where the coast is adjacent to the Serra do Mar scarps. Martinho *et al.* (submitted b) described large dunefields in the south and relatively narrower and restricted dunefields in the north. The erosion of the coastline in the south would promote more sand availability to be transported by the strong winds of this area.

Along the stretch of the RS coast from Torres to Mostardas, the Holocene barrier appears as three types: progradational, aggradational and retrogradational barriers (Fig. 4) (Dillenburg *et al.* 2000, 2003; Travessas *et al.* 2005; Dillenburg *et al.* 2004a, b; Hesp *et al.* 2005; Dillenburg *et al.* 2006, Martinho *et al.* accepted). From Torres to Atlântida Sul the barrier is progradational presenting a lagoon system at the back and a succession of overlapping transgressive dunefields separated by precipitation ridges (Hesp *et al.* 2005; Hesp *et al.* 2007; Martinho *et al.* accepted). The dunefields present on this barrier are smaller and not very well developed when compared to the others due to the local topography, climate and sand supply (Martinho *et al.* submitted b).

An aggradational barrier type is characterized by the alternation of progradational and retrogradational processes producing a quasi-stationary coastline (Morton 1994). This type of barrier is observed from Atlântida Sul to Jardim do Éden (Travessas *et al.* 2005) and at Dunas Altas (Dillenburg *et al.* 2007). Even with the coastline stability, the dunefields on this barrier are very wide and migrate landwards covering the entire Holocene barrier and silting the lakes behind the barrier (Martinho *et al.* submitted b).

Retrogradational barriers (*apud* Martinho *et al.* accepted) occur from Jardim do Éden to Mostardas, excluding the stretch around Dunas Altas. This barrier type is characterized by the coastline receding landwards (Morton 1994). The eroded sediments from the retrogradational processes apparently have been in part transferred to the dunefields which, over this barrier, are the largest and cover partially the lake deposits, locally reaching the Pleistocene barrier (Martinho *et al.* submitted b).

Dunas Altas contradicts the expected retrogradational behavior of the adjacent coastal stretches probably because it is located on an apex where there is an abrupt change in the coastline orientation to the south and north. Toldo Jr. *et al.* (2006) state that this change in coastline orientation promotes a deceleration in the LST rates.

The LST deceleration causes a “jam” in the sediments and they are partially deposited on the shoreface, creating a local positive sediment budget (Toldo Jr. *et al.* 2006). With this local positive budget, even with high wave energy, the coastal erosion and the regional retrogradational character were negated, creating an aggradational barrier around Dunas Altas.

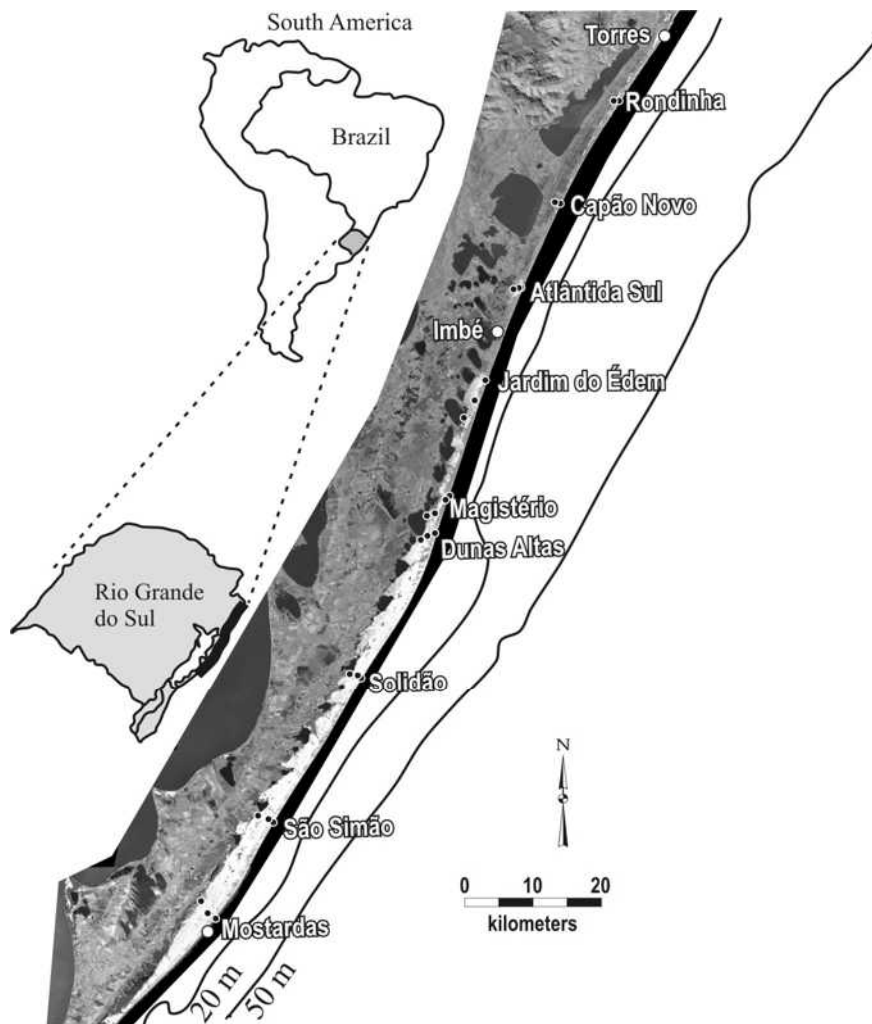


Figure 3: The study area located on the northern and mid-littoral of RS coast. Black dots indicate the location of the drill-holes in each of the nine profiles. White dots are the location of meteorological stations. The continuous lines represent the isobaths of 20m and 50m.

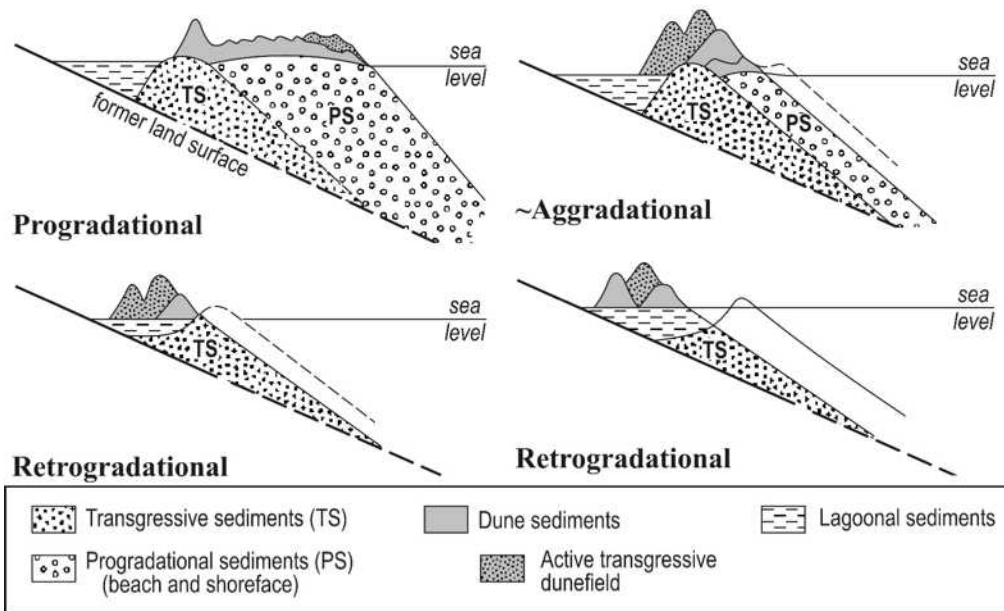


Figure 4: The barrier types present along the study area (modified from Martinho *et al.* accepted).

6.2.1. Holocene relative sea level in southern Brazil

Holocene sea level data on the RS coast is deficient due to the lack of precise paleo-sea-level indicators. Thus, the curves from the southern littoral of Santa Catarina, an adjacent area, are considered to apply to the RS coast.

There is a consensus that during the early Holocene the relative sea level (RSL) was rising and achieved the present level around 7550 calibrated (cal) yr BP and continued rising until 5000 yr approximately (Fig. 5) (Martin *et al.* 1979/1980; Suguio *et al.* 1985; Tomazelli and Villwock 1989; Tomazelli 1990; Angulo *et al.* 2006; Hesp *et al.* 2007). The discrepancies in the RSL curves start around 5000 yr BP. Suguio *et al.* (1985) and Martin *et al.* (1988), based on shell-middens and marine terrace dates, produced a sea-level curve for southern Santa Catarina State where the post-glacial marine transgression (PMT) reached 4m above the present level and two events of high frequency oscillation where the RSL would have been below present (around 4000 yr and 2500 yr BP).

Tomazelli & Villwock (1989) and Tomazelli (1990) have drawn a sea-level curve for the RS coast based on the pre-existing curves of Suguio *et al.* (1985) and Martin *et al.* (1988), on marine and lagoon terraces and on peat deposits. Tomazelli & Villwock's (1989) sea-level curve differs from Suguio and Martin's in the last 2000 yr.

They stated, based on peat outcrops on the beach face, that at 2000 yr BP the RSL was below present and since then would have been gently rising till the present level.

Angulo *et al.* (2006) critically reviewing all sea-level information along the Brazilian coast states that shell-middens and marine terraces are very poor, inaccurate and non-conclusive RSL indicators. Angulo & Giannini (1996) discuss the RSL indicators of Tomazelli & Villwock (1989) sea-level curve and state that these indicators are not sufficient to affirm a rise in RSL in the last 2000 yr in RS coast.

Angulo *et al.* (1999) and Angulo *et al.* (2006) using vermetid shells, a highly accurate RSL indicator, proposed for the southern littoral of Santa Catarina, that the maximum of the PMT was about 2.1 m above the actual position, and lasted from 5000 to 5800 cal yr BP, without a distinct peak (Angulo *et al.* 2006). After the PMT the RSL have been smoothly falling to the present level (Fig. 5) (Angulo *et al.* 1999; Ybert *et al.* 2001; Angulo *et al.* 2006). This data agrees with the tendency of the Buenos Aires curve (Isla 1989) and other curves around the Southern Hemisphere (Angulo *et al.* 2006).

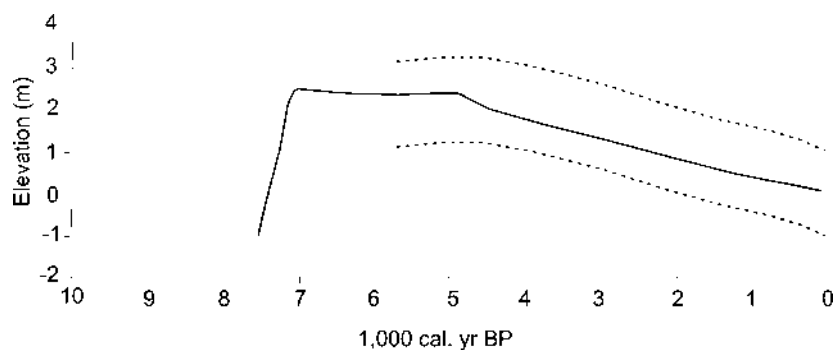


Figure 5: Dashed line represent the sea level envelope of Angulo *et al.* (2006) for the southern State of Santa Catarina. The solid line represent the paleosea-level behavior predicted by the geophysical simulations made by Milne *et al.* (2005) *apud* Angulo *et al.* (2006). Data from Angulo *et al.* (2006).

6.2.2. Climate changes during the mid to late Holocene in southern Brazil

Studies of paleoclimate on the coastal plain of Rio Grande do Sul and the highlands of Santa Catarina, State adjacent to the north of RS, identify some climate variations throughout the mid and late Holocene. During the early Holocene the climate was warm and dry (Behling 1997; Ledru *et al.* 1998; Behling *et al.* 1999; Bauermann 2003). From approximately 5000 to 4000 yr. BP the climate became more humid (Neves 1991; Prieto *et al.* 1999; Behling *et al.* 1999; Ybert *et al.* 2001). Behling (1997)

and Ybert *et al.* (2001) describe from 3000 to 2500 yr. BP a wetter period than the previous, what leads us to conclude that from 4000 to 3000 climate should be drier. Gómez *et al.* (2005), agreeing with Van Geel *et al.* (1996), state that around 2600 yr BP there was a global change in climate with the tropics becoming drier and boreal zones wetter. They describe an area near Bahía Blanca, Argentina, where the climate changed to semiarid conditions in 2610 ± 60 yr BP. Corroborating with these paleoclimatic data, Ybert *et al.* (2001) describe a drier climate from 2500 to 1500 yr BP in southern Brazil. Since 1500 yr BP until today, the area has been experiencing an increase in humidity (Behling 1997; Behling 1998; Behling *et al.* 1999; Ybert *et al.* 2001; Bauermann 2003).

In the 12 aeolian phases recognized by Hesp *et al.* (2007), four were formed from 7000 to 4500 yr BP. After 4500 yr BP at least other eight phases have developed and their morphology influenced by washouts and creeks that started to flow seawards (Hesp *et al.* 2007). This means that after the PMT maximum the RSL has initiated its slow fall and climate became a decisive factor in dunefield formation. The frequency of aeolian activation and stabilization increased possibly due to high frequencies of climate change, since ENSO (El Niño Southern Oscillations) type events started to occur in the area since \sim 4000 yr BP (Neves 1991; Behling 1997; Ybert *et al.* 2001).

6.3. METHODS

6.3.1. Drilling

The drill-holes were executed in profiles across the dunefields, from foredune to the inner dunefield limit. The number of drill-holes for each profile varied from two to four, depending on the size of the dunefield and the facility of access. A total of 26 drill-holes were executed in nine profiles along the northern and mid-littoral of RS (Fig. 3). The profiles locations were: Rondinha, Capão Novo, Atlântida Sul, Jardim do Éden, Magistério, Dunas Altas, Farol da Solidão, São Simão and Mostardas. Despite some exceptions, the profiles are composed by three drill-holes, one in the foredune, one in the center of the dunefield and one in the dunefield inner border. The exceptions are the profiles of Rondinha and Capão Novo which have only two drill-holes and Magistério profile with four drill-holes. The drilling method was by manual

percussion and the sampler was a PVC tube with 6 m in length. Due to the high number of drillings, only the most representative cores will be illustrated in this paper.

6.3.2. Dating

Sediments rich in organic matter appeared in the record of some cores as dark muds from lake bottoms or as dark sandy layers inside aeolian deposits. Performed by Beta Analytic Inc., Miami, FL, USA, eleven layers rich in organic matter were dated by AMS ^{14}C . The age of the muds provide a maximum age for aeolian deposits above them and the dark sandy layers will correspond to the age of an aeolian stabilization phase.

6.4. RESULTS

6.4.1. Sedimentary Facies

The sedimentary facies present in the cores were described and defined considering: grain size, sedimentary structures, degree of sediment compaction and presence of organic matter and vegetation in the sediment, which can indicate pedogenesis. Based on these criteria, 18 sedimentary facies were recognized. The depositional process attributed for each facies is described in Table 1.

- **FSMhc:** Fine sand, very well sorted with horizontal and cross stratification and layers with medium size sand and high compaction degree.
- **FShco:** Fine sand, very well sorted, with horizontal stratification and very high compaction degree.
- **FSmco:** Fine sand, very well to well sorted, with massive structure and high compaction degree.
- **FSi:** Fine sand, very well to well sorted, with intercalation of high compaction layers and low compaction layers, horizontal and cross stratification, truncations and rich in heavy minerals.
- **FSc:** Fine sand, very well to well sorted, with cross stratification and low sediment compaction. Vegetation like grasses may be present.
- **FSm:** Fine sand, very well sorted, massive.

- **FSmg:** Fine sand, very well to well sorted, massive structure, presenting greenish color.
- **FSmb:** Fine sand, very well to well sorted, massive structure, with bioturbation and root marks.
- **FSfom:** Fine sand, very well to well sorted, flecked, with dark color and rich in disseminated organic matter, eventually presenting root marks, high pedogenesis degree.
- **FSom:** Fine sand, very well to well sorted, with dark color indicating disseminated organic matter, a few preserved horizontal stratifications, incipient pedogenesis.
- **FShcom:** Fine sand, very well to well sorted, with horizontal and cross stratification and small layers rich in organic matter.
- **FSch:** Fine sand, very well to well sorted, with cross and horizontal stratification.
- **FSp:** Fine sand, well sorted, black, compact, massive presence of organic matter creating a peat.
- **FSv:** Fine sand amid recent vegetation (grasses).
- **FSh:** Fine sand, very well to well sorted, with horizontal stratification.
- **FSMI:** Fine sand, flecked, with irregular lenses of mud (silt and clay).
- **MSI:** Mud (silt and clay), dark, with lenses of fine sand.
- **FSMf:** Mud and fine sand, pouchy and irregular, flecked bioturbated and rich in organic matter.

Table 1: Sedimentary facies described in the cores, and their corresponding depositional process.

Facies	Depositional Processes
FSMhc	Subaqueous currents with variations in energy.
FShco	Swash and backwash currents.
FSmco	Deposition by subaqueous currents with later sedimentary structures destruction by wave's impact over the sedimentary substrate.
FSi	Intercalation of swash and backwash processes and aeolian processes.
FSc	Decrease of the aeolian flux by vegetation causing sand deposition.
FSm	Aeolian sediments that had their structure destroyed by vegetation or variations in water level.
FSmg	Sandy sediments that had their structure destroyed by vegetation or variations in water level.
FSmb	Sandy deposits that had their structure destroyed by vegetation.
FSfom	Pedogenesis developed over sandy deposits.
FSom	Incipient pedogenesis developed over aeolian deposits.
FShcom	Aeolian processes of grain flow and grain fall over vegetated surface.
FSch	Aeolian processes of grain flow and grain fall.
FSp	Advanced pedogenesis over aeolian deposits due to the vegetation.
FSv	Recent pedogenesis with aeolian deposits covered by vegetation.
FSh	Vertical piling up of sand by vegetation.
FSMI	Deposition by subaqueous currents intercalated with subaqueous suspension.
MSI	Deposition by subaqueous suspension.
FSMf	Subaqueous currents intercalated with subaqueous suspension amid vegetation.

6.4.2. Drill-hole profiles from Rondinha to Atlântida Sul

As Hesp *et al.* (2007) described, on the progradational barrier of the northern littoral the aeolian phases overlap each other but only part of the dunefield is preserved. The barchanoid and transverse dunes are blown away, with only deflation plain deposits and very low precipitation ridges remaining, covered by vegetation (Hesp *et al.* 2007). Cores from the three profiles located over this barrier type (Rondinha, Capão Novo [Fig. 6] and Atlântida Sul,) have only sandy deposits, with foreshore and backshore deposits in the base and deflation plain deposits on the top (Fig. 6). This facies succession reflects the progradational nature of the barrier in this area (Fig. 6).

By the distance from the beach and location in the aerial photo, the drill-hole made in the modern deflation plain of Rondinha, shows that the active aeolian phase is covering phase 11 of Hesp *et al.* (2007). As Hesp *et al.* (2007) found an age of 2900 years BP for phase 11, the active phase must be younger than this. In the record of the core, from the base to the top, there are beach deposits, an older aeolian deposit that might be phase 11 and the modern deflation plain deposit.

On the Capão Novo profile, the core in the foredune (CN-DF) was the longest and reached sediments of the backshore, swash zone and subaqueous foreshore (Fig. 6). The drill-hole in the deflation plain (CN-PD) has foreshore and backshore deposits in the base, an old aeolian deposit with a well developed peat deposit top that might be phase 11, and the actual deflation plain deposit covering it (Fig. 6). The limit between the backshore and foreshore deposits in this profile appears 2.5 m high. This could be the result of a higher RSL, since the actual height of the backshore/foreshore limit is approximately from 0.5 to 1.0 m in RS coast. Nevertheless, it is difficult to confirm the higher RSL due to the fact that the limit was drafted by facies and sedimentary structures description, which having a high degree of imprecision.

The cores of the northern littoral show the progradational character of the barrier, with the horizontal overlap of the aeolian phases, instead of vertical piling up. Only two aeolian phases (the modern and an older phase) cover the backshore and foreshore deposits.

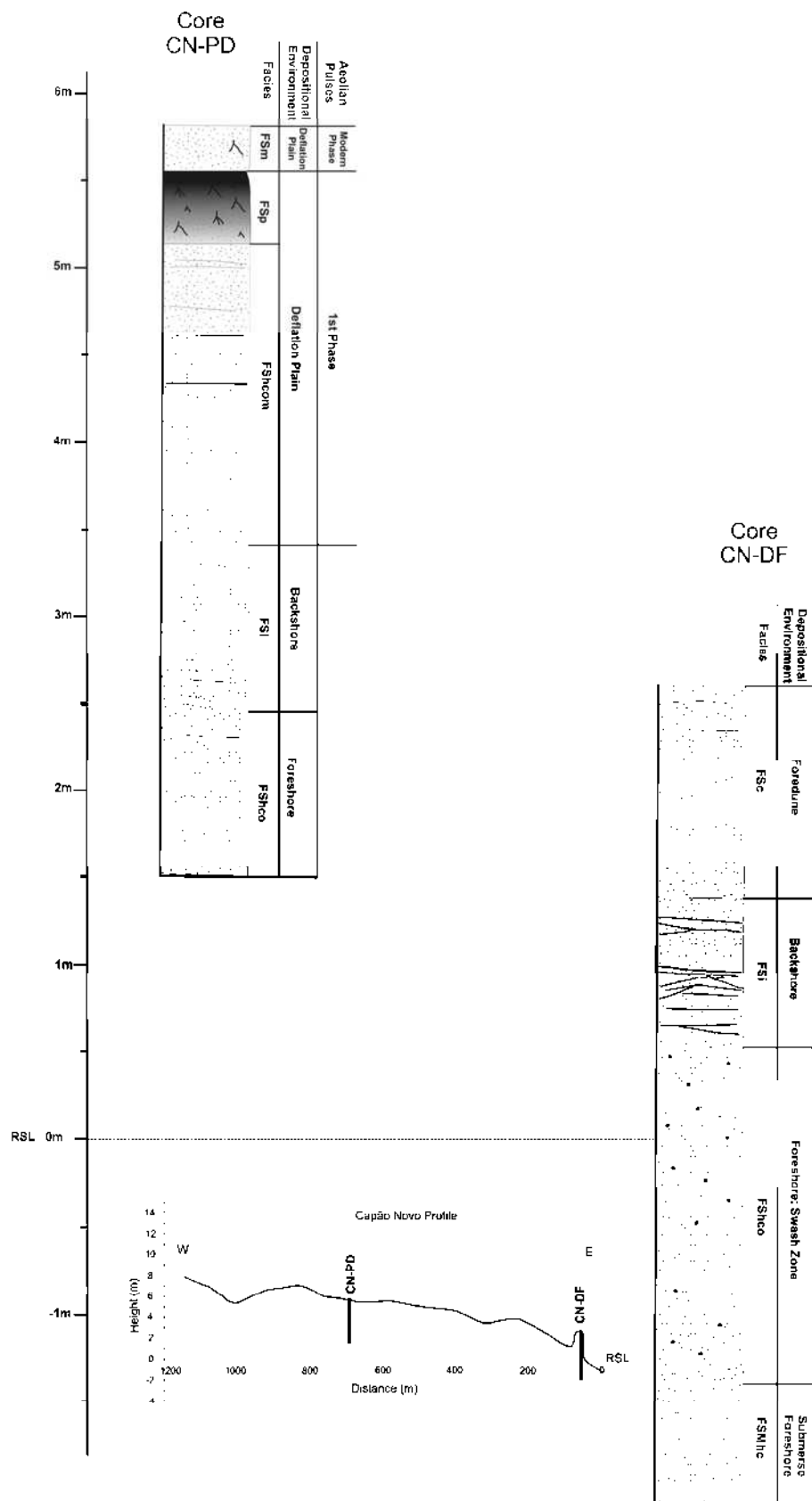


Figure 6: Capão Novo profile. Position and height of the cores in the topographic section. The diagram illustrates the cores, the observed sedimentary facies, the depositional environment in which these facies where deposited and, if discernible, the phases of aeolian activity.

6.4.3. From Jardim do Éden to Dunas Altas

As at Jardim do Éden, the barrier has been retrograding, and it was observed that there are not only aeolian and beach deposits, but also facies with mud and deposits of lacustrine marginal and bottom deposits. At the dunefield inner border (JE-BD), the dunes are silting the lake and the core in this area has muddy deposits from the lake bottom dating 3820-3460 cal yrs BP (Fig. 7, Table 2). This date gives a maximum age for the dunes in this area, meaning that aeolian sands reached the area to silt the lake after that. In the center of the dunefield (JE-PD), in the base of the core, there are deposits from the lake's margin, at the same level of the mud from the previous core (JE-BD), suggesting that they might be contemporaneous (Fig. 7). Over these deposits there is an older aeolian phase represented by deflation plain deposits with soil development, covered by the modern dunefield deposits. At the shore (JE-DF), under foredunes and backshore deposits there is a muddy deposit from the bottom of the lake with an age of 6799-6303 cal yrs BP according to Dillenburg (1994) and Travessas *et al.* (2005) (Fig. 7).

At Magistério, in the deflation plain (MA-PD, Fig. 8) the core has deposits of lake bottom at the altitude of the sea level, roughly at the same level of the mud in JE-DF and has approximately the same age 5890-5640 cal yrs BP, showing the retrogradational character of the barrier (Fig. 8, Table 2). In the center of Magistério dunefield (MA-CD), four older aeolian phases were found under the modern dunefield deposits (Fig. 8). The first one dates 4230-3970 cal yrs BP and the last one, which produced a very well developed peat, dates 2760-2460 cal yrs BP (Table 2). The core in the dunefield border (MA-BD) has basal lake margin deposits dating 970-810 cal yrs BP (Fig. 8, Table 2). This means that in the period after 2760-2460 and before 970-810 cal yrs BP aeolian sediments had not reached the MA-BD position. This might have occurred because the coastline was seawards.

At Dunas Altas, the drill-hole in the center of the dunefield (DA-CD) indicates a continuous aeolian deposition, with deflation plain deposits and dunefield deposits (Fig. 9). This area of the dunefield probably has always had a large amount of sand and due to that, it has never been completely stabilized and developed a soil layer. Variations in climate and sand supply are more perceptible in the dunefield borders, which have less sand. In the dunefield border (DA-BD) there were four older aeolian phases and the modern phase (Fig. 9). The first, a peat layer in the base, was dated at

4820-4450 cal yrs BP (Fig. 9, Table 2), being the oldest dated phase of all profiles and this phase might correspond to phase 4 of Hesp *et al.* (2007) (Fig. 1). This first and oldest phase is at a high altitude, 5.3 m above sea level. The third phase dates at 4390-4090 cal yrs BP (Fig. 9, Table 2) and it is at the same level and with the same age of the first pulse of MA-CD (from Magistério). The fourth phase is not dated but could be related to the phase of the MA-CD peat, dated at 2760-2460 cal yrs BP, since the location of the drilling is not far away, and this should be a very stable period to form such well developed peat. There is an absence of lake deposits (margin or bottom) in the cores, agreeing with Dillenburg *et al.*'s (2007) data who have described, in Dunas Altas, a 20m deep drill-hole with no muddy facies in the Holocene deposits. The absence of lake deposits and the fact that the two oldest aeolian phases were found here, might be confirming the aggradational character of the barrier around Dunas Altas, which, by its location, might have always been a higher place.

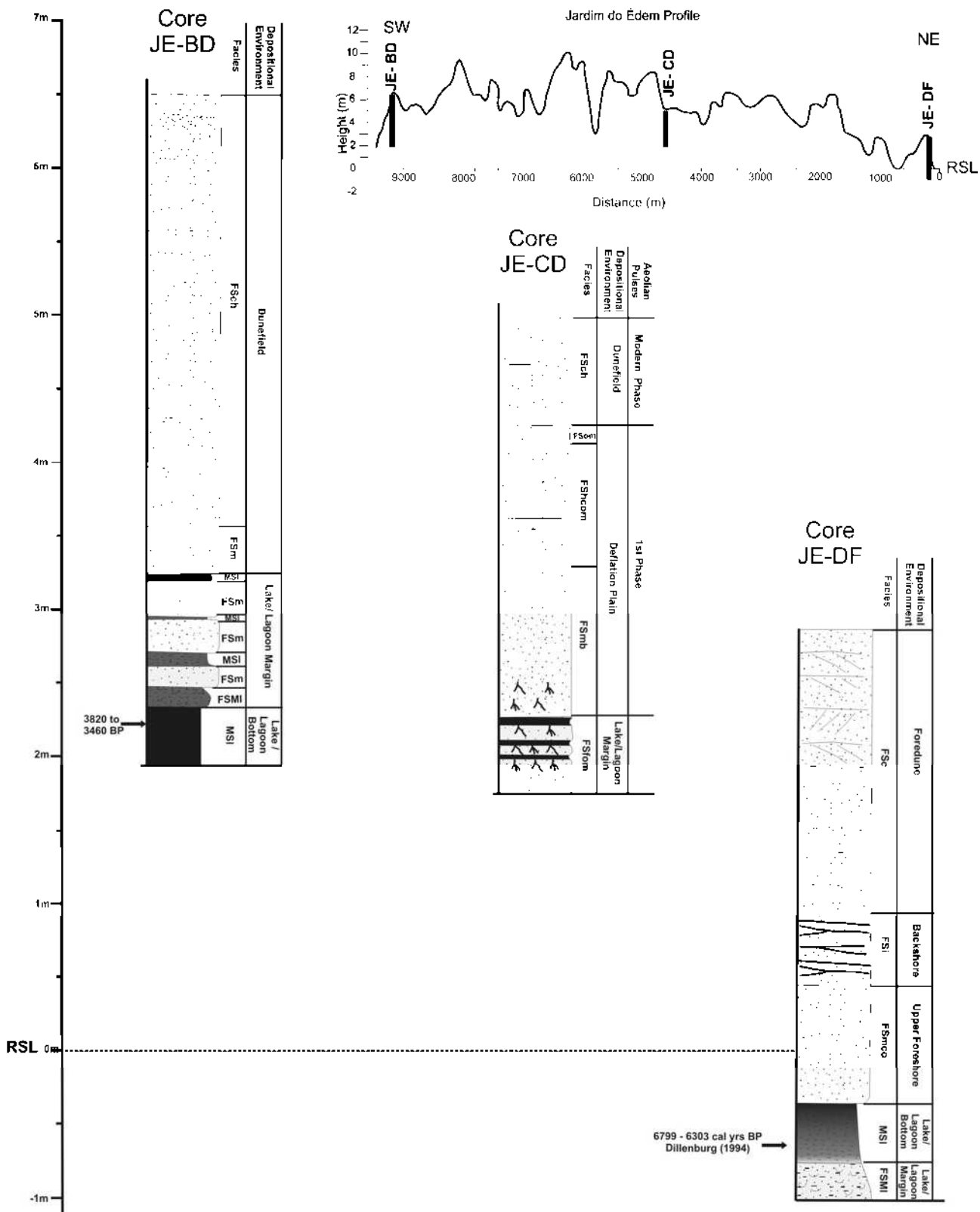


Figure 7: Jardim do Éden profile. Position and height of the cores in the topographic section. The diagram illustrates the cores, the observed sedimentary facies, the depositional environment on which these facies were deposited, the position and age of the ^{14}C samples and, if discernible, the phases of aeolian activity.

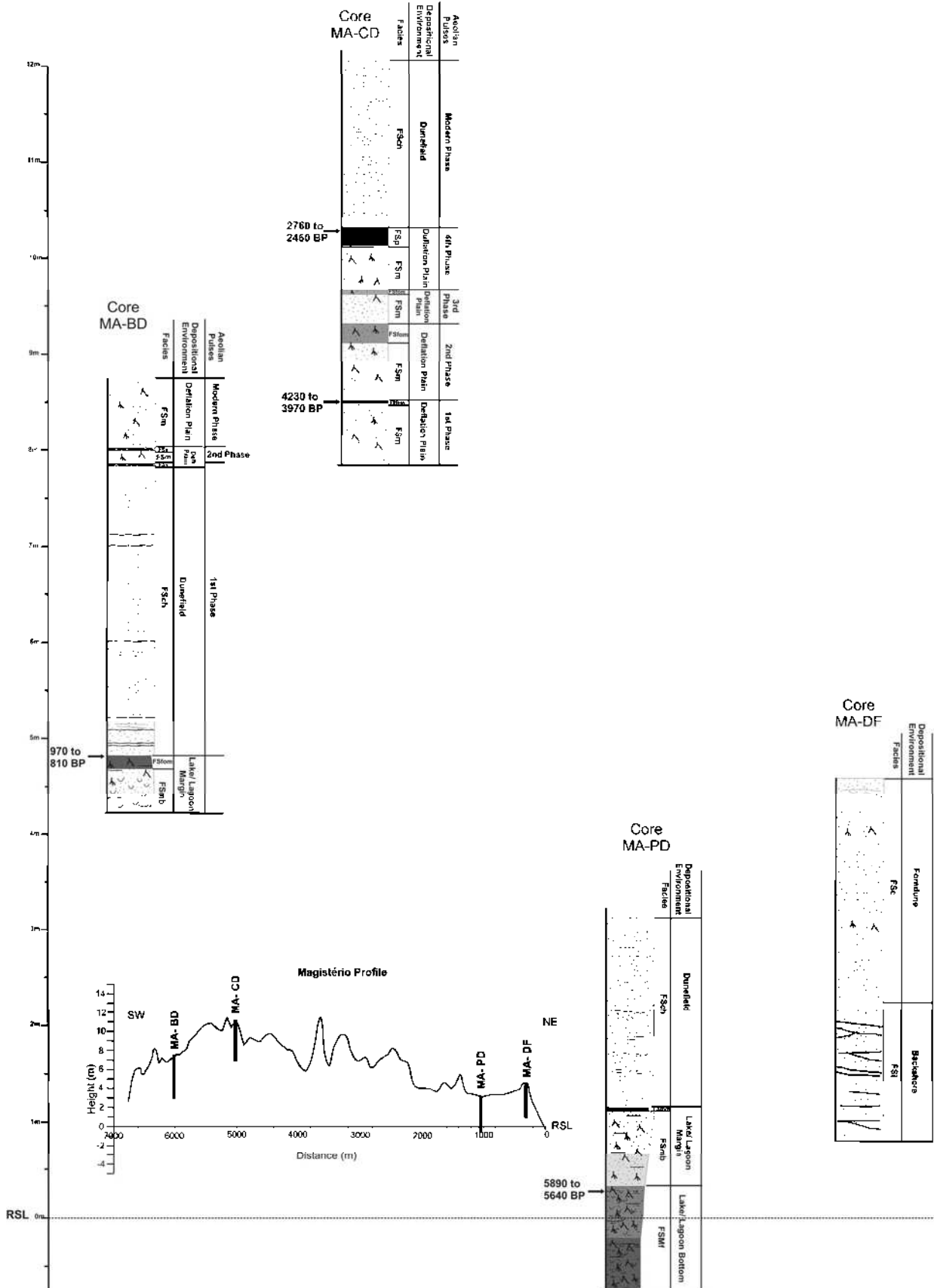


Figure 8: Magistério profile. Position and height of the cores in the topographic section. The diagram illustrates the cores, the observed sedimentary facies, the depositional environment on which these facies were deposited, the position and age of the ^{14}C samples and, if discernible, the phases of aeolian activity.

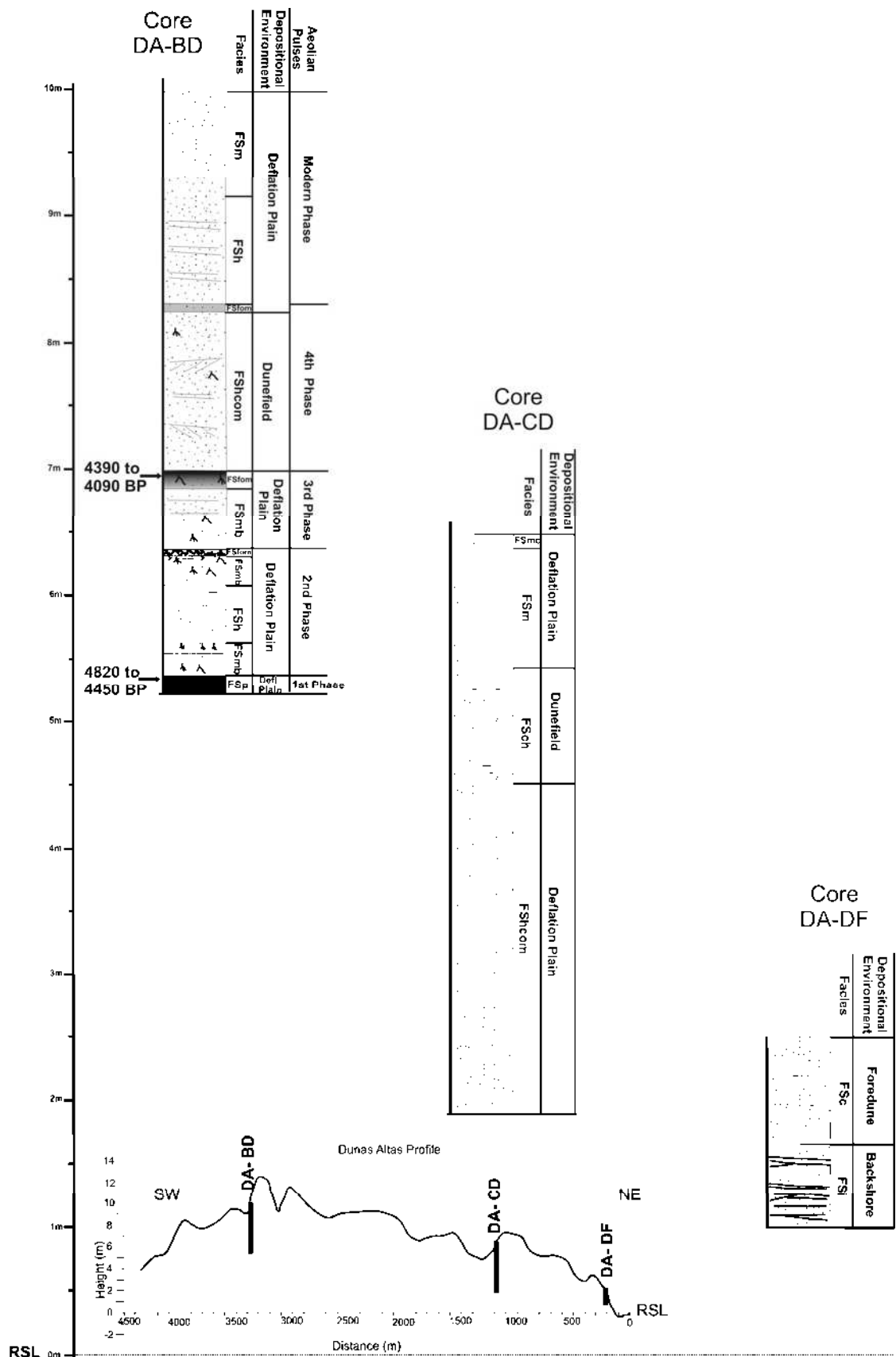


Figure 9: Dunas Altas profile. Position and height of the cores in the topographic section. The diagram illustrates the cores, the observed sedimentary facies, the depositional environment on which these facies were deposited, the position and age of the ^{14}C samples and, if discernible, the phases of aeolian activity.

6.4.4. From Solidão to Mostardas

The southernmost profiles of the study area (Solidão, São Simão and Mostardas) contrast with the others by their high altitudes. Not only are these dunefields the largest and widest (Martinho *et al.* submitted b), but they are also the highest. This information corroborates with the Martinho *et al.* (submitted b) statement that these dunefields should have a larger volume of sand in comparison with the northern dunefields.

In the drill hole made in the center of Solidão dunefield, three older phases and the modern phase were recognized, but none of them had enough content of organic matter for AMS ^{14}C dating. At the dunefield inner border (SO-BD), the altitude of the core was 12 m and, nevertheless, around an altitude of 10m a muddy sand deposit, gray, with no disseminated organic matter, but with some sparse roots was found, over aeolian deposits. Probably it is a deposit of a small local lake or creek which dated 4420-4150 cal yrs BP (Table 2). This may be evidence that a humid climate predominated during this period ceasing the local aeolian activity and giving place for deposition by subaqueous suspension. If this is true, this more humid climate would be correlated with the stabilization of phase 7 (Fig. 1), also found at MA-CD, and DA-BD.

On the São Simão profile, the drill-hole in the center of the dunefield (SS-CD), in similarity to DA-CD, has continuous aeolian deposits (Fig. 10). Down the core made in the inner border (SS-BD), at an altitude of 12m, five aeolian pulses were observed, including the modern phase (Fig. 10). The first at 1570-1410 cal yrs BP and the third at 920-710 cal yrs BP (Fig. 10, Table 2) were the strongest since they created thick peat layers. They are relatively recent and yet show high amplitude variations in climate. The high altitude of the dunes indicates that at São Simão the dunefields have been piling up at the border.

At Mostardas, with an altitude of 12m, the core located in the center of the dunefield presented two aeolian phases. The first, by its color and level could be related to the 1570-1410 cal yrs BP episode found in SS-BD. At the dunefield inner border, mud from the lake bottom was found in the core base and dated to 690-550 cal yrs BP (Table 2). This represents the maximum age that aeolian sand reached this place.

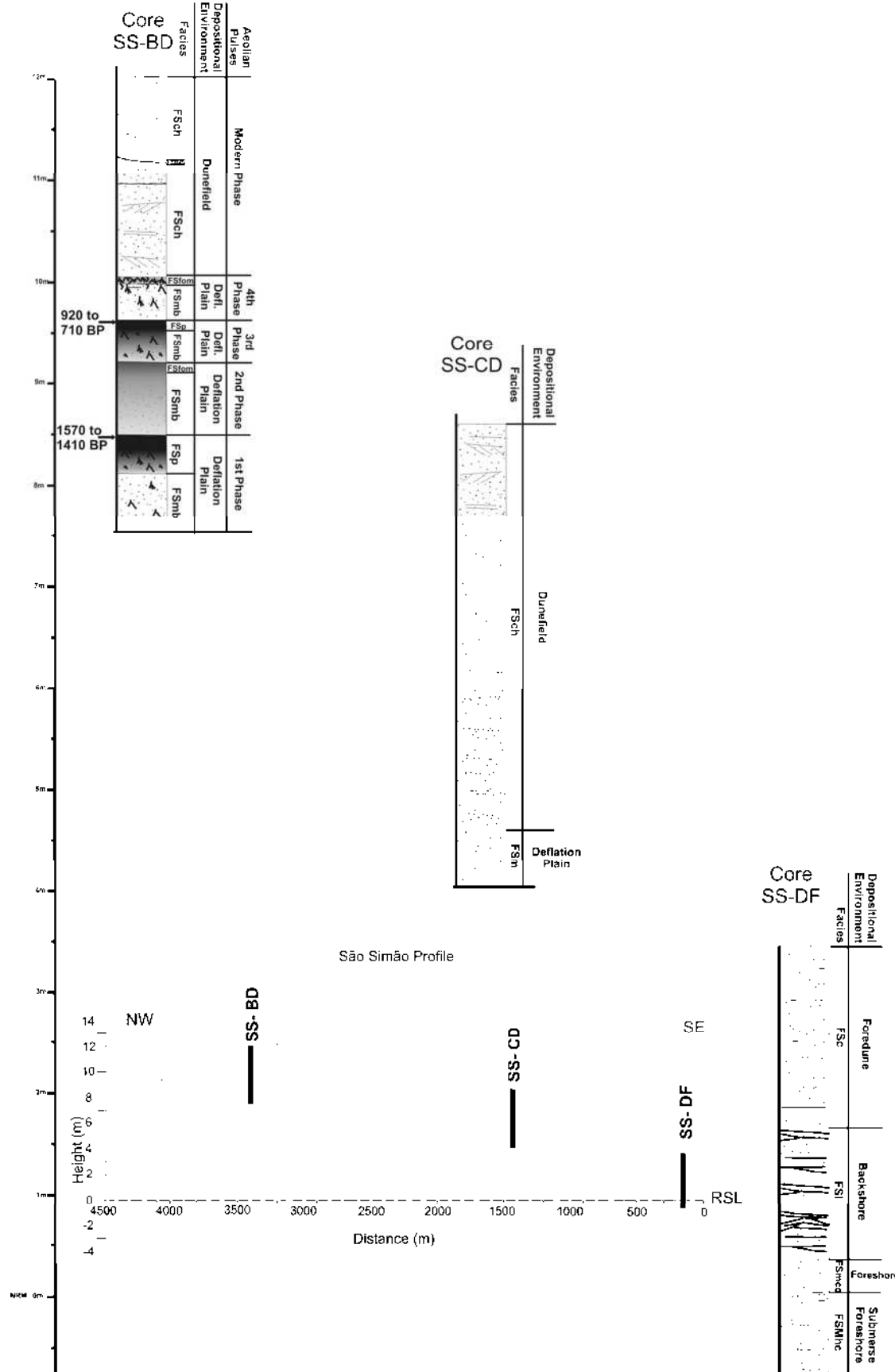


Figure 10: São Simão profile. Position and height of the cores in the topographic section. The diagram illustrates the cores, the observed sedimentary facies, the depositional environment on which these facies where deposited, the position and age of the ¹⁴C samples and, if discernible, the phases of aeolian activity.

Table 2: Organic matter samples dated by ^{14}C . ^(a) 2 sigma calibration (95% probability). ^(b) Beta Analytic Inc., FL, USA.

Samples	Environment	Depth (m)	Measured ^{14}C age (yr BP)	$^{13}\text{C}/^{12}\text{C}$ Ratio %	Conventional ^{14}C age (yr BP)	2 σ calibration age (cal yr BP) ^(a)	Lab number ^b
JE-BD	Mud from lake	4.48	3260 ± 70	-18.5	3370 ± 70	3820 to 3460	Beta - 221203
MA-PD	Mud from lake	2.78	4880 ± 40	-17.7	5000 ± 40	5890 to 5800 and 5770 to 5640	Beta - 236953
MA-CD-A	Soil	3.54	$3670 +/- 40$	-21.1	$3730 +/- 40$	4230 to 4200 and 4160 to 3970	Beta - 236952
MA-CD-B	Peat	1.74	$2440 +/- 50$	-18.8	$2540 +/- 50$	2760 to 2460	Beta - 221196
MA-BD	Soil of lake margin	3.93	$960 +/- 40$	-22.1	$1010 +/- 40$	970 to 900 and 850 to 810	Beta - 221195
DA-BD-1	Peat	4.66	$4000 +/- 40$	-18.1	$4110 +/- 40$	4820 to 4520 and 4460 to 4450	Beta - 236950
DA-BD-3	Soil	3.06	$3710 +/- 40$	-18.7	$3810 +/- 40$	4390 to 4370 and 4350 to 4320 and 4300 to 4090	Beta - 236951
SO-BD	Root frag in mud	1.16	$3740 +/- 40$	-17.9	$3860 +/- 40$	4420 to 4150	Beta - 236954
SS-BD-1	Peat	3.55	$1450 +/- 40$	-15.5	$1610 +/- 40$	1570 to 1410	Beta - 221199
SS-BD-2	Peat	2.4	$770 +/- 40$	-17.7	$890 +/- 40$	920 to 710	Beta - 221200
MO-BD	Mud from lake	4.13	$700 +/- 50$	-25.4	$690 +/- 50$	690 to 550	Beta - 221197

6.5. DISCUSSION

6.5.1. Potential of aeolian deposits preservation

Kocurek & Halvholm (1993) state that preservation of sedimentary deposits is related to accumulation below the base level of erosion. Nevertheless, in some cases, aeolian deposits could be preserved above the base level of erosion. Three factors are responsible for preservation: subsidence increasing the preservation space, incorporation of the accumulated sediments into the saturated zone, and stabilization of the sediments deposited (Kocurek & Halvholm 1993). As the neotectonics in the area are not significant during the Holocene, the possible factors that would promote aeolian deposits preservation on the RS coast are: their incorporation into the saturated zone and surface stabilization.

The placement of the accumulated sediments below the water table is possible on the RS coast in two cases, a rise in the sea-level, what would promote a rise

in water table level; or a rise in the continental water table level, by changes in climate conditions, for example.

As described above, from the early Holocene until ~5000 yr BP the aeolian deposits could be preserved on the RS coast due to the rising sea-level. Nevertheless, after ~5000 yr BP there is an accepted tendency of gentle sea-level fall, which means that sea-level was no longer responsible for the aeolian preservation. Thus, during the mid and late Holocene the preservation of the aeolian deposits has to be a consequence of the climate.

A change in climate can induce sediment preservation if the climate becomes wetter (Kocurek & Halvholm 1993). In this case the preservation can work in two forms: by raising the water table, and secondly, by increasing the moisture allowing vegetation growth and consequent stabilization of the sediments deposited (Kocurek & Halvholm 1993; Kocurek *et al.* 2001).

Thus, during wet climate phases, the aeolian activity should decrease by the increase in grain cohesion and threshold velocity. The moisture would favor vegetation growth and consequent formation of soil over the aeolian deposits. When again a dry phase started, the vegetation and moisture present in the soil would prevent the sediment erosion by the wind, preserving the deposits even above the base level of erosion and without RSL variation.

Nevertheless, sometimes the wet phases were not long enough to the complete establishment of vegetation and soil development or the sediment supply was too large, avoiding vegetation growth. In both cases, when the dry phases started the surface was not stabilized enough, and the aeolian deposits were eroded. As Kocurek & Halvholm (1993) stated: “where preservation does not occur, an unconformity must”. This unconformity, nevertheless, in the case of RS dunefields puts sand above sand making it impossible to recognize a bounding surface. For this reason, an entire aeolian phase can be deposited and be completely eroded later and no record or surface will be left to identify the phase.

This explains why at least 11 aeolian phases are recognized in the northern littoral (Hesp *et al.* 2007) while in the mid-littoral only a few phases are identified in the cores. In the northern littoral, the aeolian phases were largely preserved horizontally, as the barrier prograded. In addition, the northern dunefields are relatively smaller and have less sand, so they respond faster to small changes in climate and can be stabilized faster (Martinho *et al.* submitted b), facilitating the preservation. In the

mid-littoral, with the barrier retrograding or staying approximately in the same place, the aeolian deposits were vertically stacked. In addition, the dunefields are very large and the amount of sand is much higher (Martinho *et al.* submitted b). Thus, it takes longer to start the dunefield stabilization and vegetation growth, making them more susceptible to wind erosion.

6.5.2. Soil formation periods

Three of the eleven radiocarbon dates come from deposits from lake bottoms and contribute to an understanding of the barrier evolution, but are not very important to climate changes and dunefield evolution. The other eight dates, made in soils which mark stabilization of a dunefield, are distributed in specific time periods. The first major period of soil formation is from 4820 to 3970 yr BP comprising four samples (DA-BD-1, SO-BD, DA-BD-3, MA-CD-A) (Fig. 11). The second is in 2760-2460 cal yr BP represented by the peat of MA-CD-B sample (Fig. 11). And the third major period of soil formation is from 1570 to 710 yr BP (samples SS-BD-1, MA-BD, SS-BD-2) (Fig. 11). Radiocarbon dates of soil samples were plotted with the paleoclimatic data provided by the literature (see above). The result of this comparison is that the three major periods of soil formation coincide with periods of increased humidity (Fig. 11).

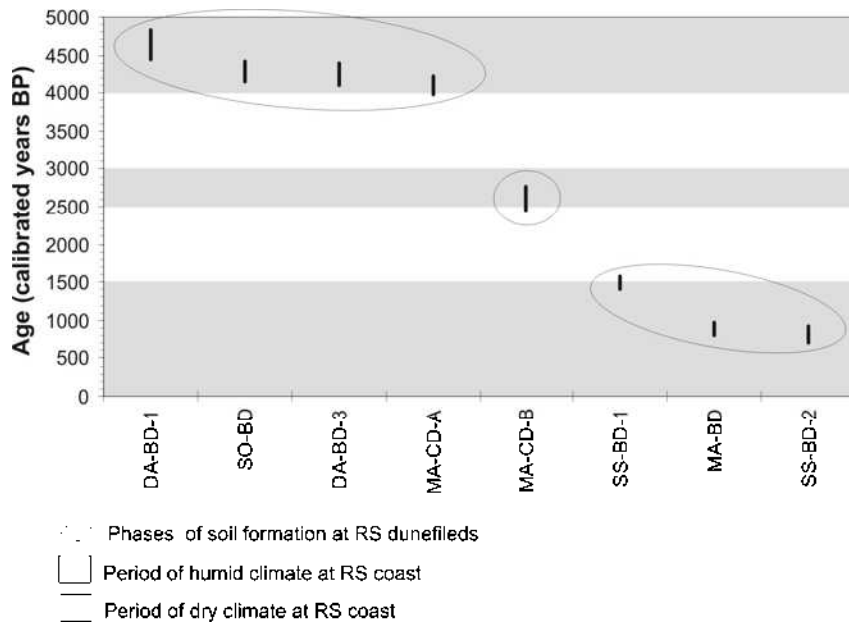


Figure 11: Radiocarbon dates of soil samples (palaeosols) plotted with paleoclimatic data (from Neves 1991; Behling 1997; Behling 1998; Ledru *et al.* 1998; Behling *et al.* 1999; Prieto *et al.* 1999; Ybert *et al.* 2001; Bauermann 2003). Gray bars represent a humid climate and white bars represent dry climates. The ellipses indicate major periods of soil formation. In the X axis are labeled the samples used to make this comparison.

Despite the major variations in climate and phases of soil formation (intervals of 500 to 1000 yrs), it is known that high frequencies of climate change (interannual to interdecadal) can start a new dunefield phase, or completely stabilize it (Martinho *et al.* submitted a, b). Such high frequency climate changes can be represented by the Southern Oscillations (SO) events (El Niño and La Niña) and by the North Atlantic Oscillations (NAO) events. These types of events started to occur on the RS coast since 4000 yr BP (Neves 1991; Behling 1997; Ybert *et al.* 2001). Agreeing with this information, Hesp *et al.* (2007) described on the northern littoral a relatively continuous formation and overlapping dunefields phases since 7000 yr BP. In theory, these high frequency phases could be preserved vertically in the mid-littoral dunefields.

In the cores analyzed in this paper, only the soil layers with enough organic matter were dated. Nevertheless, many aeolian phases and soil layers could be recognized in the cores and by facies description, despite the scarcity of material for dating. Three cores (DA-BD, MA-CD and SS-BD) have a good succession of aeolian phases, separated by soil layers with five phases each including the modern one. There are two ^{14}C dates in each of these cores. With this information it is possible to analyze the soil ages, position them in time and make a stratigraphic correlation (Fig. 12). The

stratigraphic correlation exhibited the existence of at least 10 phases of aeolian activity since 4820 yr BP (Fig. 12).

The core DA-BD, from the Dunas Altas dunefield inner border presented the oldest phases. The first recognized phase dates 4820-4450 cal yrs BP. Some time after 4820-4450 yrs and before 4390-4090 cal yrs BP a second phase developed. The third phase appears in the cores DA-BD and MA-CD, dating 4390-4090 cal yrs and 4230-3970 cal yrs BP respectively. Phases 4 and 5, present in the core MA-CD, developed in a period after 4230-3970 cal yr BP and before 2760-2460 cal yr BP, which is the date of the phase 6 (Fig. 12).

The core SS-BD from São Simão has its oldest phase dating to 1570-1410 cal yr BP. There are no records if there are more phases between this one and phase 6 (2760-2460 cal yr BP), and due to that, the first phase of the core SS-BD will be considered phase 7. Phase 8 has developed in a period after 1570-1410 cal yr BP and before 920-710 cal yr BP, the age of phase 9. Phase 10 has developed after 920-710 cal yr BP and before the modern phase (Fig. 12).

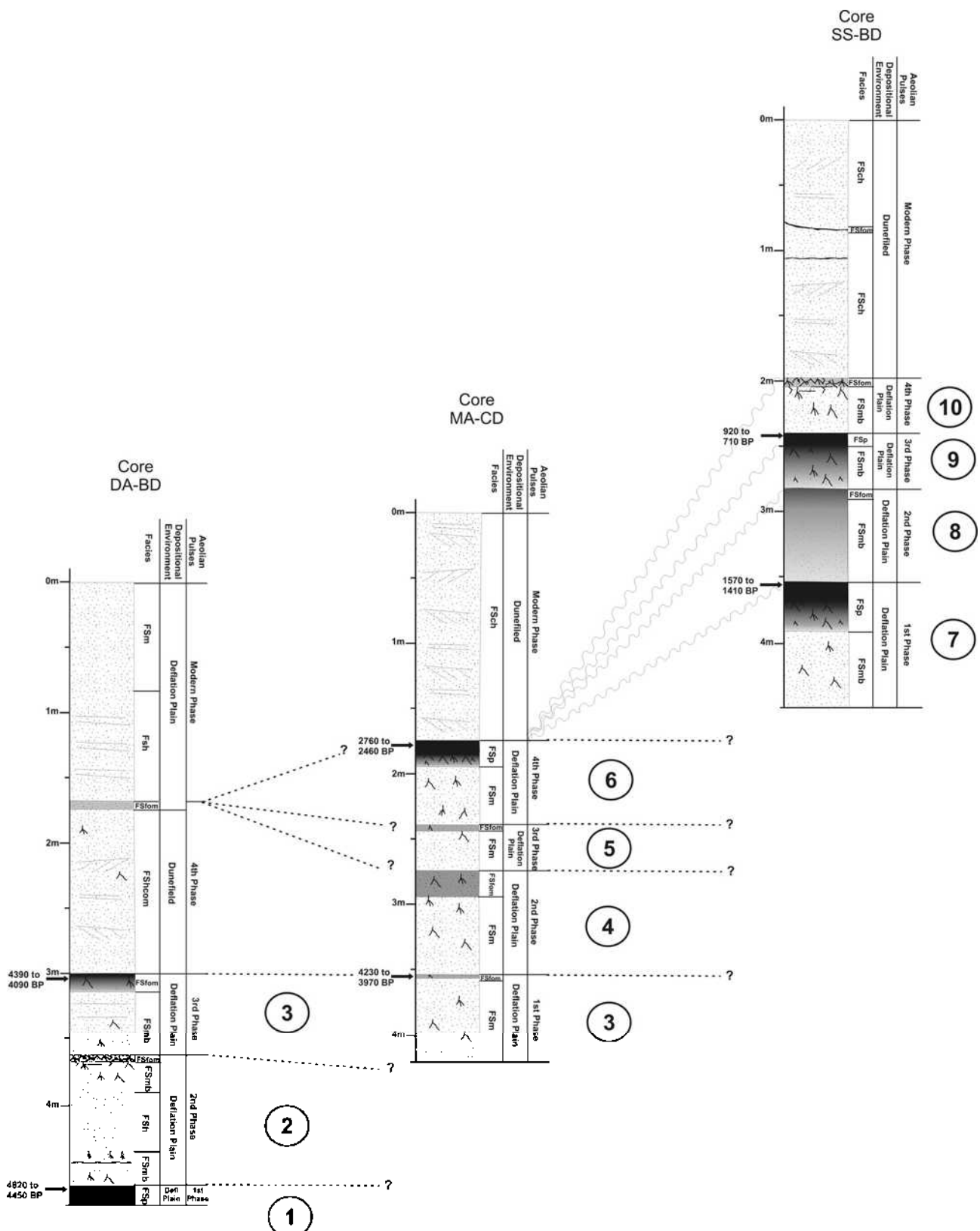


Figure 12: Stratigraphic correlation of the cores DA-BD, MA-CD and SS-BD. Along each core, the observed sedimentary facies, the depositional environment, the position and age of the ^{14}C samples and the phases of aeolian activity. Dashed lines are inferred correlations; wavy lines represent erosion and unconformity. The numbers inside the circles are the recognized phases of aeolian activity from 1 the oldest to 10 the youngest.

6.6. CONCLUSIONS

1. The stratigraphy of the cores across the profiles agreed with the barrier types previously suggested for this coastal stretch. On the northern profiles we found beach deposits under aeolian deposits, characterizing the progradation of the barrier. At Jardim do Éden and Magistério, lake deposits appear beneath aeolian deposits, a typical succession of barrier retrogradation. Dunas Altas profile, located very close to Magistério, presented only aeolian deposits, and these deposits were the oldest encountered. This suggests that the coastline has not migrated extensively, agreeing with the aggradational character of the barrier. The southernmost profiles, Solidão, São Simão and Mostardas, showed that the aeolian deposits in this area are not only very wide, but also very thick, and aeolian processes have been acting in this area for a long time. The large volume of sand in these dunefields could be the result of long-term erosion of the coast combined with a high sediment supply and the retrogradation of the barrier.
2. On the northern littoral, the preservation of aeolian phases was largely horizontal. With relatively smaller dunefields and less volume of sand, each phase of the northern dunefields was rapidly stabilized and preserved as the barrier prograded. In the mid-littoral, the phases of aeolian deposition are preserved vertically. This preservation depended on the increase in moisture, which induced the development of vegetation and soil on top of the aeolian phase, preventing the erosion. Nevertheless, if the phase was not stabilized enough, the aeolian erosion could destroy entire phases.
3. Three major periods of soil formation and dunefield stabilization were found: from 4820 to 3970 yr BP, in 2760-2460 cal yr BP and from 1570 to 710 yr BP. These periods coincide with periods where the literature cites an increase in moisture during the mid to late Holocene (Fig. 11). This coincidence of soil formation and wet climate indicates that the climate might be controlling dunefield evolution on the RS coast since 5000 yr BP.
4. The stratigraphic data of the three most representative cores were correlated, and along with the available dates from soil layers and the facies description 10 phases of aeolian activity and stabilization were recognized for the mid-littoral of the RS coast (Fig. 12):
 - Phase 1 stabilized in 4820-4450 cal yrs BP.

- Phase 2 stabilized after 4820-4450 cal yrs and before 4390-4090 cal yrs BP.
 - Phase 3 stabilized from 4390-4090 to 4230-3970 cal yrs BP.
 - Phases 4 and 5 stabilized after 4230-3970 cal yrs BP and before 2760-2460 cal yrs BP.
 - Phase 6 stabilized in 2760-2460 cal yr BP.
 - Phase 7 stabilized in 1570-1410 cal yr BP.
 - Phase 8 stabilized after 1570-1410 cal yr BP and before 920-710 cal yr BP.
 - Phase 9 stabilized in 920-710 cal yr BP.
 - Phase 10 stabilized after 920-710 cal yr BP and before the modern phase.
5. Such high frequency soil formation could be the result of high frequency events of climate change, such as SO and NAO, which started to occur on the RS coast since 4000 yr BP).

ACKNOWLEDGMENTS

This research was partly supported by grants of RECOIS-Institutos do Milênio and Conselho Nacional de Desenvolvimento Científico e Tecnológico (CNPq). We thank CNPq for the PhD Scholarship and Comissão Permanente de Aperfeiçoamento de Pessoal de Nível Superior (CAPES) for the doctorate *sandwich* scholarship to Caroline Martinho, the Dept of Geography and Anthropology at LSU and CECO at UFRGS for provision of research facilities. Sérgio Dillenburg thanks CNPq for his scholarship, and Patrick Hesp thanks LSU and UFRGS for support.

REFERENCES

- ANGULO, R.J., GIANNINI, P.C.F. 1996. Variação do nível relativo do mar nos últimos dois mil anos na Região Sul do Brasil: uma discussão. *Bol. Paranaense de Geoc.* **44:** 67–75.
- ANGULO, R.J.; GIANNINI, P.C.F.; SUGUIO, K.; PESSENCDA, L.C.R. 1999. Relative sea-level changes in the last 5500 years in the southern Brazil (Laguna-Imbituba region, Santa Catarina State) based on vermetid ^{14}C ages. *Marine Geology*, **159:** 323-339.

- ANGULO, R.J.; LESSA, G.C.; SOUZA, M.C. 2006. A critical review of the mid- to late Holocene sea-level fluctuations on the eastern brazilian coastline. *Quat Sci Reviews*, **25**: 486-506.
- BAUERMANN, S.G.; MARQUES-TOIGO, M.; BEHLING, H.; SOUZA, P.A. 2003. Análises palinológicas da turfeira de Águas Claras, planície costeira do Rio Grande do Sul, Brasil. In: IX Congresso ABEQUA, II Congresso do Quaternário dos Países de Línguas Ibéricas e II Congresso Sobre Planejamento e Gestão da Zona Costeira dos Países de Expressão Portuguesa, Recife, PE. *Anais CD*, ABEQUA.
- BEHLING, H., 1997. Late Quaternary vegetation, climate and fire history from the tropical mountain region of Morro de Itapeva, SE Brazil. *Palaeogeogr., Palaeoclimatol., Palaeoecol.* **129**: 407-422.
- BEHLING, H. 1998. Late Quaternary vegetational and climatic changes in Brazil. *Review of Palaeobotany and Palinology*, **99**: 143-156.
- BEHLING, H.; BAUER, S.; NEVES, P. 1999. Holocene environmental changes from the São Francisco de Paula region in southern Brazil. In: VII Congresso da ABEQUA. Porto Seguro. *Anais CD*, ABEQUA.
- DELANEY, P.J.V. 1963. *Quaternary Geologic History of the Coastal Plain of Rio Grande do Sul, Brazil*. Coastal Studies Series no. 7. Louisiana State University Press.
- DILLENBURG, S.R. 1994. *A Laguna de Tramandaí: Evolução Geológica e Aplicação do Método Geocronológico da Termoluminescência na Datação de Depósitos Sedimentares Lagunares*. Porto Alegre, Univ. Federal Rio Grande do Sul. Tese de Doutoramento (inéd). 113p.
- DILLENBURG, S.R.; ROY, P.S.; COWELL, P.J.; TOMAZELLI, L.J. 2000. Influence of antecedent topography on coastal evolution as tested by shoreface translation-barrier model (STM). *Journal of coastal research*, **16**(1): 71-81.
- DILLENBURG, S.R., TOMAZELLI, L.J., CLEROT, L.C.P. 2003. Gradients of wave energy as the main factor controlling the evolution of the coast of Rio Grande do Sul in southern Brazil during the Late Holocene. *Proceedings of the 5th International Symposium on Coastal Engineering and Science of Coastal Sediment Process*. New York, NY: American Society of Civil Engineers, v.1, CD, 2003.
- DILLENBURG, S.R.; TOMAZELLI, L.J.; BARBOZA, E.G. 2004a. Barrier evolution and placer formation at Bujuru southern Brazil. *Marine Geology*, **203**: 43-56.
- DILLENBURG, S.R.; ESTEVES, L.S.; TOMAZELLI, L.J. 2004b. A critical evaluation of coastal erosion in Rio Grande do Sul, Southern Brazil. *Anais da academia brasileira de ciências*, **76**(3): 611-623.
- DILLENBURG, S.R.; TOMAZELLI, L.J.; HESP, P.A.; BARBOZA, E.G.; CLEROT, L.C.P.; SILVA, D.B. 2006. Stratigraphy and evolution of a prograded, transgressive dunefield barrier in southern Brazil. *Journal of Coastal research SI* **39**: 132-135.

DILLENBURG, S.R.; BARBOZA, E.G.; TOMAZELLI, L.J.; LIMA, L.G.; BECKER, J.E.G. 2007. A Barreira Costeira de Dunas Altas no Litoral Médio do Rio Grande do Sul: um exemplo de barreira agradacional ou estacionária. In: XI Congresso da ABEQUA. Belém. *Anais CD*, ABEQUA.

DILLENBURG, S.R.; BARBOZA, E.G.; TOMAZELLI, L.J.; HESP, P.A.; CLEROT, L.C.P.; AYUP-ZOUAIN, R.N. in review. The Holocene Coastal Barriers of Rio Grande do Sul. In: DILLENBURG, S.R. & HESP, P. A. (Eds.) *Geology and Geomorphology of Holocene Coastal Barriers of Brazil*. Springer - Lecture Notes in Earth Sciences v. 107 (2008).

GARDNER, D.E. 1955. Beach-sand heavy-mineral deposits of Eastern Austrália. *BMR Bull.* No. 28, 103 pp.

GÓMEZ, E. A.; MARTÍNEZ, D.E.; BOREL, C.M.; GUERSTEIN, G.R.; CUSMINSKY, G.C. 2005. Submarine evidence of Holocene sea-level fluctuations in the Bahía Blanca estuary, Argentina. *Journal of South America Earth Sciences*, **20**: 139-155.

HESP, P. A. 1989. A review of biological and geomorphological processes involved in the initiation and development of incipient foredunes. *Proceedings of the Royal Society of Edinburgh*, **96B**: 181-201.

HESP, P.A. 1999. The beach backshore and beyond. In: SHORT, A.D. (Ed.) *Handbook of Beach and Shoreface Morphodynamics*. Chichester, Jonh Wiley & Sons Ltd, p. 145-270.

HESP, P.A. & THOM, B.G. 1990. Geomophology and evolution of active transgressive dunefields. In: NORDSTROM, K.F.; PSUTY, N.P.; CARTER, R.W.G. (Eds.) *Coastal Dunes: Form and Process*. Chichester, Jonh Wiley & Sons Ltd.

HESP, P.A.; ILLENBERGER, W; RUST, I.; McLACHLAN, A.; HYDE, R. 1989. Some aspects of transgressive dunefield and transverse dune geomorphology and dynamics, south coast, South África. *Z.Geomorph. N.F. Suppl.-Bd*, **73**: 111-123.

HESP, P.A.; DILLENBURG, S.R.; BARBOZA, E.G.; TOMAZELLI, L.J.; AYUP-ZOUAIN, R.N.; ESTEVES, L.S.; GRUBER, N.L.S.; TOLDO JR., E.E.; TABAJARA, L.L.C.A.; CLEROT, L.C.P. 2005. Beach ridges, foredunes or transgressive dunefields? Definitions and an examination of the Torres to Tramandaí barrier system, Southern Brazil. *Anais da Academia Brasileira de Ciências* **77** (3): 493-508.

HESP, P.A.; DILLENBURG, S.R.; BARBOZA, E.G.; CLEROT, L.C.P.; TOMAZELLI, L.J.; AYUP-ZOUAIN, R.N. 2007. Morphology of the Itapeva to Tramandaí transgressive dunefield barrier system and mid- to late Holocene sea level change. *Earth Surf. Process. Landforms* **32**: 407-414.

ISLA, F.I. 1989. Holocene sea-level fluctuations in the Southern Hemisphere. *Quaternary Science Reviews*, **8**: 359-368.

KOCUREK, G. & HAVHOLM, K.G. 1993. Eolian Sequence Stratigraphy – A Conceptual Framework. In: WEIMER, P. & POSAMENTIER, H. (Eds.)

Siliciclastic Sequence Stratigraphy – Recent Developments and Applications.
AAPG Memoir **58**: p.393-409.

- KOCUREK, G.; TOWNSLEY, M.; YEH, E.; HAVHOLM, K.; SWEET, M.L. 2001. Dune and dune-field development on Padre Island, Texas, with implications for interdune deposition and water-table-controlled accumulation. *Journal of Sedimentary Petrology* **62**(4): 622-635.
- LEDRU, M.P.; SALGADO-LABOURIAU, M.L.; LORSCHETTER, M.L. 1998. Vegetation dynamics in southern and central Brazil during the last 10,000 yr B.P. *Review of Palaeobotany and Palynology*, **99**: 131-142.
- LIMA, S.F.; ALMEIDA, L.E.S.B.; TOLDO JR., E.E. 2001. Estimate of longshore sediments transport from waves data to the Rio Grande do Sul coast. *Pesquisas*, **48** (2): 99-107.
- MARTIN, L., SUGUIO, K., FLEXOR, J.M., BITTENCOURT, A.C.S.P., VILAS-BOAS, G.S., 1979/1980. Le quaternaire marin brésilien (littoral pauliste, sud fluminense et bahianais). *Cahiers O.R.S.T.O.M., Série Géologie* **11**: 95–124.
- MARTIN, L.; SUGUIO, K.; FLEXOR, J.M.; AZEVEDO, A.E.G. 1988. *Mapa Geológico do Quaternário Costeiro dos Estados do Paraná e Santa Catarina*. Brasília, DNPM, 40p., 2 mapas. Série Geologia (28), Secção Geologia Básica (18).
- MARTINHO, C.T.; DILLENBURG, S.R.; HESP, P.A. (Accepted). Wave energy and longshore sediment transport gradients controlling barrier evolution in Rio Grande do Sul, Brazil. *Journal of Coastal Research*.
- MARTINHO, C.T.; HESP, P.A.; DILLENBURG, S.R.; TOMAZELLI, L.J. (Submitted a). Climate patterns and variations on the Rio Grande do Sul Coast and coastal dunefield dynamics. *Earth Surf. Process. Landforms*.
- MARTINHO, C.T.; HESP, P.A.; DILLENBURG, S.R. (Submitted b). Morphological and Temporal Variations of Transgressive dunefields of the Northern and Mid-littoral Rio Grande do Sul coast. *Geomorphology*.
- MORTON, R. A. 1994. Texas Barriers. In: DAVIS, R.A. (Ed.) *Geology of Holocene Barrier Island Systems*. Springer-Verlag, Berlin: 75-114.
- NEVES, P.C.P. 1991. *Palinologia de Sedimentos de uma Mata Tropical Paludosa em Terra de Areia, Planície Costeira Norte, RS, Brasil*. Mestrado, IG-UFRGS 166p.
- PRIETO, A.R.; LORSCHETTER, M.L.; STUTZ, S. 1999. Holocene vegetation changes in relation to the coastal evolution in Buenos Aires province (Argentina) and Rio Grande do Sul (Brazil). In: VII Congresso da ABEQUA. Porto Seguro. *Anais CD*, ABEQUA.
- SHORT, A.D. 1988a. Holocene coastal dune formation in Southern Australia: a case of study. *Sedimentary Geology*, **55**: 121-142.
- SHORT, A.D. 1988b. Wave, beach, foredune, and móible dune interactions in the Southern Australia. *Journal of Coastal Research*, Special Issue No.3, p. 05-09.

- SUGUIO, K., MARTIN, L., BITTENCOURT, A.C.S.P., DOMINGUEZ, J.M.L., FLEXOR, J.M., AZEVEDO, A.E.G. de, 1985. Flutuações do nível relativo do mar durante o Quaternário superior ao longo do litoral brasileiro e suas implicações na sedimentação costeira. *Revista Brasileira de Geociências* **15**: 273–286.
- TOLDO JR, E.E.; ALMEIDA, L.E.S.B.; NICOLODI, J.L.; ABSALONSEN, L.; GRUBER, N.L.S. 2006. O controle da deriva litorânea no desenvolvimento do campo de dunas e da antepraia no litoral médio do Rio Grande do Sul. *Pesquisas* **33** (2): 35-42.
- TOMAZELLI, L.J. 1990. *Contribuição ao Estudo dos Sistemas Depositionais Holocénicos do Nordeste da Província Costeira do Rio Grande do Sul, com Ênfase no Sistema Eólico*. Porto Alegre, Univ. Federal Rio Grande do Sul. Tese de Doutoramento (inéd). 270p.
- TOMAZELLI, L.J. 1993. Regime de ventos e taxa de migração de dunas eólicas costeiras do Rio Grande do Sul, Brasil. *Pesquisas*, **21**(1): 64-71.
- TOMAZELLI, L.J. 1994. Morfologia, organização e evolução do campo eólico costeiro do litoral norte do Rio Grande do Sul, Brasil. *Pesquisas*, **21** (1): 64-71.
- TOMAZELLI, L.J. & VILLWOCK, J.A. 1989. Processos erosivos atuais na costa do Rio Grande do Sul, Brasil: evidências de uma provável tendência contemporânea de elevação do nível relativo do mar. In: II Congresso da ABEQUA, Rio de Janeiro, 1989. ABEQUA. *Anais...*
- TOMAZELLI, L.J. & VILLWOCK, J.A. 1992. Considerações sobre o ambiente praial e deriva litorânea de sedimentos ao longo do Litoral norte do Rio Grande do Sul, Brasil. *Pesquisas*, **19** (1): 3-12.
- TOMAZELLI, L. J., VILLWOCK, J. A., DILLENBURG, S. R., BACHI, F. A., DEHNHARDT, B. A., 1998. Significance of present-day coastal erosion and marine transgression, Rio Grande do Sul, Southern Brazil. *Anais da Academia Brasileira de Ciências*, **70**(2): 221-229.
- TRAVESSAS, F. A.; DILLENBURG, S.R.; CLEROT, L.C.P. 2005. Stratigraphy and evolution of the Holocene barrier of Rio Grande do Sul between Tramandaí and Cidreira. Estratigrafia e evolução da barreira holocênica do Rio Grande do Sul no trecho Tramandaí - Cidreira (RS). *Boletim Paranaense de Geociências*, **57**: 57-73.
- TRENHAILE, A.S. 1997. Sand Dunes. In: TRENHAILE, A.S. (Ed.), *Coastal Dynamics and Landforms*. Oxford, Clarendon Press, p.144-169.
- VAN GEEL, B., BUURMAN, J., WATERBOLK, H.T., 1996. Archaeological and palaeoecological indications of an abrupt climate change in The Netherlands, and evidence for climatological teleconnections around 2650 BP. *Journal of Quaternary Science*, **11** (6): 451–460.
- VILLWOCK, J.A. 1984. Geology of the coastal province of Rio Grande do Sul, southern Brazil. A synthesis. *Pesquisas* **16**: 5-49.

VILLWOCK, J.A., TOMAZELLI, L.J., LOSS, E.L., DEHNHARDT, E.A., HORN FILHO, N.O., BACHI, F.A., DEHNHARDT, B.A., 1986. Geology of the Rio Grande do Sul Coastal Province. *Quaternary of South America and Antarctic Peninsula*, **4**: 79-97.

VILLWOCK JA, TOMAZELLI LJ. 1995. *Geologia Costeira Do Rio Grande Do Sul*. Notas Técnicas No. 8. CECO, Instituto de Geociências, UFRGS: Porto Alegre, Brasil.

YBERT, J.P.; BISSA, W.M.; KUTNER, M. 2001. Relative sea level variations and climatic evolution in southeastern and southern Brazil during the Late Holocene. *Pesquisas* **28** (2): 75-83.

CAPÍTULO 7

CONCLUSÕES FINAIS

Ao longo da costa do Rio Grande d Sul, o tipo de barreira presente é determinado pelo declive da plataforma interna, pela energia de ondas e pela taxa de transporte longitudinal de sedimentos (TLS). A energia de ondas e taxas de TLS são os principais responsáveis pelo aporte de areia para as barreiras. A variação desses fatores ao longo da costa pode causar variações no aporte sedimentar perpendicular e longitudinal à costa.

Os fatores que influenciam a morfologia dos campos de dunas são: a umidade, a capacidade de transporte do vento e o aporte sedimentar.

A umidade inibe o transporte eólico pois aumenta a coesão dos grãos, aumenta a velocidade limiar de transporte e contribui para o crescimento da vegetação, o que aumenta a rugosidade do terreno (Z_0) e encoraja a deposição (Bagnold 1941; Hesp 1989).

A capacidade de transporte dos ventos depende da sua velocidade e do tamanho dos grãos a serem transportados. Os sedimentos da barreira holocênica do RS, são sedimentos supermaturos textural e composicionalmente, evidenciando o alto grau de retrabalhamento a que foram submetidos ao longo de vários ciclos de sedimentação (Tomazelli 1990), e são considerados, portanto, uma granulação adequada para o transporte eólico (areias finas a muito finas com seleção boa a muito boa). Quanto maior a velocidade dos ventos, maior é o potencial de transporte de areia. O decréscimo na velocidade dos ventos implica na deposição de areia e influencia no crescimento da vegetação (Hesp 1989).

O aporte sedimentar para os campos de dunas depende da disponibilidade de areia para o transporte eólico no pós-praia e estirâncio (*backshore* e *foreshore*), e está diretamente ligado à variação na energia de ondas e no TLS.

Observou-se que todos os fatores acima citados variam ao longo do trecho costeiro estudado.

No trecho de Mostardas a Jardim do Éden, a plataforma interna é mais íngreme, a linha de costa é convexa e a energia de ondas e o TLS são maiores. Nessa região a precipitação é baixa e a planície costeira é larga, aberta e com baixos gradientes topográficos. Devido ao baixo gradiente topográfico, a região é mais suscetível à ventos fortes soprando de diversas direções e com os maiores potenciais de deriva (PD) eólica.

O alto gradiente da plataforma e as altas energia de ondas e taxas de TLS, de Mostardas a Jardim do Éden, provocam a erosão da linha de costa e a consequente

retrogradação da barreira. Essa erosão da linha de costa disponibiliza maior volume de areia para o transporte eólico no pós-praia e no estirâncio. Desse modo, o alto aporte sedimentar, a baixa umidade e o alto PD eólica foram responsáveis pela formação de grandes campos de dunas (chegando à 6900m de largura) nessa região.

No trecho costeiro de Atlântida Sul a Torres, onde o declive da plataforma interna é suave e a linha de costa é côncava, a energia de ondas e o TLS diminuem. Como essa região localiza-se adjacente às escarpas da Serra Geral, a umidade é mais alta, devido à precipitação de origem orográfica e o potencial de deriva (PD) eólica é menor devido à barreira topográfica imposta pelas escarpas da serra.

A baixa energia de ondas e a desaceleração do fluxo de TLS, de Atlântida Sul a Torres, cria um balanço positivo de sedimentos, promovendo a progradação da barreira. Contudo esse balanço positivo estoca areia na face litorânea (*shoreface*) e a baixa energia de ondas não tem capacidade de transportar grandes volumes dessa areia para o estirâncio e pós-praia (*foreshore* e *backshore*). Desse modo, apesar do balanço positivo, e do caráter progradante da barreira nesse trecho, o volume de areia disponível para o transporte eólico é menor. Com o baixo aporte sedimentar, alta umidade e baixo PD eólica, os campos de dunas dessa região são mais estreitos e restritos (em torno de 1400m de largura).

Na região de Dunas Altas, uma mudança abrupta na orientação da linha de costa promove a desaceleração do TLS, causando um “engarrafamento” de sedimentos no local. Esse engarrafamento cria um balanço positivo local de sedimentos, que são parcialmente depositados na face litorânea. Esse balanço positivo inibe o caráter erosivo e retrogradante da região, produzindo barreiras agradantes no local. As altas energias de onda transportam essa areia da face litorânea para o estirâncio e pós-praia disponibilizando-as para o transporte eólico.

Foi observado que alguns dos fatores responsáveis pela variação no tamanho e na morfologia dos campos de dunas ao longo da costa também variaram ao longo das últimas décadas. Na estação meteorológica de Imbé, ao longo de 55 anos de dados, foram observadas variações na precipitação e no PD eólica. Desde 1948 até 2003 (data da última informação disponível) a precipitação vem aumentando gradativamente. O PD eólica apresentou queda contínua no período de 1964 até 1988. Este aumento da precipitação e decréscimo no PD dos ventos pode ter sido crucial para a evolução dos campos de dunas nos últimos 60 anos, uma vez que agindo juntos, essa

tendência pode reduzir significativamente a taxa de migração das dunas e pode induzir o crescimento da vegetação, que é a chave para a estabilização dos campos de dunas.

Observou-se que os campos de dunas estudados também mudaram ao longo do tempo. Áreas deflacionares úmidas e vegetadas aumentaram em todos os campos de dunas desde 1948, levando-os à um processo de estabilização generalizada. Esse processo de estabilização pode ser resultante de fatores variados, incluindo mudanças temporais na umidade, ventos, ondas, freqüência de tempestades, aporte sedimentar e impactos humanos. No entanto, os únicos dados históricos disponíveis foram os de precipitação e ventos, acima citados. Não obstante, eles foram suficientes para explicar as mudanças morfológicas observadas nos campos de dunas. O aumento na precipitação e decréscimo do potencial de deriva dos ventos podem não ter sido os únicos responsáveis, mas certamente foram decisivos para o estabelecimento da atual fase de estabilização que os campos de dunas estão sofrendo.

Com as mudanças climáticas observadas ao longo das últimas décadas, os campos de dunas de Atlântida Sul a Torres, menos ativos, mais estreitos, menores e com menor volume de areia, responderam mais rápido e encontram-se em estágio avançado de estabilização. Os campos de dunas de Mostardas a Jardim do Éden, maiores, mais largos, mais ativos e com maior volume de areia levaram maior tempo para iniciarem os processos de estabilização e crescimento da vegetação. Quanto maior é o volume de areia e o tamanho do campo de dunas, maior será o intervalo de tempo para sua estabilização.

Desse modo, as variações de fatores climáticos ao longo da costa e ao longo do tempo, influenciam diretamente no comportamento morfológico espacial e temporal dos campos de dunas.

A compreensão da morfodinâmica dos campos de dunas ao longo da costa e ao longo das últimas décadas, auxilia na tentativa de entendimento da evolução desses campos de dunas ao longo do Holoceno médio e tardio (últimos 5000 anos A.P.). O estudo da evolução dos campos de dunas foi realizado a partir da análise estratigráfica dos campos de dunas.

As sucessões estratigráficas encontradas em testemunhos de sondagem concordaram com os tipos de barreiras propostos para essa região. Ao norte, os perfis de Rondinha, Capão Novo e Atlântida Sul apresentaram sucessão progradante; em Jardim do Éden e Magistério, e no trecho entre Solidão e Mostardas a sucessão é retrogradante; e em Dunas Altas foi observada agradação.

No norte, a preservação das fases eólicas foi horizontal. Com menor volume de areia, e menores campos de dunas, cada fase foi estabilizada rapidamente e preservada em superfície, enquanto a barreira progradava. No trecho entre Jardim do Éden e Mostardas, as fases de dunas foram preservadas verticalmente. Esta preservação depende do aumento da umidade, o qual induz o crescimento da vegetação e o desenvolvimento de solo no topo dos depósitos eólicos, prevenindo a erosão. Não obstante, se o período de maior umidade não for longo o suficiente para estabilizar totalmente a superfície, uma nova fase de atividade eólica pode erodir totalmente o registro de fases eólicas anteriores.

Analizando as idades ^{14}C de solos e informações sobre paleoclima observou-se que há a sobreposição de informações. Três períodos principais de formação de solo foram encontrados, de 4820 a 3970 anos cal A.P., em um período próximo de 2760-2460 anos cal A.P. e de 1570 a 710 anos cal A.P.. Esses períodos de formação de solos coincidem com períodos de clima mais úmido durante o Holoceno. Este fato indica que o clima pode estar controlando a evolução dos campos de dunas desde pelo menos 5000 anos A.P..

As informações estratigráficas dos três testemunhos mais representativos foram correlacionadas, e junto com as idades de paleossolos e a descrição de fácies puderam ser reconhecidas 10 fases de ativação e estabilização eólica para o litoral médio do RS. São elas:

- Fase 1 estabilizada em 4820-4450 anos cal A.P..
- Fase 2 estabilizada após 4820-4450 anos cal A.P. e antes de 4390-4090 anos cal A.P..
- Fase 3 estabilizada em 4390-3970 anos cal A.P..
- Fases 4 e 5 estabilizadas após 4230-3970 anos cal A.P. e antes de 2760-2460 anos cal A.P..
- Fase 6 estabilizada em 2760-2460 anos cal A.P..
- Fase 7 estabilizada em 1570-1410 anos cal A.P..
- Fase 8 estabilizada após 1570-1410 anos cal A.P. e antes de 920-710 anos cal A.P..
- Fase 9 estabilizada em 920-710 anos cal A.P..
- Fase 10 estabilizada após 920-710 anos cal A.P. e antes da fase atual, em atividade.

Variações climáticas de alta freqüência como as oscilações de sul (El Niño e La Niña) e as oscilações do Atlântico Norte podem ser responsáveis tanto pela total estabilização de campos de dunas como pelo início de uma nova fase de atividade eólica. A observada alta freqüência de formação de solos durante o Holoceno médio e tardio do litoral do RS pode ser resultado desses tipos de variações climáticas, uma vez que elas começaram a ocorrer na área de estudo a partir de 4000 anos A.P.

REFERÊNCIAS BIBLIOGRÁFICAS

- ASSINE, M.L.; PERINOTTO, J.A.J. 2001. Estratigrafia de seqüências em sistemas deposicionais siliciclásticos costeiros e marinhos. In: SEVERIANO RIBEIRO, H.J.P. (Ed.) *Estratigrafia de Seqüências – Fundamentos e Aplicações*. São Leopoldo, EDUNISINOS, 305-339.
- BAGNOLD, R.A. 1941. *The Physics of Blown Sand and Desert Dunes*. London, Chapman & Hall, 265p.
- BARLETTA, R.C. 2000. *Efeito da interação oceano-atmosfera sobre a morfodinâmica das praias do litoral central do Rio Grande do Sul, Brasil*. Rio Grande, Fundação Universidade Federal de Rio Grande, Dissertação de mestrado. 134p.
- BORÓWKA, R.K. 1990. The Holocene development and present morphology of the Leba dunes, Baltic coast of Poland. In: NORDSTROM, K.F.; PSUTY, N.P.; CARTER, R.W.G. (Eds.) *Coastal Dunes: Form and processes*. Chichester, John Wiley & Sons Ltd, 289-313.
- BOYD, R.; DALRYMPLE, R.; ZAITLIN, B.A. 1992. Classification of clastic coastal depositional environments. *Sedimentary Geology*, **80**: 139-150.
- BRESSOLIER, C.; FROIDEFOUND, J.M.; THOMAS, Y.F. 1990. Chronology of coastal dunes in the South-West of France. *Catena Supplement* **18**: 101-107.
- BROOKFIELD, M.E., 1977. The origin of bounding surfaces in ancient aeolian sandstones. *Sedimentology* **24**: 303-332.
- CALLIARI, L.J. & KLEIN, A.H.F. 1993. Características morfodinâmicas e sedimentológicas das praias oceânicas entre Rio Grande e Chuí, RS. *Pesquisas*, **20** (1): 48-56.
- CARTER, R.W.G. 1988. *Coastal Environments*. Academic Press, London, 617 pp.
- CLARKE, M.L.; RENDELL, H.M.; PYE, K.; TASTET, J.P.; PONTEE, N.I.; MASSÉ, L. 1999. Evidence for the timing of dune development on the Aquitaine coast, southwest France. *Z. Geomorph. N.F. Suppl.Bd* **116**: 147-163.
- CURRAY, J.R. 1964. Transgressions and regressions. In: MILLER, R.L. (Ed.), *Papers in Marine Geology*, Shepard commemorative volume. Macmillan, New York, N.Y., pp.175-203.
- DILLENBURG, S.R. 1994. *A Laguna de Tramandaí: Evolução Geológica e Aplicação do Método Geocronológico da Termoluminescência na Datação de Depósitos Sedimentares Lagunares*. Porto Alegre, Univ. Federal Rio Grande do Sul. Tese de Doutoramento (inéd.). 113p.
- DILLENBURG, S.R.; ROY, P.S.; COWELL, P.J.; TOMAZELLI, L.J. 2000. Influence of antecedent topography on coastal evolution as tested by shoreface translation-barrier model (STM). *Journal of coastal research*, **16**(1): 71-81.
- DILLENBURG, S.R., TOMAZELLI, L.J., CLEROT, L.C.P. 2003. Gradients of wave energy as the main factor controlling the evolution of the coast of Rio Grande do Sul in southern Brazil during the Late Holocene. *Proceedings of the 5th*

International Symposium on Coastal Engineering and Science of Coastal Sediment Process. New York, NY: American Society of Civil Engineers, v.1, CD, 2003.

FISHER, W.L. 1983. *Facies Analysis in Reservoir Geology*. Ouro Preto, Univ.Federal Ouro Preto. Apostila de Curso (inéd.). 66p.

FISHER, W.L. & McGOWEN, J.H. 1969. Depositional systems in Wilcox Group (Eocene) of Texas and their relation to occurrence of oil and gas. *Bull. Am. Assoc. Petrol. Geologists*, **53** (1): 30-54.

FRYBERGER, S.G.; DEAN, G. 1979. Dune forms and wind regime. In: MCKEE, E.D. (Ed.) *A Study of Global Sand Seas*. USGS, Professional paper **1052**:137-169.

GIANNINI, P.C.F. 1993. *Sistemas Depositionais no Quaternário Costeiro entre Jaguaruna e Imbituba, SC*. São Paulo, Inst. Geoc. Univ. S. Paulo. Tese de Doutoramento (inéd.) 2v, 2 mapas, 439p..

GIANNINI, P.C.F. 1998. Associações de fácies eólicas ativas na costa centro-sul de Santa Catarina. *Anais da Acad. Bras. Ciências*, **70**(3): 696.

GIANNINI, P.C.F. 2002. Complexo lagunar centro-sul catarinense- valioso patrimônio sedimentológico, arqueológico e histórico. In: SCHOBENHAUS, C.; CAMPOS, D.A.; QUEIROZ, E.T.; WINGE, M.; BERBERT-BORN, M. (Eds.) *Sítios geológicos e paleontológicos do Brasil*. Brasília, DNPM, p.213-222.

GIANNINI, P.C.F. & SANTOS, E.R. 1994. Padrões de variação espacial e temporal na morfologia de dunas de orla costeira no Centro-Sul catarinense. *Bol. Paranaense de Geociências*, **42**: 73-96.

GIANNINI, P.C.F.; SAWAKUCHI, A.O.; MARTINHO, C.T. 2001a. A estratigrafia de seqüências na evolução das dunas costeiras de Santa Catarina, Sul do Brasil. In: I CONGRESSO DO QUATERNÁRIO DOS PAÍSES DE LÍNGUA IBÉRICA, Lisboa. *Actas*, GTPEQ., AEQUA, SGP. p. 117-120.

GIANNINI, P.C.F.; SAWAKUCHI, A.O.; MARTINHO, C.T. 2001b. O nível do mar e as dunas eólicas no litoral centro-sul catarinense: um modelo de estratigrafia de seqüências no Quaternário. In: VIII CONGRESSO ABEQUA, Imbé, RS. *Boletim de resumos*, ABEQUA. p. 45-46.

GIANNINI, P.C.F.; ASSINE, M.L.; BARBOSA, L.M.; BARRETO, A.M.F.; CARVALHO, A.M.; CLAUDINO-SALES, V.; MAIA, L.P.; MARTINHO, C.T.; PEULVAST, J.P.; SAWAKUCHI, A.O. & TOMAZELLI, L.J. 2005. Dunas Eólicas Costeiras e Interiores. In: SOUZA, C.R.G.; SUGUIO, K.; DE OLIVEIRA, P.E. & OLIVEIRA, A.M.S. (Eds.). *Quaternário do Brasil*. Holos Editora, São Paulo. 235-257.

GODDARD, E.N. 1975. *The Rock Color Chart Committee*. Geological Society of America Boulder, Colorado, USA.

GOLDSMITH, V. 1985. Coastal dunes. In: DAVIES Jr., R.A. (Ed.), *Coastal sedimentary environments*. New York, Spring-Verlag. p. 303-378.

- HESP, P.A. 1983. Morphodynamics of incipient foredunes in New South Wales, Austrália. In: BROOKFIELD, M.E. & AHLBRANDT, T.S. eds. *Eolian Sediments and Processes*. Amsterdam, Elsevier. p. 325-342 (Developments in Sedimentology, 38).
- HESP, P.A. 1988. Morphology, dynamics and internal stratification of some established foredunes in Southeast Austrália. *Sediment. Geol.*, **55** (1/2): 17-41.
- HESP, P. A. 1989. A review of biological and geomorphological processes involved in the initiation and development of incipient foredunes. *Proceedings of the Royal Society of Edinburgh*, **96B**: 181-201.
- HESP, P.A. 1999. The beach backshore and beyond. In: SHORT, A.D. (Ed.) *Handbook of Beach and Shoreface Morphodynamics*. Chichester, Jonh Wiley & Sons Ltd, p. 145-270.
- HESP, P.A. 2000. *Coastal sand dunes. Form and Function*. CDNV Technical Bulletin No. 4. Massey University, 28 pp.
- HESP, P.A. 2004. Coastal dunes in the Tropics and Temperate Regions: Location, formation, morphology and vegetation processes. In: MARTINEZ, M. & PSUTY, N. (Eds.) *Coastal Dunes, Ecology and Conservation. Ecological Studies* v. 171. Springer-Verlag, Berlin: 29-49.
- HESP, P.A. & THOM, B.G. 1990. Geomophology and evolution of active transgressive dunefields. In: NORDSTROM, K.F.; PSUTY, N.P.; CARTER, R.W.G. (Eds.) *Coastal Dunes: Form and Process*. Chichester, Jonh Wiley & Sons Ltd, 253-287.
- HESP, P.A. & SHORT, A.D., 1999. Barrier Morphodynamics. In: SHORT, A.D. (Ed.) *Handbook of Beach and Shoreface Morphodynamics*. Chichester, Jonh Wiley & Sons Ltd, p. 307-333.
- ILLENBERGER, W.K. 1988. The Holocene evolution of the Sundays estuary and adjacent coastal dunefields, Algoa Bay, South Africa. In: DARDIS, G.F. & MOON, B.P. (Eds.) *Geomorphological Studies in Southern Africa*. Balkema, Rotterdam, 389-405.
- ILLENBERGER, W.K. & VERHAGEN, B.T. 1990. Environmental history and dating of coastal dunefields. *Suid-Afrikaanse Tydskrif vir Wetenskap* **86**: 311-314.
- INGLE, J.C. 1966. *The movement of beach sand: an analysis using florescent grains*. Devel. in Sedimentology v. 5. Amsterdam, Elsevier.
- KARPETA, W.P. 1990. The morphology of Permian palaeodunes – a reinterpretation of the Bridgnorth Sandstone around Bridgnorth, England, in the light of modern dune studies. *Sediment. Geol.*, **69** (1/4): 59-75.
- KOCUREK, G. 1981. Significance of interdune deposits and bounding surfaces in eolian dune sands. *Sedimentology*, **28**(6):753-780.
- KOCUREK, G. 1988. First-order and super bounding surfaces in eolian sequences - Bounding surfaces revisited. *Sediment. Geol.*, **56**(1/4):193-206.

- KOCUREK, G. & HAVHOLM, K.G. 1993. Eolian Sequence Stratigraphy – A Conceptual Framework. In: WEIMER, P. & POSAMENTIER, H. (Eds.) *Siliciclastic Sequence Stratigraphy – Recent Developments and Applications*. AAPG Memoir **58**: p.393-409.
- LIMA, S.F.; ALMEIDA, L.E.S.B.; TOLDO JR., E.E. 2001. Estimate of longshore sediments transport from waves data to the Rio Grande do Sul coast. *Pesquisas* **48** (2): 99-107.
- LOOPE, W.L.; ARBOGAST, A.F. 2000. Dominance of an ~150-year cycle of sand-supply change in the Late Holocene dune-building along the Eastern Shore of Lake Michigan. *Quaternary Research*, **54**: 414-422.
- MARCOMINI, S.C.; MAIDANA N. 2006. Response of eolian ecosystems to minor climatic changes. *Journal of Coastal Research* **SI 39**: 204-208.
- MARTINHO, C.T. 2004. *Morfodinâmica e sedimentologia de campos de dunas transgressivos da região de Jaguaruna-Imbituba, Santa Catarina*. São Paulo, Inst. Geoc. Univ. S. Paulo. Dissertação de Mestrado, (inéd.) 108p.
- MARTINHO, C.T. 2006. *Evolução Holocênica de Barreiras e Campos de Dunas Transgressivos*. Porto Alegre, Univ. Federal Rio Grande do Sul. Monografia de Qualificação, (inéd.) 33p.
- MARTINHO, C.T.; GIANNINI, P.C.F.; SAWAKUCHI, A.O. 2003. Fácies morfológicas e fácies deposicionais de campos de dunas transgressivos ativos da região de Jaguaruna-Imbituba, SC. In: IX CONGRESSO ABEQUA, II CONGRESSO DO QUATERNÁRIO DOS PAÍSES DE LÍNGUAS IBÉRICAS e II CONGRESSO SOBRE PLANEJAMENTO E GESTÃO DA ZONA COSTEIRA DOS PAÍSES DE EXPRESSÃO PORTUGUESA, Recife, PE. *Anais*, arquivo eletrônico em CD, 5p., 102.pdf.
- MARTINHO, C.T.; GIANNINI, P.C.F.; SAWAKUCHI, A.O. 2006. Morphological and depositional facies of transgressive dunefields in the Imbituba-Jaguaruna region, Santa Catarina State, Southern Brazil. *Journal of Coastal Research*, **SI 39**: 673-677.
- MORTON, R. A. 1994. Texas Barriers. In: DAVIS, R.A. (Ed.) *Geology of Holocene Barrier Island Systems*. Springer-Verlag, Berlin: 75-114.
- MURRAY, A.S. & CLEMMENSEN, L.B. 2001. Luminescence dating of Holocene aeolian sand movement, Thy, Denmark. *Quaternary Sciences Reviews*, **20**: 751-754.
- NORDSTROM, K. F.; PSUTY, N.; CARTER, B. 1990. *Coastal dunes. Forms and process*. Jonh Wiley & Sons. Chichester. 392 pp.
- ORFORD, J.D. 2005. The controls on Late-Holocene coastal dune formation on leeside coasts of the British Isles. *Z. Geomorph. N. F.*, **141**: 135-152.

- PATTERSON, D.C. & BLAIR, R.J. 1983. Visually determined wave parameters. In: Sixth Australian Conference on Coastal & Ocean Engineering, 1983, Gold Coast. pp. 151-155.
- PYE, K. 1983. Formation and history of Queensland coastal dunes. *Z. Geomorph. N.F.* Suppl.-Bd **45**: 175-204.
- PYE, K. & BOWMAN, G.M. 1984. The Holocene marine transgression as a forcing function in episodic dune activity on the Eastern Australian Coast. In: THOM, B.G. (Ed.) *Coastal Geomorphology in Australia*. Academic Press Australia, 179-196.
- PYE, K. & RHODES, E.G. 1985. Holocene development of an episodic transgressive dune barrier, Ramsay Bay, North Queensland, Australia. *Marine Geology*, **64**: 189-202.
- ROY, P.S.; COWELL, P.J.; FERLAND, M.A.; THOM, B.G. 1994. Wave-dominated coasts. In: CARTER, R.W.G. & WOODROFFE, C.D. (Eds.) *Coastal evolution, Late Quaternary Shoreline Morphodynamics*. Cambridge, Cambridge University Press, p.121-186.
- SHEPARD, M., 2000. Coasts, the edge of the land. In: SAUNDERS, B.G.R. (Ed.) *The South of the North. Manawatu and Its Neighbours*. Palmerston North, Massey University, p. 34-39.
- SHORT, A.D. 1988b. Holocene coastal dune formation in Southern Australia: a case of study. *Sedimentary Geology*, **55**: 121-142.
- SHORT, A.D. & HESP, P.A. 1982. Wave, beach and dune interactions in South-eastern Australia. *Marine Geol.*, **48**(4): 259-284.
- SHULMEISTER, J. & LEES, B. 1992. Morphology and chronostratigraphy of coastal dunefield: Groote Eylandt, northern Australia. *Geomorphology* **5**: 521-534.
- SOARES, P.C. 1992. *Tectônica Sinsedimentar Cíclica na Bacia do Paraná - Controles*. Curitiba, Dpto. Geologia Univ. Fed. Paraná. Tese Prof. Titular (inéd.). 131p.
- STOKES, W.L. 1968. Multiple parallel - truncation bedding planes a feature of wind deposited sandstone formations. *J. Sediment. Petrol.*, **38**(2): 510-515.
- TALBOT, M.R. 1985. Major bounding surfaces in aeolian sandstones - a climatic model. *Sedimentology*, **32**: 257-265.
- TASTET, J.P.; PONTEE, N.I. 1998. Morpho-chronology of coastal dunes in Médoc. A new interpretation of Holocene dunes in Southwestern France. *Geomorphology* **25**: 93-109.
- TOLDO JR, E.E.; ALMEIDA, L.E.S.B.; NICOLODI, J.L.; ABSALONSEN, L.; GRUBER, N.L.S. 2006. O controle da deriva litorânea no desenvolvimento do campo de dunas e da antepraia no litoral médio do Rio Grande do Sul. *Pesquisas* **33** (2): 35-42.

- TOMAZELLI, L.J. 1990. *Contribuição ao Estudo dos Sistemas Depositionais Holocénicos do Nordeste da Província Costeira do Rio Grande do Sul, com Ênfase no Sistema Eólico*. Porto Alegre, Univ. Federal Rio Grande do Sul. Tese de Doutoramento (inéd). 270p.
- TOMAZELLI, L.J. 1993. Regime de ventos e taxa de migração de dunas eólicas costeiras do Rio Grande do Sul, Brasil. *Pesquisas*, **21**(1): 64-71.
- THOM, B.G.; BOWMAN, G.M.; ROY, P.S. 1981. Late Quaternary evolution os coastal sand barriers, Port Stephens – Myall Lakes area, Central New South Wales, Australia. *Quaternary Research* **15**: 345-364.
- U.S. ARMY, CECW-EW, 2003. *Coastal engineering manual*. Corps of Engineers Internet Publishing Group, Washington, DC, USA. EM 1110-2-1100.
- WESCHENFELDER, J. & ZOUAIN, R.N.A. 2002. Variabilidade morfodinâmica das praias oceânicas entre Imbé e Arroio do Sal, RS, Brasil. *Pesquisas em Geociências*, **29**(1): 3-13.
- WILSON, P.; ORFORD, J.D.; KNIGHT, J.; BRALEY, S.M.; WINTLE, A.G. 2001. Late-Holocene (post-4000 years BP) coastal dune development in Northumberland, northeast England. *The Holocene*, **11** (2): 215-229.

ANEXO A

DESCRIÇÃO DAS FÁCIES SEDIMENTARES

FÁCIES SEDIMENTARES

- **AFMhc:** Areia fina, muito bem selecionada, com estratificação sub-horizontal a horizontal, estratificação cruzada e níveis com areia média.
- **AFhco:** Areia fina, muito bem selecionada, com estratificação sub-horizontal a horizontal e com alto grau de compactação.
- **AFmco:** Areia fina, muito bem a bem selecionada, maciça, com alto grau de compactação.
- **AFi:** Areia fina, muito bem a bem selecionada, com intercalação de níveis com alto grau de compactação e níveis com baixo grau de compactação, com estratificação cruzada e planar, truncamentos e rico em minerais pesados.
- **AFc:** Areia fina, muito bem a bem selecionada, com estratificação cruzada e baixo grau de compactação dos sedimentos. Pode apresentar raízes de gramíneas.
- **AFm:** Areia fina, muito bem selecionada, maciça.
- **AFme:** Areia fina, muito bem a bem selecionada, maciça apresentando coloração esverdeada.
- **AFmb:** Areia fina, muito bem a bem selecionada, maciça com bioturbação e marcas de raízes.
- **AFmmo:** Areia fina, muito bem a bem selecionada, mosqueada, com coloração escura e rica em matéria orgânica disseminada, eventualmente apresenta marcas de raízes, alto grau de pedogênese.
- **AFmo:** Areia fina, muito bem a bem selecionada, com coloração escura indicando a presença de matéria orgânica disseminada, algumas estratificações planares preservadas apresentando pedogênese incipiente.
- **AFhemo:** Areia fina, muito bem a bem selecionada, com estratificação sub-horizontal a horizontal, estratificação cruzada e níveis ricos em matéria orgânica.
- **AFch:** Areia fina, muito bem a bem selecionada, com estratificações cruzadas e estratificação sub-horizontal a horizontal.
- **AFT:** Areia fina, bem selecionada, coloração preta evidenciando presença maciça de matéria orgânica turfosa, compacta.
- **AFv:** Areia fina em meio à vegetação atual (gramíneas).

- **AFh:** Areia fina, muito bem a bem selecionada com estratificação sub-horizontal a horizontal.
- **AFL:** Areia fina, mosqueada com lentes irregulares de lama (silte e argila).
- **LAl:** Lama (silte e argila) escura com lentes de areia fina.
- **AFLb:** Bolsões irregulares de lama e areia fina, mosqueados, bioturbados, rico em marcas de raízes.

PROCESSOS DEPOSIONAIS

Fácies	Processos Depositionais
AFMphc	Correntes subaquosas com variações de energia.
AFhco	Correntes subaquosa de saca e ressaca.
AFmco	Deposição por corrente subaquosa e posterior destruição das estruturas sedimentares devido ao impacto da quebra de ondas no substrato sedimentar.
AFi	Intercalação de deposição por correntes subaquosa de saca e ressaca e por processos eólicos.
AFc	Diminuição do fluxo eólico pela vegetação, ocasionando deposição de areia.
AFm	Depósitos arenosos que tiveram sua estrutura destruída pela vegetação ou pela variação do lençol freático.
AFme	Depósitos arenosos que tiveram sua estrutura destruída pela variação do lençol freático.
AFmb	Depósitos arenosos que tiveram sua estrutura destruída pela vegetação.
AFmmo	Pedogênese desenvolvida sobre depósitos arenosos.
AFmo	Pedogênese incipiente desenvolvida sobre depósitos arenosos.
AFhemo	Processos eólicos de fluxo e queda de grãos, em superfície vegetada.
AFch	Processos eólicos fluxo e queda de grãos.
AFt	Pedogênese avançada sobre depósitos arenosos devido à colonização por vegetação.
AFv	Pedogênese atual com depósitos eólicos cobertos por vegetação
AFh	Empilhamento vertical de areia pela vegetação
AFL	Intercalação de corrente subaquosa e suspensão subaquosa
LAl	Deposição por suspensão subaquosa
AFLb	Intercalação de corrente subaquosa e suspensão subaquosa em meio à vegetação

ANEXO B

LOCALIZAÇÃO DOS PERFIS E TESTEMUNHOS

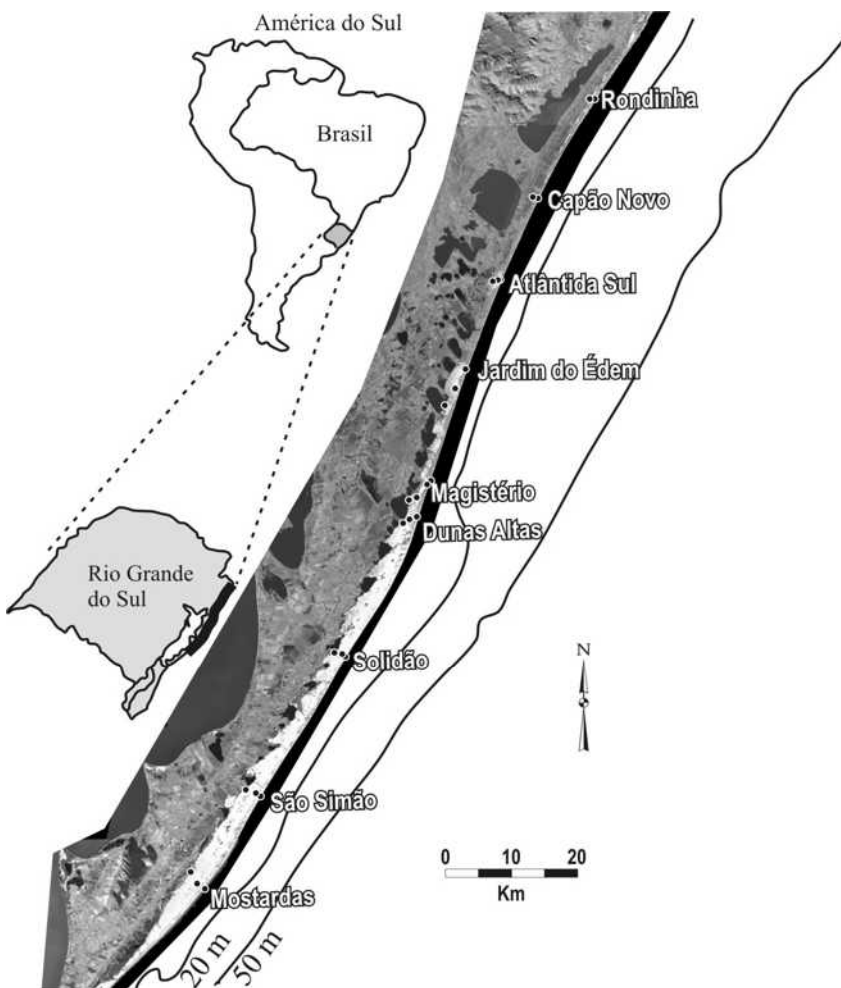


Figura 1: Localização os perfis ao longo do litoral

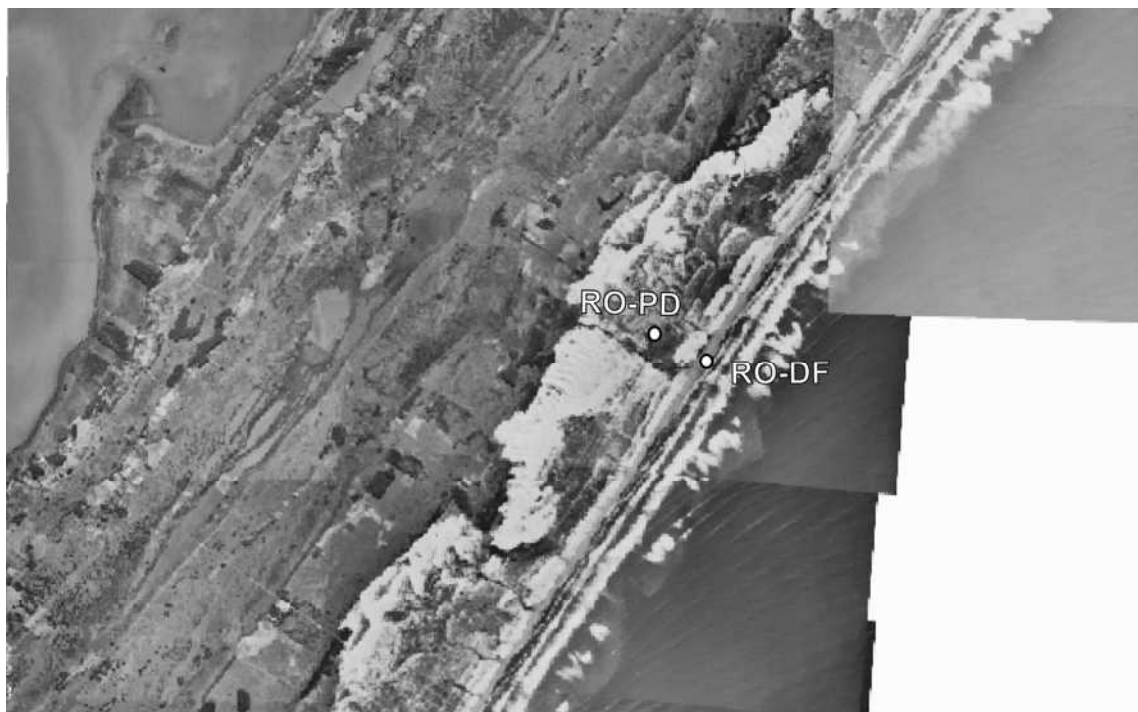


Figura 2: Localização dos testemunhos no perfil de Rondinha. Foto aérea de 1974, escala 1:40.000.

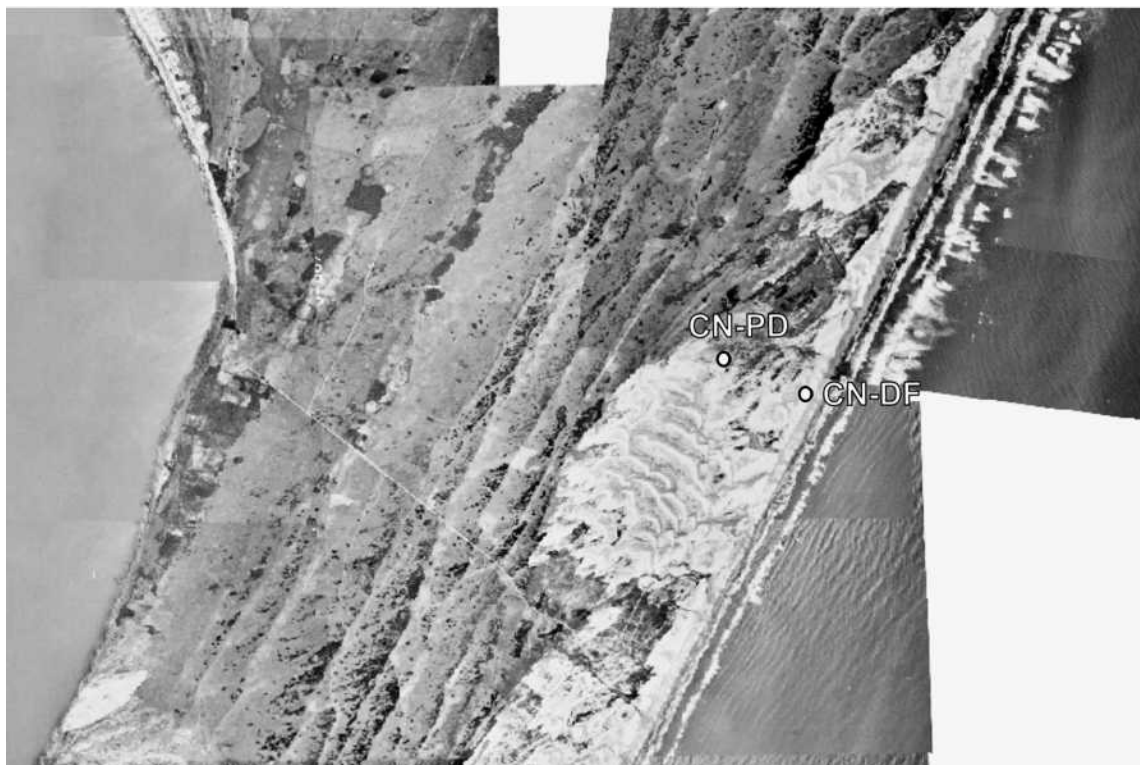


Figura 3: Localização dos testemunhos no perfil de Capão Novo. Foto aérea de 1974, escala 1:40.000.

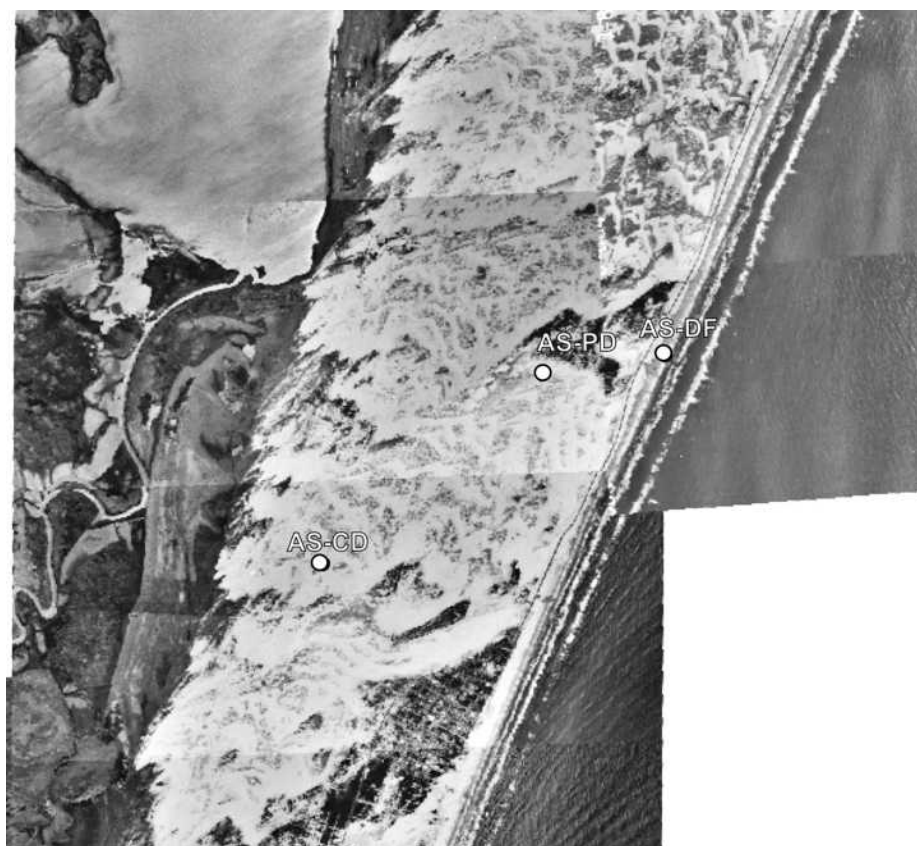


Figura 4: Localização dos testemunhos no perfil de Atlântida Sul. Foto aérea de 1974, escala 1:40.000.

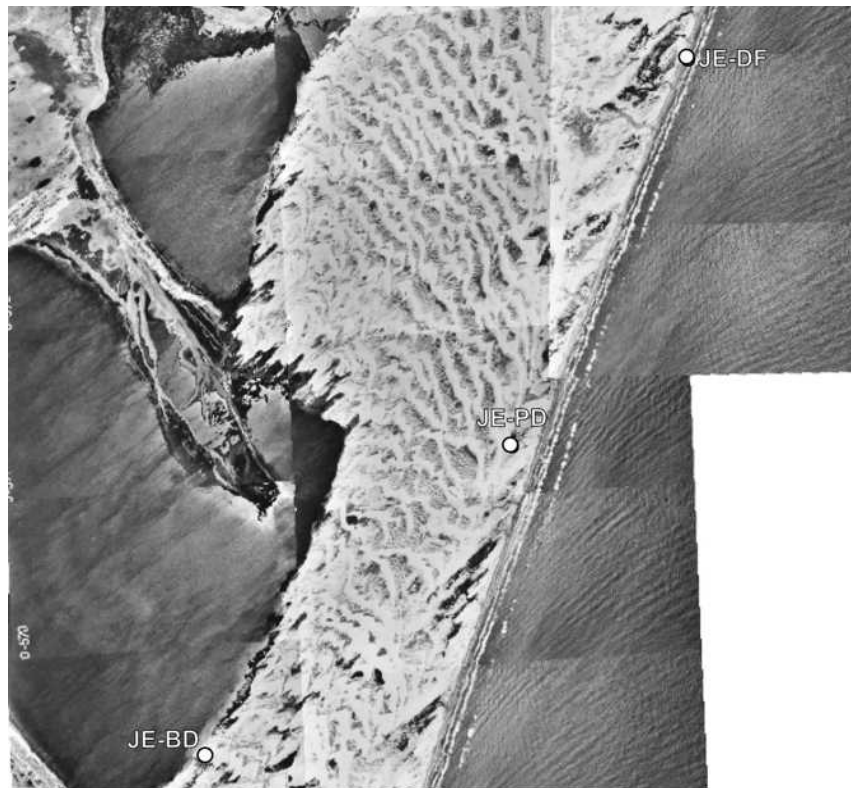


Figura 5: Localização dos testemunhos no perfil de Jardim do Éden. Foto aérea de 1974, escala 1:60.000.

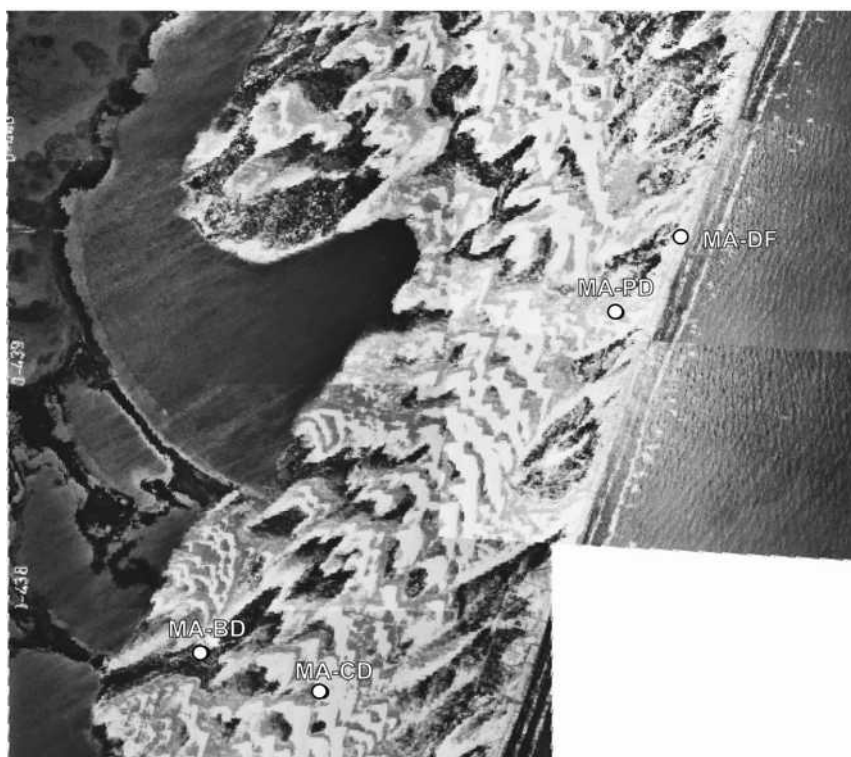


Figura 6: Localização dos testemunhos no perfil de Magistério. Foto aérea de 1974, escala 1:45.000.

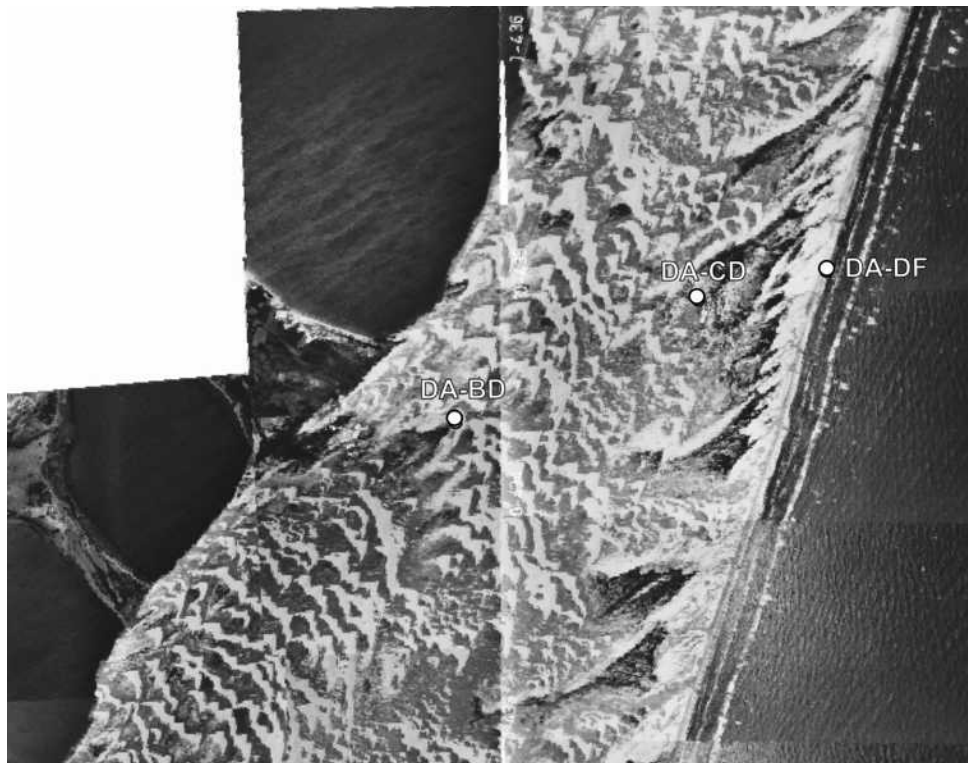


Figura 7: Localização dos testemunhos no perfil de Dunas Altas. Foto aérea de 1974, escala 1:45.000.

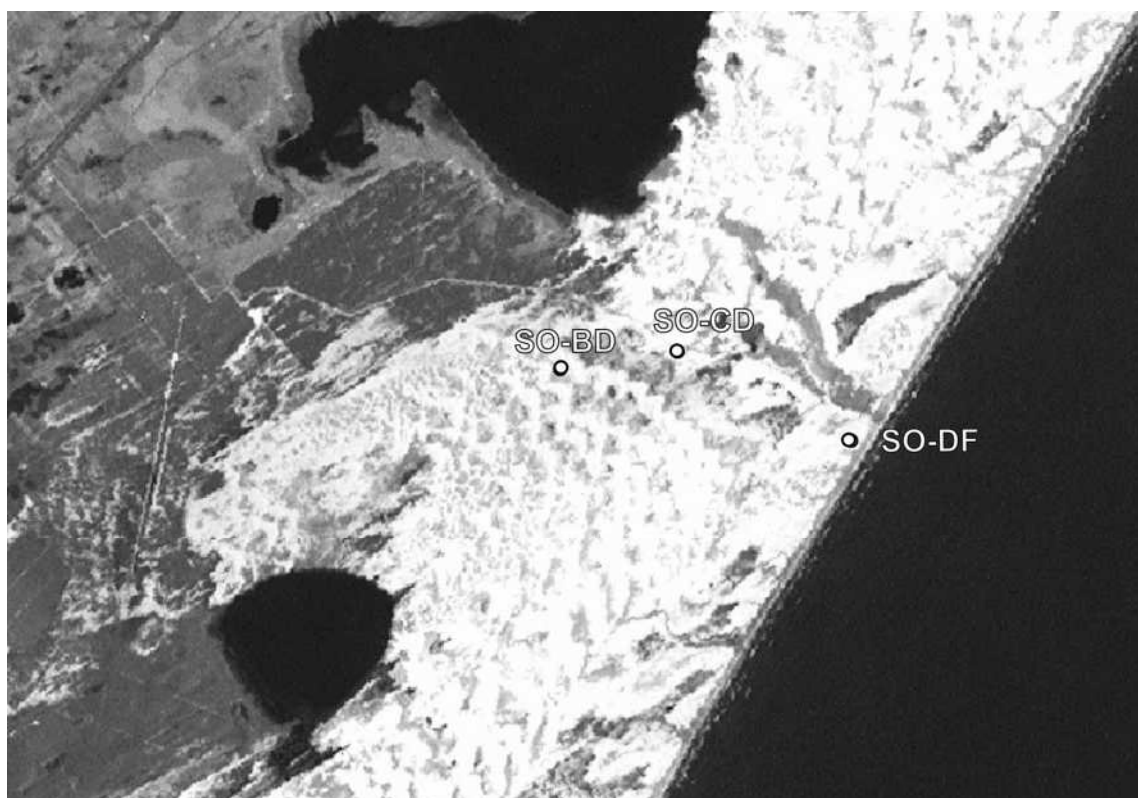


Figura 8: Localização dos testemunhos no perfil de Solidão. Imagem de satélite de 1999, escala 1:45.000.

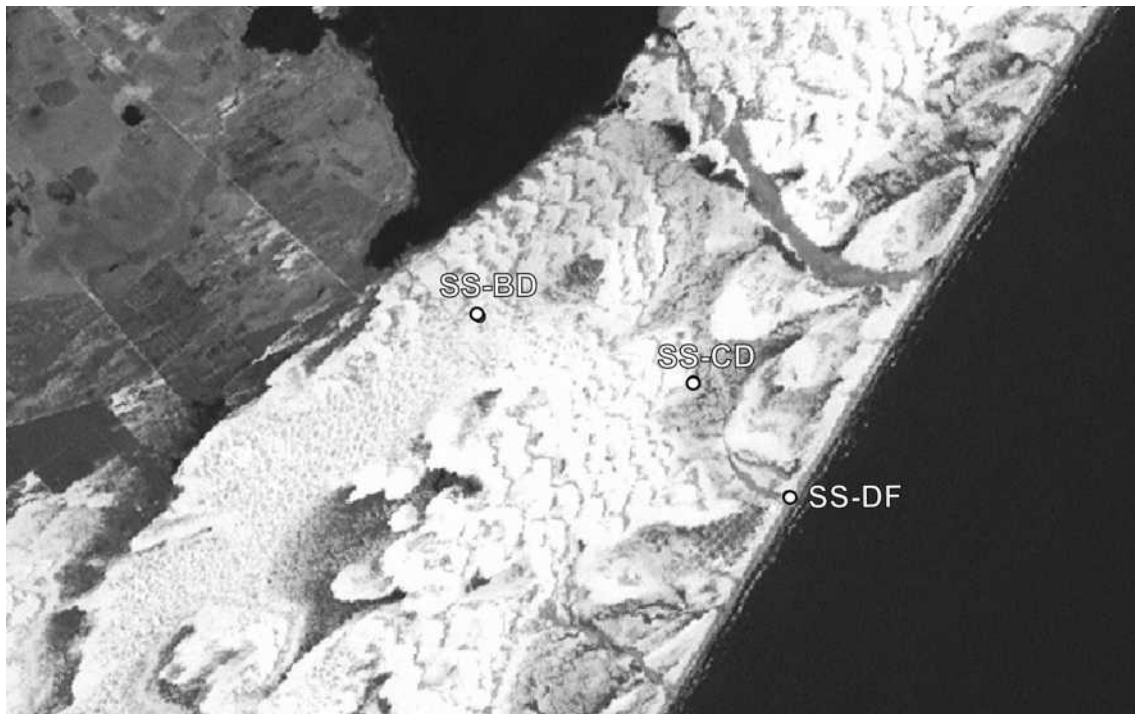


Figura 9: Localização dos testemunhos no perfil de São Simão. Imagem de satélite de 1999, escala 1:45.000.

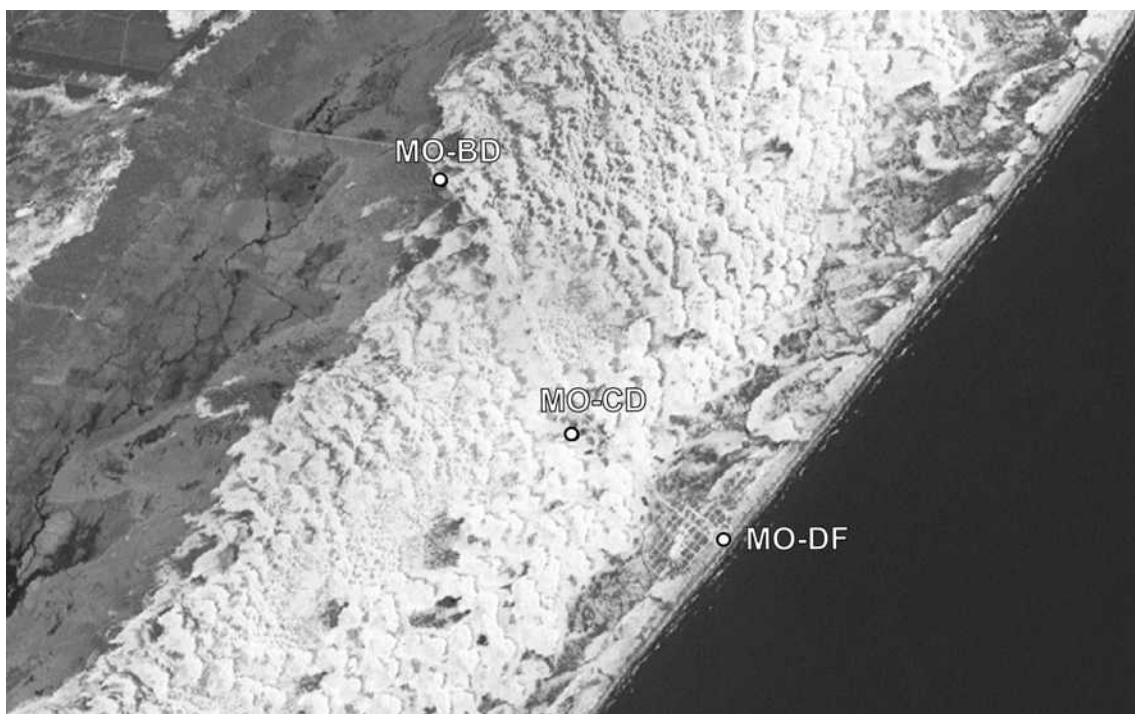


Figura 10: Localização dos testemunhos no perfil de Mostardas. Imagem de satélite de 1999, escala 1:55.000.

ANEXO C

TESTEMUNHOS DE SONDAGEM

ANEXO D

PERFIS COM OS TESTEMUNHOS DE SONDAGEM

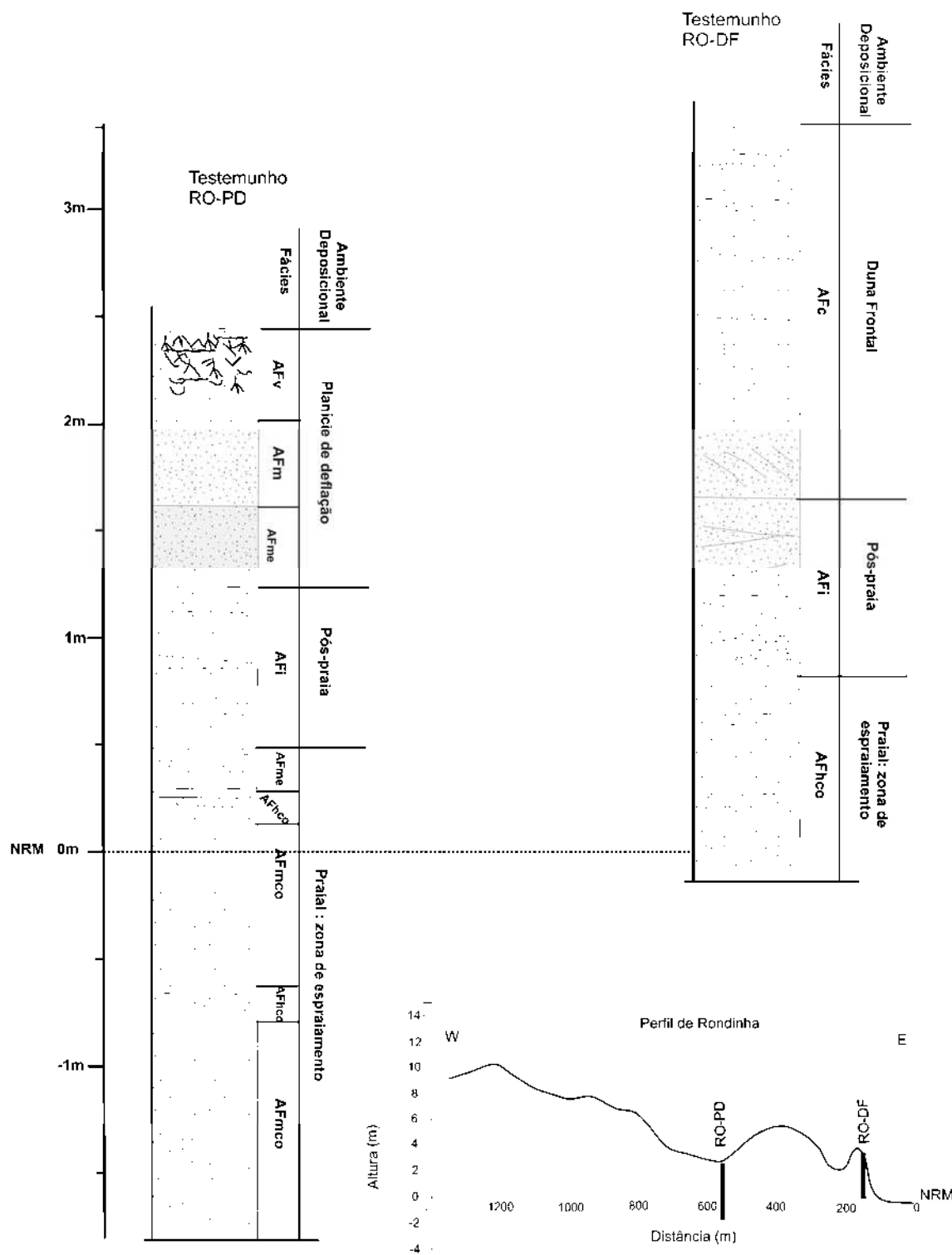


Figura 1: Perfil de Rondinha. Posição e altura dos testemunhos na seção topográfica. Seção estratigráfica dos testemunhos, apresentando as fácies sedimentares, o ambiente deposicional no qual as facies foram depositadas e as fases de atividade eólica, quando reconhecidas.

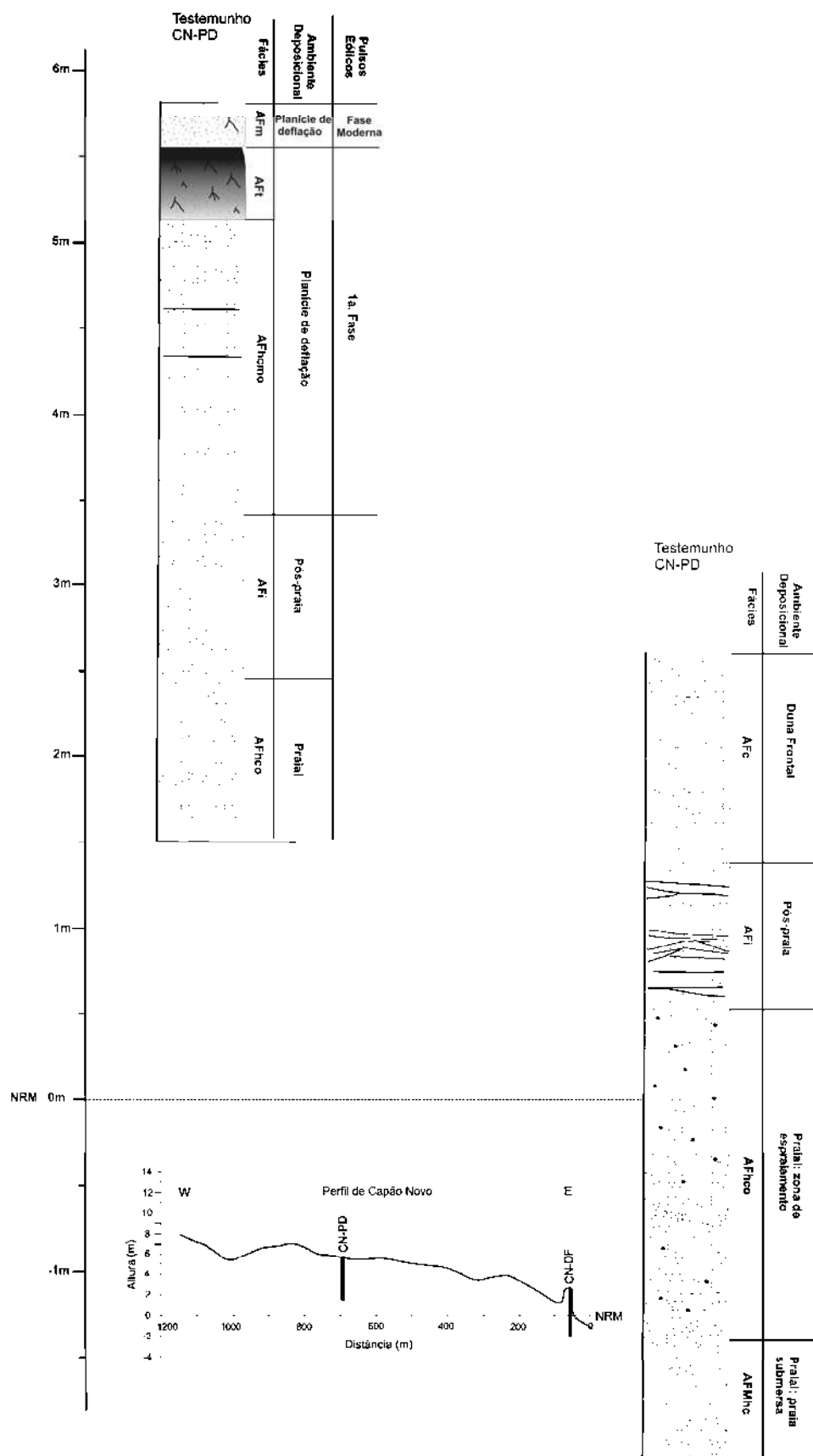


Figura 2: Perfil de Capão Novo. Posição e altura dos testemunhos na seção topográfica. Seção estratigráfica dos testemunhos, apresentando as fácies sedimentares, o ambiente deposicional no qual as facies foram depositadas e as fases de atividade eólica, quando reconhecidas.

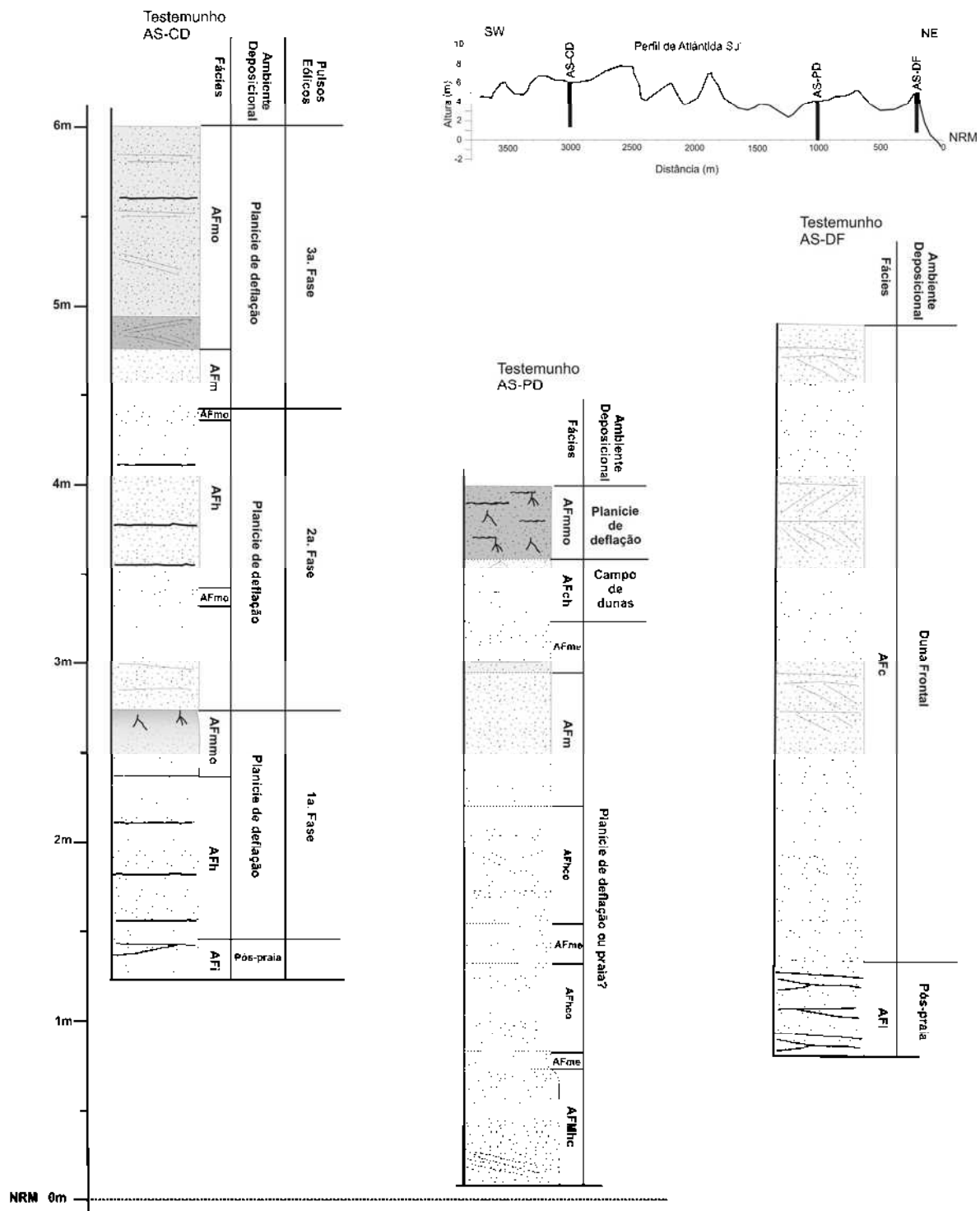


Figura 3: Perfil de Atlântida Sul. Posição e altura dos testemunhos na seção topográfica. Seção estratigráfica dos testemunhos, apresentando as fácies sedimentares, o ambiente deposicional no qual as facies foram depositadas e as fases de atividade eólica, quando reconhecidas.

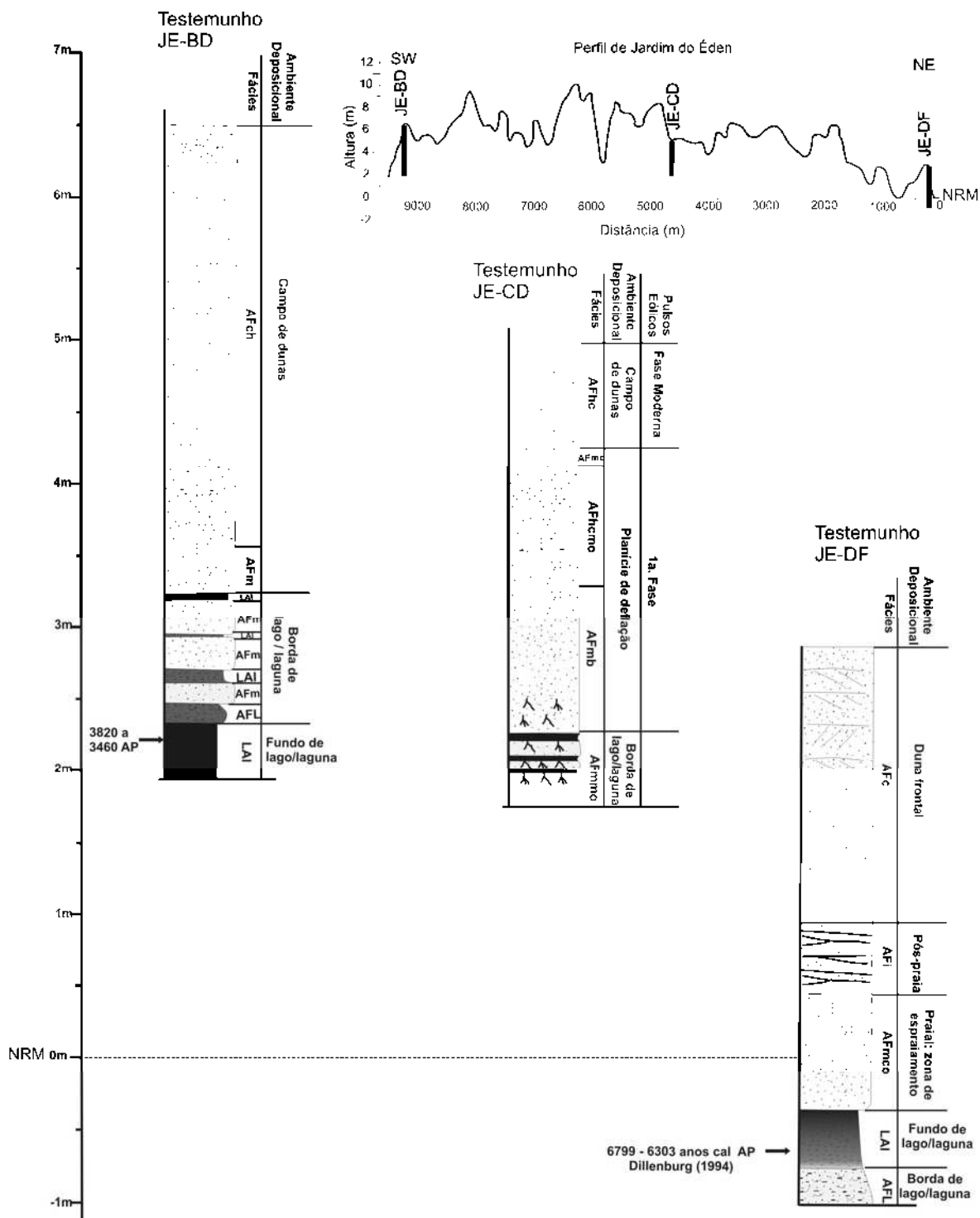


Figura 4: Perfil de Jardim do Éden. Posição e altura dos testemunhos na seção topográfica. Seção estratigráfica dos testemunhos, apresentando as fácies sedimentares, o ambiente deposicional no qual as facies foram depositadas e as fases de atividade eólica, quando reconhecidas.

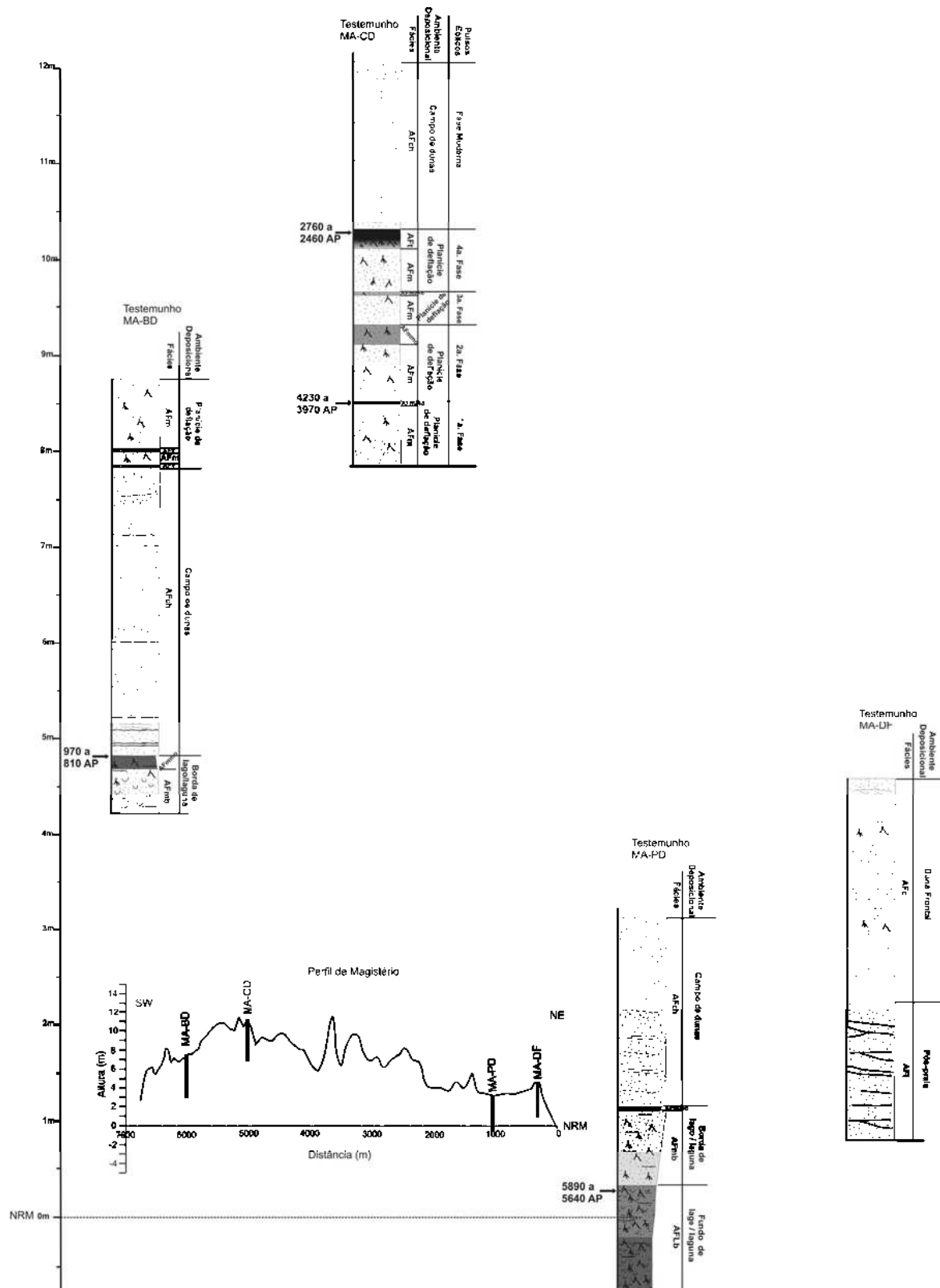


Figura 5: Perfil de Magistério. Posição e altura dos testemunhos na seção topográfica. Seção estratigráfica dos testemunhos, apresentando as fácies sedimentares, o ambiente deposicional no qual as facies foram depositadas e as fases de atividade eólica, quando reconhecidas.

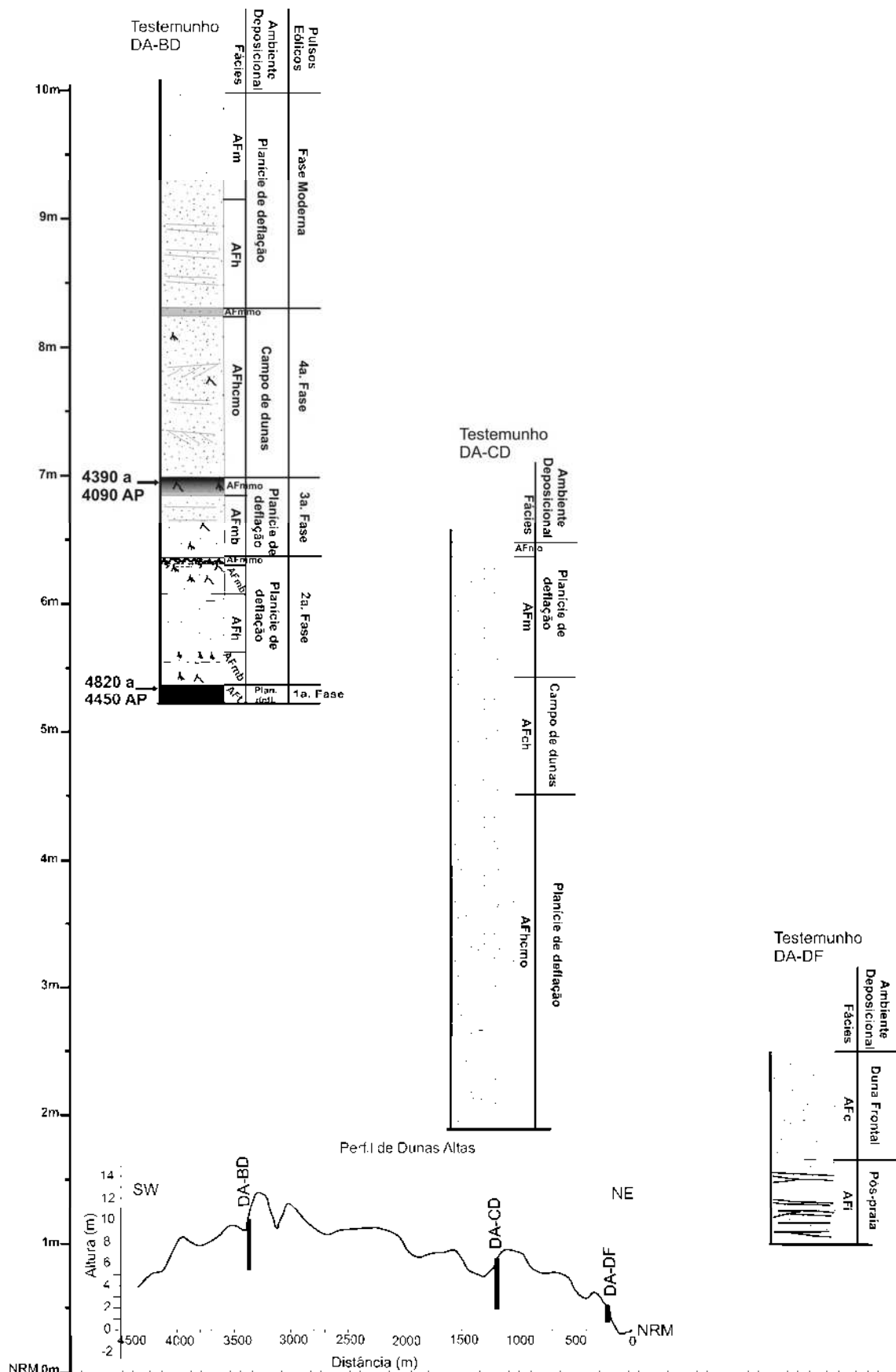


Figura 6: Perfil de Dunas Altas. Posição e altura dos testemunhos na seção topográfica. Seção estratigráfica dos testemunhos, apresentando as fácies sedimentares, o ambiente deposicional no qual as facies foram depositadas e as fases de atividade eólica, quando reconhecidas.

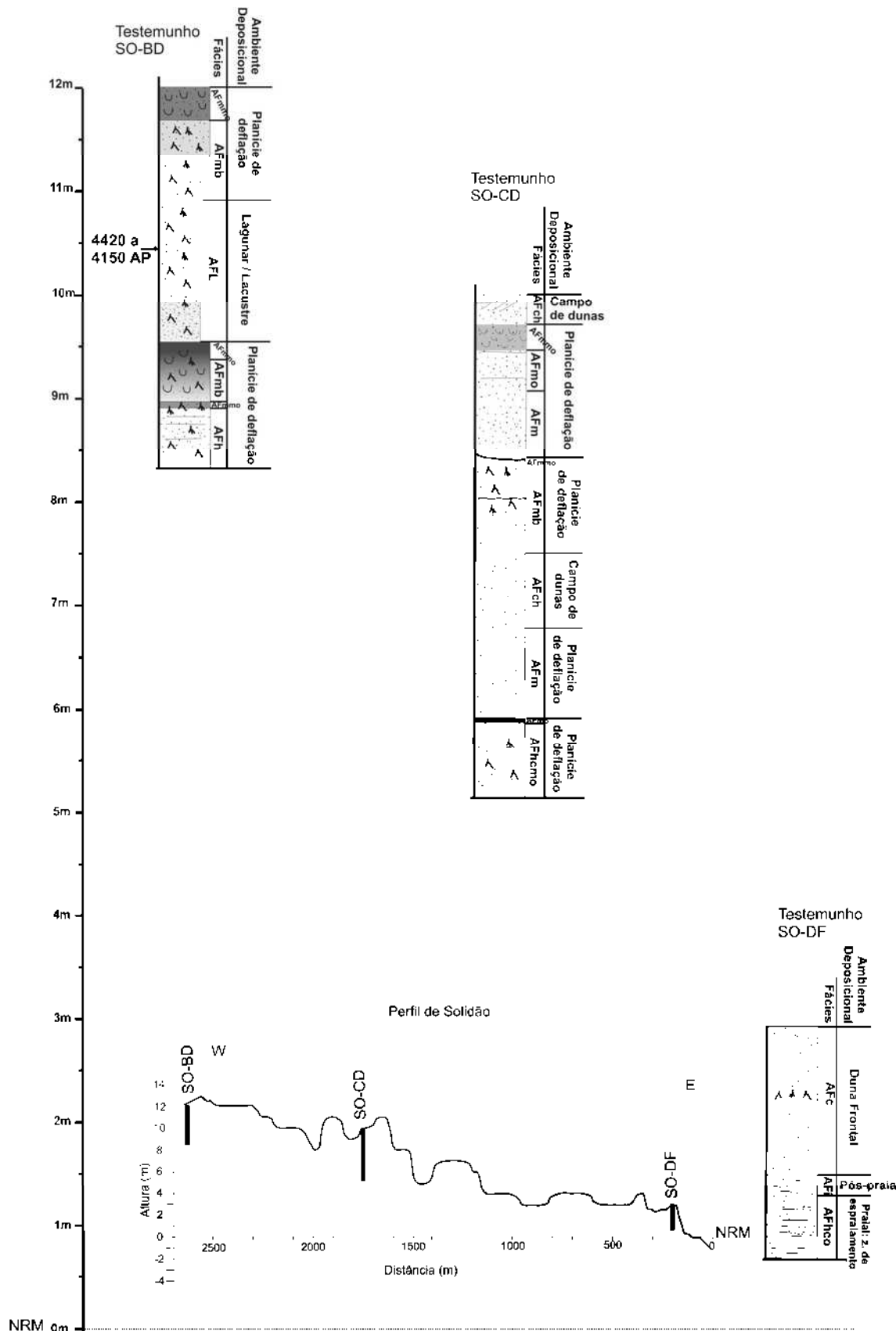


Figura 7: Perfil de Solidão. Posição e altura dos testemunhos na seção topográfica. Seção estratigráfica dos testemunhos, apresentando as fácies sedimentares, o ambiente deposicional no qual as facies foram depositadas e as fases de atividade eólica, quando reconhecidas.

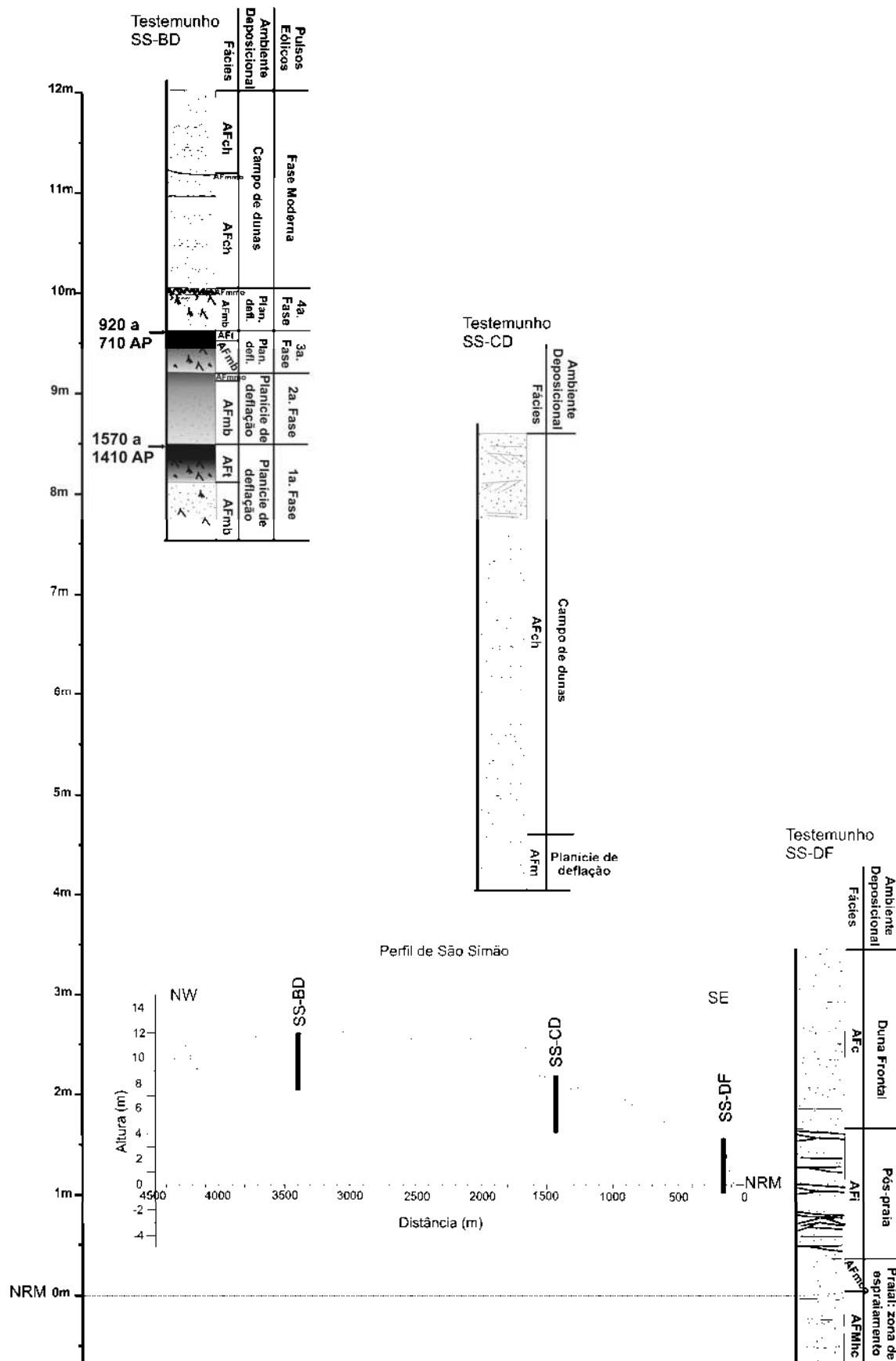


Figura 8: Perfil de São Simão. Posição e altura dos testemunhos na seção topográfica. Seção estratigráfica dos testemunhos, apresentando as fácies sedimentares, o ambiente deposicional no qual as facies foram depositadas e as fases de atividade eólica, quando reconhecidas.

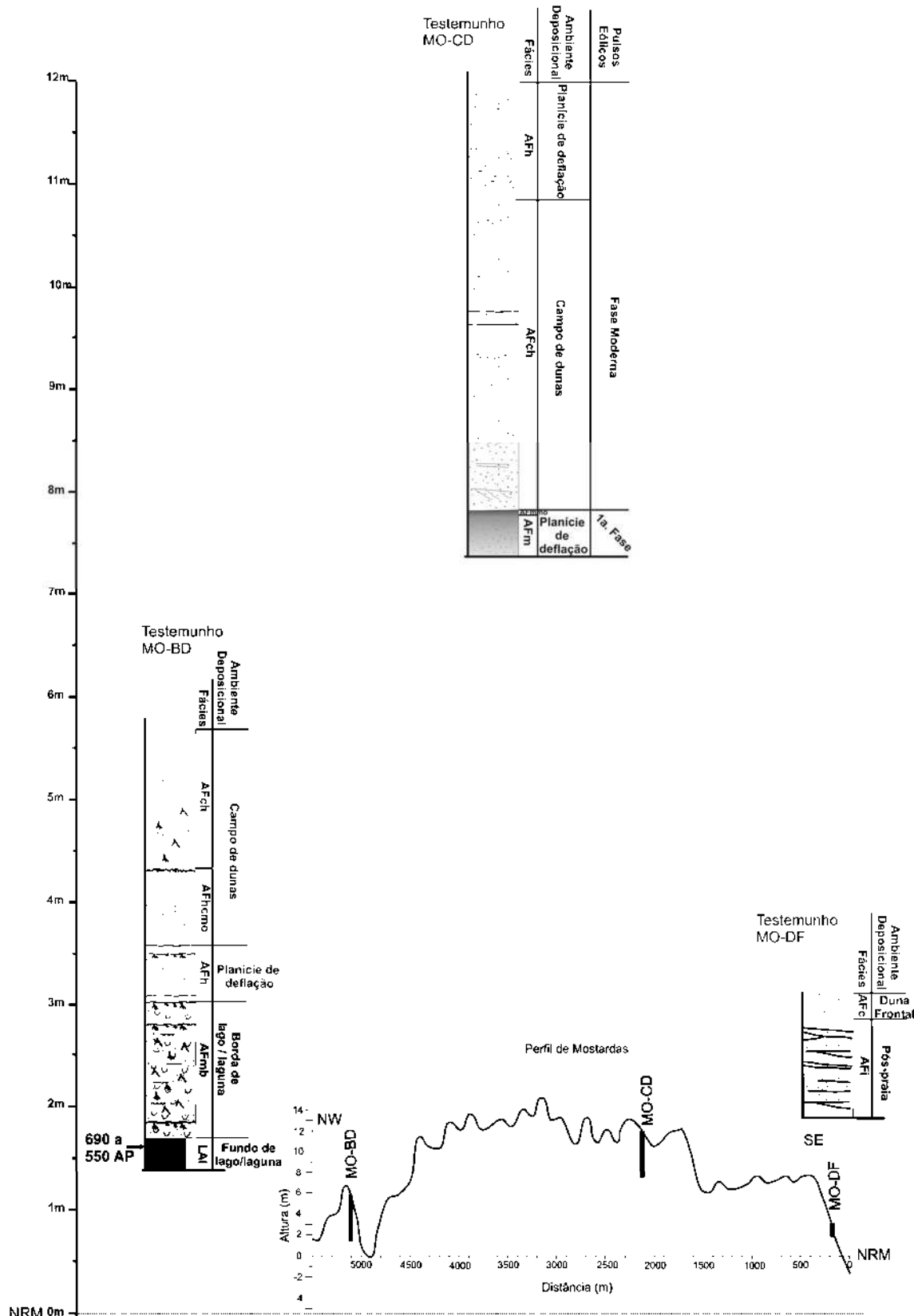


Figura 9: Perfil de Mostardas. Posição e altura dos testemunhos na seção topográfica. Seção estratigráfica dos testemunhos, apresentando as fácies sedimentares, o ambiente deposicional no qual as facies foram depositadas e as fases de atividade eólica, quando reconhecidas.

Livros Grátis

(<http://www.livrosgratis.com.br>)

Milhares de Livros para Download:

[Baixar livros de Administração](#)

[Baixar livros de Agronomia](#)

[Baixar livros de Arquitetura](#)

[Baixar livros de Artes](#)

[Baixar livros de Astronomia](#)

[Baixar livros de Biologia Geral](#)

[Baixar livros de Ciência da Computação](#)

[Baixar livros de Ciência da Informação](#)

[Baixar livros de Ciência Política](#)

[Baixar livros de Ciências da Saúde](#)

[Baixar livros de Comunicação](#)

[Baixar livros do Conselho Nacional de Educação - CNE](#)

[Baixar livros de Defesa civil](#)

[Baixar livros de Direito](#)

[Baixar livros de Direitos humanos](#)

[Baixar livros de Economia](#)

[Baixar livros de Economia Doméstica](#)

[Baixar livros de Educação](#)

[Baixar livros de Educação - Trânsito](#)

[Baixar livros de Educação Física](#)

[Baixar livros de Engenharia Aeroespacial](#)

[Baixar livros de Farmácia](#)

[Baixar livros de Filosofia](#)

[Baixar livros de Física](#)

[Baixar livros de Geociências](#)

[Baixar livros de Geografia](#)

[Baixar livros de História](#)

[Baixar livros de Línguas](#)

[Baixar livros de Literatura](#)

[Baixar livros de Literatura de Cordel](#)

[Baixar livros de Literatura Infantil](#)

[Baixar livros de Matemática](#)

[Baixar livros de Medicina](#)

[Baixar livros de Medicina Veterinária](#)

[Baixar livros de Meio Ambiente](#)

[Baixar livros de Meteorologia](#)

[Baixar Monografias e TCC](#)

[Baixar livros Multidisciplinar](#)

[Baixar livros de Música](#)

[Baixar livros de Psicologia](#)

[Baixar livros de Química](#)

[Baixar livros de Saúde Coletiva](#)

[Baixar livros de Serviço Social](#)

[Baixar livros de Sociologia](#)

[Baixar livros de Teologia](#)

[Baixar livros de Trabalho](#)

[Baixar livros de Turismo](#)